THE UNIVERSITY OF MICHIGAN

INDUSTRY PROGRAM OF THE COLLEGE OF ENGINEERING

THE DYNAMIC RESPONSE OF HEAT EXCHANGERS WITH SINUSOIDAL TIME DEPENDENT INTERNAL HEAT GENERATION

Wen-Jei Yang

A dissertation submitted in partial fulfillment
of the requirements for the degree of
Doctor of Philosophy in The
University of Michigan
1960

June, 1960

IP-434

Doctoral Committee:

Professor John A. Clark, Chairman
Assistant Professor Vedat S. Arpaci
Assistant Professor Bernard A. Galler
Associate Professor Frederick G. Hammitt
Professor Joseph E. Shigley

ACKNOWLEDGMENT

The writer sincerely extends his utmost gratitude and pays his respect to his Chairman, Professor John A. Clark for his excellent instructions and sincere encouragement. The writer is indebted particularly to his committee and Assistant Professor Herman Merte, Jr. for their invaluable advices. To the technicians and Mrs. Frank Martin, secretary at the laboratory, the writer wishes to extend his sincere thanks. The assistance of the Department of Mechanical Engineering in providing materials, instrumentation and equipment for the experimental work and the Horace H. Rackham School of Graduate Studies for a financial grant aiding in the cost of machine computation are gratefully acknowledged.

The cooperation of the Industry Program of the College of Engineering in the preparation of the manuscript is highly appreciated.

TABLE OF CONTENTS

TABLE OF CONTENTS (CONT'D)

LIST OF TABLES

LIST OF FIGURES

LIST OF FIGURES (CONT'D)

LIST OF FIGURES (CONT'D)

LIST OF FIGURES (CONT'D)

LIST OF FIGURES (CONT'D)

LIST OF FIGURES (CONT'D)

NOMENCLATURE *

A	area of the fluid in contact with wall, sq. ft.
$A_t, A_\theta, A_{\Delta t}, A_{t\infty}, A_{\theta\infty}, A_{\Delta t\infty}$.	See Chapter III and Appendix E
a	flow area of fluid, sq. ft.
a^1	cross-sectional area of wall, sq. ft.
a_1	$\frac{(r_o^2 - r_i)^2}{2r_i\ h} = \frac{1}{(\rho Cp)_w K_w}$ $ft^3 hr\,°F/Btu$
a_2	$\frac{(\rho Cp)_\omega (r_o^2 - r_i^2)}{2r_i\ h} = \frac{1}{K_w}$ hr
a_3	$\frac{\rho Cp\ r_i}{2h} = \frac{1}{K}$ hr
a_4	$\frac{\rho Cp r_i u}{2h} = \frac{u}{K}$ ft
$B_t, B_\theta, B_{\Delta t}, B_{t\infty}, B_{\theta\infty}, B_{\Delta t\infty}$.	See Chapter III and Appendix E
b_1	$a_1 + a_2 = \frac{M+1}{K}$ hr
b_2	$a_2\ a_3 = \frac{M}{K^2}$ hr^2
$C_1, C_2, \ldots C_6$	constant coefficients, dimensionless
c	circumference (wetted perimeter) $= \pi d_i$, ft
C_p	specific heat of the fluid, Btu/lb_m deg F
C_{pw}	specific heat of the wall, Btu/lb_m deg F
D	differential operator, $D_x = \frac{d}{dx}$ and $D_\tau = \frac{d}{d\tau}$
$D_1, D_2, D_3, \ldots$	constant coefficients, dimensionless
d_o	outside diameter of the tube, ft
d_i	inside diameter of the tube, ft

---

* See page xviii for representation of temperature symbols.

E	voltage, volt
Ea	amplitude of voltage, volt
e	internal energy, Btu/lb_m
$F_{13}...F_{16}$	see Appendix D
F(D)	system operational function
$\overline{F}(s)$	transfer function; $\overline{F}_t(s)$, of the fluid temperature; $\overline{F}_\Theta(s)$, of the wall temperature; $\overline{F}(s)_{\Delta t}$, of the fluid-wall temperature difference, dimensionless
$\lvert\overline{F}(i\omega)\rvert$	$\frac{Y}{\Phi}$ = amplitude ratio; $\lvert\overline{F}_t(i\omega)\rvert = \frac{(T_\infty)_{\omega=\omega}}{(T_\infty)_{\omega=0}}$, of the fluid temperature; $\lvert\overline{F}_\Theta(i\omega)\rvert = \frac{(\Theta_\infty)_{\omega=\omega}}{(\Theta_\infty)_{\omega=0}}$, of the wall temperature; $\lvert\overline{F}_{\Delta t}(i\omega)\rvert = \frac{(\Delta T_\infty)_{\omega=\omega}}{(\Delta T_\infty)_{\omega=0}}$, of the fluid-wall temperature difference, dimensionless
$G_{13}...G_{16}$	see Appendix D
h	coefficient of heat transfer between the wall and the fluid, based on the film temperature, $Btu/hr\text{-}ft^2\text{-}deg\ F$; h_x, of local values; h_m, of mean values; h_∞, at large $\frac{x}{d_o}$ where the local value is constant
h	enthalpy, Btu/lb_m
I	current, ampere
I_a	amplitude of current, ampere
I_o	Bessel function of first kind, zeroth order (modified or hyperbolic type)
Im	imaginary part of a complex number

Jc	$(St)(Pr)_f^{2/3}$, dimensionless, Jcx, of local value; Jcm, of mean value
k	the k-th term of the series
K	$(\frac{h}{\rho C_p})(\frac{A}{V})$ for fluid, $(hr)^{-1}$
K_w	$(\frac{h}{\rho C_p})_w(\frac{A}{V})_w$ for wall, $(hr)^{-1}$
m	mass, lb_m
M	heat capacity ratio $= \frac{a_2}{a_3} = \frac{K}{K_w}$
Pr	Prandtl number, dimensionless; $(Pr)_f$, based on the film temperature
P_x	rate of work done by system, Btu/hr
p	pressure, psia
p_a	amplitude of power input, Btu/ft^3hr
p_{xo}''	initial power input $= (\frac{q}{A})(\frac{A}{V})_\infty = \frac{(3412)(Kw)}{\pi(d_o^2-d_i^2)L}$, Btu/ft^3hr
$\Delta p_x''$	Change in power input, Btu/ft^3hr
q/A	heat flux $= \frac{(3412)(Kw)}{\pi d_i L}$ Btu/hr-ft^2, $(q/A)_x$, of local value
$(q/A)_o$	initial heat flux, Btu/hr-ft^2
q	heat flow rate, Btu/hr
Re	real part of a complex number or Reynolds number based on the film temperature
r_o	outside radius of the tube, ft
r_i	inside radius of the tube, ft
St	Stanton number, dimensionless

s	Laplace variable, $(hr)^{-1}$ or $s = K(x/u)$, dimensionless
$t(x,\tau)$	temperature of the fluid = $t_1(x,o) + t_2(x,\tau)$, deg F
$t_1(x,o)$	steady-state component of fluid temperature, deg F
$t_1^*(x,\tau)$	steady-state fluid temperature at x for $p_x'' = p_{xo}'' + \Phi$, deg F
$t_2(x,\tau)$	transient component of fluid temperature, deg F
$t_o(\tau)$	temperature of the fluid entering coolant channel, $t_o(\tau) = t_o + t_o^*(\tau)$, deg F
$t_o^*(\tau)$	transient component of the fluid entering coolant channel, deg F
t_o	steady-state component of temperature of the fluid entering coolant channel, deg F
$T(x,\tau)$	amplitude of transient component of fluid temperature defined in Equations (76), (79) and (84), deg F
u	velocity of the fluid, ft/hr
v	specific volume, ft^3/lbm
V	volume of the fluid = $\pi d_1^2 L/4$, ft^3
V_w	volume of the wall = $\omega(d_o^2-d_1^2)L/4$, ft^3
w	fluid flow rate lbm/hr
x	axial distance, ft
Y	amplitude of the transient component of the output
α	phase-shift; α_t, of fluid temperature; α_θ, of wall temperature; $\alpha_{\Delta t}$, of fluid-wall temperature difference, degree of angle
γ	see Appendix C
$\Delta t(x,\tau)$	fluid-wall temperature difference = $\theta - t$, deg F

$\Delta T(x,\tau)$	amplitude of transient component of fluid-wall temperature difference, deg F
δ	see Appendix C
$\Theta(x,\tau)$	wall temperature = $\Theta_1(x,o) + \Theta_2(x,\tau)$, deg F
$\Theta_1(x,o)$	steady-state component of wall temperature, deg F
$\Theta_2(x,\tau)$	transient component of wall temperature, deg F
$\theta(x,\tau)$	amplitude of transient component of wall temperature, deg F
$\Lambda(\tau)$	see Appendix D
$\pi(\tau)$	see Appendix D
ρ	density, lbm/ft^3
τ	time, hr
τ^*	$\tau - \frac{x}{u}$, hr
τ'	time of inlet lag of a fluid particle, hr
$\phi(\tau)$	disturbance, or transient in volumetric heat generation rate, Btu/hr-ft^3
Φ	amplitude of disturbance, or amplitude of transient in volumetric heat generation rate, Btu/hr-ft^3
$\psi_2, \ldots, \psi_8$	see Appendix D
ω	circular frequency, rad./hr
$\omega\tau'$	dimensionless inlet lag of a fluid particle
$\bar{(\ )}$	transformed function

Subscripts

+	upper envelope
-	lower envelope

bar	mean value (except Laplace transformed function)
∞	at steady-periodic state
t	fluid temperature
θ	wall temperature
Δt	fluid-wall temperature difference

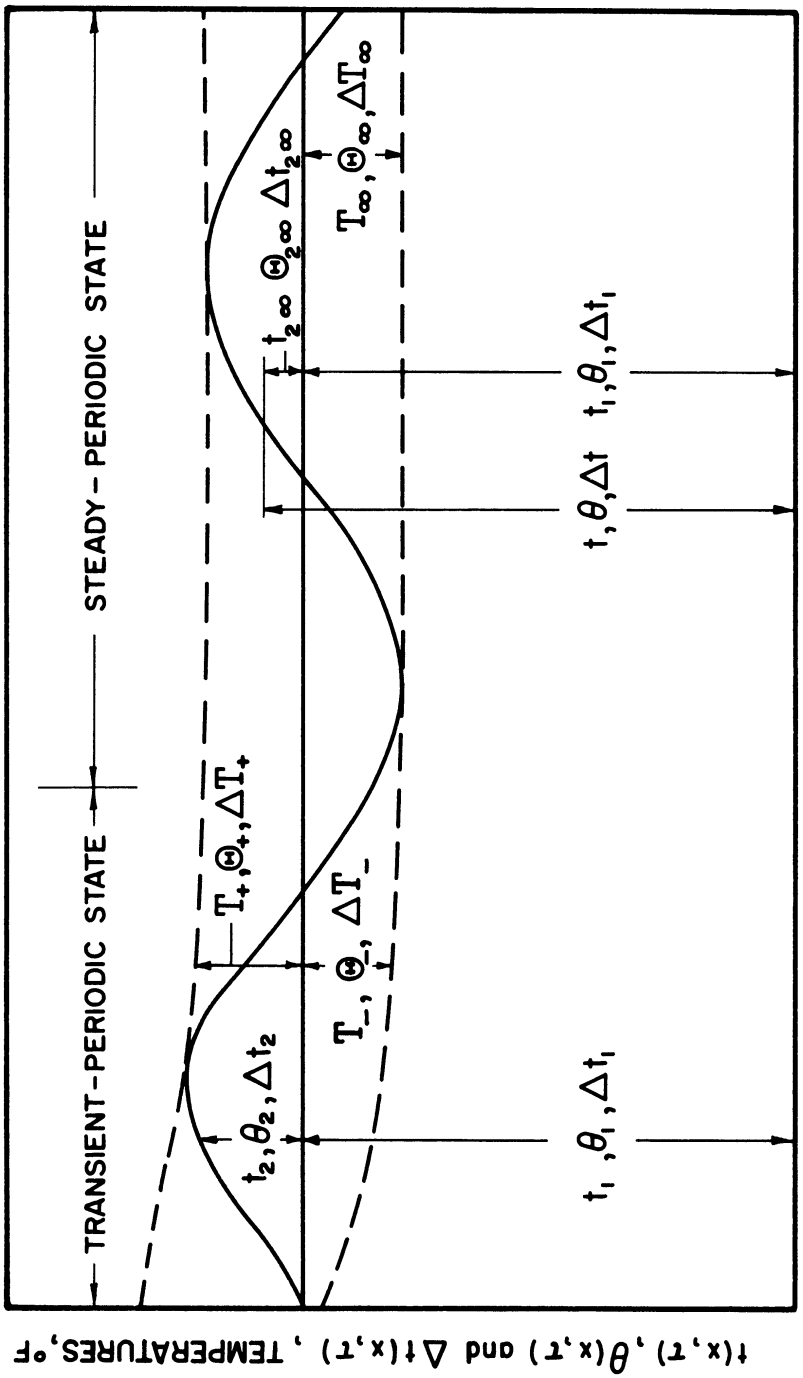

Representation of Temperature Symbols.

CHAPTER I

INTRODUCTION

Problems concerning the dynamics of thermal processes possessing characteristics attributed to capacitance (specific heat and density) and resistance (heat transfer coefficient) are continuously arising in engineering practice where temperature control is necessary.

The controllability of the output is decided by the dynamic characteristics of the system subjected to various external disturbances.

The dynamic response of a fluid flowing through an insulated pipe subjected to a step, and sinusoidal disturbance on inlet temperature were investigated by J. W. Rizika[9], P. Profos[20] and Y. Takahashi[7,8]. The dynamic response of the same system with a step and linear change in the rate of heat generation were studied by Professors J. A. Clark and V. S. Arpaci in a series of technical papers.[1,2,3] This thesis is the extension of their work on a similar heat exchanger but differing in that the rate of heat generation from the internal heat source is sinusoidally time dependent. The heat exchanger and the fluid are considered as a system. The fluid temperature, the wall temperature and the fluid-wall temperature difference are taken as the outputs, corresponding to variations of internal heat generation, which are considered as the input or disturbance. The previous work[1,2,3] have presented the solutions to the step and ramp response while this work reports the investigation of the frequency response of the wall temperature, fluid temperature and fluid-wall temperature difference owing to the periodic disturbance in the rate of

heat generation. In case both the fluid inlet temperature and the rate of heat generation change the results on the outputs are superposable because of the linearity in the entire system.

The understanding of the dynamic characteristics of a physical system is necessary in order that it be able to be controlled. The response of a dynamic system may be found by imposing a disturbance at one point in the system, holding all variables but one constant. The disturbance may be a step, sinusoidal, linear, or an exponential function with respect to time, and the corresponding response is called step, sinusoidal or frequency, ramp, exponential response, respectively.

In general, it is preferable to express the dynamic behavior of a system by means of a step, and-or frequency response.

Step response is recommended because of its clearness in representation and fullness of physical significance. Also it is sometimes easier to impose experimentally. The experimentally determined response can be approximated by a suitable mathematical expression which then can be used to determine the dynamic characteristics of the system to other disturbances.

Steady-periodic response or frequency response is important for two reasons:

1) If the response of a linear system to sinusoidal imputs of all frequencies is known, it is possible to know the response of the system to any other type of disturbance on the input, since any arbitrary function, according to the Fourier theorem, can be synthesized by superimposing an infinite number of sine waves of different frequencies.

If the arbitrary function is periodic in time, one can use a Fourier series of sine waves to represent it; if the function is not periodic, a Fourier integral is used to represent it.

2) Frequence response is also extremely helpful in predicting the stability of a closed-loop system, if the frequency response of an open-loop system is known.

Furthermore, frequency response may also be determined experimentally by simply applying all frequencies and then plotting the transfer locus as a function of frequency.

This powerful method of frequency-response study was originally and thoroughly developed for use in feedback amplifier design and subsequently has been widely applied to the servomechanism as well as process control fields. It is now realized that servomechanism and the control of heat exchangers are basically the same and therefore the method of study used in servomechanism can be applied directly to heat exchanger by merely changing in terminology and point of view or emphasis.

The investigation of the dynamic behavior in the transient-periodic state has often been ignored since it is usually a more complicated problem and the period will decay after a certain time interval followed by the steady-periodic state. Two convenient ways to determine the rapidness of the decay of the transient periodic-state are: (a) to measure the time required for the amplitudes of the transient periodic oscillation of temperatures to reach 99 percent of that of the steady-state oscillation. (The specification of 99 per cent is admittedly somewhat arbitrary.) (b) to measure the logarithmic increment which may be defined as the natural logarithm of the ratio of any two successive amplitudes.

The research was conducted in the Heat Transfer and Thermodynamics Laboratory of the Department of Mechanical Engineering.

CHAPTER II

GENERAL THEORY

The operating conditions of a system may be divided into three time regiemes: steady state, quasi-steady state and transient state as shown in Figure 1.

Steady-state exists for a system when the disturbance (or input) and output quantities are both constant with time. A system is under the quasi-steady state, when the disturbance changes so slow that the output follows with the change without any disturbance on the equilibrium of the entire system. A system is under the transient state when the relationship between the input and the output is different from the relationship that would exist under steady or quasi-steady states for the same system.

Transient state of a system under the sinusoidal disturbance may further be divided into steady-periodic and transient-periodic states. As the sinusoidal disturbance is imposed on the system, the system starts to respond, the output being oscillatory with growing amplitude but due to the inertness the system generally possesses, it is not sinusoidal. The system at this period is said to be under the transient-periodic state although each period of the oscillations may not be the same. After a certain time, the output will finally become sinusoidal, perhaps with an altered amplitude and a phase shift relative to the disturbance. The system is then in the steady-periodic state.

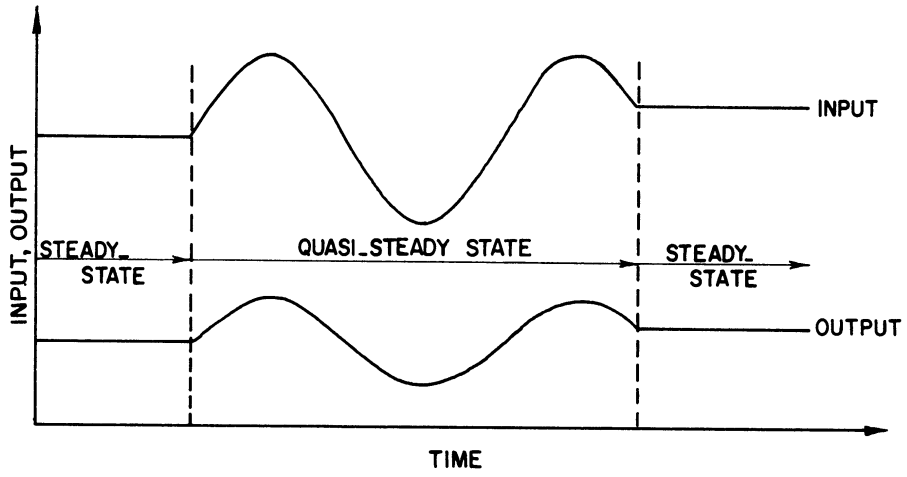

(a) Input and Output Variations Under Steady and Quasi-Steady States.

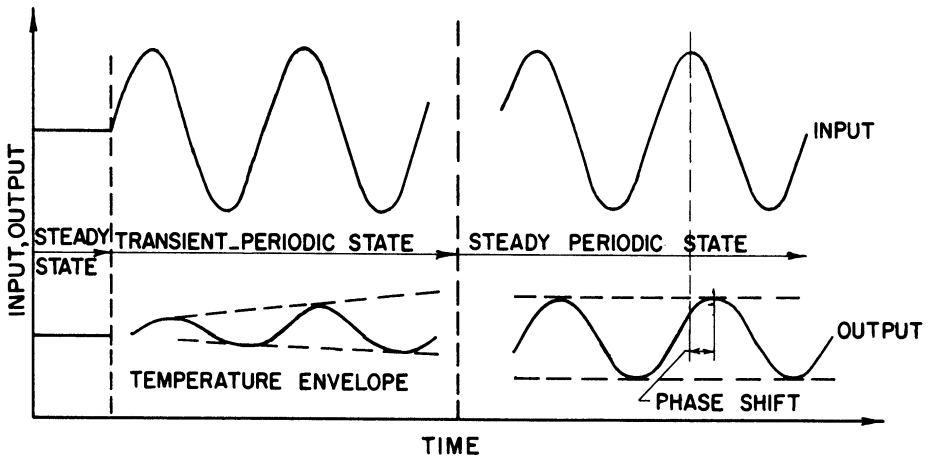

(b) Input and Output Variations Under Steady and Dynamic States.

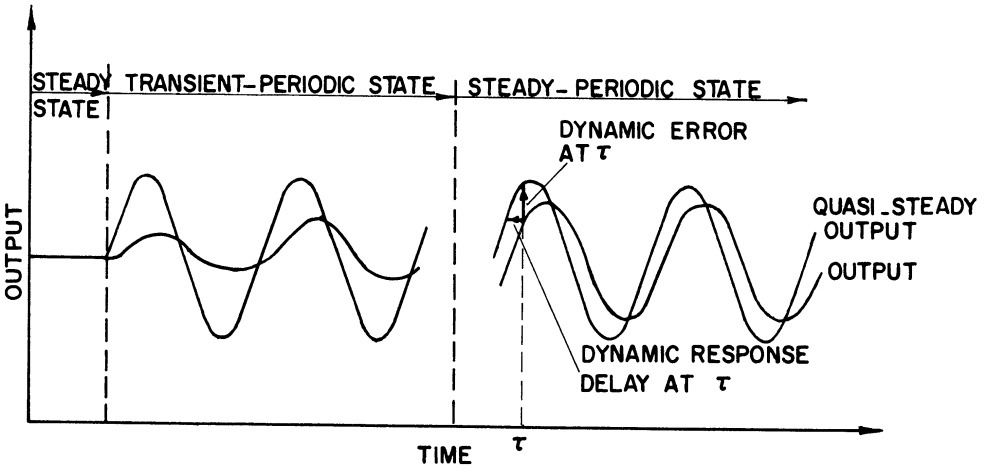

(c) Output Response Under Dynamic Conditions.

Figure 1. Steady and Dynamic Operating Conditions.

A. Dynamic Response at Steady-Periodic State

In the field of Automatic control, the method of Laplace transform is very widely applied to initial-value problems of linear ordinary differential equation with constant coefficients since the Laplace transform is defined as an operation on a function defined for $\tau > 0$. But in "Operational Methods in Applied Mathematics" Oxford University Press, by H. S. Carslaw and J. C. Jaeger, they had shown it is also applicable to linear partial differential equations with coefficients that are independent of τ and with boundary conditions partially described as initial-value conditions in τ.

For example, for dynamic-response problems of heat exchangers expressed by a linear partial differential equation with two independent variables length x and time τ, τ can be removed from the original equation by applying the Laplace transformation. The resultant equation containing s, the Laplace variable, as a parameter is a linear ordinary differential equation having a single independent variable x, and may be solved by using the remaining boundary conditions.

For simplicity, a second order system is taken as an example. Its response characteristics may be expressed by a linear partial differential equation in y as a function of x and τ having constant coefficients, as Equation (1), below. The following method of analysis is general and can be applied to any linear system of a higher order expressed by two independent variables and possessing coefficients that are independent of τ. Any two specific quantities in the solution of the transformed equation are compared, still bear a linear relation. If one

of them is considered to be a disturbance and the other an output, the ratio of output to disturbance is still the function of the parameter s, the Laplace variable.(29)

Consider such a linear transfer system* of the second order which can be expressed by the equation

$$C_1\frac{\partial^2 y}{\partial x^2} + C_2\frac{\partial^2 y}{\partial x \partial \tau} + C_3\frac{\partial^2 y}{\partial \tau^2} + C_4\frac{\partial y}{\partial x} + C_5\frac{\partial y}{\partial \tau} + C_6 y = D_1\phi + D_2\frac{d\phi}{d\tau} + D_3\frac{d^2\phi}{d\tau^2} \quad , \tag{1}$$

with initial conditions as required by a later transformation of Equation (1) into the Laplace variable,

$$y(x,0) = y_o$$

$$\frac{\partial y(x,0)}{\partial \tau} = y_o^{(1)}$$

$$\frac{\partial^2 y(x,0)}{\partial \tau^2} = y_o^{(2)}$$

where y is the output due to ϕ, the input or transient disturbance which is a function of τ. $C_1,\ldots C_6$ and $D_1,\ldots D_3$ are constant coefficients.

Since the equation is linear, the principle of superposition of solutions applies. Let $y = y_1 + y_2$, where y_1 is a complementary and y_2 is a particular solution of the equation. Physically, the complimentary solution signifies the effect of initial disturbance on output, thus it may also be called the steady-state component of the output. The

---

* A transfer system is defined as an arrangement in which any physical quantity ϕ - the input to the system - is converted into a second quantity y - the output - which bears a unique relation to the first.(30)

particular solution signifies the transient effect of the disturbance on output, thus may be called the transient component of the output.

Upon the substitution of the general solution $y = y_1 + y_2$, into the original equation as well as into its initial and boundary conditions, two equations are obtained, one expressing the steady-state, the other the transient behavior of the system, each having its own initial and boundary conditions.

The steady-state component y_1 is the solution of the homogeneous equation

$$C_1\frac{\partial^2 y_1}{\partial x^2} + C_2\frac{\partial^2 y_1}{\partial x \partial \tau} + C_3\frac{\partial^2 y_1}{\partial \tau^2} + C_4\frac{\partial y_1}{\partial x} + C_5\frac{\partial y_1}{\partial \tau} + C_6 y_1 = 0 \quad , \tag{2}$$

with the initial conditions:

$$y_1(x,0) = y_0$$

$$\frac{\partial y_1(x,0)}{\partial \tau} = y_0^{(1)}$$

$$\frac{\partial^2 y_1(x,0)}{\partial \tau^2} = y_0^{(2)}$$

The transient component y_2 is the solution of the non-homogeneous equation

$$C_1\frac{\partial^2 y_2}{\partial x^2} + C_2\frac{\partial^2 y_2}{\partial x \partial \tau} + C_3\frac{\partial^2 y_2}{\partial \tau^2} + C_4\frac{\partial y_2}{\partial x} + C_5\frac{\partial y_2}{\partial \tau} + C_6 y_2 = D_1\phi + D_2\frac{d\phi}{d\tau} + D_3\frac{d^2\phi}{d\tau^2} \tag{3}$$

with the boundary conditions:

$$y_2(x,0)=0$$

$$\frac{\partial y_2(x,0)}{\partial \tau}=0$$

$$\frac{\partial^2 y_2(x,0)}{\partial \tau^2}=0$$

To solve the Equations (2) and (3) by the Laplace transform, we multiply both sides of the equations by $e^{-s\tau}$ and integrate each term from $\tau = 0$ to $\tau = \infty$. By terms, this gives the following set of equations,

$$L\left[\frac{\partial^2 y}{\partial x^2}\right]=\frac{d^2\bar{y}}{dx^2}$$

$$L\left[\frac{\partial^2 y}{\partial x \partial \tau}\right]=L\left[\frac{\partial^2 y}{\partial \tau \partial x}\right]=-\frac{dy_0}{dx}+s\frac{d\bar{y}}{dx}$$

$$L\left[\frac{\partial^2 y}{\partial \tau^2}\right]=-y_0^{(1)}-sy_0+s^2\bar{y}$$

$$L\left[\frac{\partial y}{\partial x}\right]=\frac{d\bar{y}}{dx}$$

$$L\left[\frac{\partial y}{\partial \tau}\right]=-y_0+s\bar{y}$$

$$L[y]=\bar{y}$$

$$L[\phi]=\bar{\phi}$$

$$L\left[\frac{d\phi}{d\tau}\right]=-\phi(0)+s\bar{\phi}=s\bar{\phi}$$

$$L\left[\frac{d^2\phi}{d\tau^2}\right]=-\phi^{(1)}(0)-s\phi(0)+s^2\bar{\phi}=s^2\bar{\phi}$$

Upon substitution of the above set into Equations (2) and (3) they become ordinary differential equations with x as the independent variable, as follows,

$$C_1\frac{d^2\bar{y}_1}{dx^2}+C_2\left(s\frac{d\bar{y}_1}{dx}-\frac{dy_0}{dx}\right)+C_3\left(-y_0^{(1)}-sy_0+s^2\bar{y}_1\right)+C_4\frac{d\bar{y}_1}{dx}+C_5\left(-y_0+s\bar{y}_1\right)+C_6\bar{y}_1=0$$

$$C_1\frac{d^2\bar{y}_2}{dx^2}+C_3\,s\frac{d\bar{y}_2}{dx}+C_3s^2\bar{y}_2+C_4\frac{d\bar{y}_2}{dx}+C_5s\bar{y}_2+C_6\bar{y}=D_1\bar{\phi}+D_2s\bar{\phi}+D_3s^2\bar{\phi}$$

Rearranging the above equations, one obtains

$$C_1\frac{d^2\bar{y}_1}{dx^2}+(C_2s+C_4)\frac{d\bar{y}_1}{dx}+(C_3s^2+C_5s+C_6)\bar{y}_1=C_3y_0^{(1)}+C_3sy_0+C_5y_0+C_2\frac{dy_0}{dx} \qquad (4)$$

$$C_1\frac{d^2\bar{y}_2}{dx^2}+(C_2s+C_4)\frac{d\bar{y}_2}{dx}+(C_3s^2+C_5s+C_6)\bar{y}_2=(D_1+D_2s+D_3s^2)\bar{\phi} \qquad (5)$$

Equations (4) and (5) may be expressed in the form of

$$A_2\frac{d^2\bar{y}}{dx^2}+A_1(s)\frac{d\bar{y}}{dx}+A_0(s)\bar{y}=B(s) \qquad (6)$$

which has a general solution

$$\bar{y}=E_1(s)e^{p_1(s)x}+E_2(s)e^{p_2(s)x}+\frac{B(s)}{A_0(s)} \qquad (7)$$

where $E_1(s)$ and $E_2(s)$ are coefficients which must be determined by the boundary conditions and $p_1(s)$ and $p_2(s)$ are roots of the corresponding homogeneous differential equation:

$$A_2\frac{d^2\bar{y}}{dx^2}+A_1(s)\frac{d\bar{y}}{dx}+A_0(s)\bar{y}=0 \quad . \tag{8}$$

For the higher order system, the differential equation after Laplace transformation is of the n-th order and can be expressed as

$$A_n(s)\frac{d^n\bar{y}}{dx^n}+A_{n-1}(s)\frac{d^{n-1}\bar{y}}{dx^{n-1}}+\cdots\cdots\cdots+A_0(s)\bar{y}=B(s) \tag{9}$$

Then the solution of the homogeneous equation

$$A_n(s)\frac{d^n\bar{y}_1}{dx^n}+A_{n-1}(s)\frac{d^{n-1}\bar{y}_1}{dx^{n-1}}+\cdots\cdots\cdots+A_0(s)\bar{y}_1=0 \quad , \tag{10}$$

may be found by using the exponential expression

$$\bar{y}_1=e^{p(s)x} \tag{11}$$

Upon the substitution of $\bar{y}_1$ into the homogeneous equation, the equation is converted into an algebraic equation

$$A_n(s)p^n(s)+A_{n-1}(s)p^{n-1}(s)+\cdots\cdots\cdots+A_0(s)=0 \quad . \tag{12}$$

Now if $p_1(s)$, $p_2(s)$, ..., $p_n(s)$ be the n roots of Equation (12), then the complementary solution will be

$$\bar{y}_1 = C_1(s)e^{p_1(s)x} + C_2(s)e^{p_2(s)x} + \text{---------} + C_n(s)e^{p_n(s)x}$$

The particular solution of Equation (9) is found by inspection to be

$$\bar{y}_2 = \frac{B(s)}{A_0(s)}$$

Therefore the general solution to Equation (9) can be expressed by

$$\bar{y} = \bar{y}_1 + \bar{y}_2 \tag{13}$$

The constants $C_1(s)$, $C_2(s)$, ..., $C_n(s)$ must be determined by the boundary conditions.

One then obtains a complete solution by an inverse Laplace transformation of $\bar{y}$, as,

$$y = y_1 + y_2 \tag{14}$$

In general, if a physical system is stable, the transient effect of y_1 will decay after a considerable time and only y_2 constitutes the complete description of the dynamical behavior of the system. In other words, the initial disturbance* has no effect on the dynamic behavior of the system subsequent to $\tau = 0$. Therefore, only y_2, the transient effect needs to be considered. This happens when the poles of the complementary solution are all located to the left of the imaginary axis on s-plane.

---

* The initial disturbance is the disturbance caused by the initial steady-state.

The solution of Equation (5) can be expressed by

$$\bar{y}_2 = \frac{D_1 + D_2 S + D_3 S^2}{C_1 D_x^2 + (C_2 S + C_4) D_x + (C_3 S^2 + C_5 S + C_6)} \bar{\Phi} = \bar{F}(S) \cdot \bar{\Phi} \qquad (15)$$

where $\bar{F}(s)$ is called the transfer function of the system. Physically it is the ratio of the Laplace transform of an output and the Laplace transform of its disturbance, and completely defines the dynamic performance of the system.

The performance of a system may be described either by a scalar or by a vector performance operator as shown in Figure 2.(32)

1. Scalar Performance Operators

If a system is free from inertness, (for instance heat capacity and thermal resistance in thermal systems), the output is directly proportional to its input without delay in response. This may be expressed by

$$y_2 = C\Phi \quad ,$$

where C is the proportionality constant. However, the system generally possesses a certain inertness, which creates an extended period of response. Then the direct proportionality between y and ϕ represents only the finally attained steady-state. For those systems having inertness, the previous equation must be replaced by

$$y_2 = F(D_\tau)\Phi \quad ,$$

where y_2 is a scalar output quantity and ϕ, a scalar input quantity. The symbol (D_τ) represents a function of the differential operator $D_\tau = d/d\tau$ operating on ϕ at all orders of differentiation. $F(D_\tau)$ is called the system operational function.

a) SCALAR PERFORMANCE OPERATORS

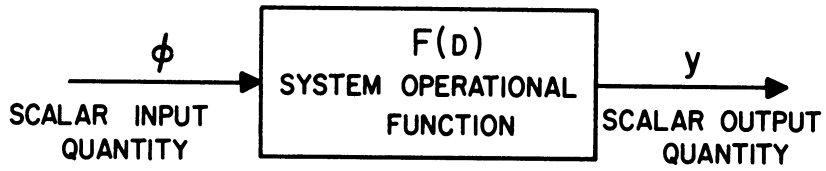

SCALAR OUTPUT QUANTITY = [SYSTEM OPERATIONAL FUNCTION] X [SCALAR INPUT QUANTITY]

b) VECTOR PERFORMANCE OPERATORS

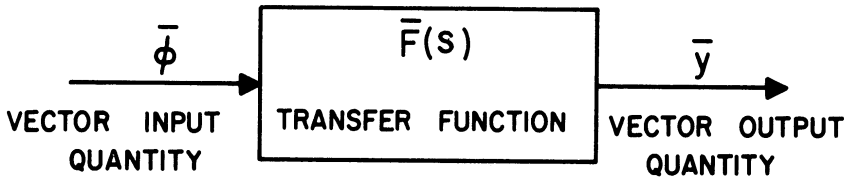

VECTOR OUTPUT QUANTITY = [TRANSFER FUNCTION] X [VECTOR INPUT QUANTITY]

Figure 2. The Scalar and Vector Performance Operations of a System.

2. Vector Performance Operators

The vector performance of the system is described by an equation

$$\bar{y}_2 = \bar{F}(s) \cdot \bar{\Phi}$$

The vector output quantity $\bar{y}_2$ is equal to the product of the transfer function $\bar{F}(s)$, and the vector input quantity, $\bar{\phi}$. This definition has an advantage over the scalar performance operator in that it describes not only magnitude changes but also phase relationships.

3. Frequency Response

If the disturbance $\phi(\tau)$ is sinusoidal, it may be written by

$$\phi(\tau) = \Phi e^{i\omega\tau} \quad , \tag{16}$$

where Φ is the amplitude and ω is the circular frequency. Since the system is linear, after a sufficient time, the output y_2 will become sinusoidal with the same frequency as the disturbance but with a different amplitude and a phase-shift relative to the disturbance ϕ. Let Y be the amplitude and α the phase-shift, then the output may be written as

$$y_2 = Y e^{i(\omega\tau - \alpha)} \tag{17}$$

It must be emphasized that Equation (17) holds only at steady-periodic state at which Y is the function of length x and frequency ω and is periodic in time over the interval $2\pi/\omega$. From Equation (17) the following are obtained:

$$\frac{\partial y_2}{\partial x} = \frac{dY}{dx} e^{i(\omega\tau - \alpha)}$$

$$\frac{\partial^2 y_2}{\partial x^2} = \frac{d^2Y}{dx^2} e^{i(\omega\tau - \alpha)}$$

$$\frac{\partial^2 y_2}{\partial x \partial \tau} = \frac{dY}{dx} (i\omega) e^{i(\omega\tau - \alpha)}$$

$$\frac{\partial y_2}{\partial \tau} = Y(i\omega) e^{i(\omega\tau - \alpha)}$$

$$\frac{\partial^2 y_2}{\partial \tau} = Y(i\omega)^2 e^{i(\omega\tau - \alpha)}$$

Substituting these equations into Equation (5), one obtains

$$\left[C_1 \frac{d^2Y}{dx^2} + C_2(i\omega)\frac{dY}{dx} + C_3(i\omega)^2 Y + C_4 \frac{dY}{dx} + C_5(i\omega)Y + C_6 Y\right] e^{i(\omega\tau - \alpha)}$$

$$= \left[D_1 \Phi + D_2(i\omega)\Phi + D_3(i\omega)^2 \Phi\right] e^{i\omega\tau}$$

or

$$C_1 \frac{d^2}{dx^2}(Ye^{-i\alpha}) + C_2(i\omega)\frac{d}{dx}(Ye^{-i\alpha}) + C_3(i\omega)^2(Ye^{-i\alpha}) + C_4 \frac{d}{dx}(Ye^{-i\alpha})$$

$$+ C_5(i\omega)(Ye^{-i\alpha}) + C_6(Ye^{-i\alpha}) = D_1\Phi + D_2(i\omega)\Phi + D_3(i\omega)^2\Phi \qquad (18)$$

One finds, therefore, the solution expressed by Equation (17) is correct since the time function $e^{i\omega\tau}$ vanishes. By solving Equation (18) for the unknown quantity $Ye^{-i\alpha}$ one obtains

$$\frac{Ye^{-i\alpha}}{\Phi} = \frac{D_1 + D_2(i\omega) + D_3(i\omega)^2}{CD_x^2 + [C_2(i\omega) + C_4]D_x + C_3(i\omega)^2 + C_5(i\omega) + C_6} = \bar{F}(i\omega) \qquad (19\text{-a})$$

Combining Equation (15) with the Laplace transformations of Equations (16) and (17), yields

$$\frac{\bar{y}_2}{\bar{\Phi}} = \frac{Ye^{-i\alpha}}{\Phi} = \frac{D_1 + D_2 S + D_3 S^2}{C_1 D_x^2 + (C_2 S + C_4) D_x + C_3 S^2 + C_5 S + C_6} \tag{19-b}$$

Equations (19-a) and (19-b) are identical if $s = i\omega$. For the frequency response of a system represented by an ordinary differential equation, the literature in the fields of cybenetics[29], control engineering[30] and servomechanisms[28] have demonstrated the principle of substituting s in $\bar{F}(s)$ by $i\omega$. There have been many papers[4,5,6,7,8,20,22,26] treating the frequency response of the system expressed by a partial differential equation by the same principle. It is believed that the previous derivation is the first attempt to prove the applicability of the principle to the system with two independent variables x and τ.

The complex quantity $Ye^{-i\alpha}/\Phi$ is a function of x, the system constants and the angular frequency ω. $\bar{F}(i\omega)$ is generally called the transfer function of frequency response. From the above analysis if one knows the function $\bar{F}(s)$ of any system, called the system transfer function in Equation (15), one may find $\bar{F}(i\omega)$ as a function of frequency ω by merely substituting $s = i\omega$. Now from Equation (19-a)

$$\bar{F}(i\omega) = |\bar{F}(i\omega)| e^{-i\alpha} \tag{20}$$

where,

$$|\bar{F}(i\omega)| = \frac{Y}{\Phi} \tag{21}$$

The absolute value of $\bar{F}(i\omega)$ forms the amplitude-ratio response function. The term α represents the angular difference in phase (or phase shift) between Y and Φ resulting from an oscillation or the disturbance of frequency ω imposed on the system.

It must be noted that the output due to a sinusoidal disturbance is given by the pure imaginary component of the complex solution $\overline{y_2} = \bar{F}(i\omega)\overline{\phi}$, since the sinusoidal disturbance is expressed by the pure imaginary component of $\phi = \Phi e^{i\omega\tau}$. Therefore

$$y_2 = |\bar{F}(i\omega)|\Phi \sin(\omega\tau - \alpha) \tag{22}$$

with

$$\alpha = \tan^{-1}\left\{-\frac{Im[\bar{F}(i\omega)]}{Re[\bar{F}(i\omega)]}\right\} \tag{23}$$

If the frequency ω of a disturbance decreases towards zero, that is, the system tends to the quasi-steady process, the disturbance $\phi(\tau)$ approaches a constant value equal to Φ, which is independent of time. The quantity represented by $\bar{F}(s)$ at $s = 0$, expressed by $\bar{F}(0)$, is the ratio of output to disturbance under the quasi-steady process at $\omega = 0$. Takahashi points out in Reference 8 that for a two-fluid heat exchanger, $\bar{F}(0)$ signifies the cold-side heat exchanger effectiveness, if $\bar{F}(i\omega)$ is defined as the ratio of the outlet temperature amplitude of the cold fluid and the inlet temperature amplitude of the hot fluid. For the problem of one fluid flowing along an insulated solid wall, $\bar{F}(i\omega)$ is defined as the ratio of the inlet and outlet temperature amplitudes of the same fluid, thus $\bar{F}(0)$ is equal to unity.

4. Representations of Sinusoidal Performance Characteristics

The response of a system to a sinusoidal disturbance $\phi = \Phi \sin\omega\tau$ is, in general terms, $y_2 = Y\sin(\omega\tau-\alpha)$. The relationship between two or more sinusoidal variations of the same frequency (both disturbance and outputs) is important and may be shown on the rotating vector diagram. By the complex angle convention the phase angle is positive for counter-clockwise angular displacement meaning that the phase shift shown is actually negative.

In order to visualize the response characteristics, it is much more descriptive to show it on the Bode type diagram by plotting the amplitude and phase-shift versus frequency since it is known that the output function is sinusoidal. Furthermore, the amplitude and phase-shift are a function of frequency so that a periodic steady-state sinusoidal response may be considered in the frequency domain rather than the time domain. For a system composed of several transfer elements in series, the transfer function of the system is equal to the product of the transfer function of the components.

The sinusoidal performance characteristics of a system can also be represented by a polar diagram in a complex plane, which is called transfer locus. It is represented by a polar plot with amplitude-ratio and phase-shift shown in vector form with frequency as a parameter. It shows the real and imaginary parts of the frequency function as projections on the real and imaginary axes of a vector with a length proportional to the amplitude-ratio and making an angle with the clockwise direction of the real axes, equal to the phase-shift.

The transfer locus of any system uniquely describes the dynamic characteristics of the system. If two physical systems have identical transfer loci, the systems must be dynamically equivalent even though they belong to different categories of energy systems, such as, a mechanical system and a pheumatic one.

5. Parameters Affecting the Decay Time of the Transient Periodic State

For the system represented by an ordinary differential equation, the transient response is determined by the roots of the characteristic equation of the system. For the system expressed by a partial differential equation, the response is determined by the real part of the poles (which determines the time constants) of the system transfer function,

$$\bar{F}(s)=\frac{\bar{\theta}_2}{\bar{\phi}}$$

The inverse Laplace transformation of $1/s+C$ gives $e^{-c\tau}$. If the transfer function has poles $-C_1$, $-C_2$, $-C_3$, ..., its inverse Laplace transform gives the components $e^{-C_1\tau}$, $e^{-C_2\tau}$, $e^{-C_3\tau}$, ... If the real part of all the poles of $\bar{F}(s)$ are negative in sign, the transient-periodic state vanishes with increasing values of time. The time required for the transient period to decay is inversely proportional to the magnitude of these negative valued real parts of these poles of $\bar{F}(s)$, which lie to the left of the imaginary axis on the s-plane. Therefore for the rapid decay in the transient period, these poles should lie as far to the left of the imaginary axis as possible. On the other hand, should the poles of $\bar{F}(s)$ fall to the right side of the imaginary axis on the s-plane, the time constant will be positive and the response of the system will be ever

increasing in time. Such a condition is dynamically unstable. Domains of both stable and unstable systems are shown in the s-plane in Figure 3.

6. Relationship Between Step- and Frequency-Responses

For a linear transfer system, its transfer function may be expressed by the ratio of output to its disturbance both in Laplace transform notation as

$$\bar{F}(s)=\frac{\bar{y}}{\bar{\phi}} \tag{24}$$

If the system is subject to a step-change in disturbance

$$\phi(\tau)=0 \qquad \text{for} \qquad 0>\tau>-\infty \ ,$$

and,

$$\phi(\tau)=\Phi \qquad \text{for} \qquad \infty>\tau>0 \ .$$

Or, in Laplace transform notation,

$$\bar{\phi}=0 \qquad \text{for} \qquad 0>s>-\infty \ ,$$

and,

$$\bar{\phi}=\frac{\Phi}{s} \qquad \text{for} \qquad \infty>s>0 \ .$$

Then the transfer function for step change may be expressed by

$$\bar{F}(s)=\frac{\bar{y}_{step}}{\Phi/s} \ ,$$

and by inverse transformation,

$$y_{step}(\tau)=\frac{\Phi}{2\pi i}\int_{-i\infty}^{i\infty}\frac{\bar{F}(s)}{s}e^{s\tau}ds \tag{25}$$

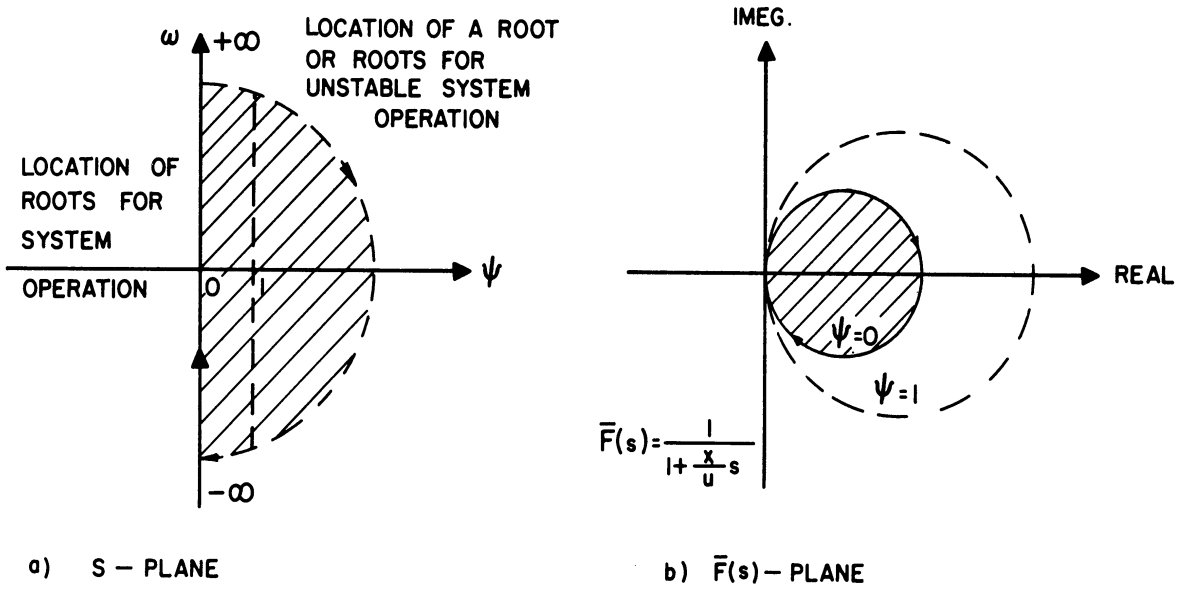

Figure 3. S- and $\bar{F}(s)$- Planes.

Now if $s = i\omega$, then

$$y_{step}(\tau) = \frac{\Phi}{2\pi i}\int_{-i\infty}^{i\infty} \frac{\bar{F}(i\omega)}{i\omega} e^{i\omega\tau} d(i\omega)$$

or

$$\frac{y_{step}(\tau)}{\Phi} = \frac{1}{2\pi i}\int_{-i\infty}^{i\infty} \frac{\bar{F}(i\omega)}{\omega} e^{i\omega\tau} d\omega \qquad (26)$$

Here y_{step}/Φ is the ratio of output to the disturbance of a system subjected to a step change in some input quantity, or disturbance. The function $\bar{F}(i\omega)$ is the transfer function of the system for frequency response. Therefore, Equation (26) represents the relationship between the step-response and the frequency response of the system.*

According to the Fourier theorem, any function, periodic or non-periodic may be resolved into a series of harmonic oscillations, if the function is single-valued and sectionally continuous. Therefore a step function disturbance $\phi(\tau)$ may be resolved into a series of individual harmonic oscillations as follows:

$$\phi(\tau) = \sum_{n=-\infty}^{\infty} \phi_n(\omega_n) e^{i\omega_n\tau} \qquad (27)$$

where $\phi_n(\omega_n)$ is the amplitude of the Fourier oscillation of frequency ω_n.

Here $\phi(\tau) = 0$ for $0 > \tau > -\infty$,

and, $\phi(\tau) = \Phi$ for $\infty > \tau > 0$.

---

* See Reference 22 for its application.

According to the Fourier integral, Equation (27) may be written as

$$\phi(\tau) = \int_{-\infty}^{\infty} \phi_n(\omega_n) e^{i\omega_n \tau} d\omega_n \qquad (28)$$

where

$$\phi_n(\omega_n) = \frac{1}{2\pi} \int_{o}^{\infty} \phi(\tau) e^{-i\omega_n \tau} d\tau$$

Hence, $\phi_n(\omega_n) = 0$ for $0 > \tau > -\infty$,

and $\phi_n(\omega_n) = \frac{\Phi}{2\pi\omega_n i}$ for $\infty > \tau > 0$. (29)

From Equation (29), one obtains the following relationship

$$\frac{2\pi\phi_n(\omega_n) i}{\Phi} = \frac{1}{\omega_n} \qquad (30)$$

Equation (30) is an imaginary quantity which may be interpreted as vector of magnitude $2\pi\phi_n(\omega_n)/\Phi$ and having a constant phase angle of $\pi/2$ for each frequency, ω_n. Equation (30) shows $2\pi\phi_n(\omega_n)i/\Phi$ vs. ω_n* to be a continuous hyperbolic curve. Substituting Equation (29) into Equation (28), one obtains

$$\frac{\phi(\tau)}{\Phi} = \frac{1}{2\pi i} \int_{-i\infty}^{i\infty} \frac{e^{i\omega_n \tau}}{i\omega_n} d(i\omega_n) \qquad (31)$$

The right side of Equation (31) equals to unity**, which satisfies and is consistent with the imposed condition that $\phi(\tau)/\Phi = 1$ for $0 < \tau < \infty$.

---

* Reference 30, page 28, the curve is called frequency spectrum of the step function.

** Reference 30, page 42 to 44.

Differentiating Equation (26) and substituting $\Phi/2\pi\omega i = \phi(\omega)$ obtained from Equation (30) yields,

$$dy_{step}(\tau) = \bar{F}(i\omega)\phi(\omega)e^{i\omega\tau}d\omega \tag{32}$$

Equation (32) shows the relationship between the component disturbance and its corresponding component output. The step response $y_{2_{step}}$ due to the disturbance $\phi(\tau)$ is the Fourier integral of the individual harmonic oscillation expressed by Equation (32).

Equation (26) and (31) show that both the output and its disturbance for a step-response contain all frequencies ranging from $-\infty$ to ∞, although the minus frequencies are physically meaningless. Therefore, it is concluded that since the transfer function completely defines a system, both step- and frequency-response completely characterize the dynamic behavior or the frequency relationships of the system. Furthermore there is only one corresponding step-response for each frequency response and vice versa.

B. Dynamic Behavior at the Transient-Periodic State

The complete solution of the dynamic response of a system with a sinusoidal disturbance must include its dynamic behavior under the transient- as well as the steady-periodic state. In this case $\phi(\tau) = \Phi\sin\omega\tau$ and the transient periodic response may be found by substituting the Laplace transform of $\phi(\tau)$, $\Phi = \Phi/1+s^2$, into Equation (15) and performing the inverse Laplace transformation, as follows,

$$\bar{y}_2 = \bar{F}(s)\frac{\Phi}{s^2+1}$$

$$y_2 = \frac{1}{2\pi i}\int_{\xi-i\infty}^{\xi+i\infty} e^{s\tau}\bar{F}(s)\frac{\Phi}{s^2+1}\,ds \tag{33}$$

where ξ is chosen in the s-plane to lie to the right of any singularity of $\overline{F}(s)\frac{\Phi}{1+s^2}$. The results of this operation of inverse transformation is usually given in most text books or mathematical tables on operational mathematics for various forms of the function $\overline{F}(s)\frac{\Phi}{1+s^2}$. The product of transformed functions may be treated by the method of convolution, that is, a technique of the inverse transformation for product of functions.

CHAPTER III

GENERAL THEORY APPLIED TO THE SINUSOIDAL RESPONSE OF THE HEAT EXCHANGERS WITH ONE FLUID

A. Analysis

The physical system analyzed is shown in Figure 4. This consists of a circular tube through which a coolant flow steadily, and in the solid walls of which energy is generated. In the steady state, all of this energy appears as a flow of heat at the interface between coolant and solid causing the coolant to increase in enthalpy (and temperature) as it flows through the tube. The outside surface of the tube is adiabatic. During the transient, however, both the tube-wall material and the coolant experience local temperature excursions, the magnitude of the former and their difference being evaluated here as a function of distance and time. A circular tube has been selected for convenience in comparison of theory and experiment. Where a non-symmetrical geometry is involved in the analysis, such as a triangular flow cross section, the results may be reduced to an area-to-volume ratio and to a degree of approximation, can be used for other geometry for which the restraints on the solution apply. The solution will be valid as presented for flow inside circular tubes and between parallel plates.

The following assumptions are imposed on the solution:

a. The fluid temperature and velocity are constant across the flow cross section.

b. The duct wall temperature does not depend on radius. Valid for thin-walled metallic systems.

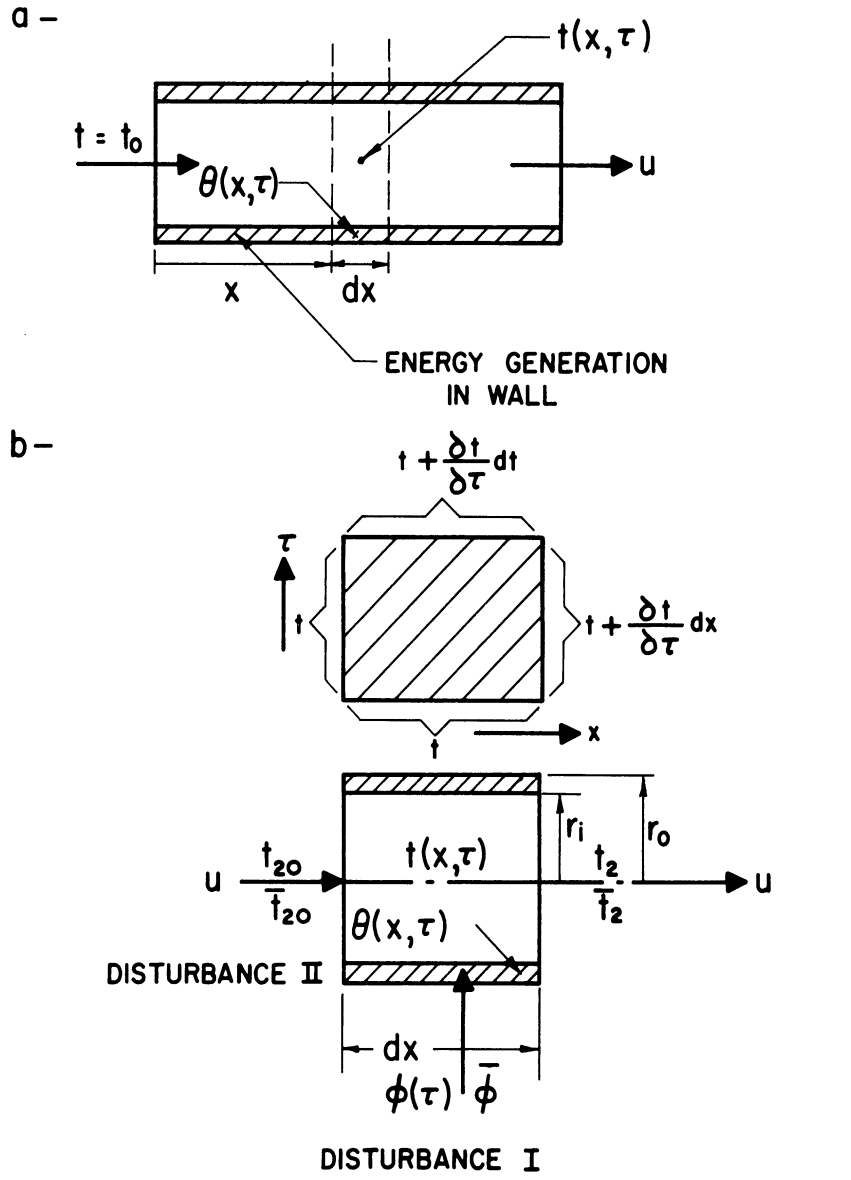

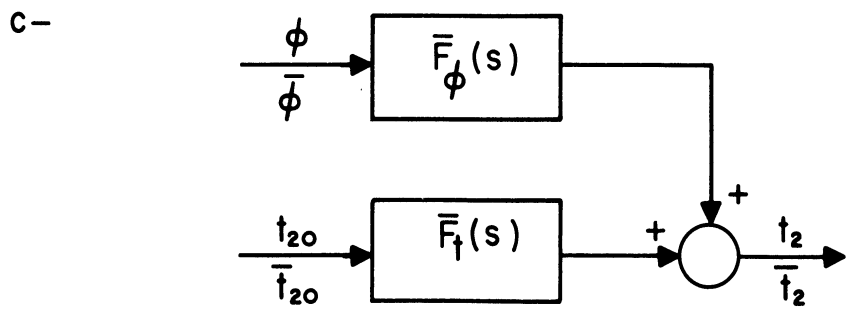

Figure 4. Simulated Coolant Channel.

c. Axial heat conduction is negligible in both fluid and duct walls and heat flows only to the coolant. This is a reasonable assumption when the Peclet number exceeds 100 The outer surface is adiabatic.

d. The heat-transfer coefficient is constant with length and time.

e. The fluid is incompressible and all fluid properties are constant. The flow channel has constant area.

f. Energy (heat) generation within the walls is constant with length but is time-dependent.

g. The temperature of the fluid entering the duct $t_o(\tau)$ is a function of time and equal to $t_o + t_o^*(\tau)$. At the initial steady-state, it is constant and equal to t_o.

With these assumptions, the application of the First Law of Thermodynamics and the law of conservation of mass for an incompressible fluid to the system shown in Figure 4-b produces the following two differential equations, one for the duct wall, the other for the fluid. Details of this derivation are outlined in Appendix A.

Wall

$$-(\theta - t) + a_1 p_x''(\tau) = a_2 \frac{\partial \theta}{\partial \tau} \tag{34}$$

Fluid

$$(\theta - t) = a_3 \frac{\partial t}{\partial \tau} + a_4 \frac{\partial t}{\partial x} \tag{35}$$

For a circular tube and in generalized terms the constants are written:

$$a_1 = \frac{r_o^2 - r_i^2}{2 r_i h} = \frac{1}{(\rho c_p)_w K_w}$$

$$a_2 = \frac{(\rho c_p)_w (r_o^2 - r_i^2)}{2 r_i h} = \frac{1}{K_w}$$

$$a_3 = \frac{\rho c_p r_i}{2h} = \frac{1}{K} \qquad (36)$$

$$a_4 = \frac{\rho c_p r_i u}{2h} = \frac{u}{K}$$

$$p_x''(\tau) = p_{xo}'' + \phi(\tau)$$

where p_{xo}'' is the initial uniform volumetric heat-generation rate and $\phi(\tau)$ is the arbitrary time-variant volumetric heat generation rate function, having a zero value at zero time, which introduces the transient into the system. As shown in Chapter II and Appendix A both functions $\theta(x,\tau)$ and $t(x,\tau)$ may be split into two components one being a steady-state part $\theta_1(x,0)$ and $t_1(x,0)$ the other of the transient component $\theta_2(x,\tau)$ and $t_2(x,\tau)$. The dynamic characteristics of the system is completely governed by the transient component and is free from the initial effect. Therefore it is necessary only to carry out detailed mathematical analysis of the transient components.

Hence the governing differential equations become

Wall:

$$-(\theta_2 - t_2) + \frac{\phi(\tau)}{(\rho c_p)_w K_w} = \frac{1}{K_w}\left(\frac{\partial \theta_2}{\partial \tau}\right) \qquad (37)$$

Fluid:

$$\theta_2 - t_2 = \frac{1}{K}\left(\frac{\partial t_2}{\partial \tau}\right) + \frac{u}{K}\left(\frac{\partial t_2}{\partial x}\right) \qquad (38)$$

Applying the method of Laplace transform to Equations (37) and (38)and solving for $\bar{\theta}_2$ and $\bar{t}_2$ with the appropriate boundary conditions, expressed by Equations (A-21), (A-22) and (A-23), one obtains

$$\bar{t}_2 = \bar{t}_o^* e^{\frac{-s\left(\frac{M}{K^2}s+\frac{M+1}{K}\right)\frac{Kx}{u}}{1+\frac{M}{K}s}} + \bar{\phi}\frac{1}{(\rho c_p)_w K_w s\left(\frac{M}{K^2}s+\frac{M+1}{K}\right)}\left[1-e^{-\frac{s\left(\frac{M}{K^2}s+\frac{M+1}{K}\right)\frac{Kx}{u}}{1+\frac{M}{K}s}}\right] \tag{39}$$

$$\bar{\theta}_2 = \bar{t}_o^*\frac{e^{\frac{-s\left(\frac{M}{K^2}s+\frac{M+1}{K}\right)\frac{Kx}{u}}{1+\frac{M}{K}s}}}{1+\frac{M}{K}s} + \bar{\phi}\frac{1}{(\rho c_p)_w K_w s\left(\frac{M}{K^2}s+\frac{M+1}{K}\right)}\left[1+\frac{s}{K}-\frac{e^{\frac{-s\left(\frac{M}{K^2}s+\frac{M+1}{K}\right)\frac{Kx}{u}}{1+\frac{M}{K}s}}}{1+\frac{M}{K}s}\right] \tag{40}$$

$$\Delta\bar{t}_2 = -\bar{t}_o^*\frac{\frac{M}{K}s\, e^{\frac{-s\left(\frac{M}{K^2}s+\frac{M+1}{K}\right)\frac{Kx}{u}}{1+\frac{M}{K}s}}}{1+\frac{M}{K}s} + \bar{\phi}\frac{1}{(\rho c_p)_w K_w\left(\frac{M}{K^2}s+\frac{M+1}{K}\right)}\left[\frac{1}{K}+\frac{\frac{M}{K}e^{\frac{-s\left(\frac{M}{K^2}s+\frac{M+1}{K}\right)\frac{Kx}{u}}{1+\frac{M}{K}s}}}{1+\frac{M}{K}s^2}\right] \tag{41}$$

$\bar{t}_2$, $\bar{\theta}_2$ and $\Delta\bar{t}_2$ represent the outputs due to two independent disturbances $\bar{t}_o^*$ and $\bar{\phi}$ as shown schematically in Figure 4-c.

B. Frequency Response

If the temperature of the fluid entering the duct is constant and equal to t_o Equations (39), (40), and (41) reduce to

$$\bar{t}_2 = \bar{\phi}\frac{1}{(\rho c_p)_w K_w s\left(\frac{M}{K^2}s+\frac{M+1}{K}\right)}\left[1-e^{-\frac{s\left(\frac{M}{K^2}s+\frac{M+1}{K}\right)\frac{Kx}{u}}{1+\frac{M}{K}s}}\right] \tag{42}$$

$$\bar{\theta}_2 = \bar{\phi} \frac{1}{(\rho c_p)_w K_w S\left(\frac{M}{K^2}S + \frac{M+1}{K}\right)} \left[1 + \frac{S}{K} - \frac{e^{\frac{-S\left(\frac{M}{K^2}S + \frac{M+1}{K}\right)\frac{Kx}{u}}{1+\frac{M}{K}S}}}{1+\frac{M}{K}S} \right] \tag{43}$$

$$\Delta\bar{t}_2 = \bar{\phi} \frac{1}{(\rho c_p)_w K_w \left(\frac{M}{K^2}S + \frac{M+1}{K}\right)} \left[\frac{1}{K} + \frac{\frac{M}{K} e^{\frac{-S\left(\frac{M}{K^2}S + \frac{M+1}{K}\right)\frac{Kx}{u}}{1+\frac{M}{K}S}}}{1+\frac{M}{K}S} \right] \tag{44}$$

or

$$\frac{\bar{t}_2}{\frac{\bar{\phi}}{(\rho c_p)_w K_w}\frac{Kx}{u}} = \frac{1}{S\frac{Kx}{u}\left(\frac{M}{K^2}S + \frac{M+1}{K}\right)} \left[1 - e^{\frac{-S\left(\frac{M}{K^2}S + \frac{M+1}{K}\right)\frac{Kx}{u}}{1+\frac{M}{K}S}} \right] \tag{45}$$

$$\frac{\bar{\theta}_2}{\frac{\bar{\phi}}{(\rho c_p)_w K_w}\frac{Kx}{u}} = \frac{1}{S\left(1+\frac{Kx}{u}\right)\left(\frac{M}{K^2}S + \frac{M+1}{K}\right)} \left[1 + \frac{S}{K} - \frac{e^{\frac{-S\left(\frac{M}{K^2}S + \frac{M+1}{K}\right)\frac{Kx}{u}}{1+\frac{M}{K}S}}}{1+\frac{M}{K}S} \right] \tag{46}$$

$$\frac{\Delta\bar{t}_2}{\frac{\bar{\phi}}{(\rho c_p)_w K_w}\frac{Kx}{u}} = \frac{1}{\left(\frac{M}{K^2}S + \frac{M+1}{K}\right)} \left[\frac{1}{K} + \frac{\frac{M}{K} e^{\frac{-S\left(\frac{M}{K^2}S + \frac{M+1}{K}\right)\frac{Kx}{u}}{1+\frac{M}{K}S}}}{1+\frac{M}{K}S} \right] \tag{47}$$

since

$$\frac{\phi(\tau)\frac{Kx}{u}}{(\rho c_p)_w K_w} = \frac{\Phi\frac{Kx}{u}}{(\rho c_p)_w K_w} \sin\omega\tau = \frac{\Delta(q/A)}{h}\frac{Kx}{u}\sin\omega\tau \quad , \tag{48}$$

and

$$t_2(x,\tau)=\left[T_\infty(x)\right]_{\omega=\omega}\sin(\omega\tau-\alpha_t) \tag{49}$$

are in the forms of Equations (16) and (17) respectively, according to Equation (21), one can express the amplitude-ratio response of the fluid temperature as

$$\left|\bar{F}_t(i\omega)\right|=\frac{\left[T_\infty(x)\right]_{\omega=\omega}}{\frac{\Delta(q/A)}{h}\frac{Kx}{u}} \tag{50}$$

But

$$\frac{\Delta(q/A)}{h}\frac{Kx}{u}=t_1^*(x,\tau)-t_1(x,0)=\left[T_\infty(x)\right]_{\omega=0} \tag{51}$$

where $t_1^*(x,\tau)$ is the steady-state fluid temperature at x for $p_x'' = p_{xo}'' + \Phi$, or the maximum fluid temperature corresponding to $\omega = 0$, hence

$$\left|\bar{F}_t(i\omega)\right|=\frac{\left[T_\infty(x)\right]_{\omega=\omega}}{\left[T_\infty(x)\right]_{\omega=0}} \tag{52}$$

Similarly, one obtains the following relationships for the wall temperature and the fluid-wall temperature difference.

$$\left|\bar{F}_\theta(i\omega)\right|=\frac{\left[\Theta_\infty(x)\right]_{\omega=\omega}}{\frac{\Phi(1+\frac{Kx}{u})}{(\rho c_p)_w K_w}}=\frac{\left[\Theta_\infty(x)\right]_{\omega=\omega}}{\frac{\Delta(q/A)}{h}(1+\frac{Kx}{u})}=\frac{\left[\Theta_\infty(x)\right]_{\omega=\omega}}{\left[\Theta_\infty(x)\right]_{\omega=0}} \tag{53}$$

$$\left|\bar{F}_{\Delta t}(i\omega)\right|=\frac{\left[\Delta T_\infty(x)\right]_{\omega=\omega}}{\frac{\Phi}{(\rho c_p)_w K_w}}=\frac{\left[\Delta T_\infty(x)\right]_{\omega=\omega}}{\frac{\Delta(q/A)}{h}}=\frac{\left[\Delta T_\infty(x)\right]_{\omega=\omega}}{\left[\Delta T_\infty(x)\right]_{\omega=0}} \tag{54}$$

For fluid temperature.

$$|F_t(i\omega)| = \frac{[T_\infty(x)]_{\omega=\omega}}{[T_\infty(x)]_{\omega=0}} = \frac{\sqrt{1+\left(\frac{M+1}{M\omega}\right)^2}}{\frac{KX}{U}\left[1+\left(\frac{M\omega}{K}\right)^2\right]e^{\delta\frac{(M+1)^2}{M}}}\left\{\left[-\frac{e^{\delta}}{\sqrt{1+\left(\frac{M+1}{M\omega}\right)^2}}+\sin\left(\gamma+\tan^{-1}\frac{M\omega}{K}\right)\right]^2\right.$$

$$\left.+\left[-\frac{e^{\delta}}{\sqrt{1+\left(\frac{M\omega}{K}\right)^2}}+\cos\left(\gamma+\tan^{-1}\frac{M\omega}{K}\right)\right]^2\right\}^{1/2} \qquad (55)$$

$$\alpha_t = \tan^{-1}\left\{\frac{\frac{e^{\delta}}{\sqrt{1+\left(\frac{M\omega}{K}\right)^2}}-\cos\left[\gamma+\tan^{-1}\left(\frac{M\omega}{K}\right)\right]}{-\frac{e^{\delta}}{\sqrt{1+\left(\frac{M+1}{M\omega}\right)^2}}+\sin\left[\gamma+\tan^{-1}\left(\frac{M\omega}{K}\right)\right]}\right\} \qquad (56)$$

For wall temperature

$$|F_\theta(i\omega)| = \frac{[\theta_\infty(x)]_{\omega=\omega}}{[\theta_\infty(x)]_{\omega=0}} = \frac{\sqrt{\left(\frac{M+1}{M\omega}-\frac{M\omega}{K}\right)^2+(M+2)^2}}{\left[1+\left(\frac{M+1}{M\omega}\right)^2\right]\frac{1}{M}\left(\frac{M\omega}{K}\right)^2\left(1+\frac{KX}{U}\right)\left[1+\left(\frac{M\omega}{K}\right)^2\right]e^{\delta}}\left\{\left[\frac{\frac{1}{M}e^{\delta}\left[1+\left(\frac{M\omega}{K}\right)^2\right]}{\sqrt{\left[\left(\frac{M+1}{M\omega}\right)-\frac{M\omega}{K}\right]^2+(M+2)^2}}+\sin\left(\gamma+\tan^{-1}\frac{M+2}{\frac{M+1}{M\omega}-\frac{M\omega}{K}}\right)\right]^2\right.$$

$$\left.+\left[-\frac{\left(\frac{M+1}{M\omega}+\frac{1}{M}\frac{M\omega}{K}\right)e^{\delta}\left[1+\left(\frac{M\omega}{K}\right)^2\right]}{\sqrt{\left[\left(\frac{M+1}{M\omega}\right)-\frac{M\omega}{K}\right]^2+(M+2)^2}}+\cos\left(\gamma+\tan^{-1}\frac{M+2}{\frac{M+1}{M\omega}-\frac{M\omega}{K}}\right)\right]^2\right\}^{1/2} \qquad (57)$$

$$\alpha_\theta = \tan^{-1}\left\{\frac{\frac{\left(\frac{M+1}{M\omega}+\frac{1}{M}\frac{M\omega}{K}\right)e^{\delta}\left[1+\left(\frac{M\omega}{K}\right)^2\right]}{\sqrt{\left(\frac{M+1}{M\omega}-\frac{M\omega}{K}\right)^2+(M+2)^2}}-\cos\left(\gamma+\tan^{-1}\frac{M+2}{\frac{M+1}{M\omega}-\frac{M\omega}{K}}\right)}{\frac{\frac{1}{M}e^{\delta}\left[1+\left(\frac{M\omega}{K}\right)^2\right]}{\sqrt{\left(\frac{M+1}{M\omega}-\frac{M\omega}{K}\right)^2+(M+2)^2}}+\sin\left(\gamma+\tan^{-1}\frac{M+2}{\frac{M+1}{M\omega}-\frac{M\omega}{K}}\right)}\right\} \qquad (58)$$

For fluid-wall temperature difference

$$\left|\bar{F}_{\Delta t}(i\omega)\right| = \frac{\left[\Delta T_{\infty}(x)\right]_{\omega=\omega}}{\left[\Delta T_{\infty}(x)\right]_{\omega=0}} = \frac{\sqrt{\left(-\frac{M+1}{M\omega}+\frac{M\omega}{K}\right)^2+(M+2)^2}}{\frac{1}{M}\left(\frac{M\omega}{K}\right)\left[1+\left(\frac{M+1}{M\omega}\right)^2\right]\left[1+\left(\frac{M\omega}{K}\right)^2\right]e^{\delta}} \left\{\left[\frac{\frac{M+1}{M\omega}\left(1+\left(\frac{M\omega}{K}\right)^2\right)e^{\delta}\frac{1}{M}}{\sqrt{\left(-\frac{M+1}{M\omega}+\frac{M\omega}{K}\right)^2+(M+2)^2}}\right.\right.$$

$$\left.\left.-\sin\left[\gamma+\tan^{-1}\frac{-\frac{M+1}{M\omega}+\frac{M\omega}{K}}{M+2}\right]\right]^2+\left[\frac{\frac{1}{M}\left[1+\left(\frac{M\omega}{K}\right)^2\right]e^{\delta}}{\sqrt{\left(-\frac{M+1}{M\omega}+\frac{M\omega}{K}\right)^2+(M+2)^2}}+\cos\left[\gamma+\tan^{-1}\frac{-\frac{M+1}{M\omega}+\frac{M\omega}{K}}{M+2}\right]\right]^2\right\}^{1/2} \quad (59)$$

$$\alpha_{\Delta t} = \tan^{-1}\left\{\frac{\frac{\frac{1}{M}\left[1+\left(\frac{M\omega}{K}\right)^2\right]e^{\delta}}{\sqrt{\left(-\frac{M+1}{M\omega}+\frac{M\omega}{K}\right)^2+(M+2)^2}}+\cos\left[\gamma+\tan^{-1}\frac{-\frac{M+1}{M\omega}+\frac{M\omega}{K}}{M+2}\right]}{\frac{\frac{M+1}{M\omega}\left[1+\left(\frac{M\omega}{K}\right)^2\right]e^{\delta}\frac{1}{M}}{\sqrt{\left(-\frac{M+1}{M\omega}+\frac{M\omega}{K}\right)^2+(M+2)^2}}-\sin\left[\gamma+\tan^{-1}\frac{-\frac{M+1}{M\omega}+\frac{M\omega}{K}}{M+2}\right]}\right\} \quad (60)$$

Here δ and γ are defined in Equations (C-15) and (C-16), Appendix C.

Temperatures at the transient-periodic state will decay after some time and only the steady-state temperatures remain. Temperatures and fluid-wall temperature difference at the steady-periodic state are represented by the following equations:

$$t_{2\infty}(x,\tau) = \left|\bar{F}_t(i\omega)\right|\left[T_{\infty}(x)\right]_{\omega=0}\sin(\omega\tau-\alpha_t) \quad (61)$$

$$\theta_{2\infty}(x,\tau) = \left|\bar{F}_{\theta}(i\omega)\right|\left[\theta_{\infty}(x)\right]_{\omega=0}\sin(\omega\tau-\alpha_{\theta}) \quad (62)$$

$$\Delta t_{2\infty}(x,\tau) = \left|\bar{F}_{\Delta t}(i\omega)\right|\left[\Delta T_{\infty}(x)\right]_{\omega=0}\sin(\omega\tau-\alpha_{\Delta t}) \quad (63)$$

The significance of these results and their comparison with experiment is discussed later in section D.

C. Response in Transient-Periodic State

The complete solutions for t_2, θ_2 and Δt_2 may be obtained by performing the inverse transformation on Equation (42), (43), and (44). It must be noted that $\theta(x,\tau) - \theta(x,0)$ and $t(x,\tau) - t(x,0)$ are identical with $\theta_2(x,\tau)$ and $t_2(x,\tau)$ since $\theta(x,0) = \theta_1(x,0)$ and $t(x,0) = t_1(x,0)$.

The nature of the mathematical attack on this problem produces solutions for $\theta_2(x,\tau)$, $t_2(x,\tau)$ and $\Delta t_2(x,\tau)$ in two domains of physical time:

Case 1. A physical time following the introduction of the transient which is greater than zero but equal to or less than x/u

Case 2. A physical time τ is greater than x/u.

Case 1 $\quad 1 \geq \tau u/x \geq 0$

Wall temperature

$$\frac{\theta(x,\tau)-\theta(x,0)}{\frac{\Delta(q/A)}{h}\left(1+\frac{Kx}{u}\right)} = \frac{M}{(M+1)\frac{M\omega}{K}\left(1+\frac{Kx}{u}\right)}\left\{1+\frac{\frac{1}{M}e^{-(M+1)\frac{K\tau}{M}}}{1+\left(\frac{M+1}{M\omega}{K}\right)^2}\right.$$

$$\left.+\frac{\sqrt{\left[\frac{1}{M}\left(\frac{M+1}{M\omega}{K}\right)^2\right]+\left[1+\frac{1}{M}+\left(\frac{M+1}{M\omega}{K}\right)^2\right]^2}}{1+\left(\frac{M+1}{M\omega}{K}\right)^2}\sin\left[\omega\tau-\tan^{-1}\left[\frac{1+\frac{1}{M}+\left(\frac{M+1}{M\omega}{K}\right)^2}{\frac{1}{M}\left(\frac{M+1}{M\omega}{K}\right)}\right]\right]\right\} \qquad (64)$$

Fluid-wall temperature difference

$$\frac{\Delta t(x,\tau)-\Delta t(x,0)}{\frac{\Delta(q/A)}{h}} = \frac{\frac{1}{M\omega}{K}}{1+\left(\frac{M+1}{M\omega}{K}\right)^2}\left\{e^{-(M+1)\frac{K\tau}{M}}+\sqrt{1+\left(\frac{M+1}{M\omega}{K}\right)^2}\sin\left[\omega\tau-\tan^{-1}\frac{\frac{M\omega}{K}}{M+1}\right]\right\} \qquad (65)$$

Fluid temperature

$$\frac{t(x,\tau)-t(x,0)}{\frac{\Delta(q/A)}{h}\frac{Kx}{u}}=\frac{\frac{M}{\frac{M\omega}{K}}}{\frac{Kx}{u}(M+1)}\left\{1-\frac{e^{\frac{-(M+1)K\tau}{M}}}{1+\left(\frac{M+1}{\frac{M\omega}{K}}\right)^2}+\frac{\frac{M+1}{\frac{M\omega}{K}}\sqrt{1+\left(\frac{M+1}{\frac{M\omega}{K}}\right)^2}}{1+\left(\frac{M+1}{\frac{M\omega}{K}}\right)^2}\sin\left[\omega\tau-\tan^{-1}\left(-\frac{M+1}{\frac{M\omega}{K}}\right)\right]\right\} \tag{66}$$

Case 2 $\tau u/x \geq 1$

Wall temperature

$$\frac{\Theta(x,\tau)-\Theta(x,0)}{\frac{\Delta(q/A)}{h}\left(1+\frac{Kx}{u}\right)}=\frac{M}{(M+1)\frac{M\omega}{K}\left(1+\frac{Kx}{u}\right)}\left\{1+\frac{\frac{1}{M}e^{\frac{-(M+1)K\tau}{M}}}{1+\left(\frac{M+1}{\frac{M\omega}{K}}\right)^2}-e^{-\frac{Kx}{u}}\left[\psi_2^{**}\left(\frac{Kx}{u},\frac{K\tau^*}{M}\right)\right.\right.$$

$$\left.\left.-\frac{\frac{1}{M}e^{\frac{-(M+1)K\tau^*}{M}}}{1+\left(\frac{M+1}{\frac{M\omega}{K}}\right)^2}\psi_4\left[\frac{1}{M}\left(\frac{Kx}{u}\right),M\left(\frac{K\tau^*}{M}\right)\right]\right]+\sqrt{A_\theta^2+B_\theta^2}\sin\left[\omega\tau^*-\tan^{-1}\left(-\frac{B_\theta}{A_\theta}\right)\right]\right\} \tag{67}$$

$$A_\theta=\sin\frac{\omega x}{u}+\frac{\frac{1}{M}}{1+\left(\frac{M+1}{\frac{M\omega}{K}}\right)^2}\left(\frac{M+1}{\frac{M\omega}{K}}\cos\frac{\omega x}{u}+\sin\frac{\omega x}{u}\right)$$

$$+\frac{e^{-\frac{Kx}{u}\left(\frac{M+1}{\frac{M\omega}{K}}\right)}}{1+\left(\frac{M+1}{\frac{M\omega}{K}}\right)^2}\left[\frac{M+1}{\frac{M\omega}{K}}\psi_8\left(\frac{Kx}{u},\frac{K\tau^*}{M},\frac{M\omega}{K}\right)+\psi_7\left(\frac{Kx}{u},\frac{K\tau^*}{M},\frac{M\omega}{K}\right)\right] \tag{68}$$

$$B_\theta=-\cos\frac{\omega x}{u}+\frac{\frac{1}{M}}{1+\left(\frac{M+1}{\frac{M\omega}{K}}\right)^2}\left(\frac{M+1}{\frac{M\omega}{K}}\sin\frac{\omega x}{u}-\cos\frac{\omega x}{u}\right)$$

$$+\frac{e^{-\frac{Kx}{u}\left(\frac{M+1}{\frac{M\omega}{K}}\right)}}{1+\left(\frac{M+1}{\frac{M\omega}{K}}\right)^2}\left[\frac{M+1}{\frac{M\omega}{K}}\psi_7\left(\frac{Kx}{u},\frac{K\tau^*}{M},\frac{M\omega}{K}\right)-\psi_8\left(\frac{Kx}{u},\frac{K\tau^*}{M},\frac{M\omega}{K}\right)\right] \tag{69}$$

Fluid-wall temperature difference

$$\frac{\Delta t(x,\tau)-\Delta t(x,0)}{\frac{\Delta(q/A)}{h}} = \frac{\frac{M}{\frac{Mw}{K}}}{1+\left(\frac{M+1}{\frac{Mw}{K}}\right)^2}\left\{\left[e^{-(M+1)\frac{K\tau}{M}} + \frac{e^{-\frac{Kx}{u}}e^{-(M+1)\frac{K\tau^*}{M}}}{M}\right]\psi_4\left[\frac{1}{M}\left(\frac{Kx}{u}\right), M\left(\frac{K\tau^*}{M}\right)\right]\right.$$

$$\left. + \sqrt{A_{\Delta t}^2 + B_{\Delta t}^2}\,\sin\left[\omega\tau^* - \tan^{-1}\left(-\frac{B_{\Delta t}}{A_{\Delta t}}\right)\right]\right\} \tag{70}$$

$$A_{\Delta t} = \frac{M+1}{\frac{Mw}{K}}\cos\frac{\omega x}{u} + \sin\frac{\omega x}{u} + e^{-\frac{Kx}{u}}\left[\frac{M+1}{\frac{Mw}{K}}\psi_7\left(\frac{Kx}{u}, \frac{K\tau^*}{M}, \frac{Mw}{K}\right)\right.$$

$$\left. - \psi_8\left(\frac{Kx}{u}, \frac{K\tau^*}{M}, \frac{Mw}{K}\right)\right] \tag{71}$$

$$B_{\Delta t} = \frac{M+1}{\frac{Mw}{K}}\sin\frac{\omega x}{u} - \cos\frac{\omega x}{u} + e^{-\frac{Kx}{u}}\left[-\psi_7\left(\frac{Kx}{u}, \frac{K\tau^*}{M}, \frac{Mw}{K}\right)\right.$$

$$\left. - \frac{M+1}{\frac{Mw}{K}}\psi_8\left(\frac{Kx}{u}, \frac{K\tau^*}{M}, \frac{Mw}{K}\right)\right] \tag{72}$$

Fluid temperature

$$\frac{t(x,\tau)-t(x,0)}{\frac{\Delta(q/A)}{h}\frac{Kx}{u}} = \frac{\frac{M}{\frac{Mw}{K}}}{\frac{Kx}{u}(M+1)}\left\{1 - \frac{e^{-(M+1)\frac{K\tau}{M}}}{1+\left(\frac{M+1}{\frac{Mw}{K}}\right)^2} + e^{-\frac{Kx}{u}}\left[-\psi_2^{**}\left(\frac{Kx}{u}, \frac{K\tau^*}{M}\right)\right.\right.$$

$$\left.\left. - \frac{e^{-(M+1)\frac{K\tau^*}{M}}}{1+\left(\frac{M+1}{\frac{Mw}{K}}\right)^2}\psi_4\left[\frac{1}{M}\left(\frac{Kx}{u}\right), M\left(\frac{K\tau^*}{M}\right)\right] + \sqrt{A_t^2+B_t^2}\,\sin\left[\omega\tau^* - \tan\left(-\frac{B_t}{A_t}\right)\right]\right\} \tag{73}$$

$$A_t = \sin\frac{\omega x}{u} - \frac{1}{1+\left(\frac{M+1}{\frac{Mw}{K}}\right)^2}\left(\frac{M+1}{\frac{Mw}{K}}\cos\frac{\omega x}{u} + \sin\frac{\omega x}{u}\right) + \frac{e^{-\frac{Kx}{u}}}{1+\left(\frac{M+1}{\frac{Mw}{K}}\right)^2}\left[\left[\frac{M+1}{\frac{Mw}{K}}\right)^2 + M + 1\right]\psi_8\left(\frac{Kx}{u}, \frac{K\tau^*}{M}, \frac{Mw}{K}\right)$$

$$\left. - \frac{1}{M}\left(\frac{M+1}{\frac{Mw}{K}}\right)\psi_7\left(\frac{Kx}{u}, \frac{K\tau^*}{M}, \frac{Mw}{K}\right)\right\} \tag{74}$$

$$B_t = -\cos\frac{\omega x}{u} - \frac{1}{1+\left(\frac{M+1}{M\omega}K\right)^2}\left(\frac{M+1}{M\omega}K\sin\frac{\omega x}{u} - \cos\frac{\omega x}{u}\right) + \frac{e^{-\frac{Kx}{u}}}{1+\left(\frac{M+1}{M\omega}K\right)^2}\left\{\left[\left(\frac{M+1}{M\omega}K\right)^2 + M + 1\right]\right.$$

$$\left. \cdot\, \psi_7\left(\frac{Kx}{u}, \frac{K\tau^*}{M}, \frac{M\omega}{K}\right) + \frac{1}{M}\left(\frac{M+1}{M\omega}K\right)\psi_8\left(\frac{Kx}{u}, \frac{K\tau^*}{M}, \frac{M\omega}{K}\right)\right\} \qquad (75)$$

where, A_θ, B_θ, A_t, B_t, $A_{\Delta t}$ and $B_{\Delta t}$ are defined in Equations (68), (69), (71), (72), (74) and (75).

The envelopes formed by the points of the maximum amplitudes of the temperatures and temperature difference may be obtained by substituting sines equal to ± 1.0 into Equations (64), (65), (66), (67), (70) and (73). Let Θ_+, T_+ and ΔT_+ be the upper envelope and Θ_-, T_- and ΔT_- lower envelope amplitudes. The equations obtained by substituting sine = +1.0 give the upper envelope of the amplitudes while sine = -1.0 give their lower envelopes. With these definitions and substitutions, the following equations for these envelopes are obtained.

Case 1 $1 \geq \tau u/x \geq 0$

Wall temperature

$$\frac{[\Theta(x,\tau)]_{+,-}}{\frac{\Delta(q/A)}{h}\left(1+\frac{Kx}{u}\right)} = \frac{M}{(M+1)\frac{M\omega}{K}\left(1+\frac{Kx}{u}\right)}\left\{1 + \frac{\frac{1}{M}e^{-(M+1)\frac{K\tau}{M}}}{1+\left(\frac{M+1}{M\omega}K\right)^2} \pm \frac{\sqrt{\left[\frac{1}{M}\left(\frac{M+1}{M\omega}K\right)\right]^2 + \left[1+\frac{1}{M}+\left(\frac{M+1}{M\omega}K\right)^2\right]^2}}{1+\left(\frac{M+1}{M\omega}K\right)^2}\right\}$$

(76)

Fluid-wall temperature difference

$$\frac{[\Delta T(x,\tau)]_{+,-}}{\frac{\Delta(q/A)}{h}} = \frac{\frac{M}{M\omega/K}}{1+\left(\frac{M+1}{M\omega/K}\right)^2}\left\{ e^{-\frac{(M+1)K\tau}{M}} \pm \sqrt{1+\left(\frac{M+1}{M\omega/K}\right)^2} \right\} \tag{77}$$

Fluid temperature

$$\frac{[T(x,\tau)]_{+,-}}{\frac{\Delta(q/A)}{h}\frac{Kx}{u}} = \frac{\frac{M}{M\omega/K}}{\frac{Kx}{u}(M+1)}\left\{ 1 - \frac{e^{-\frac{(M+1)K\tau}{M}}}{1+\left(\frac{M+1}{M\omega/K}\right)^2} \pm \frac{\frac{M+1}{M\omega/K}\sqrt{1+\left(\frac{M+1}{M\omega/K}\right)^2}}{1+\left(\frac{M+1}{M\omega/K}\right)^2} \right\} \tag{78}$$

Case 2 $\tau u/x \geq 1$

Wall temperature

$$\frac{[\Theta(x,\tau)]_{+,-}}{\frac{\Delta(q/A)}{h}\left(1+\frac{Kx}{u}\right)} = \frac{M}{(M+1)\frac{M\omega}{K}\left(1+\frac{Kx}{u}\right)}\left\{ 1 + \frac{\frac{1}{M}e^{-\frac{(M+1)K\tau}{M}}}{1+\left(\frac{M+1}{M\omega/K}\right)^2} - e^{-\frac{Kx}{u}}\left\| \psi_2^{**}\left(\frac{Kx}{u},\frac{K\tau^*}{M}\right) \right.\right.$$

$$\left.\left. - \frac{\frac{1}{M}e^{-\frac{(M+1)K\tau^*}{M}}}{1+\left(\frac{M+1}{M\omega/K}\right)^2} I_4\left[\frac{1}{M}\left(\frac{Kx}{u}\right), M\left(\frac{K\tau^*}{M}\right)\right] \right\| \pm \sqrt{A_\theta^2 + B_\theta^2} \right\} \tag{79}$$

Fluid-wall temperature difference

$$\frac{[\Delta T(x,\tau)]_{+,-}}{\frac{\Delta(q/A)}{h}} = \frac{\frac{M}{M\omega/K}}{1+\left(\frac{M+1}{M\omega/K}\right)^2}\left\{ \left\| e^{-\frac{(M+1)K\tau}{M}} + \frac{e^{-\frac{Kx}{u}}e^{-\frac{(M+1)K\tau^*}{M}}}{M} I_4\left[\frac{1}{M}\left(\frac{Kx}{u}\right), M\left(\frac{K\tau^*}{M}\right)\right] \right\| \pm \sqrt{A_{4t}^2 + B_{4t}^2} \right\} \tag{80}$$

Fluid-temperature

$$\frac{[T(x,\tau)]_{+,-}}{\frac{\Delta(q/A)}{h}\frac{Kx}{u}} = \frac{\frac{M}{\frac{Mw}{K}}}{\frac{Kx}{u}(M+1)}\left\{1-\frac{e^{-(M+1)\frac{K\tau}{M}}}{1+\left(\frac{M+1}{\frac{Mw}{K}}\right)^2}+e^{-\frac{Kx}{u}}\left[-\psi_2^{**}\left(\frac{Kx}{u},\frac{K\tau^*}{M}\right)\right.\right.$$
$$\left.\left.-\frac{e^{-(M+1)\frac{K\tau^*}{M}}}{1+\left(\frac{M+1}{\frac{Mw}{K}}\right)^2}\psi_4\left[\frac{1}{M}\left(\frac{Kx}{u}\right),M\left(\frac{K\tau^*}{M}\right)\right]\right]\pm\sqrt{A_t^2+B_t^2}\right\} \qquad (81)$$

After the transient-periodic state has vanished, the steady-periodic oscillations of the temperatures will be observed. The envelope will be symmetric about the abscissca (time axis) and has a magnitude expressed by Θ_∞, ΔT_∞ and T_∞. These may be expressed by the following equations obtained from Equations (79), (80) and (81) by substituting $\tau = \infty$ and $\tau^* = \infty$.

Wall temperature

$$\frac{[\Theta_\infty(x)]_{+,-}}{\frac{\Delta(q/A)}{h}\left(1+\frac{Kx}{u}\right)} = \pm\frac{M\sqrt{A_{\theta\infty}^2+B_{\theta\infty}^2}}{(M+1)\frac{Mw}{K}\left(1+\frac{Kx}{u}\right)} \qquad (82)$$

Fluid-wall temperature difference

$$\frac{[\Delta T_\infty(x)]_{+,-}}{\frac{\Delta(q/A)}{h}} = \pm\frac{\frac{M}{\frac{Mw}{K}}\sqrt{A_{\Delta t\infty}^2+B_{\Delta t\infty}^2}}{1+\left(\frac{M+1}{\frac{Mw}{K}}\right)^2} \qquad (83)$$

Fluid temperature

$$\frac{[T_\infty(x)]_{+,-}}{\frac{\Delta(q/A)}{h}\frac{Kx}{u}} = \pm\frac{\frac{M}{\frac{Mw}{K}}\sqrt{A_{t\infty}^2+B_{t\infty}^2}}{\frac{Kx}{u}(M+1)} \qquad (84)$$

Equations (82), (83) and (84) also represent the frequency response (amplitude-ratio) of the fluid and wall temperatures and the fluid-wall temperature difference. They are identical with those previously obtained by using $|\overline{F}(i\omega)|$. The corresponding phase-shift may be obtained from Equations (67), (70) and (73) [or from Equations (E-24), (E-27), and (E-30)] as follows:

Wall temperature

$$\alpha_\theta = \frac{\omega x}{u} + \tan^{-1}\left(-\frac{B_{\theta\infty}}{A_{\theta\infty}}\right) \tag{85}$$

Fluid-wall temperature difference

$$\alpha_{\Delta t} = \frac{\omega x}{u} + \tan^{-1}\left(-\frac{B_{\Delta t\infty}}{A_{\Delta t\infty}}\right) \tag{86}$$

Fluid temperature

$$\alpha_t = \frac{\omega x}{u} + \tan^{-1}\left(-\frac{B_{t\infty}}{A_{t\infty}}\right) \tag{87}$$

$A_{\theta\infty}$, $B_{\theta\infty}$, $A_{\Delta t\infty}$, $B_{\Delta t\infty}$, $A_{t\infty}$ and $B_{t\infty}$ may be obtained from Equations (68), (69), (71), (72), (74) and (75) by substituting $\tau^* = \infty$, or directly from Equations (E-25), (E-26), (E-28), (E-29), (E-31) and (E-32) as follows:

$$A_{\theta\infty} = \sin\frac{\omega x}{u} + \frac{\frac{1}{M}}{1+\left(\frac{M+1}{M\omega}\right)^2}\left(\frac{M+1}{M\omega}\cos\frac{\omega x}{u} + \sin\frac{\omega x}{u}\right)$$

$$+ \frac{e^{-\frac{Kx}{u}\left(\frac{M+1}{M\omega}\right)}}{1+\left(\frac{M+1}{M\omega}\right)^2}\left[\frac{M+1}{M\omega}\psi_8\left(\frac{Kx}{u}, \infty, \frac{M\omega}{K}\right) + \psi_7\left(\frac{Kx}{u}, \infty, \frac{M\omega}{K}\right)\right] \tag{88}$$

$$B_{\theta_\infty} = -\cos\frac{\omega x}{u} + \frac{1}{M}\frac{1}{1+\left(\frac{M+1}{M\omega}\right)^2}\left(\frac{M+1}{M\omega}\sin\frac{\omega x}{u} - \cos\frac{\omega x}{u}\right)$$

$$+ \frac{e^{-\frac{Kx}{u}\left(\frac{M+1}{M\omega}\right)}}{1+\left(\frac{M+1}{M\omega}\right)^2}\left[\frac{M+1}{M\omega}\psi_7\left(\frac{Kx}{u},\infty,\frac{M\omega}{K}\right) - \psi_8\left(\frac{Kx}{u},\infty,\frac{M\omega}{K}\right)\right] \qquad (89)$$

$$A_{\Delta t_\infty} = \frac{M+1}{M\omega}\cos\frac{\omega x}{u} + \sin\frac{\omega x}{u} + e^{-\frac{Kx}{u}}\left[\frac{M+1}{M\omega}\psi_7\left(\frac{Kx}{u},\infty,\frac{M\omega}{K}\right)\right.$$

$$\left. - \psi_8\left(\frac{Kx}{u},\infty,\frac{M\omega}{K}\right)\right] \qquad (90)$$

$$B_{\Delta t_\infty} = \frac{M+1}{M\omega}\sin\frac{\omega x}{u} - \cos\frac{\omega x}{u} + e^{-\frac{Kx}{u}}\left[-\psi_7\left(\frac{Kx}{u},\infty,\frac{M\omega}{K}\right) - \frac{M+1}{M\omega}\psi_8\left(\frac{Kx}{u},\infty,\frac{M\omega}{K}\right)\right] \qquad (91)$$

$$A_{t_\infty} = \sin\frac{\omega x}{u} - \frac{1}{1+\left(\frac{M+1}{M\omega}\right)^2}\left(\frac{M+1}{M\omega}\cos\frac{\omega x}{u} + \sin\frac{\omega x}{u}\right) + \frac{e^{-\frac{Kx}{u}}}{1+\left(\frac{M+1}{M\omega}\right)^2}\left\{\left[\left(\frac{M+1}{M\omega}\right)^2 + M + 1\right]\right.$$

$$\left. \cdot\,\psi_8\left(\frac{Kx}{u},\infty,\frac{M\omega}{K}\right) - \frac{1}{M}\left(\frac{M+1}{M\omega}\right)\psi_7\left(\frac{Kx}{u},\infty,\frac{M\omega}{K}\right)\right\} \qquad (92)$$

$$B_{t_\infty} = -\cos\frac{\omega x}{u} - \frac{1}{1+\left(\frac{M+1}{M\omega}\right)^2}\left(\frac{M+1}{M\omega}\sin\frac{\omega x}{u} - \cos\frac{\omega x}{u}\right) + \frac{e^{-\frac{Kx}{u}}}{1+\left(\frac{M+1}{M\omega}\right)^2}\left\{\left[\left(\frac{M+1}{M\omega}\right)^2 + M + 1\right]\right.$$

$$\left. \cdot\,\psi_7\left(\frac{Kx}{u},\infty,\frac{M\omega}{K}\right) + \frac{1}{M}\left(\frac{M+1}{M\omega}\right)\psi_8\left(\frac{Kx}{u},\infty,\frac{M\omega}{K}\right)\right\} \qquad (93)$$

Using the results for the steady periodic response, the conditions corresponding to the maximum amplitudes (Θ_+ and Θ_-, etc.) of the transient-periodic oscillation to reach 99 per cent of the steady-state value (Θ_∞, etc.) are expressed as follows:

Case 1 $1 \geq \tau u/x \geq 0$

Wall temperature

$$\frac{[\Theta(x,\tau)]_{+,-}}{[\Theta_\infty(x)]} = 0.99 = 1 + \frac{\frac{1}{M} e^{-(M+1)\frac{K\tau}{M}}}{1+\left(\frac{M+1}{Mw}\right)^2 \pm \sqrt{\left[\frac{1}{M}\left(\frac{M+1}{Mw}\right)\right]^2 + \left[1+\frac{1}{M}+\left(\frac{M+1}{Mw}\right)^2\right]^2}} \tag{94}$$

Fluid-wall temperature difference

$$\frac{[\Delta T(x,\tau)]_{+,-}}{[\Delta T_\infty(x)]} = 0.99 = 1 \pm \frac{e^{-(M+1)\frac{K\tau}{M}}}{\sqrt{1+\left(\frac{M+1}{Mw}\right)^2}} \tag{95}$$

Fluid temperature

$$\frac{[T(x,\tau)]_{+,-}}{[T_\infty(x)]} = 0.99 = 1 - \frac{e^{-(M+1)\frac{K\tau}{M}}}{1+\left(\frac{M+1}{Mw}\right)^2 \pm \frac{M+1}{Mw}\sqrt{1+\left(\frac{M+1}{Mw}\right)^2}} \tag{96}$$

Case 2 $\tau u/x \geq 1$

Wall temperature

$$\frac{[\Theta(x,\tau)]_{+,-}}{[\Theta_\infty(x)]} = 0.99 = \frac{1+\frac{\frac{1}{M} e^{-(M+1)\frac{K\tau}{M}}}{1+\left(\frac{M+1}{Mw}\right)^2} - e^{-\frac{Kx}{u}}\left[\psi_2^{**}\left(\frac{Kx}{u}, \frac{K\tau^*}{M}\right) - \frac{\frac{1}{M} e^{-(M+1)\frac{K\tau^*}{M}}}{1+\left(\frac{M+1}{Mw}\right)^2}\psi_4\left[\frac{1}{M}\left(\frac{Kx}{u}\right), M\left(\frac{K\tau^*}{M}\right)\right]\right] \pm \sqrt{A_\theta^2 + B_\theta^2}}{\sqrt{A_{\theta\infty}^2 + B_{\theta\infty}^2}} \tag{97}$$

Fluid-wall temperature difference

$$\frac{[\Delta T(x,\tau)]_{+,-}}{[\Delta T_\infty(x)]} = 0.99 = \frac{e^{-(M+1)\frac{K\tau}{M}} + \frac{e^{-\frac{Kx}{u}} e^{-(M+1)\frac{K\tau^*}{M}}}{M} \psi_4\left[\frac{1}{M}\left(\frac{Kx}{u}\right), M\left(\frac{K\tau^*}{M}\right)\right] \pm \sqrt{A^2_{\Delta t} + B^2_{\Delta t}}}{\sqrt{A^2_{\Delta t_\infty} + B^2_{\Delta t_\infty}}} \qquad (98)$$

Fluid temperature

$$\frac{[T(x,\tau)]_{+,-}}{[T_\infty(x)]} = 0.99 = \frac{1 - \frac{e^{-(M+1)\frac{K\tau}{M}}}{1+\left(\frac{M+1}{M}\right)^2} + e^{-\frac{Kx}{u}}\left[-\psi_2^{**}\left(\frac{Kx}{u}, \frac{K\tau^*}{M}\right) - \frac{e^{-(M+1)\frac{K\tau^*}{M}}}{1+\left(\frac{M+1}{M}\right)^2}\right] \psi_4\left[\frac{1}{M}\left(\frac{Kx}{u}\right), M\left(\frac{K\tau^*}{M}\right)\right] \pm \sqrt{A_t^2 + B_t^2}}{\sqrt{A^2_{t_\infty} + B^2_{t_\infty}}} \qquad (99)$$

D. Dynamic Response of the Heat Exchanger Having a Zero Wall-Fluid Heat-Capacity Ratio

For a heat exchanger with zero wall-fluid heat-capacity ratio, ($M = 0$), the transfer function of the fluid temperature may be obtained from Equation (45) by substituting from the identity $(\rho\, Cp)_w K_w = \rho\, CpVK/V_w$ and setting M equal to zero. It yields

$$\bar{F}_t(s) = \frac{\bar{t}_2}{\frac{V_w}{\rho C_p V}\frac{x}{u}\bar{\Phi}} = \frac{1 - e^{-s\frac{x}{u}}}{s\frac{x}{u}} \qquad (100)$$

Substituting s by $i\omega$, Equation (100) becomes

$$\bar{F}_t(i\omega) = \frac{1 - e^{-i\omega\frac{x}{u}}}{i\omega\frac{x}{u}} = \frac{1}{\omega\frac{x}{u}}\left[\sin\frac{\omega x}{u} + i\left(\cos\frac{\omega x}{u} - 1\right)\right] \qquad (101)$$

The absolute value of Equation (101) is

$$\left|\bar{F}_t(i\omega)\right| = \frac{1}{\frac{\omega x}{u}}\sqrt{\left(\sin\frac{\omega x}{u}\right)^2+\left(\cos\frac{\omega x}{u}-1\right)^2} = \frac{1}{\frac{\omega x}{u}}\sqrt{2\left(1-\cos\frac{\omega x}{u}\right)} \tag{102}$$

Since $$\frac{V_w}{\rho C_p V}\frac{x}{u}\Phi = \frac{\Delta\left(q/A\right)}{h}\left(\frac{Kx}{u}\right) = \left[T_\infty(x)\right]_{\omega=0} ,$$

Equation (102) expresses the ratio of the temperature amplitude-ratio at $\omega = \omega$ to $\omega = 0$. Therefore, one may express Equation (102) as

$$\frac{\left[T_\infty(x)\right]_{\omega=\omega}}{\left[T_\infty(x)\right]_{\omega=0}} = \frac{\sqrt{2\left(1-\cos\frac{\omega x}{u}\right)}}{\frac{\omega x}{u}} \tag{103}$$

Equation (103) is the amplitude-ratio response of the fluid temperature. The corresponding phase-shift may be obtained from Equation (101) as

$$\alpha_t = \tan^{-1}\left(\frac{1-\cos\frac{\omega x}{u}}{\sin\frac{\omega x}{u}}\right) \tag{104}$$

Response in the transient-periodic state may be obtained as follows by substituting $M = 0$ into Equation (66) and (73). It must be noted that $s = Kx/u = M\,K_w x/u$ and for $M = 0$, s is equal to zero. From (G-17), (G-18), and (G-19) the functions $\psi_2(Kx/u, K\tau^*/M)$, $\psi_7(Kx/u, K\tau^*/M, M\omega/K)$ and $\psi_8(Kx/u, K\tau^*/M, M\omega/K)$ are identically zero for $M = 0$.

Case 1 $\quad 1 \geq \tau u/x \geq 0$

$$\frac{t_2(x,\tau)}{\frac{V_w}{\rho C_p V}\frac{x}{u}\Phi} = \frac{1-\cos\omega\tau}{\frac{\omega x}{u}} , \tag{105}$$

Case 2 $\tau u/x \geq 1$

$$\frac{t_2(x,\tau)}{\frac{V_w}{\rho C_p V}\Phi\frac{x}{u}} = \frac{\sqrt{2\left(1-\cos\frac{\omega x}{u}\right)}}{\frac{\omega x}{u}} \sin\left[\omega\tau - \tan^{-1}\left(\frac{1-\cos\frac{\omega x}{u}}{\sin\frac{\omega x}{u}}\right)\right] \tag{106}$$

Since $(V_w/\rho C_p V)(\Phi x/u)$ is equal to $(t_{2\infty})_{\omega=0}$ and Equation (106) is in the same form as Equation (22), one obtains

$$\frac{[T_\infty(x)]_{\omega=\omega}}{[T_\infty(x)]_{\omega=0}} = \frac{\sqrt{2\left(1-\cos\frac{\omega x}{u}\right)}}{\frac{\omega x}{u}} \tag{107}$$

$$\alpha_t = \tan^{-1}\left(\frac{1-\cos\frac{\omega x}{u}}{\sin\frac{\omega x}{u}}\right) \tag{108}$$

The results for the dynamic response of the heat exchanger with zero heat capacity ratio are also derived independently in Appendix F.

The dimensionless frequencies $\omega x/u$ for the maximum and minimum amplitude-ratios of the fluid temperature may be obtained by differentiating Equation (103) with respect to $\omega x/u$ and setting it equal to zero. A dimensionless frequency satisfying the equation

$$\frac{\omega x}{u}\sin\frac{\omega x}{u} + 2\cos\frac{\omega x}{u} - 2 = 0 \tag{109}$$

is the one corresponding to either a maximum or a minimum amplitude-ratio evaluated by Equation (103).

To explain the phenomena of resonance in the amplitude-ratio and phase-shift of the fluid temperature, one may imagine a fluid particle entering the heat exchanger when the time-dependent power input (or heat generation) is $p_x''(\tau) = p_{xo}'' + \Phi \sin\omega\tau'$, as shown in Figure 5. After the particle travels through the heat exchanger for a time interval of τ, the heat balance on the particle can be expressed as

$$\rho C_p V \frac{dt}{d\tau} = V_w \left[p_{xo}'' + \Phi \sin(\omega\tau - \omega\tau') \right] \tag{110}$$

where $\omega\tau'$ may be called the inlet lag of the fluid particle, Figure 5.

Integrating Equation (110) from $\omega\tau=0$ to $\omega\tau=\omega\tau$, yields

$$t(\tau) - t_o = \frac{p_{xo}'' V_w \tau}{\rho C_p V} + \frac{\Phi V_w}{\rho C_p V \omega} \left[\cos\omega\tau' - \cos(\omega\tau - \omega\tau') \right] . \tag{111}$$

Now, for the case of $\omega=0$,

$$t_{(\tau)_{\omega=0}} - t_o = \frac{p_{xo}'' V_w \tau}{\rho C_p V} + \frac{\Phi V_w \tau}{\rho C_p V} , \tag{112}$$

and for the initial steady-state

$$t_1(\tau) - t_o = \frac{p_{xo}'' V_w \tau}{\rho C_p V} , \tag{113}$$

where $t_1(\tau)$ is the steady-state component of the particle temperature. From Equations (111), (112) and (113), one obtains then

$$t_2(\tau) = t(\tau) - t_1(\tau) = \frac{\Phi V_w}{\rho C_p V \omega} \left[\cos\omega\tau' - \cos(\omega\tau - \varphi') \right] , \tag{114}$$

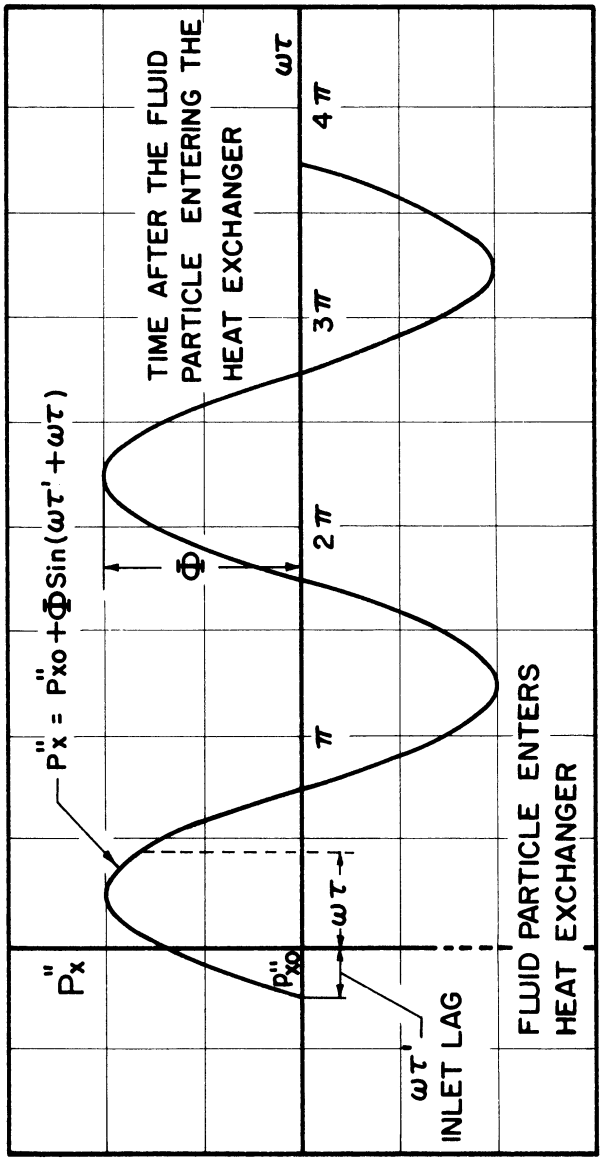

Figure 5. Diagram Demonstrating the Time Relationship Between the Power Input (or Heat Generation) and Flow of the Fluid Particle.

and

$$t_{2_{\omega=0}}(\tau) = t_{\omega=0}(\tau) - t_1(\tau) = \frac{\Phi V_w \tau}{\rho C_p V} \quad . \tag{115}$$

Dividing Equation (114) by Equation (115), one obtains the amplitude-ratio of the temperature of the fluid particle as observed by an observer attached to the particle, as follows,

$$\frac{t_2(\tau)}{t_{2_{\omega=0}}(\tau)} = \frac{\cos\omega\tau' - \cos(\omega\tau - \omega\tau')}{\omega\tau}$$

$$= \frac{\sqrt{2(1-\cos\omega\tau)}}{\omega\tau} \sin\left[\omega\tau - \tan^{-1}\left(\frac{1-\cos\omega\tau}{\sin\omega\tau}\right)\right] \quad , \tag{116}$$

or

$$\frac{t_2(\tau)}{t_{2_{\omega=0}}(\tau)} = \left[\frac{t_2(\tau)}{t_{2_{\omega=0}}(\tau)}\right]_{max} \sin\left[\omega\tau' - \tan^{-1}\left(\frac{1-\cos\frac{\omega x}{u}}{\frac{\omega x}{u}}\right)\right] \quad , \tag{117}$$

where

$$\left[\frac{t_2(\tau)}{t_{2_{\omega=0}}(\tau)}\right]_{max} = \pm \frac{\sqrt{2(1-\cos\omega\tau)}}{\omega\tau} \tag{118}$$

It is seen from Equation (117) that $t_2(\tau)/t_{2_{\omega=0}}$ equals $(t_2(\tau)/t_{2_{\omega=0}})_{max}$, when

$$\omega\tau' = \frac{\pi}{2} + 2n\pi + \tan^{-1}\left(\frac{1-\cos\omega\tau}{\sin\omega\tau}\right) \quad \text{for + sign,} \tag{119}$$

and

$$\omega\tau' = \frac{3\pi}{2} + 2n\pi + \tan^{-1}\left(\frac{1-\cos\omega\tau}{\sin\omega\tau}\right) \quad \text{for - sign,} \tag{120}$$

where n = 0, 1, 2, ...

It is also seen from Equation (117), that $t(\tau) = t_1(\tau)$ when $\omega\tau' = \tan^{-1}(1-\cos\omega\tau)/\sin\omega\tau) = 0$, that is

$$\omega\tau = 2n\pi \quad \text{and} \quad \omega\tau - 2\omega\tau' = 2n\pi \tag{121}$$

Equation (118) is the envelope of the temperature oscillations of the fluid particles of the different inlet lags.

The transfer function of the wall temperature of the heat exchanger with zero wall-fluid heat capacity ratio, (M=0) may be obtained from Equation (46) by substituting from the identity $(\rho Cp)_w K_w = \rho CpVK/V_w$ and setting M equal to zero. It yields

$$\bar{F}_\theta(S) = \frac{\bar{\theta}_2}{\frac{V_w}{\rho C_p V K}\left(1+\frac{Kx}{u}\right)\bar{\phi}} = \frac{K}{S\left(1+\frac{Kx}{u}\right)}\left[1+\frac{S}{K} - e^{-\frac{Sx}{u}}\right] \tag{122}$$

Substituting s by iω into Equation (122), one obtains

$$\bar{F}_\theta(i\omega) = \frac{K}{i\omega\left(1+\frac{Kx}{u}\right)}\left[1+\frac{i\omega}{K} - e^{-\frac{i\omega x}{u}}\right]$$

$$= \frac{\frac{K}{\omega}}{1+\frac{Kx}{u}}\sqrt{\left(\cos\frac{\omega x}{u}-1\right)^2 + \left(\frac{\omega}{K}+\sin\frac{\omega x}{u}\right)^2}\, e^{i\tan^{-1}\left(\frac{\cos\frac{\omega x}{u}-1}{\frac{\omega}{K}+\sin\frac{\omega x}{u}}\right)} \tag{123}$$

Therefore, the amplitude-ratio and phase-shift of the wall temperature

can be expressed as

$$\left|\bar{F}_\theta(i\omega)\right| = \frac{\left[\theta_\infty(x)\right]_{\omega=\omega}}{\left[\theta_\infty(x)\right]_{\omega=0}} = \frac{\frac{K}{\omega}}{1+\frac{Kx}{u}}\sqrt{\left(\cos\frac{\omega x}{u}-1\right)^2+\left(\frac{\omega}{K}+\sin\frac{\omega x}{u}\right)^2} \tag{124}$$

$$\alpha_\theta = \tan^{-1}\left(\frac{1-\cos\frac{\omega x}{u}}{\sin\frac{\omega x}{u}}\right) \tag{125}$$

These results are shown in Figure 25-b and 26-b. The wall-fluid heat capacity ratio M is defined as the ratio $(\rho Cp)_W V_W/\rho CpV$ or as K/K_W. M = 0 could exist for (i) K_W equal to infinity [or $(\rho Cp)_W = 0$] but K is finite, that is, the fluid has a finite heat capacity, and (ii) K_W equals to infinity and (ρCp) is equal to infinity. Equations (124) and (125) express the dynamic response for case (i). For case (ii) Equations (124) and (125) become

$$\left|\bar{F}_\theta(i\omega)\right| = 1 \tag{126}$$

$$\alpha_\theta = 0 \tag{127}$$

For some limiting cases, Equations (124) and (125) can be reduced as follows:

$$\lim_{\omega\to\infty}\left|\bar{F}_\theta(i\omega)\right| = \frac{1}{1+\frac{Kx}{u}} \tag{128}$$

$$\lim_{\omega\to\infty}\alpha_\theta = 0 \tag{129}$$

Equations (128) and (129) indicate that the amplitude-ratio of the wall temperature is asympotic to $1/(1+Kx/u)$ and its phase-shift asymptotic to zero with increase in the frequency ω, as shown in Figures 25-b

and 26-b. For large values of K, Equations (124) and (125) become

$$\lim_{K\to\infty} |\bar{F}_\theta(i\omega)| = \frac{2(1-\cos\frac{\omega x}{u})}{\frac{\omega x}{u}} \tag{130}$$

$$\lim_{K\to\infty} \alpha_\theta = \tan^{-1}\left(\frac{1-\cos\frac{\omega x}{u}}{\sin\frac{\omega x}{u}}\right) \tag{131}$$

Equations (130) and (131) are identical with Equations (103) and (104) indicating that the amplitude-ratio and phase-shift are function of $\omega x/u$ alone. Physically, Equations (103), (104), (130) and (131) signify that the amplitude-ratio and phase-shift of the fluid and wall temperature are the same providing that the heat capacities of both fluid and wall are zero. For small values of Kx/u, Equations (124) and (125) may be simplified as

$$\lim_{\frac{Kx}{u}\to 0} |\bar{F}_\theta(i\omega)| = 1 \tag{132}$$

$$\lim_{\frac{Kx}{u}\to 0} \alpha_\theta = 0 \tag{133}$$

For M = 0 case, Equation (47) becomes

$$\bar{F}_{\Delta t}(s) = 1 \tag{134}$$

Therefore the amplitude-ratio and phase-shift of the fluid-wall temperature difference can be expressed as

$$|\bar{F}_{\Delta t}(i\omega)| = 1 \tag{135}$$

$$\alpha_{\Delta t} = 0 \tag{136}$$

A discussion of these results is found in the next section.

E. Discussion of Theoretical Results

The constant M has been defined as follows:

$$M = \frac{a_2}{a_3} = \frac{(\rho C_p)_w}{\rho C_p} \frac{r_o^2 - r_i^2}{r_i^2} = \frac{(\rho C_p V)_w}{\rho C_p V}$$

$$= \frac{\text{total heat capacity of wall material}}{\text{total heat capacity of fluid}}$$

$$= \frac{K}{K_w} \tag{137}$$

where

$$K = \frac{h(\frac{A}{V})}{\rho C_p} = \text{fluid time constant}$$

$$K_w = \frac{h(\frac{A}{V})_w}{(\rho C_p)_w} = \text{wall time constant}$$

M is a heat-capacity ratio depending on geometry as well as materials. For the usual materials and geometry it may be expected that M will vary from near zero for water-steel systems with thin metal walls to something in excess of 1000 for similar air-steel systems.

1. Frequency Response

According to the definition of the transfer function for the wall and fluid temperatures, and the fluid-wall temperature difference, as shown by Equations (45), (46) and (47), the amplitude-ratio all are unity at s = 0, and zero at S = ∞ as shown in Table I. These same results are obtained from Equations (55), (57) and (59) for $\omega = 0$.

Under the quasi-steady process, that is, $\omega \approx 0$, the response of the transient component of the fluid temperature, t_2, the wall temperature, θ_2, and the fluid-wall temperature difference, Δt_2, are completely in phase with the time-wise variation in the rate of internal heat generation within the wall. Their amplitudes under the condition of a zero frequency oscillation as shown earlier in regard to Equations (51), (53) and (54) are:

$$\left[T_{\infty}(x)\right]_{\omega=0} = \frac{\Phi \frac{Kx}{U}}{(\rho c_p)_w K_w} = \frac{\Delta\left(q/A\right)}{h}\frac{Kx}{U} \tag{138}$$

$$\left[\Theta_{\infty}(x)\right]_{\omega=0} = \frac{\Phi\left(1+\frac{Kx}{U}\right)}{(\rho c_p)_w K_w} = \frac{\Delta\left(q/A\right)\left(1+\frac{Kx}{U}\right)}{h} \tag{139}$$

$$\left[\Delta T_{\infty}(x)\right]_{\omega=0} = \frac{\Phi}{(\rho c_p)_w K_w} = \frac{\Delta\left(q/A\right)}{h} \tag{140}$$

TABLE I

ASYMPTOTIC VALUES OF THE TRANSFER FUNCTIONS AT s=0 AND s=∞

Transfer Function	s=0	s=∞
$\bar{F}_t(s)$	1	0
$\bar{F}_\theta(s)$	1	0
$\bar{F}_{\Delta t}(s)$	1	0

TABLE II

ASYMPTOTIC VALUES OF THE AMPLITUDE-RATIOS AND PHASE-SHIFTS AT ω=0,∞ AND M=0,∞

	ω=0	ω=∞	M=0 *	M=∞
$\lvert\bar{F}_t(i\omega)\rvert$	1	0	Resonance	0
$\lvert\bar{F}_\theta(i\omega)\rvert$	1	0	Resonance	0
$\lvert\bar{F}_{\Delta t}(i\omega)\rvert$	1	0	1	0
α_t	0	$\tan^{-1}\left(\frac{e^{-\delta}\sin\gamma}{1-e^{-\delta}\cos\gamma}\right)$	Resonance	0
α_θ	0	$\pi/2$	Resonance	0
$\alpha_{\Delta t}$	0	$\pi/2$	0	0

TABLE III

ASYMPTOTIC LIMITS OF THE TEMPERATURE-RESPONSE FUNCTIONS FOR THE VALUES OF ω=0,∞ AND M=0,∞ IN THE FIRST TIME DOMAIN

Function	M=0 *	M=∞	ω=0	ω=∞
$\frac{t_2(x,\tau)}{\frac{\Delta(q/A)}{h}\frac{Kx}{u}}$	$\frac{1-\cos\omega\tau}{\frac{\omega x}{u}}$	0	1	0
$\frac{\theta_2(x,\tau)}{\frac{\Delta(q/A)}{h}(1+\frac{Kx}{u})}$	$\frac{1-\cos\omega\tau+\frac{\omega}{K}\sin\omega\tau}{\frac{\omega}{K}(1+\frac{Kx}{u})}$	0	1	0
$\frac{\Delta t_2(x,\tau)}{\frac{\Delta(q/A)}{h}}$	$\sin\omega\tau$	0	1	0

* See Table IV

where, Φ is the transient amplitude of power input to the wall, which can be expressed as

$$\Phi = \Delta\left(\frac{q}{A}\right)\left(\frac{A}{V}\right)_w \tag{141}$$

Here $\Delta(q/A)$ is the increase in the steady-state heat flux, and $(A/V)_w$ is the ratio of the wetted area of the wall to the volume of the wall. $\Delta(q/A)/h$ is the increase in the steady-state value of the fluid-wall temperature difference, and Kx/u is the product of a fluid time constant K and a fluid transit time x/u.

The asymptotic values of the amplitude-ratio of the fluid and wall temperatures and the fluid-wall temperature difference as shown in Equations (55), (57) and (59) are all unity at $\omega = 0$ and zero at $\omega = \infty$. For the zero wall-fluid heat capacity ratio, ($M = 0$), the amplitude-ratio of the fluid and wall temperature has a phenomenon of resonance as will be shown later. At the very large values of heat capacity ratio M, those values for the fluid and wall temperatures and the fluid-wall temperature difference all approach zero.

In the case of finite wall-fluid heat capacity ratio, M, the phase-shift of the fluid and wall temperatures and the fluid-wall temperature difference as shown in Equations (56), (58) and (60) are all zero at zero frequency. At very large values of ω, those of the wall temperature and the fluid-wall temperature difference approach $\pi/2$ while that of the fluid temperature as shown in Equation (56) becomes equal to $\tan^{-1}\left(\frac{e^{-\gamma}\sin\gamma}{1-e^{-\gamma}\cos\gamma}\right)$, which oscillates about a phase shift of 180 degrees. The phase-shift of

the fluid temperature possesses resonance phenomenon for all values of M as will be discussed later, although those of the wall temperature and the fluid-wall temperature difference also resonate at large Kx/u. At large values of M all the phase shifts approach zero. These are shown in Table II.

The frequency response characteristics of the wall and fluid temperatures and the fluid-wall temperature difference as shown in Equations (55) - (60), are all functions of four dimensionless parameters: M, $M\omega/K$, Kx/u and $\omega x/u$, of which $M\omega/K$ is not independent since there exists the relationship $M\omega/K = (M)(\omega x/u) \Big/ (Kx/u)$. Typical theoretical results for M = 0.561, K_w = 2470 is plotted on the Bode type diagram (amplitude ratio versus frequency) in Figures 6, 7 and 8 and are shown by the solid line. Also shown are experimental results which will be discussed later. The wall and fluid temperatures and the fluid-wall temperature difference are given in Figures 9 and 10 for a complete range of the dimensionless parameters. These theoretical results predict the phenomena of resonance in the amplitude-ratio and phase-shift which is characteristics of a distributed parameter system having periodic, distributed disturbances. In such a case the amplitude-ratio ultimately decreases to zero with increasing frequency, although it passes through points of resonance.

The theoretical results for the frequency response of the wall temperature and the fluid-wall temperature differences are shown in Figures 9b, 9c, 10b and 10c. These results are similar to those of the fluid temperature, discussed below, except for the phase angle of the fluid-wall temperature difference shown in Figure 10c which is unique in that it has characteristics of phase advance at large Kx/u.

The effects of the parameters M, Kx/u and $\omega x/u$ on the amplitude-ratio, first resonance amplitude-ratio, phase-shift and first resonance

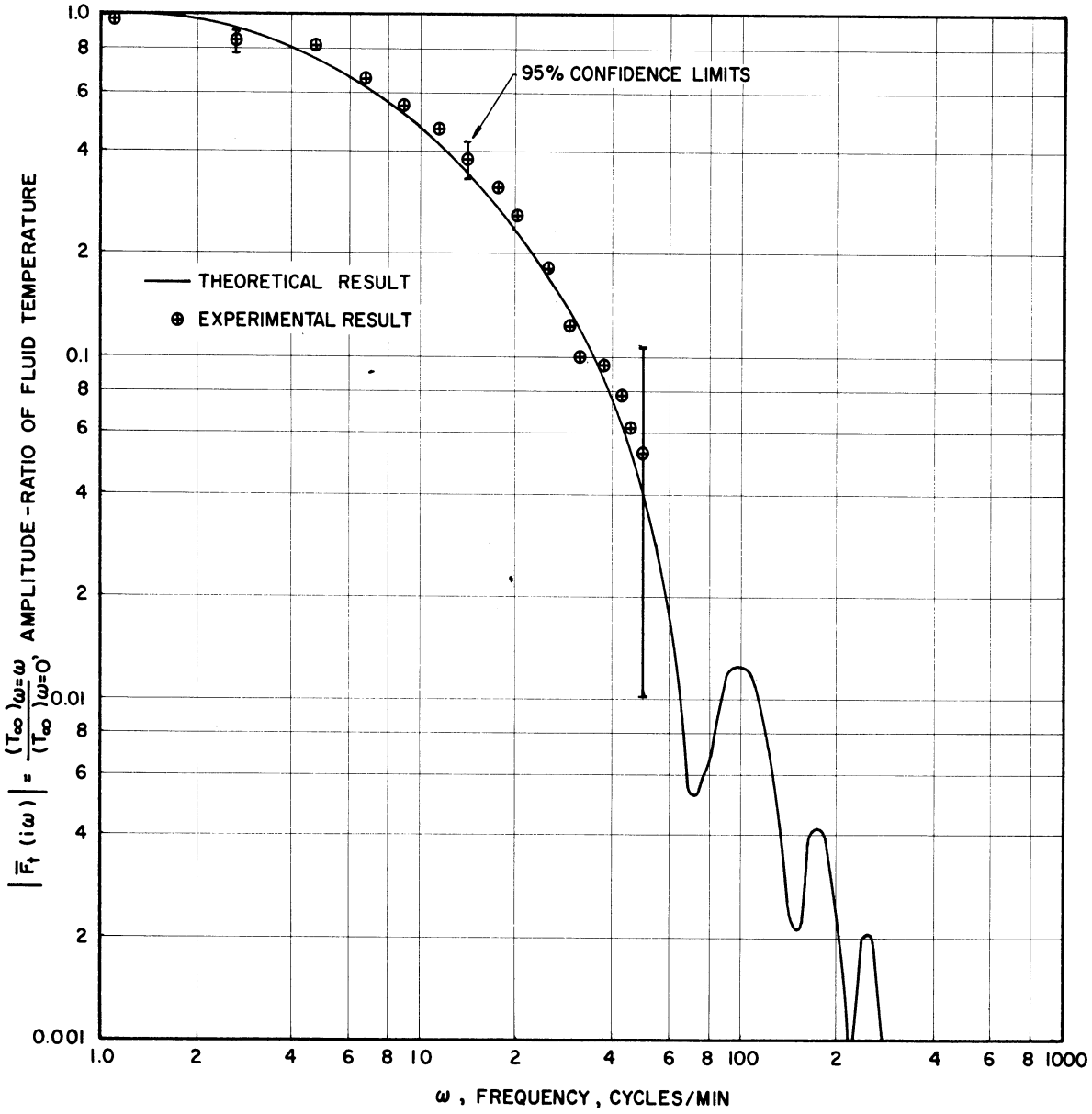

Figure 6-a. Amplitude-Ratio Response of Fluid Temperature at $Kx/u = 0.321$, $M = 0.561$, $K_w = 2470$, $P_a/P_{ox}" = 0.218$.

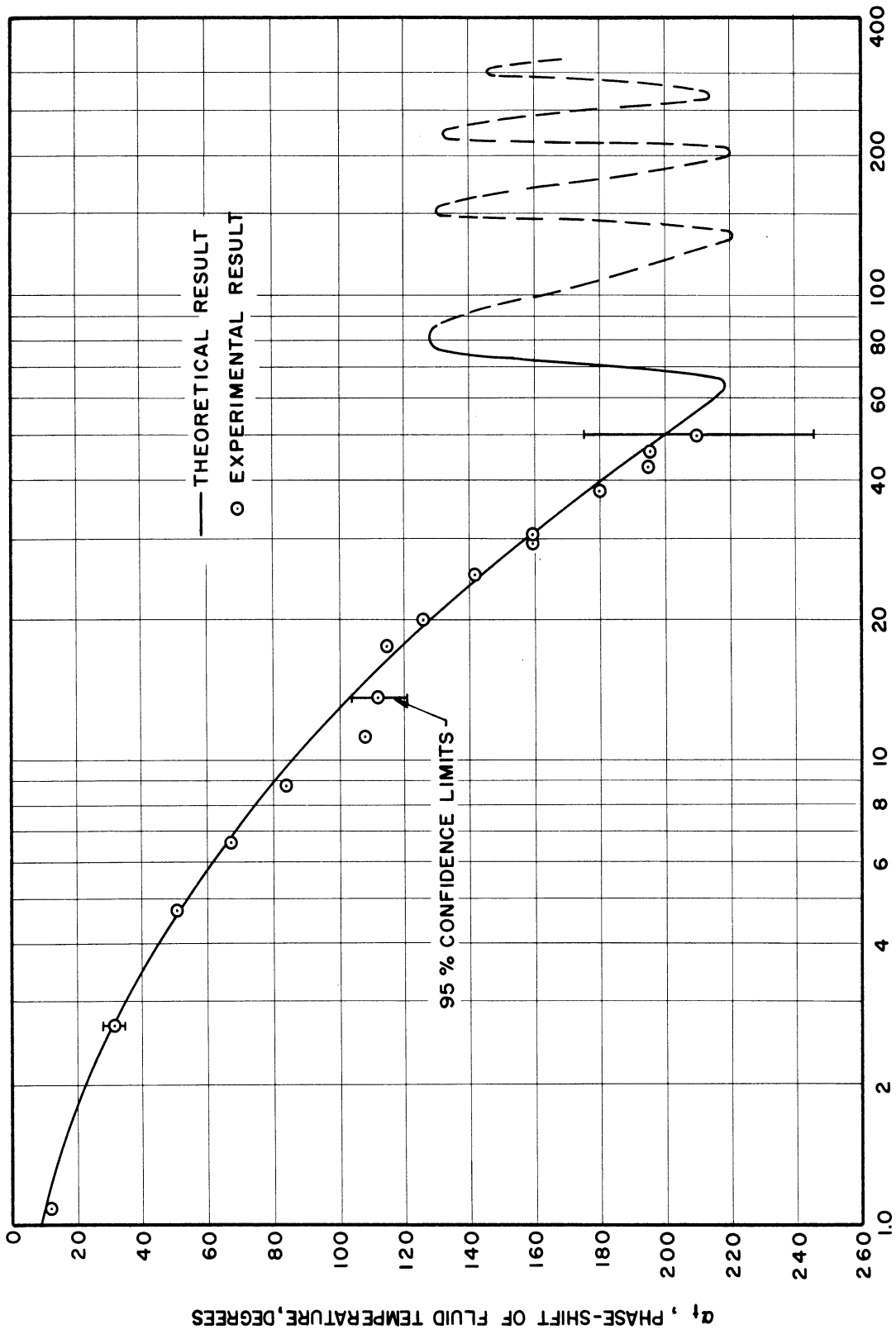

Figure 6-b. Phase-Shift Response of Fluid Temperature at Kx/u = 0.321, M = 0.561, K_w = 2470, P_a/P_{ox}" = 0.218.

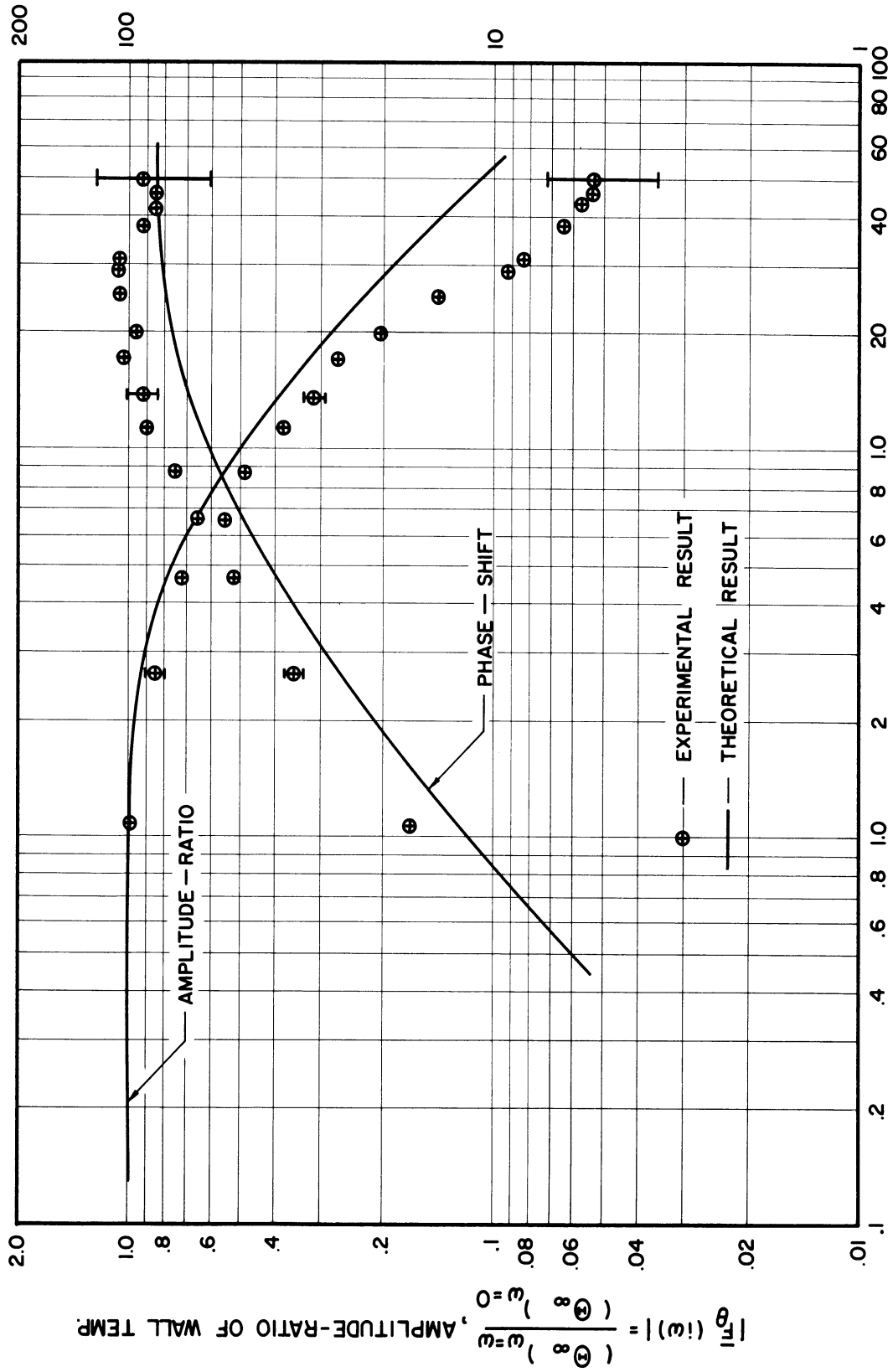

Figure 7. Frequency Response of Wall Temperature at $Kx/u = 0.161$, $M = 0.561$, $K_w = 2470$, $P_a/P_{xo}" = 0.218$.

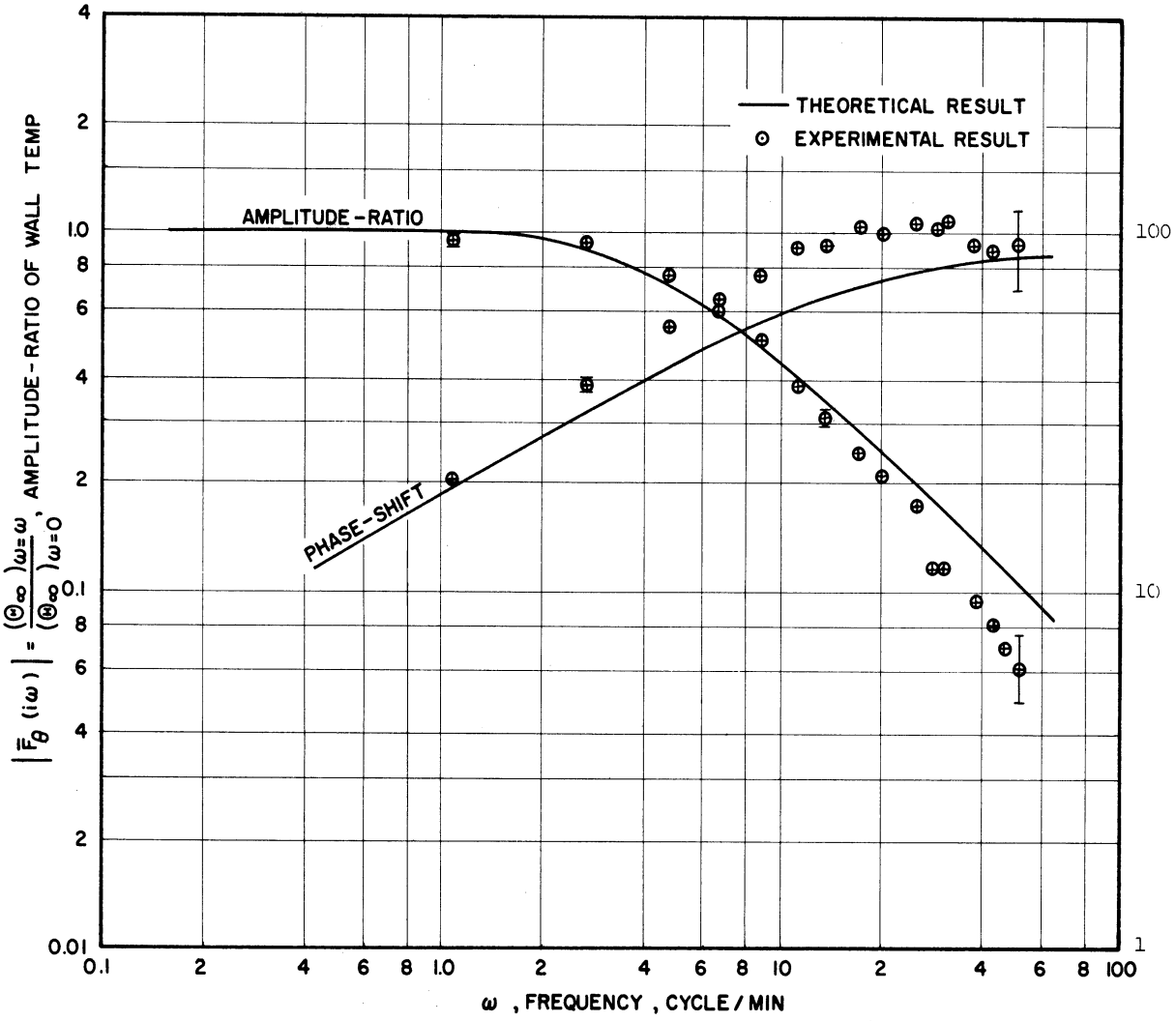

Figure 8. Frequency Response of Wall Temperature at Kx/u = 0.302, M = 0.561, K_w = 2470, P_a/P_{xo}" = 0.218.

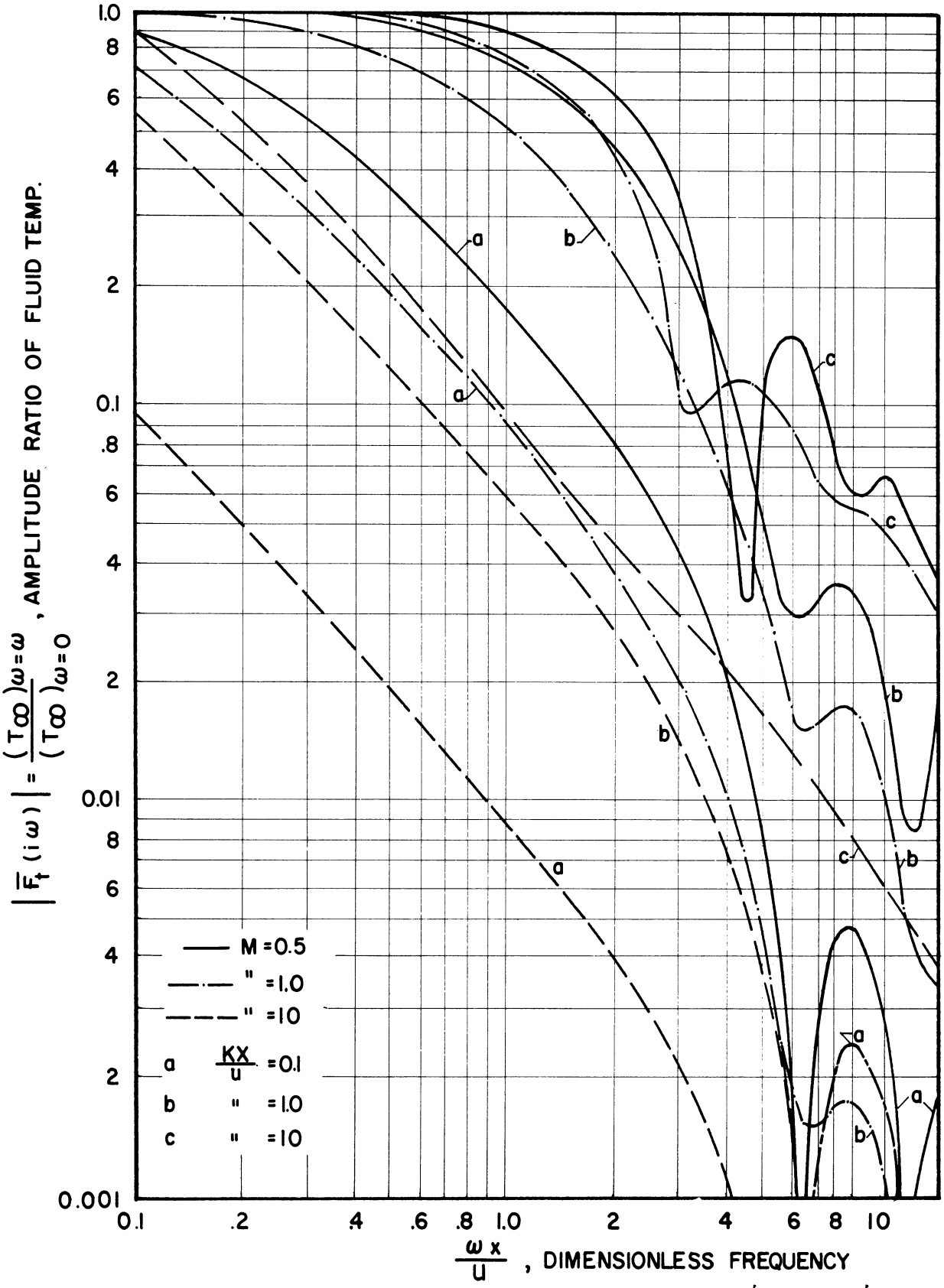

Figure 9-a. Effect of the Parameters M, Kx/u and ωx/u on the Amplitude-Ratio Response of Fluid Temperature.

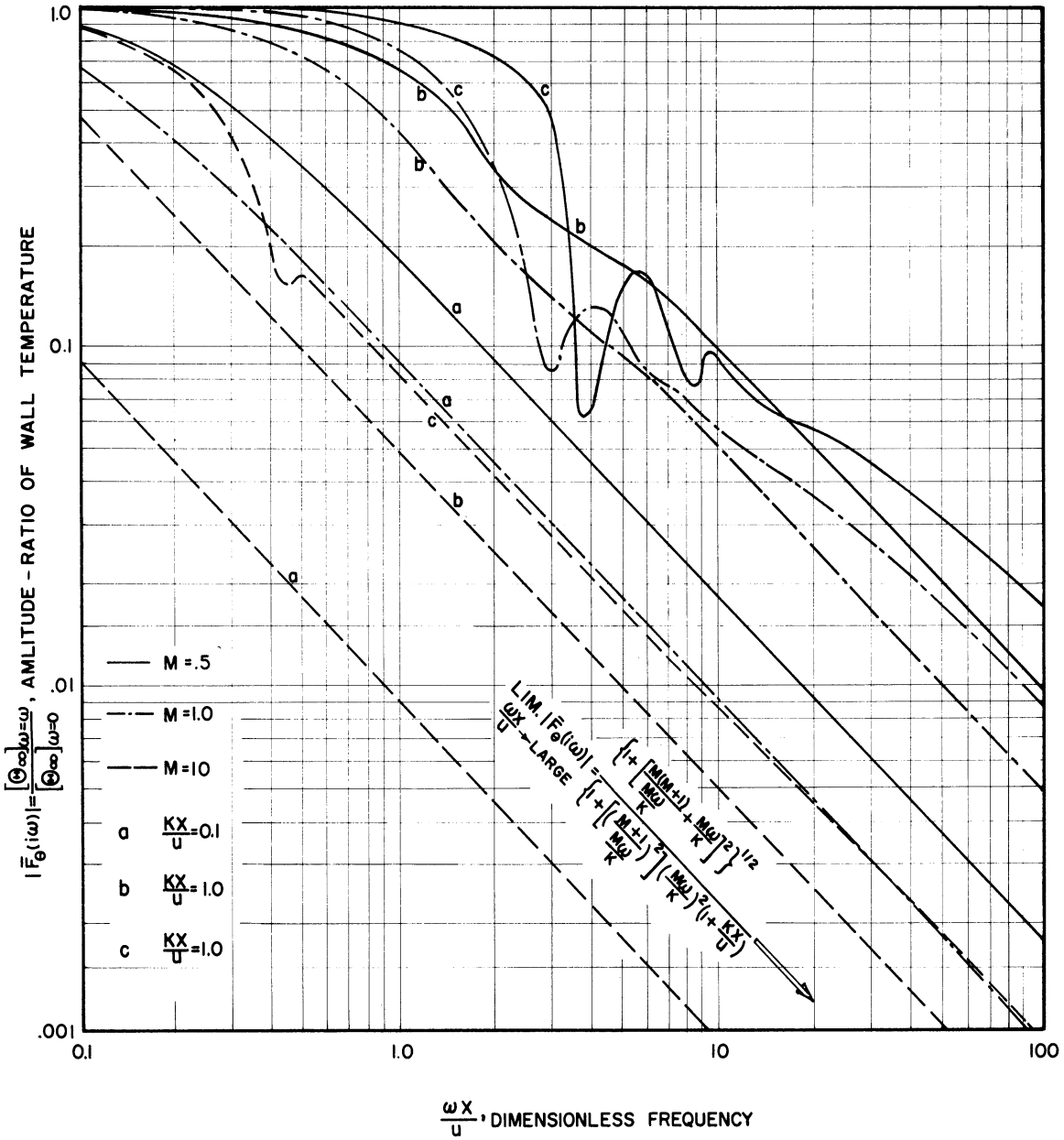

Figure 9-b. Effect of the Parameters M, Kx/u and ωx/u on the Amplitude-Ratio Response of the Wall Temperature.

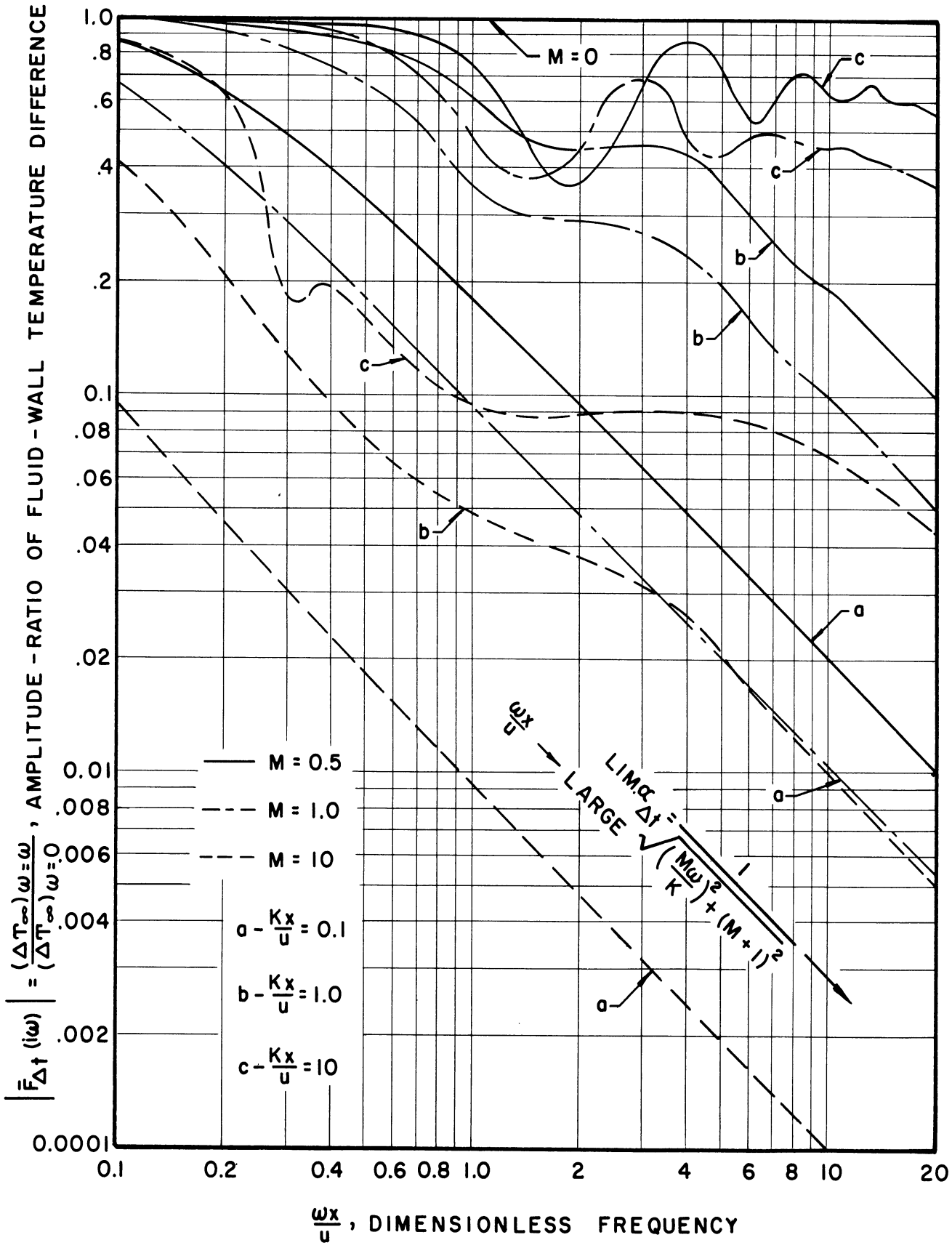

Figure 9-c. Effects of the Parameters, M, Kx/u and ωx/u on the Amplitude-Ratio Responses of the Fluid-Wall Temperature Difference.

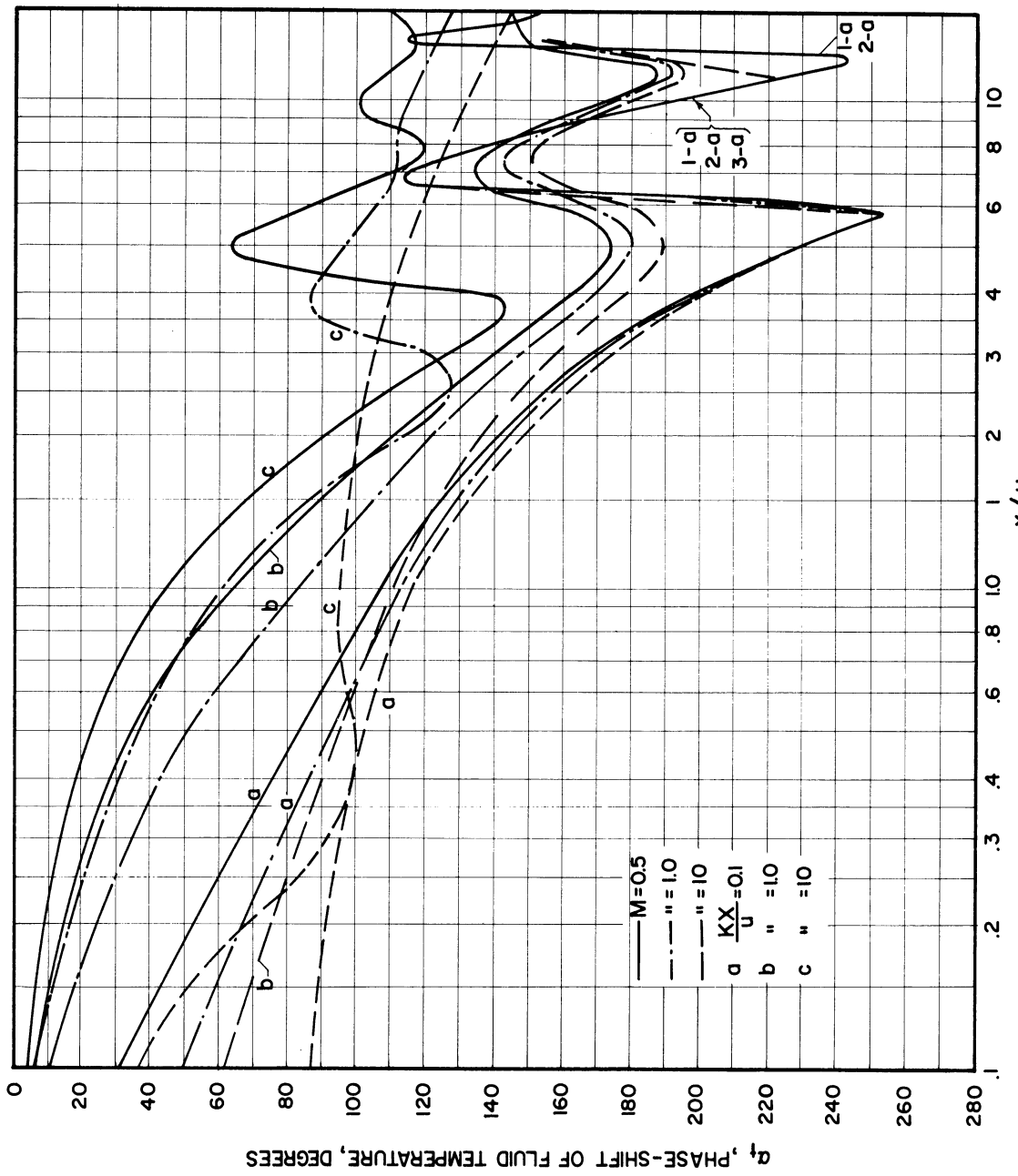

Figure 10-a. Effect of the Parameters M, Kx/u, and ωx/u on the Phase-Shift Response of Fluid Temperature.

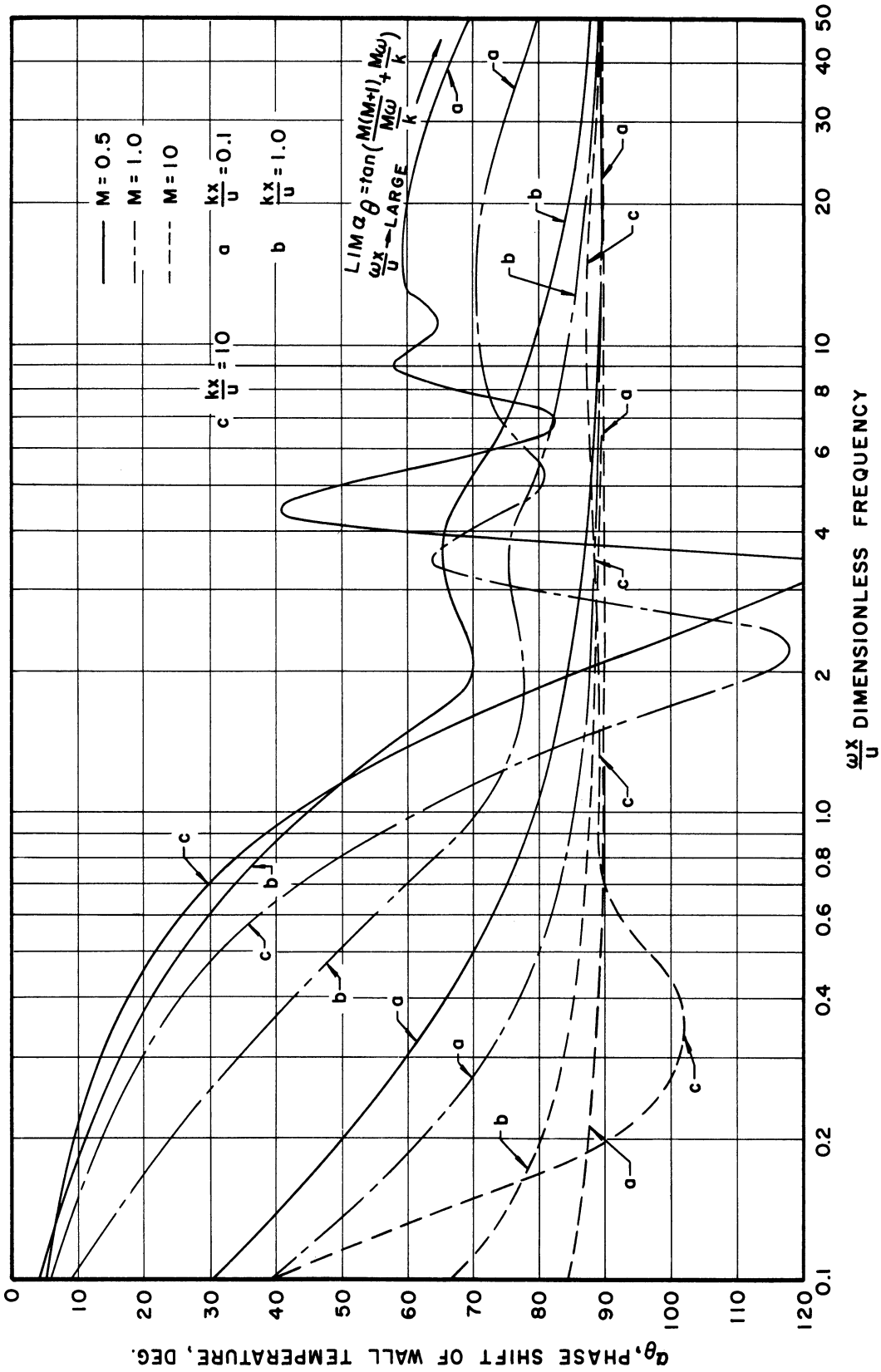

Figure 10-b. Effect of the Parameters M, Kx/u and ωx/u on the Phase-Shift Response of the Wall Temperature.

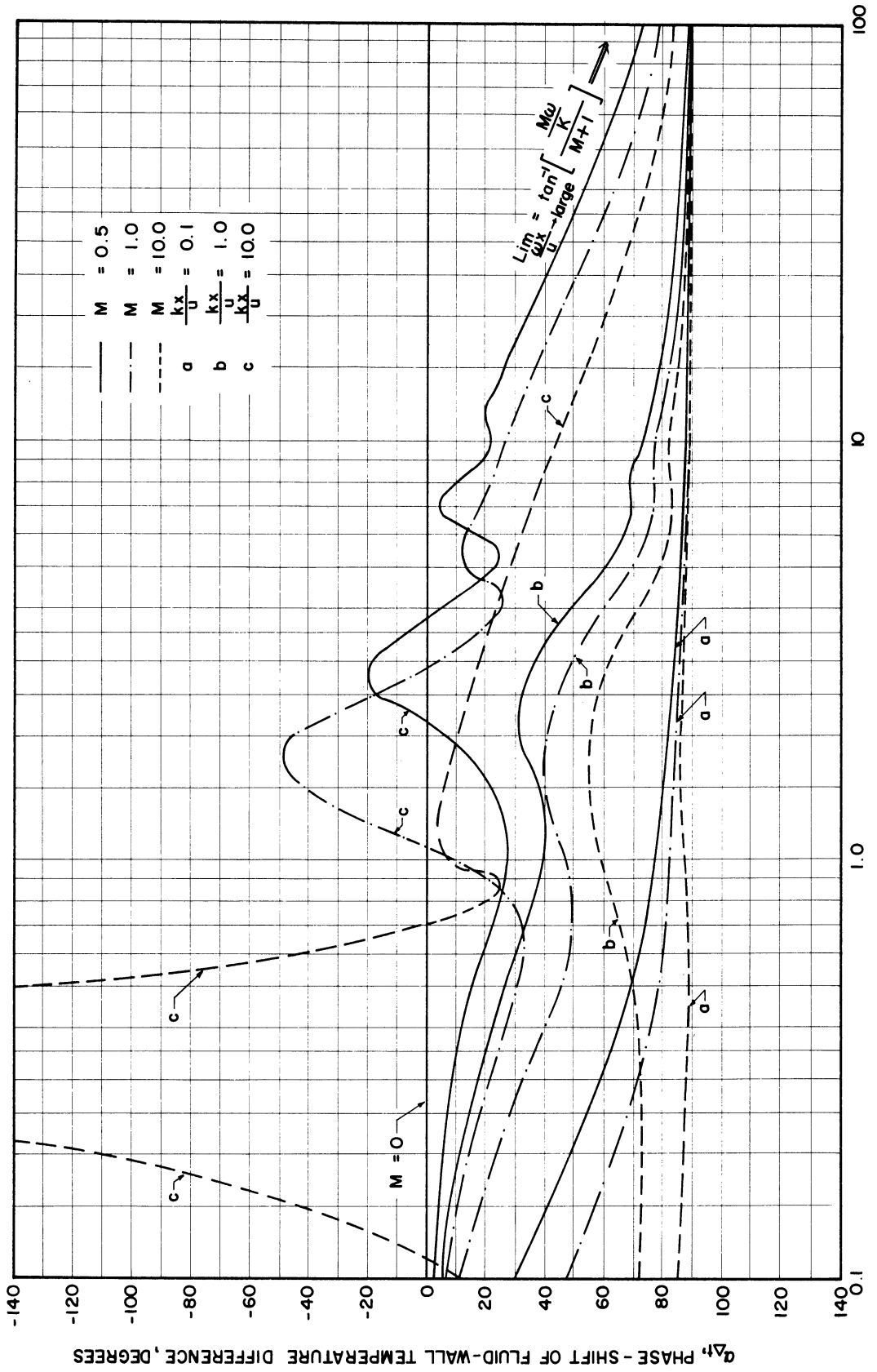

Figure 10-c. Effect of the Parameters, M, Kx/u and ωx/u on the Phase-Shift Response of the Fluid-Wall Temperature Difference.

phase-shift of the fluid temperature are shown in Figures 9-a, 10-a, 11 and 12. These figures indicate that at a small value of Kx/u, an increase in the heat capacity ratio causes a continuous decrease in the amplitude-ratio and increase in the phase-shift. The amplitude-ratio at the first resonance decreases its magnitude considerably accompanied by decrease in its resonance frequency for change in M from zero to 0.5. As M increases from 0.5 the first resonance amplitude-ratio decreases continuously at constant resonance dimensionless frequency $\omega x/u$. On the contrary, the phase-shift at the first resonance increases abruptly accompanied by increase in the resonance frequency for change in M from zero to 0.1. With M greater than 0.5 the magnitude of the first resonance phase-shift is practically constant with constant resonance frequency. At high Kx/u an increase in the heat capacity ratio causes a decrease in the amplitude-ratio and increase in phase-shift. The first resonance amplitude-ratio decreases gradually accompanied by the continuous decrease in the resonance frequency for increase in M. The first resonance phase-shift increases considerably at lower M and then increases very gradually for M of greater than unity. This change in the magnitude of the first resonance phase-shift with increase in M is accompanied by the continuous decrease in the resonance frequency. For heat capacity ratio of higher than 10 the magnitude of the resonance amplitude-ratio becomes essentially zero. Similar effects on the phase-shift and resonance phase-shift are observed except the resonance of the phase-shift at the heat capacity ratio of 10 is still finite.

The effects of Kx/u on the amplitude-ratio and phase-shift at the first resonance may be seen from Figures 11 and 12. Here the first

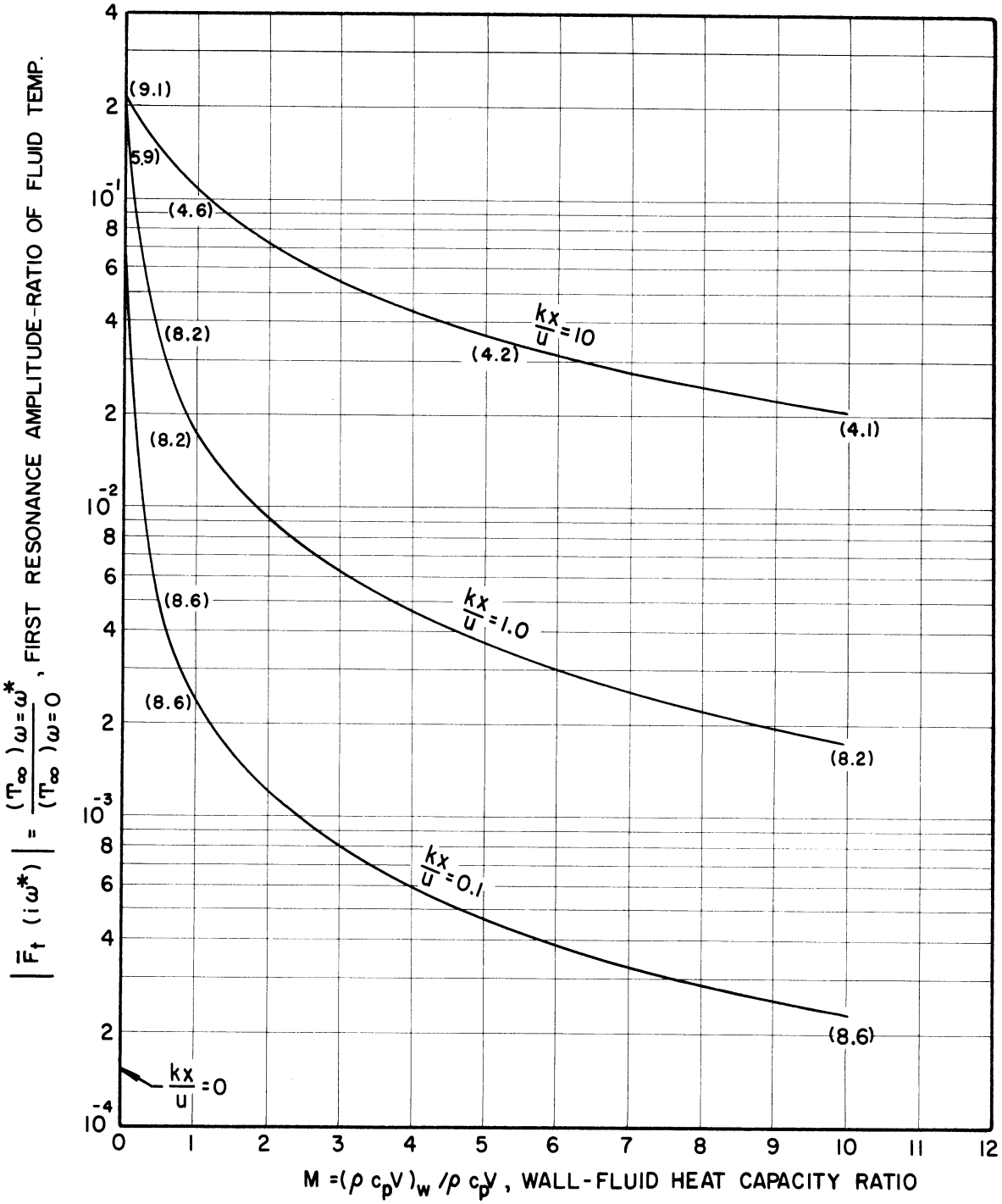

Figure 11. Effects of the Parameters M, Kx/u and ωx/u on the First Resonance Amplitude-Ratio of Fluid Temperature.

NOTE: Bracketed quantity ( ) on curve is value of ωx/u at first resonance frequency, ω*.

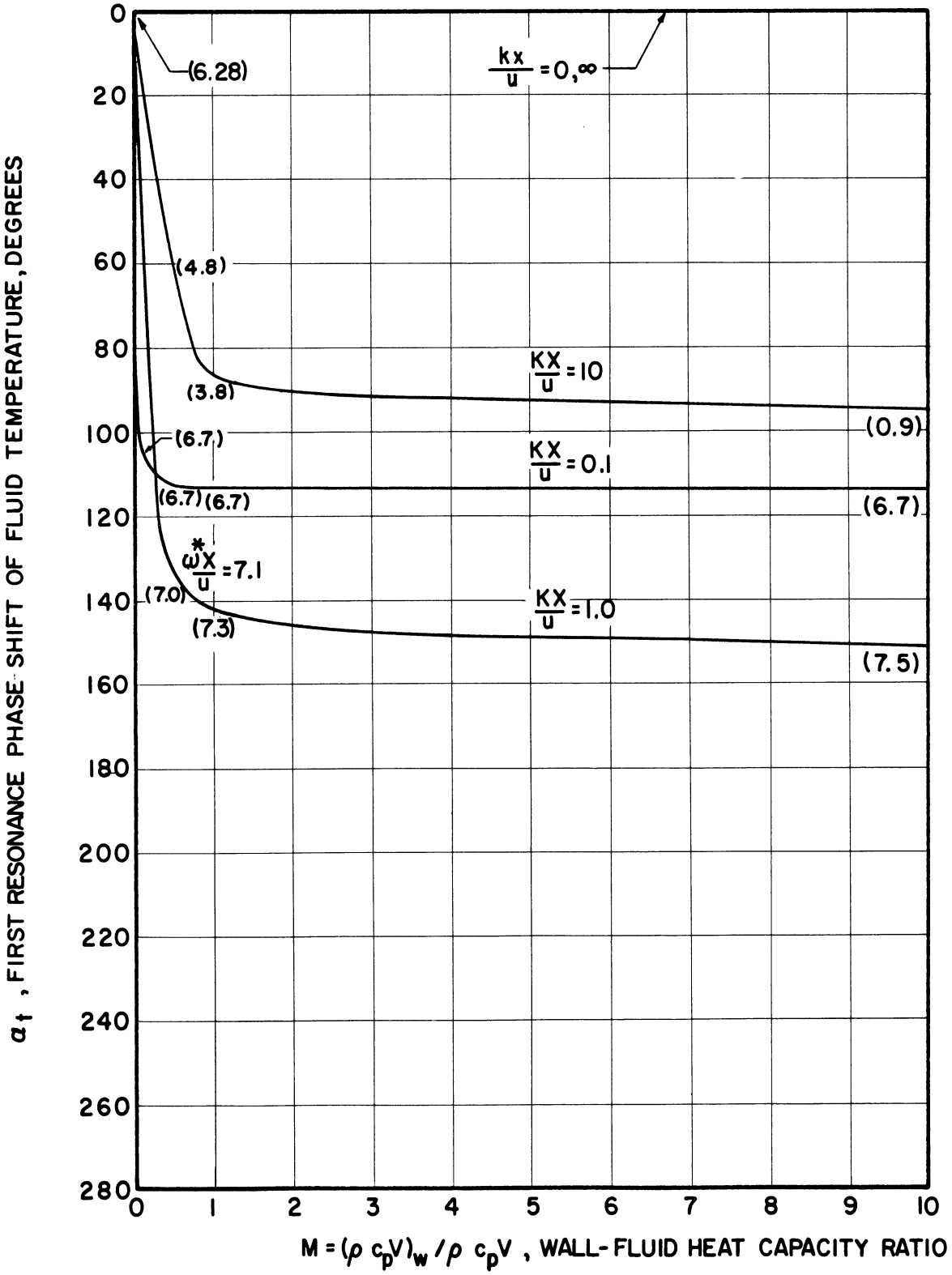

Figure 12. Effects of the Parameters M, $\omega x/u$ and Kx/u on the First Resonance Phase Shift of Fluid Temperature.

NOTE: Bracketed quantity ( ) on curve is value of $\omega x/u$ at first resonance frequency, ω^*.

resonance amplitude-ratio continuously increases as Kx/u increases but the first resonance phase-shift increases from zero with increase in Kx/u and then decreases with further increase in Kx/u, until zero at Kx/u equal to infinity. Physically speaking, as the heat-capacity ratio is increased the heat capacity of the wall relative to the fluid is increased. Consequently, it is equivalent to the increase in the inertness of the system to damp its dynamic characteristics thus causing a decrease in both the amplitude-ratio and the resonance amplitude-ratio, an increase in phase-shift and the resonance phase-shift, and the shifting of the resonance frequency to a lower value.

2. Response at the Transient-Periodic State

The dynamic behavior of the wall and fluid temperature and the fluid-wall temperature difference as shown in Equations (64) through (75) are all functions of six dimensionless parameters M, $M\omega/K$, Kx/u, $\omega x/u$, $K\tau/M$ and $\omega\tau$ among which the parameters Kx/u and $\omega\tau$ are not independent, since

$$\frac{Kx}{u}=\frac{M\left(\frac{\omega x}{u}\right)}{\frac{M\omega}{K}} \qquad \text{and} \qquad \omega\tau=\left(\frac{K\tau}{M}\right)\left(\frac{M\omega}{K}\right)$$

As the system reaches its steady-periodic state the dynamic behavior becomes independent of the parameter $K\tau/M$ and $\omega\tau$, as already discussed in part 1.

Transfer functions expressed by Equations (45), (46) and (47) demonstrate that the Laplace variable $s = -K/M$ is the multiple poles of the infinite order and $s = -\frac{1+M}{\frac{M}{K}}$ is the singular poles, of the wall and

fluid temperatures and the fluid-wall temperature difference. Physically

$$\frac{K}{M} = \frac{h(A/V)_w}{(\rho C_p)_w} = \frac{hA}{(\rho C_p V)_w} \tag{142}$$

where $(\rho CpV)_w$ is the wall heat capacity, 1/hA the surface resistance, and M/K the capacity lag. Therefore the transient state (under any kind of disturbance) of the wall and fluid temperatures and fluid-wall temperature difference decay exponentially with two products: of a physical time τ and the wall time constant K/M and of a physical time τ and $\frac{M+1}{\frac{M}{K}}$. The principle is discussed in References 28 and 29.

Owing to the relative complexity of the equations governing the time domain $\tau x/u \geq 1$ the effects of the various physical parameters on the dynamic characteristics of the wall temperature, the fluid temperature and the fluid-wall temperature difference is briefly discussed in the time domain $0 \leq \tau x/u \leq 1$ for the sinusoidal transient in $\phi(\tau)$.

For a small value of the heat capacity ratio M, Equations (64), (65) and (66) approaches

$$\frac{t_2(x,\tau)}{\Delta\frac{(q/A)}{h}\frac{Kx}{u}} = \frac{1-\cos\omega\tau}{\omega x/u} \tag{143-a}$$

$$\frac{\theta_2(x,\tau)}{\Delta\frac{(q/A)}{h}(1+\frac{Kx}{u})} = \frac{1-\cos\omega\tau}{\frac{\omega}{K}(1+\frac{Kx}{u})} + \frac{\sin\omega\tau}{1+\frac{Kx}{u}} \tag{143-b}$$

$$= \sin\omega\tau \qquad (\text{For } K=0 \text{ only}) \tag{143-c}$$

$$\frac{\Delta t_2(x,\tau)}{\Delta\frac{(q/A)}{h}} = \sin\omega\tau \tag{143-d}$$

in case K=0 the amplitude-ratio of the wall temperature θ_2 oscillates between two values, maximum value +1 and minimum value -1. No transient-periodic state exists, since for small M, the heat capacity of the wall

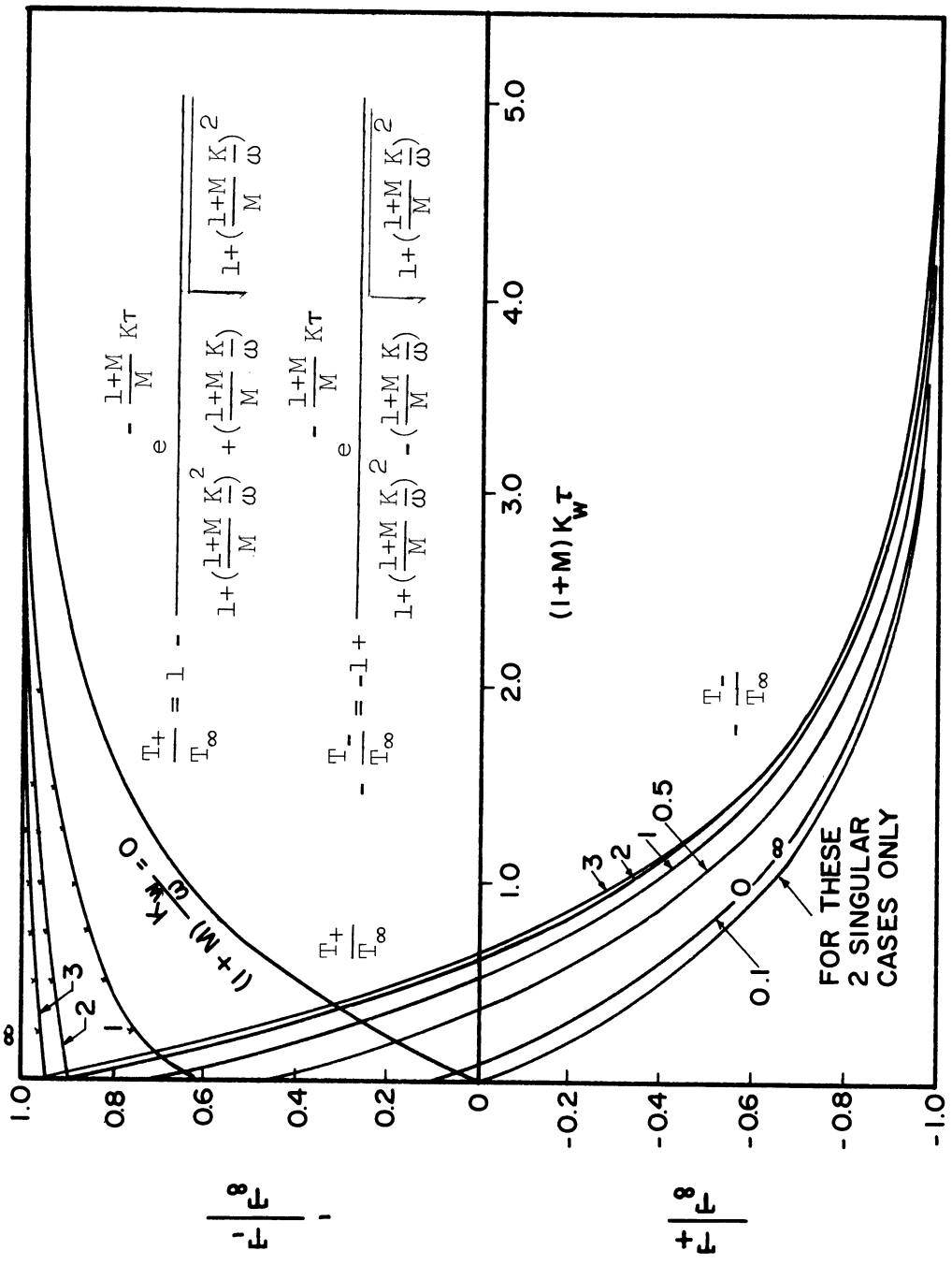

Figure 13. Envelopes Formed by the Points of the Maximum Amplitudes of the Fluid Temperature in the First Time Domain, $1 \geq \tau u/x \geq 0$.

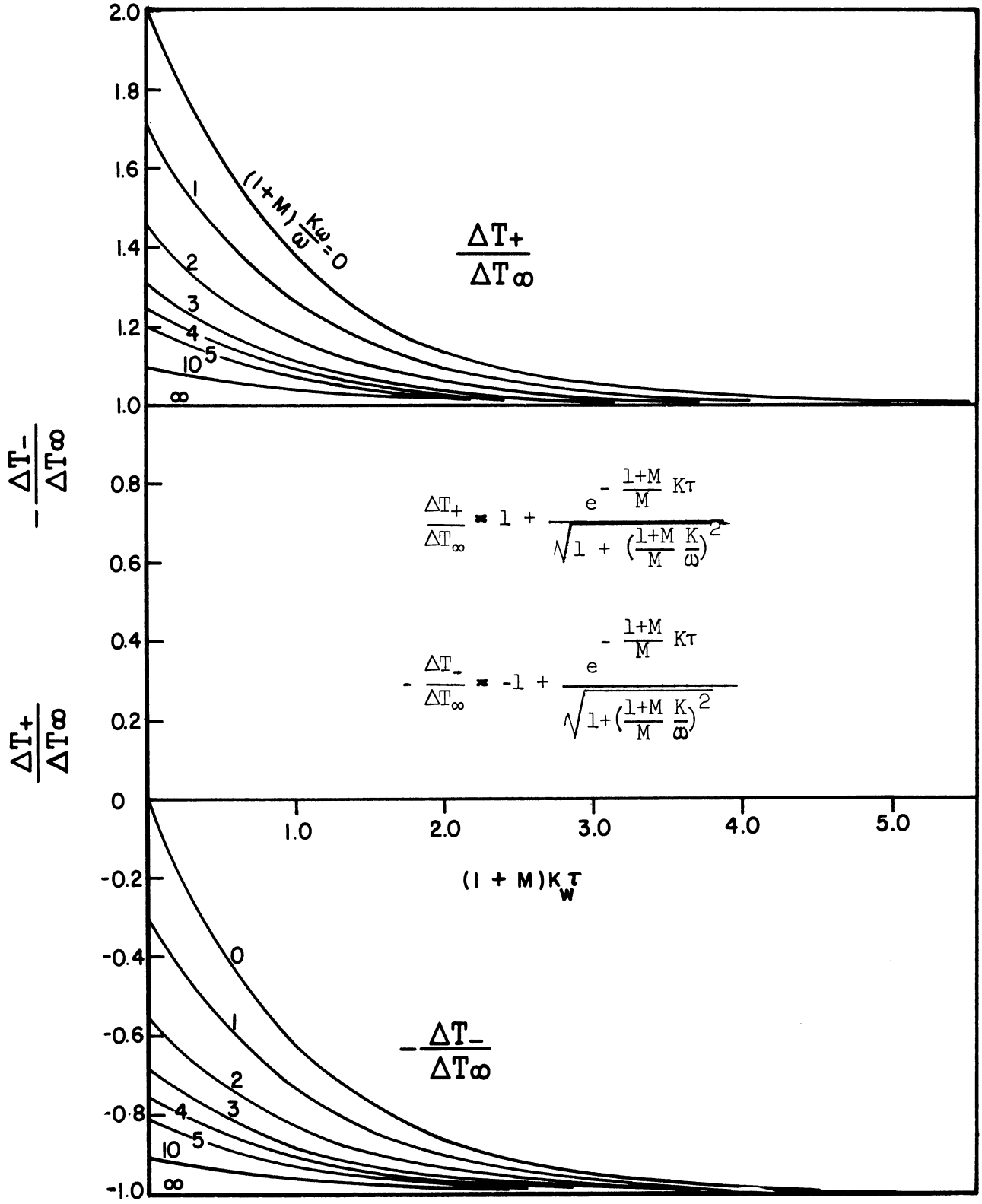

Figure 14. Envelopes Formed by the Points of the Maximum Amplitudes of the Fluid-Wall Temperature Difference in the First Time Domain, $0 \geq \tau u/x \geq 1$.

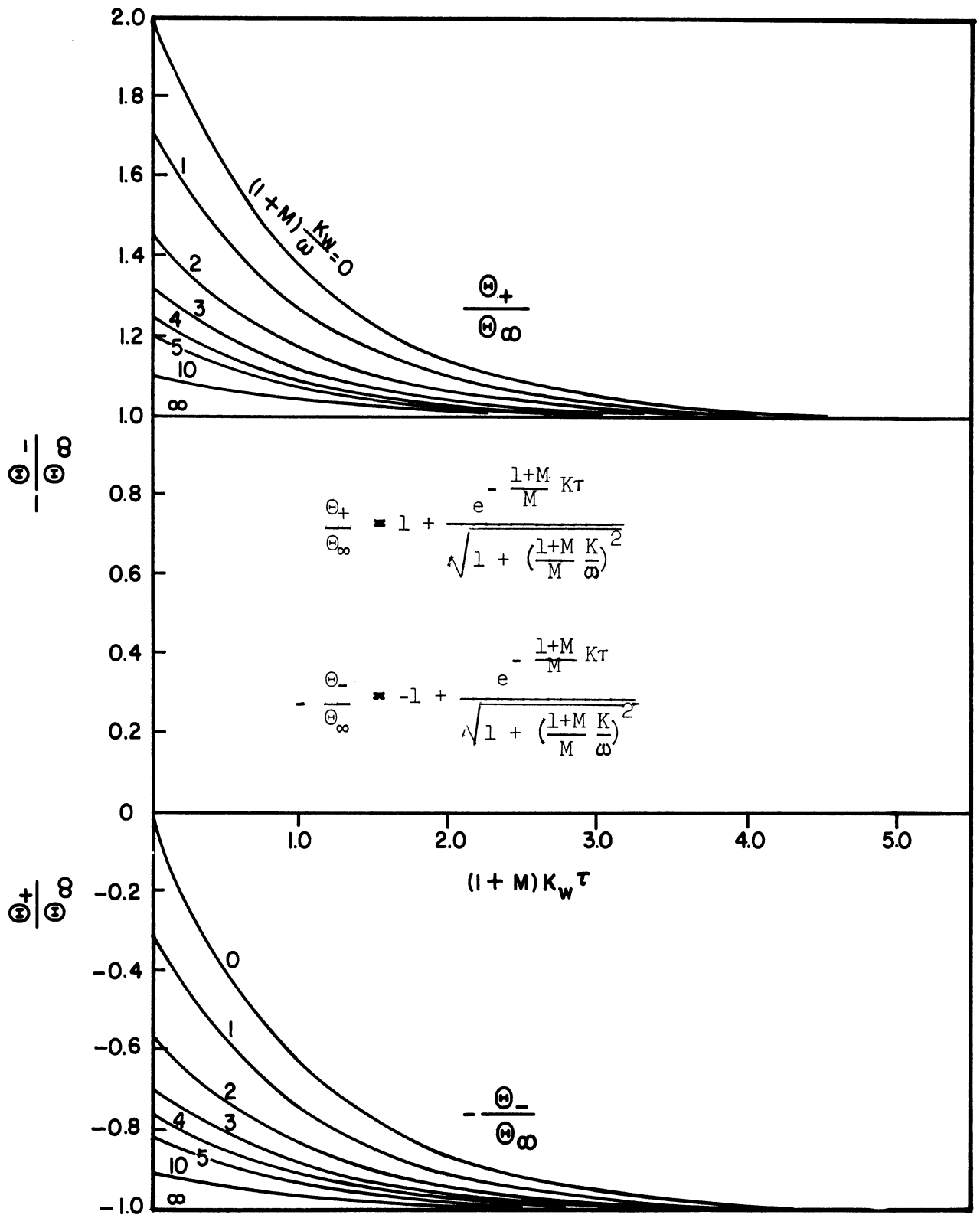

Figure 15. Envelopes Formed by the Points of the Maximum Amplitudes of the Wall Temperature for M= in the First Time Domain, $1 \geq \tau u/x \geq 0$.

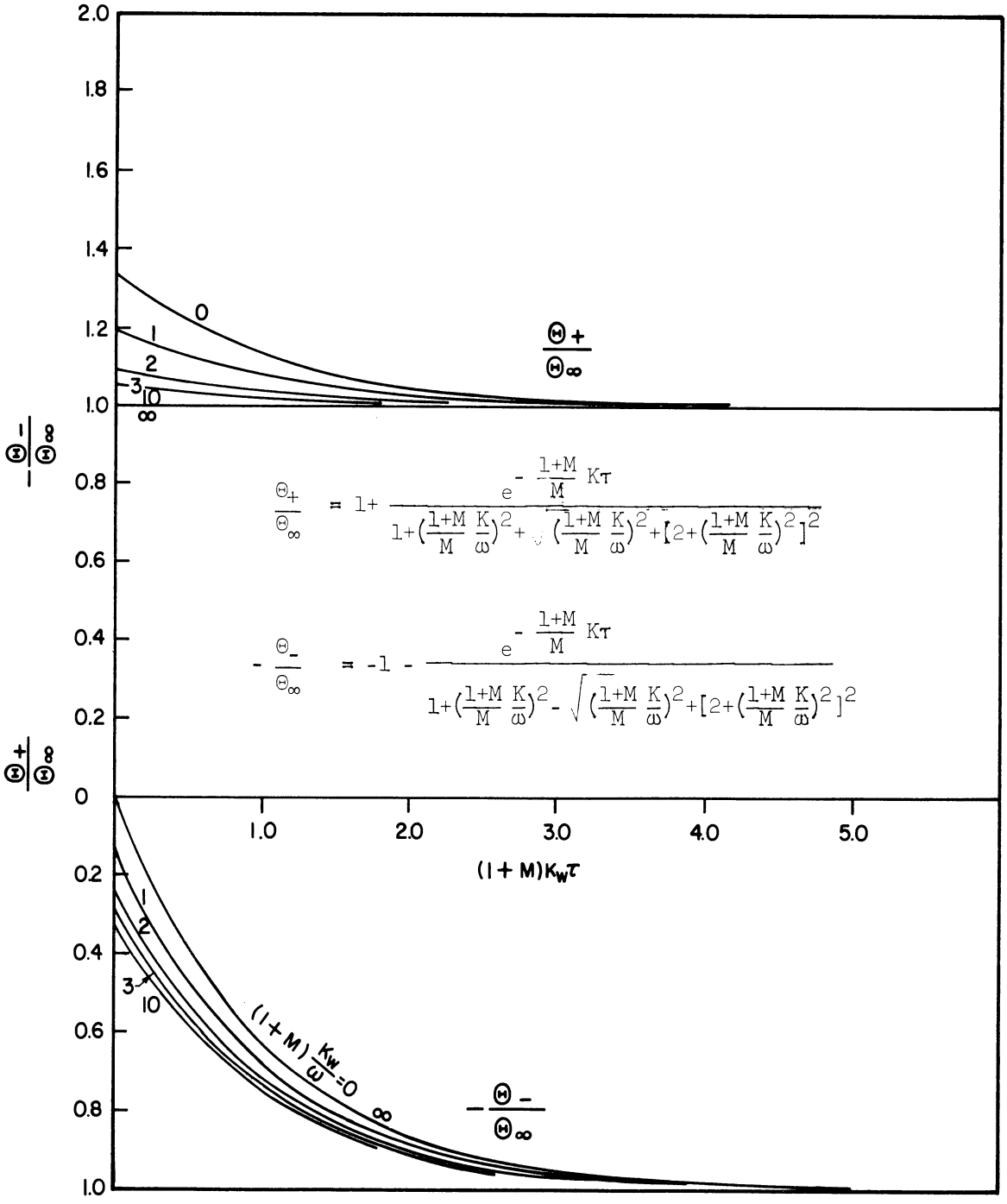

Figure 16. Envelopes Formed by the Points of the Maximum Amplitudes of the Wall Temperature For M = 1, in the First Time Domain $1 \geq \tau u/x \geq 0$.

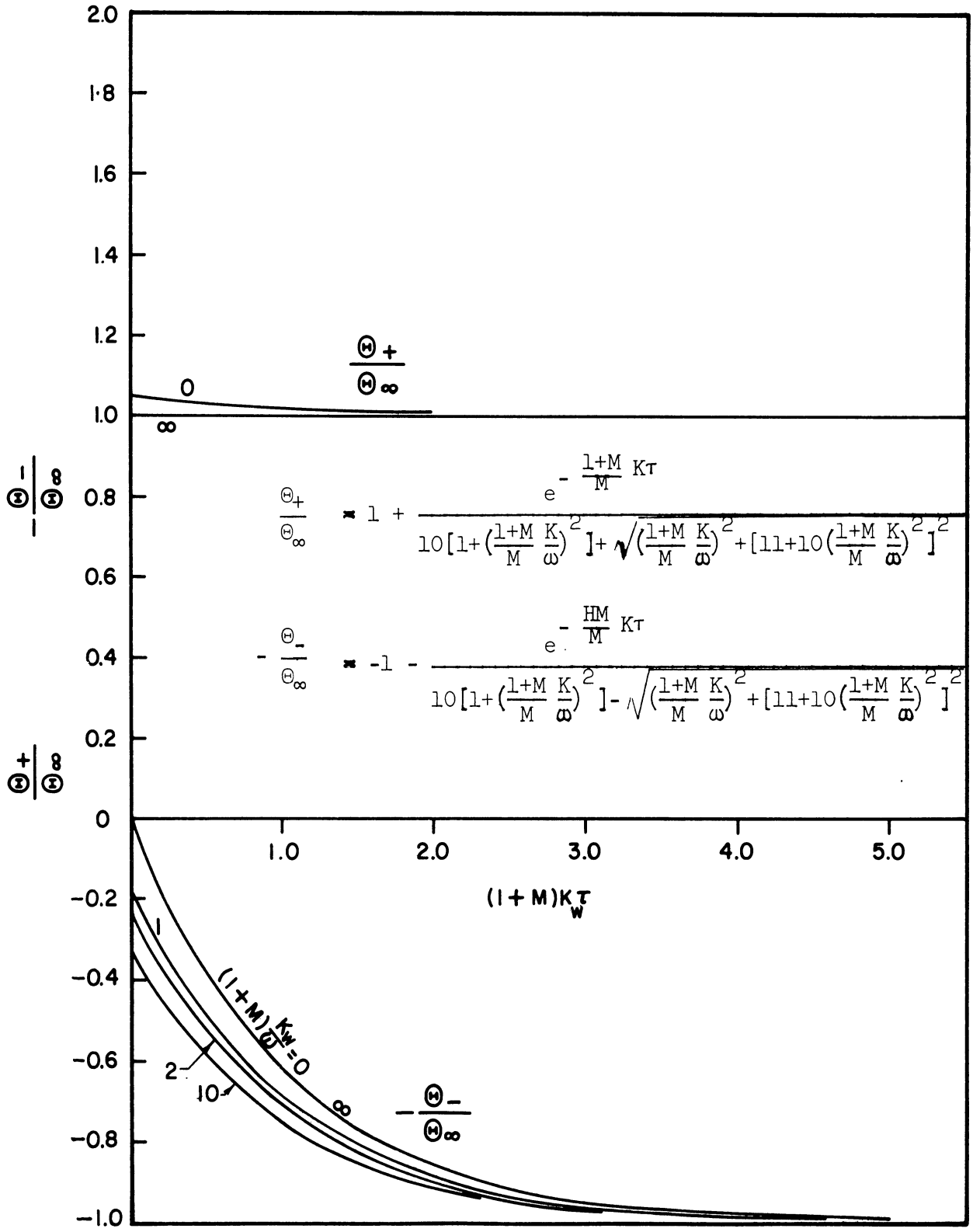

Figure 17. Envelopes Formed by the Points of the Maximum Amplitudes of the Wall Temperature for M = 10, in the First Time Domain, $1 \geq \tau u/x \geq 0$.

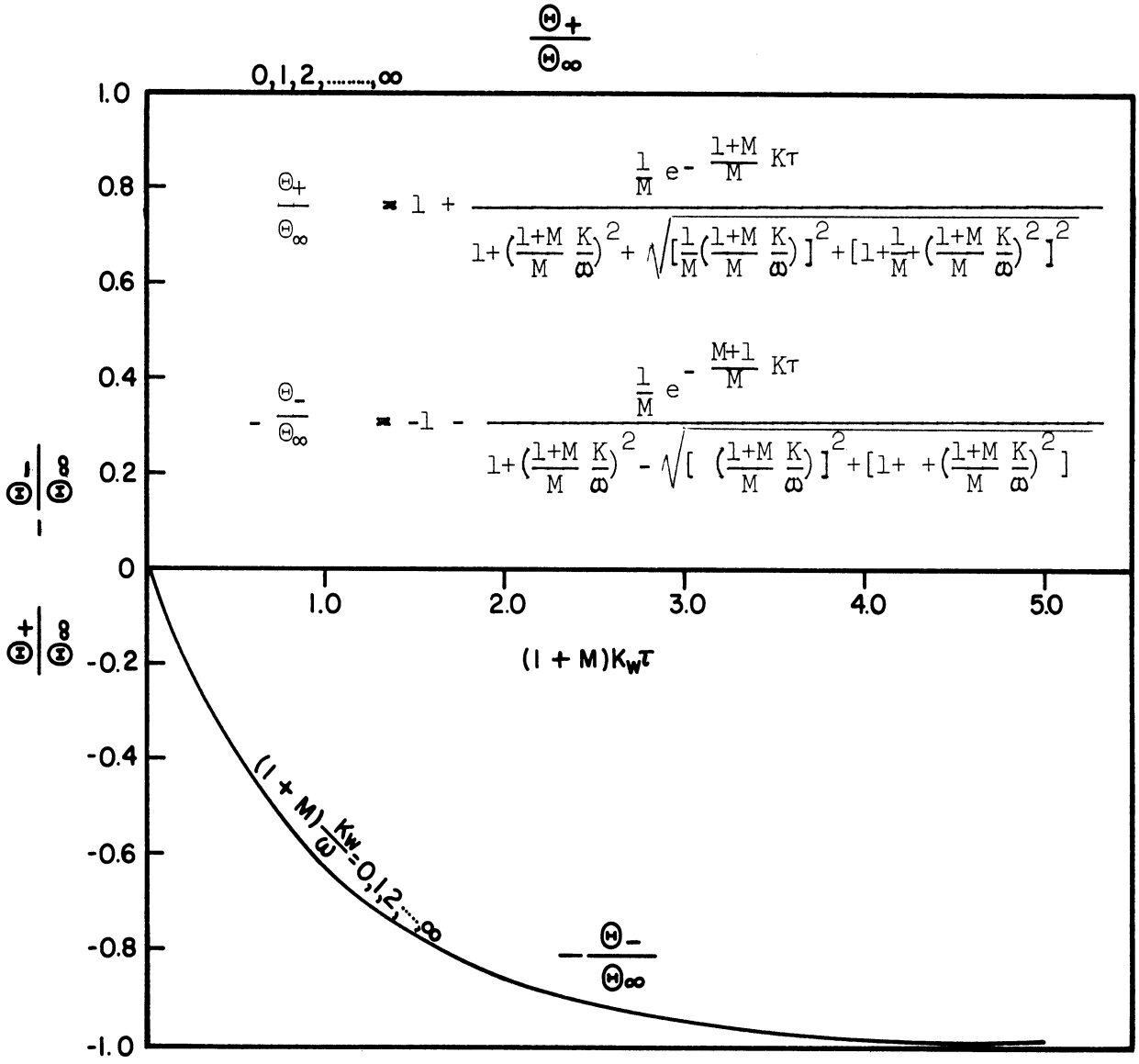

Figure 18. Envelopes Formed by the Points of the Maximum Amplitudes of the Wall Temperature for M = 1000, in the First Time Domain, $1 \geq \tau u/x \geq 0$.

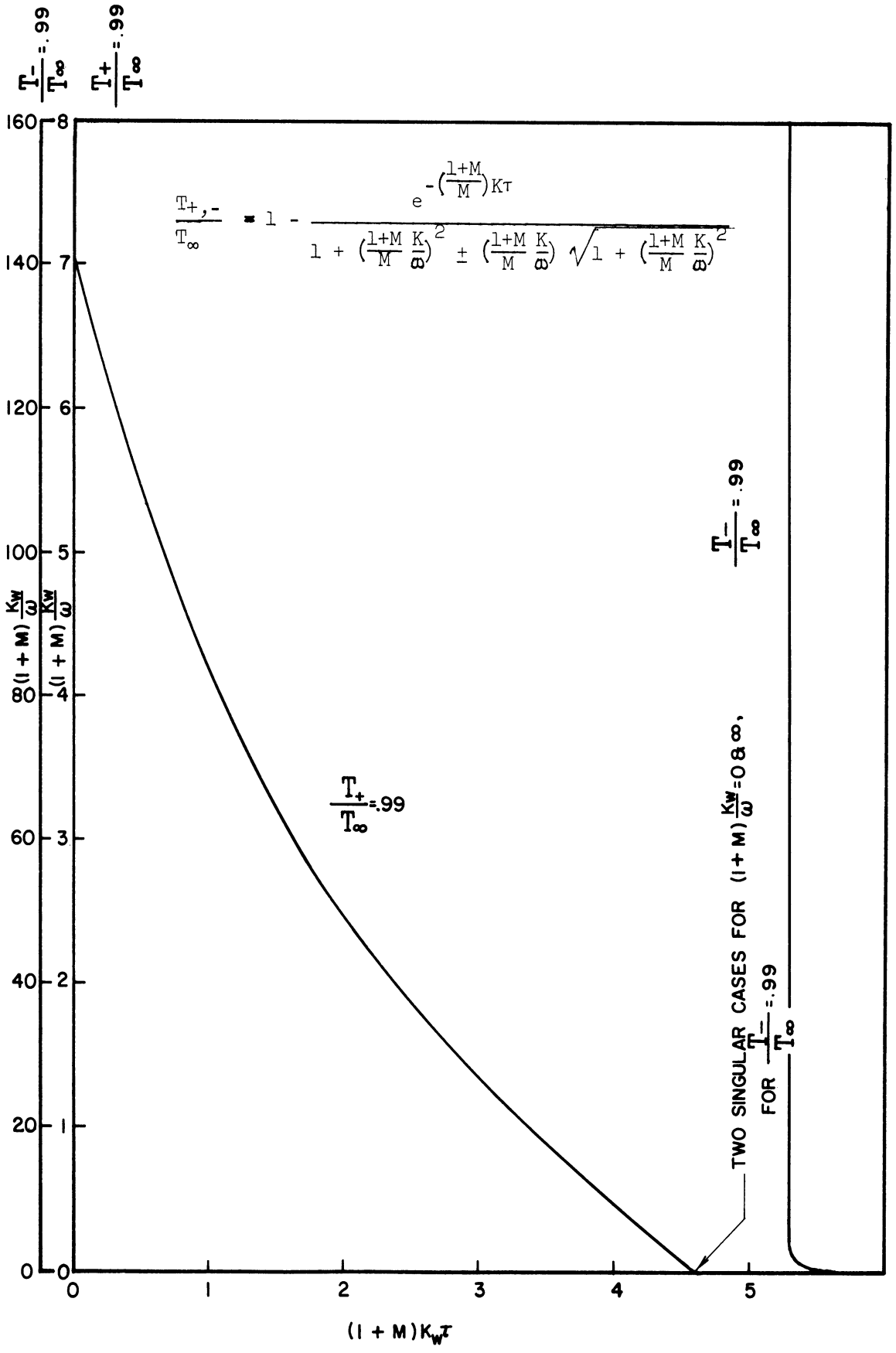

Figure 19. Time Required by $[T(x,\tau)]_{+,-}$ to Reach 99 Per Cent of $[T_\infty(x)]_{+,-}$ in the First Time Domain, $1 \geq \tau u/x \geq 0$.

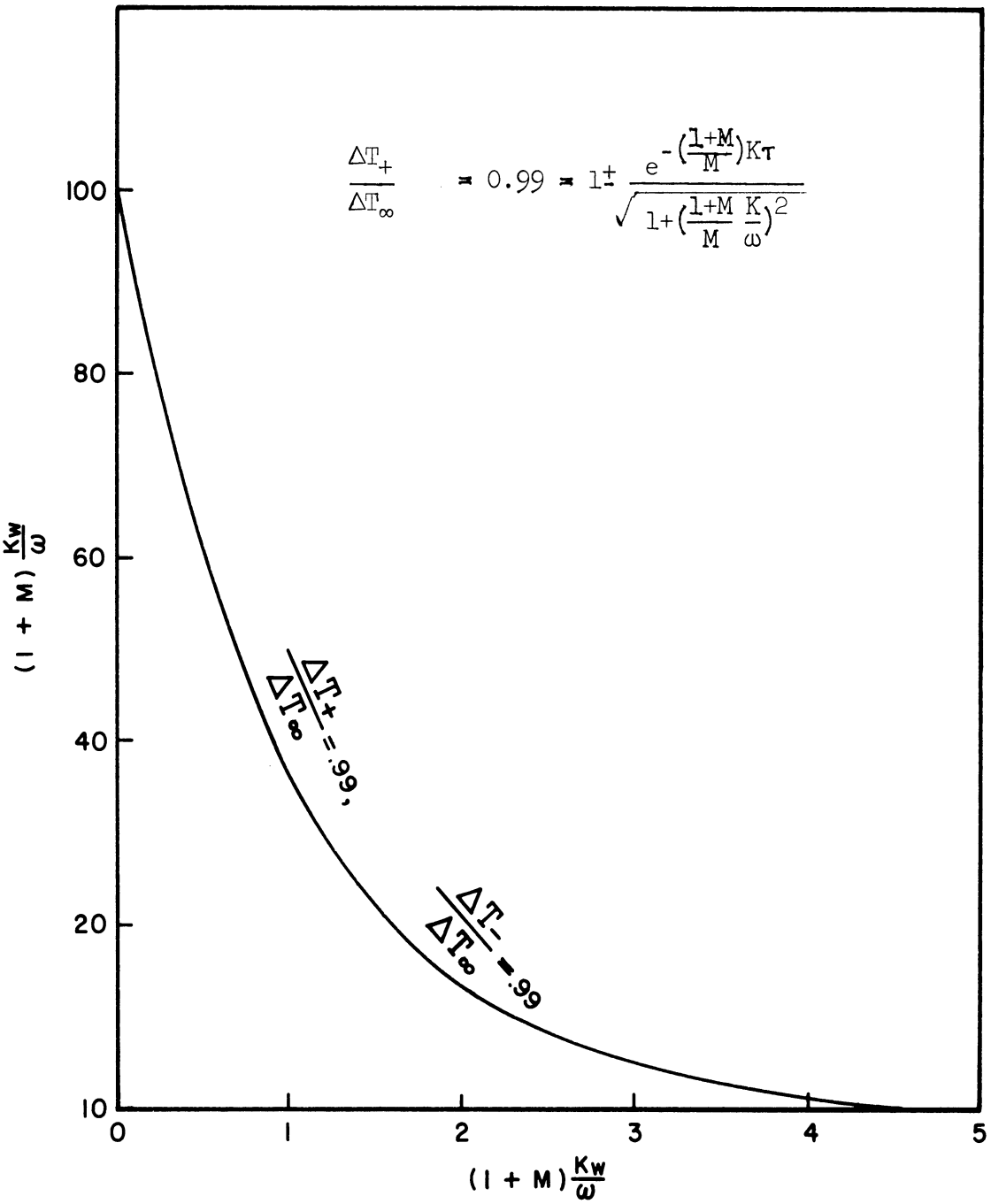

Figure 20. Time Required by $[T(x,\tau)]_{+,-}$ to Reach 99 Per Cent of $[\Delta T_\infty(x)]_{+,-}$ in the First Time Domain, $1 \geq \tau u/x \geq 0$.

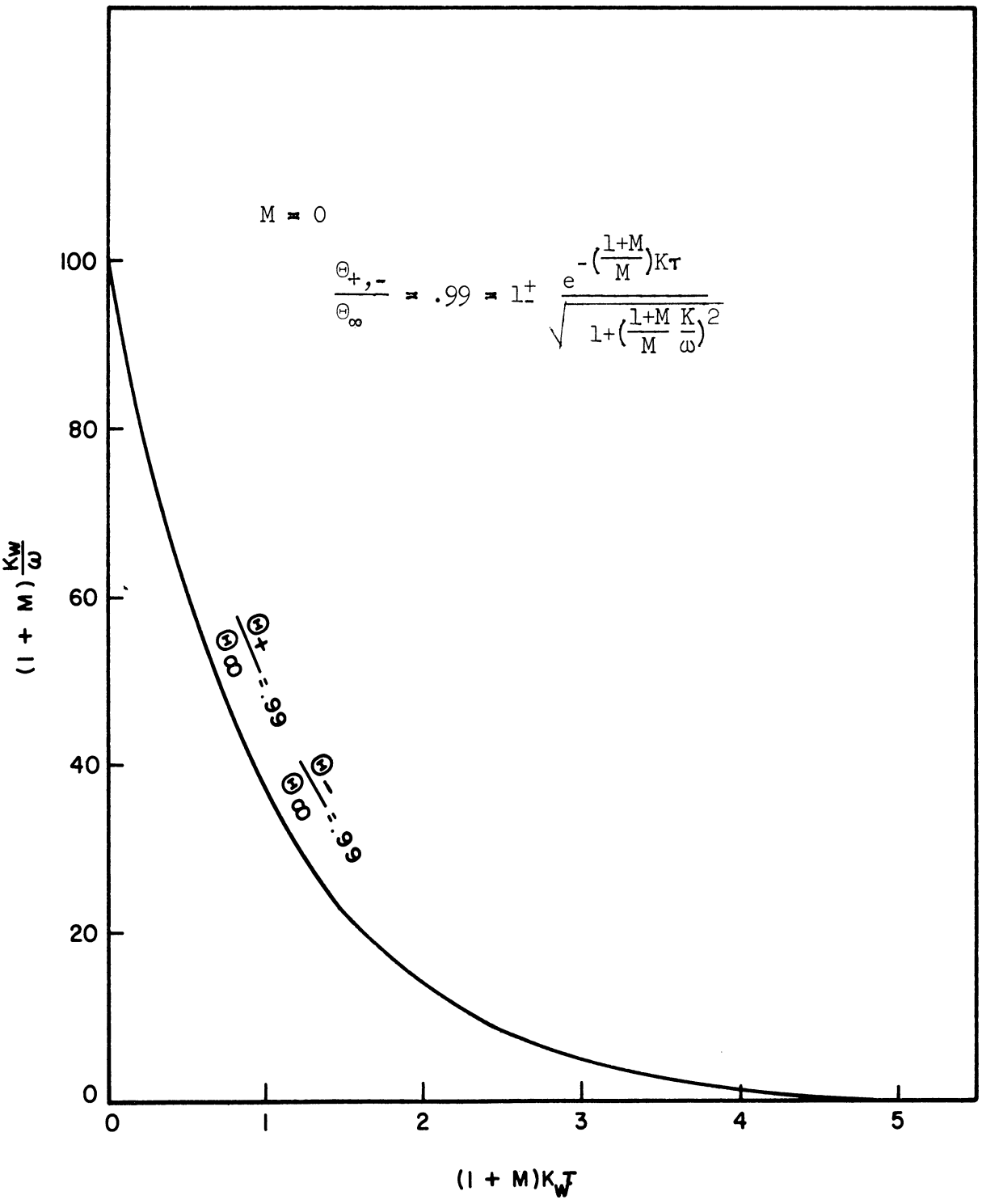

Figure 21. Time Required by $[\Theta(x,\tau)]_{+,-}$ to Reach 99 Per Cent of $[\Theta_\infty(x)]_{+,-}$ for M=0 in the Time Domain, $1 \geq \tau u/x \geq 0$.

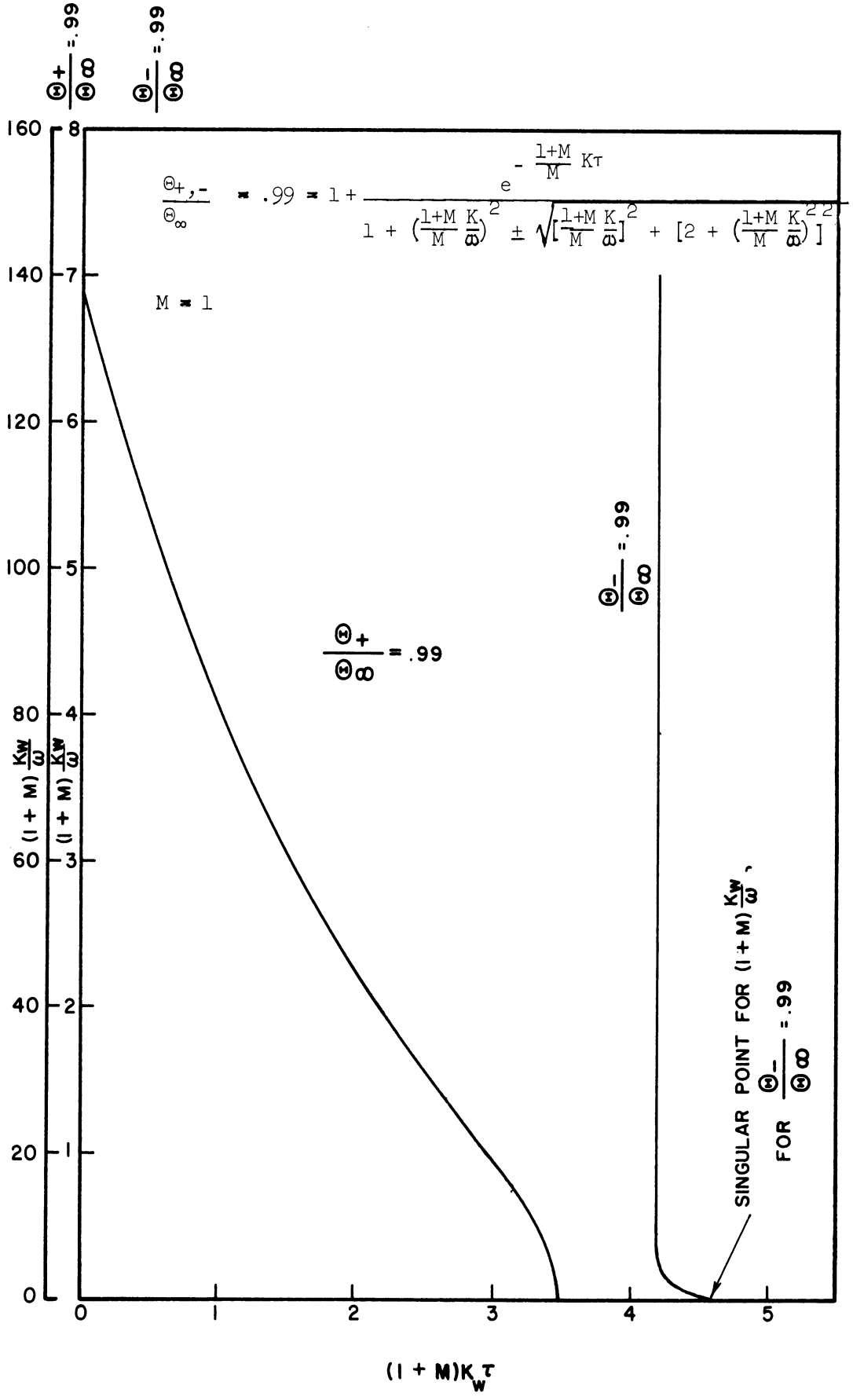

Figure 22. Time Required by $[\Theta(x,\tau)]_{+,-}$ to Reach 99 Per Cent of $[\Theta_\infty(x)]_{+,-}$ for M=1 in the Time Domain, $1 \geq \tau u/x \geq 0$.

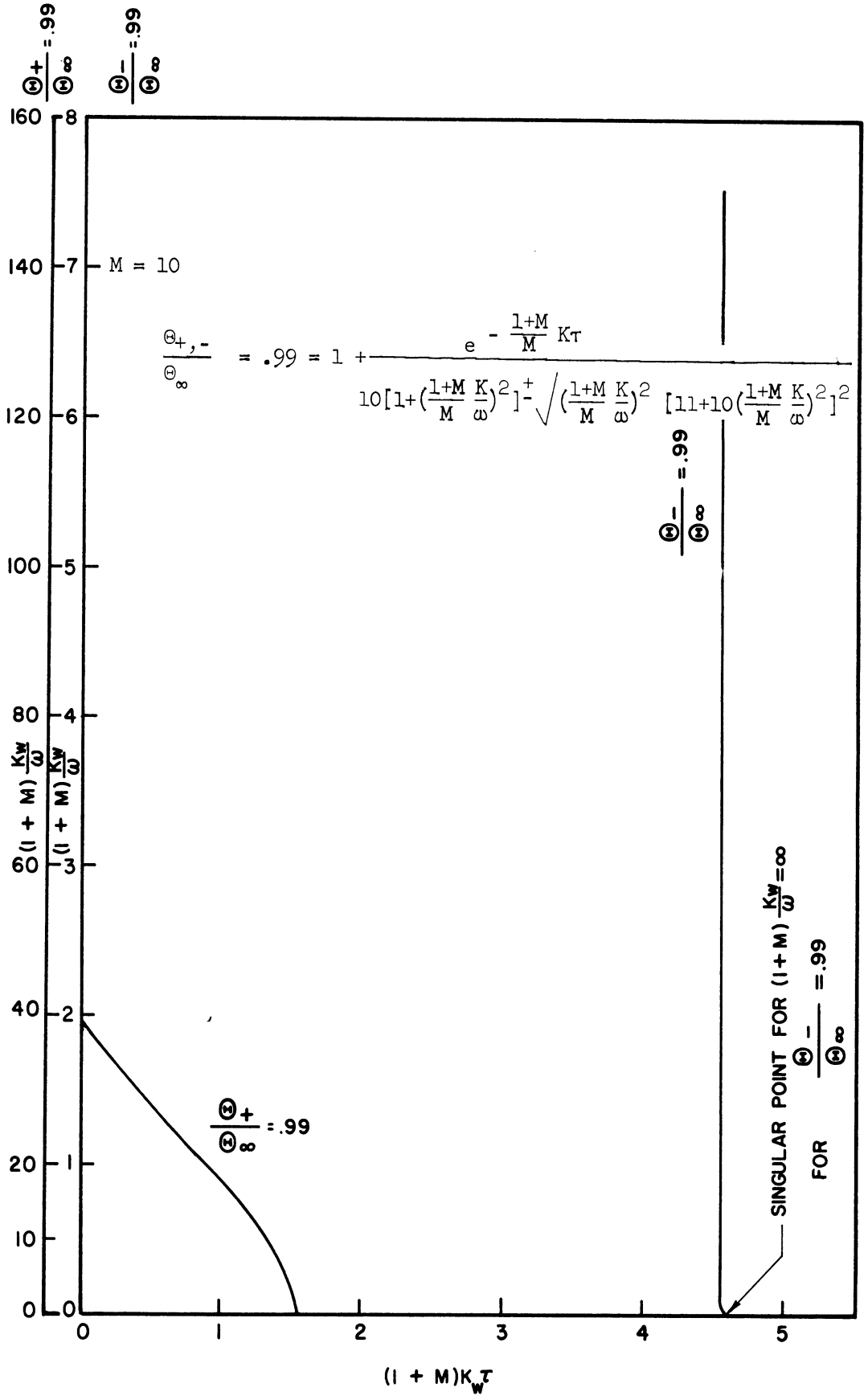

Figure 23. Time Required by $[\Theta(x,\tau)]_{+,-}$ to Reach 99 Per Cent of $[\Theta_\infty(x)]_{+,-}$ for M = 10 in the Time Domain, $1 \geq \tau u/x \geq 0$.

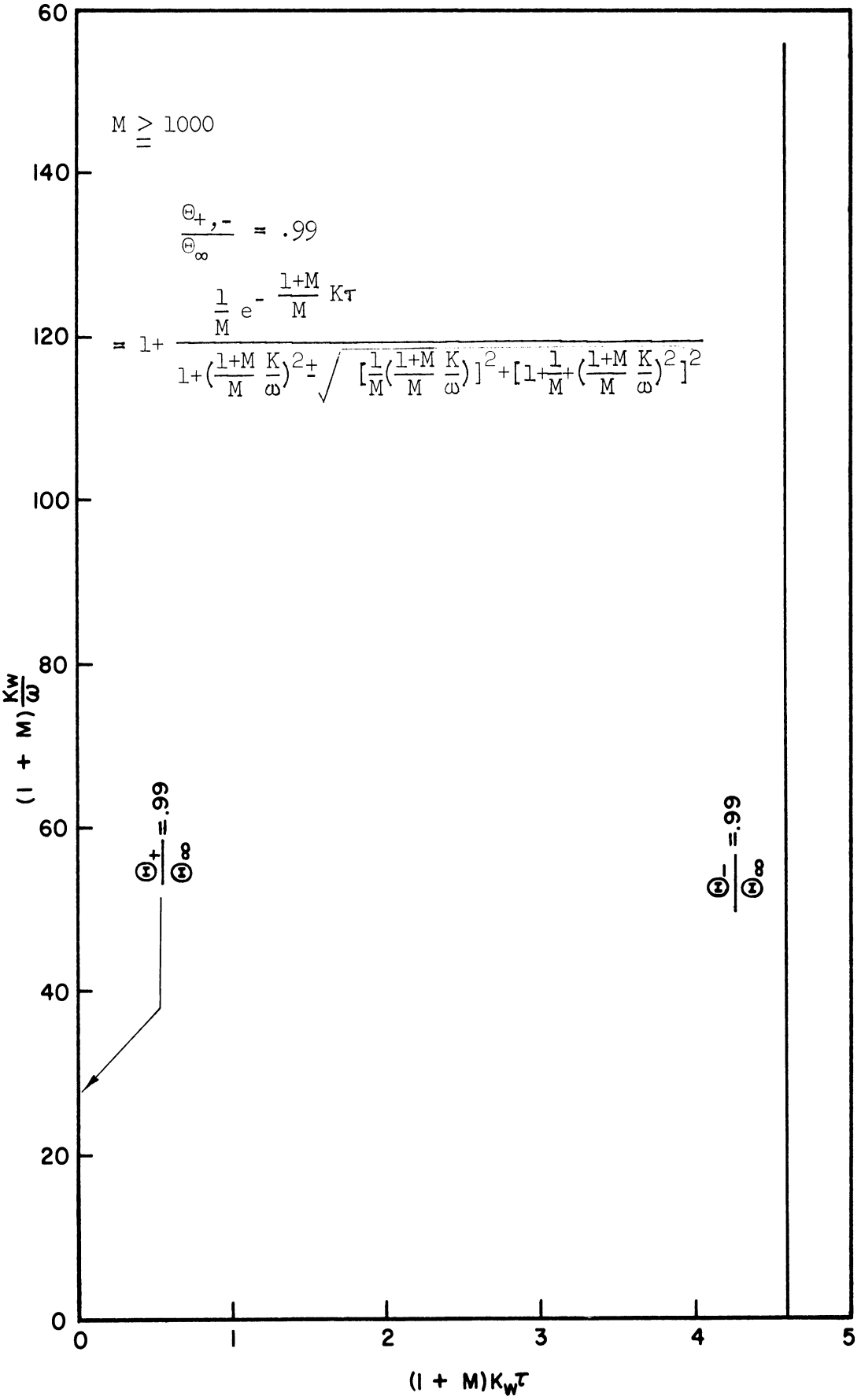

Figure 24. Time Required by $[\Theta(x,\tau)]_{+,-}$ to Reach 99 Per Cent of $[\Theta_\infty(x)]_{+,-}$ for M = 1000 in the Time Domain, $1 \geq \tau u/x \geq 0$.

relative to the fluid is small and the wall responds rapidly to power transients. For large values of M the amplitude-ratio of the wall temperature approaches zero. The amplitude-ratio of the wall temperature is unity at $\omega = 0$ and approaches zero with increase in frequency for a fixed M but increases with Kx/u. The results for the response of the fluid temperature for a small M are discussed in the following section. But for the fluid-wall temperature difference, the same responses as the wall temperature are observed for $M = 0$, $M = \infty$ and $\omega = \infty$. The asymptotic limits of the temperature response functions for the values of $M = 0$, and $\omega = \infty$ are given in Table III.

The envelopes as indicated in Equations (76), (77) and (78) formed by the points of the maximum amplitudes of the fluid and wall temperatures and the fluid-wall temperature difference in the first time domain are shown in Figures 13, 14, 15, 16, 17 and 18. The envelopes of the maximum amplitude of the wall and fluid temperatures and wall-fluid temperature difference in the dimensionless forms is a function of $\frac{M+1}{\frac{K}{M}}$ and ω but is independent of x in this domain as shown by equations in Figures 13-18. Figures 19, 20, 21, 22, 23 and 24 show the time required for the envelopes of the transient-periodic oscillation of the wall and fluid temperatures and the fluid-wall temperature difference in the first time domain to reach the 99 per cent of their steady state values.

3. Dynamic Response of the Heat Exchanger Having a Zero-Wall-Fluid Heat-Capacity Ratio

For a heat exchanger having a zero heat-capacity ratio M, Equation (105) indicates that the fluid temperature has a lag of $\pi/2$ with respect to the power input in the time domain $1 \geq \tau u/x \geq 0$. In this time

domain, the amplitude-ratio of the fluid temperature becomes zero periodically in 2π at $\omega\tau = 2n\pi$, where $n = 0, 1, 2, \ldots$, with a constant maximum amplitude-ratio of $\frac{2}{\frac{\omega x}{u}}$ at constant $\frac{\omega x}{u}$ as indicated in Equation (105). The amplitude-ratio is a function of ω, x/u and τ and the maximum value of the amplitude-ratio, a function of $\omega x/u$. For this case of $M = 0$, the amplitude-ratio of the fluid temperature becomes a function of just one parameter $\omega x/u$, as indicated in Equations (103) and (104) or (107) and (108) and does not exhibit a transient-periodic characteristic. Equations (103) and (104), which show the response of the amplitude-ratio and phase-shift, are also presented graphically in Figures 25-a and 26-a. They demonstrate that the fluid temperature amplitude-ratio decreases from unity to zero and the phase-shift increases from zero to 180 degrees for changes in the dimensionless frequency $\omega x/u$ from zero to 2π. As the dimensionless frequency $\omega x/u$ increases from 2π, the amplitude ratio increases from zero, reaches a maximum when $\omega x/u$ is of the order of 3π and then decreases to zero at 4π. During the same period of the frequency change, the phase-shift increases from zero to 180 degrees. The phenomenon of resonance occurs every 2π interval of the dimensionless frequency, with consecutive decrease in the magnitudes of the resonance amplitude-ratios, and repeats in the phase-shift change from zero to 180 degrees. A dimensionless frequency $\omega x/u$ satisfying Equation (109) is the one corresponding to either a maximum or minimum amplitude-ratio, which could be evaluated by Equation (103).

The phenomenon of resonance of the fluid temperature in a heat exchanger having $M = 0$ may be explained as follows: The internal heat sources of the heat exchanger generate an uniformly distributed sinusoidally

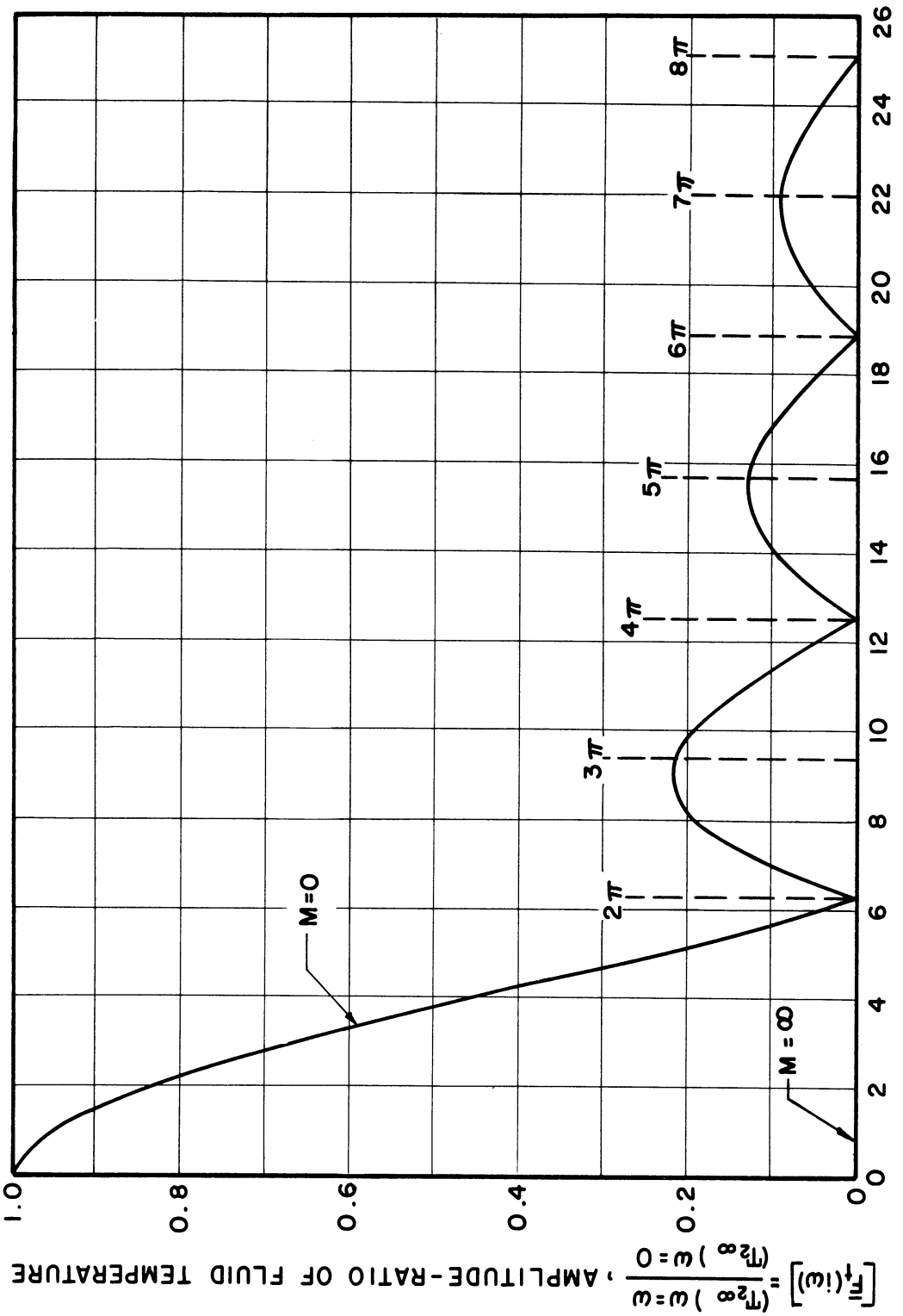

Figure 25-a. Amplitude-Ratio Response of the Fluid Temperature for M=0.

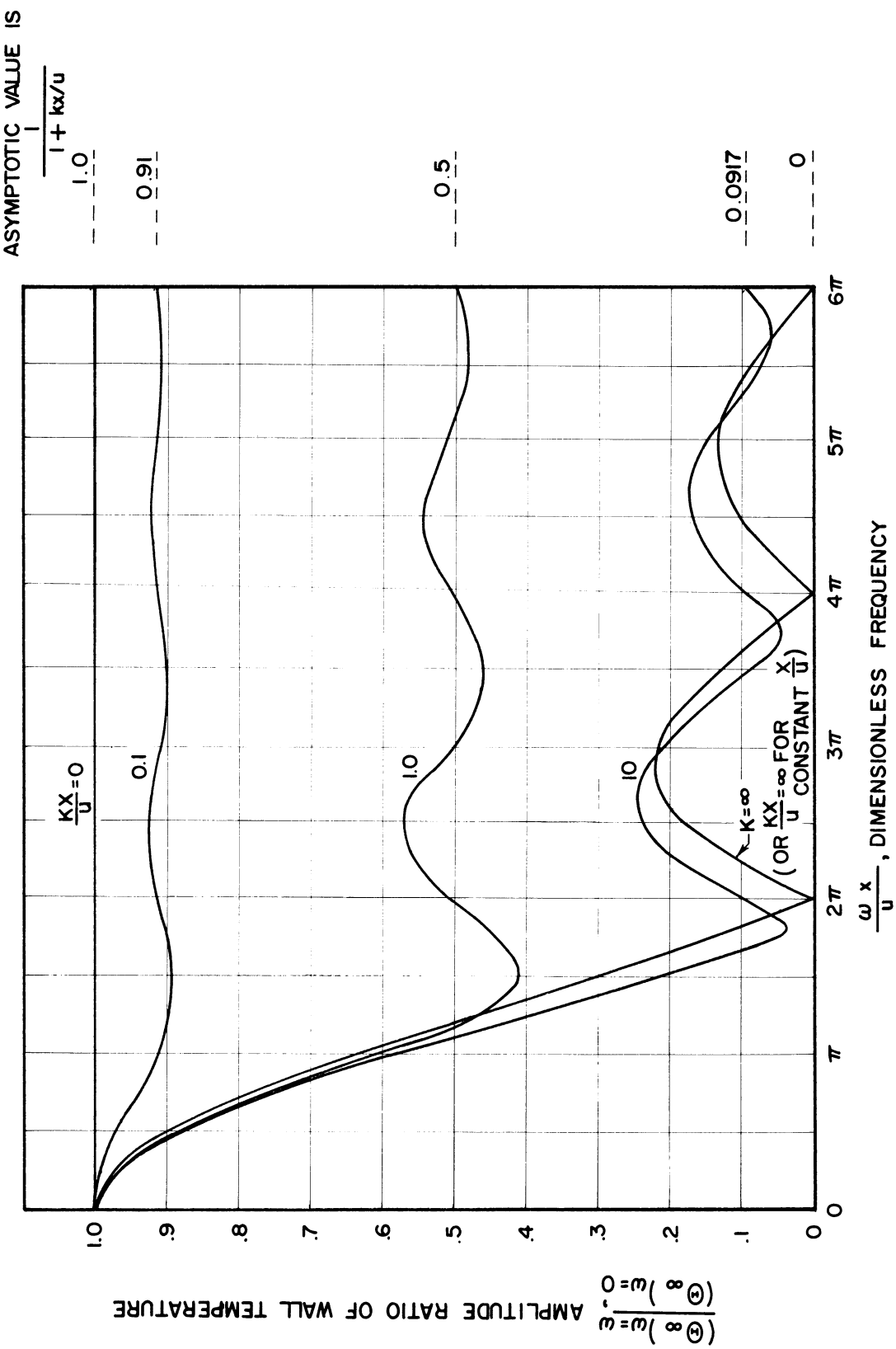

Figure 25-b. Amplitude-Ratio Response of the Wall Temperature for M=0.

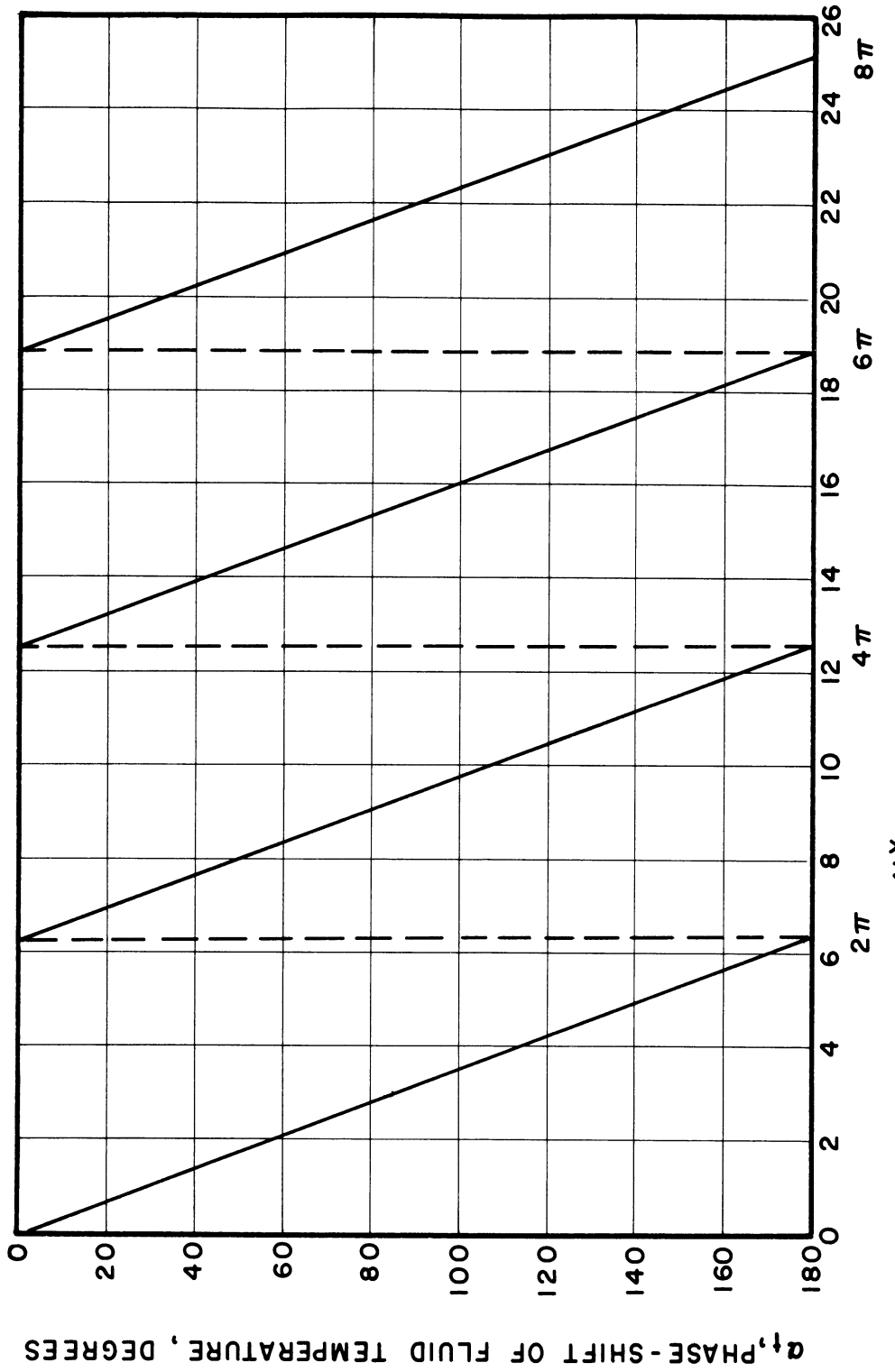

Figure 26-a. Phase-Shift Response of the Fluid Temperature for M=0.

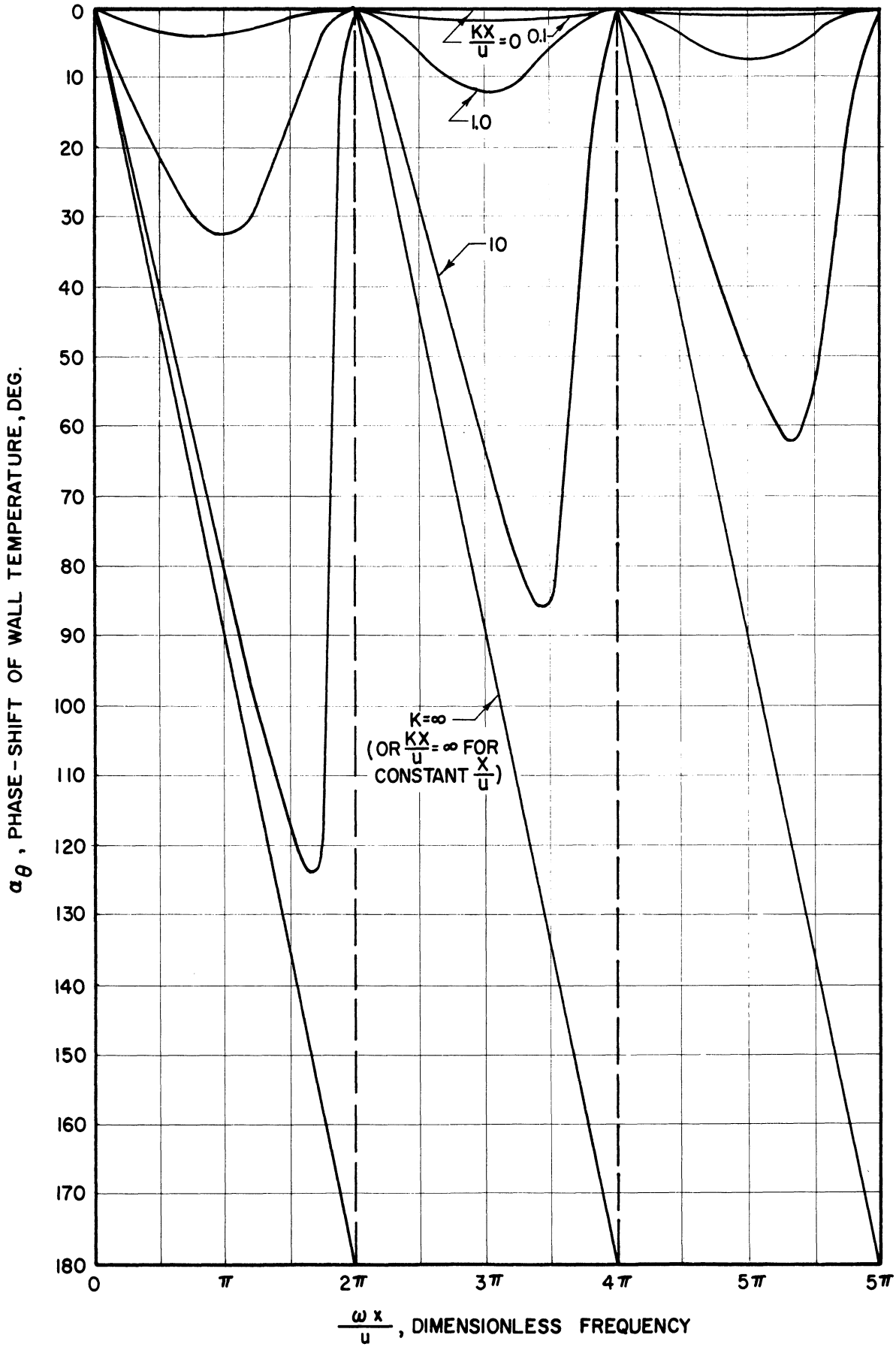

Figure 26-b. Phase-Shift Response of the Wall Temperature for M=0.

time variant heat energy having a frequency ω. Imagine a fluid particle which enters the heat exchanger at $\tau = 0$ at which time the heat generation is given by $p_x'' = p_{xo}'' + \Phi \sin\omega\tau'$, as shown in Figure 5. The change in the thermal state of the particle is graphically shown in Figure 27. The temperature amplitude-ratio of the particle changes as a function of $\omega\tau'$, which may be called the inlet lag and $\omega\tau$, where τ is the elapsed time after the particle has entered the heat exchanger, as shown in Equation (116). Figure 27 demonstrates that for a zero inlet lag $\omega\tau'$, the temperature amplitude-ratio of the fluid particle increases following the increase in heat generation and reaches its maximum at the dimensionless time $\omega\tau > \pi/2$ and less than π after the heat generation rate reaches its maximum. It then decreases reaching zero at $\omega\tau = 2\pi$ when the heat generation returns to its mean value. As the particle travels further along the heat exchanger, the temperature amplitude-ratio of the particle repeat periodically in 2π, with a gradual decrease in its maximum values.

Physically speaking this is due to the fact that temperature $t(\tau)$ of the particle at $\omega\tau = 2\pi, 4\pi, \ldots$ is equal to the steady-state component of its temperature $t_1(\tau)$. In other words, the transient component of its temperature $t_2(\tau)$ equals to zero, since there is no net increase or decrease in the enthalpy of the particle. At $\omega\tau = 2\pi, 4\pi, \ldots$ the total heat generation during each period is equal to the heat generated by its steady-state component during that period, therefore, the temperature of the fluid particle at $\omega\tau = 2\pi, 4\pi, \ldots$ must be equal to that of the steady-state component $t_1(\tau)$. Figure 11 also shows that the temperature amplitude-ratio of the particles having different values in $\omega\tau'$ have zero values at $\omega\tau = 2\pi, 4\pi, \ldots$. This could be confirmed by

TABLE IV

SUMMARY OF EQUATIONS FOR DYNAMIC RESPONSE
OF HEAT EXCHANGERS HAVING M=0

(a) $1 \geq \tau u/x \geq 0$

$$t_2 = \frac{\Delta(q/A)}{h}\frac{1-\cos\omega\tau}{\frac{\omega}{K}} \qquad \frac{t_2}{t_{2\omega=0}} = \frac{t_2}{\frac{\Delta(q/A)}{h}\frac{Kx}{u}} = \frac{1-\cos\omega\tau}{\omega x}$$

$$\theta_2 = \frac{\Delta(q/A)}{h}\frac{1-\cos\omega\tau}{\frac{\omega}{K}} + \frac{\Delta(q/A)}{h}\sin\omega\tau \qquad \frac{\theta_2}{\theta_{2\omega=0}} = \frac{\theta_2}{\frac{\Delta(q/A)}{h}\left(1+\frac{Kx}{u}\right)} = \frac{1-\cos\omega\tau+\frac{\omega}{K}\sin\omega\tau}{\frac{\omega}{K}\left(1+\frac{Kx}{u}\right)}$$

$$\Delta t_2 = \frac{\Delta(q/A)}{h}\sin\omega\tau \qquad \frac{\Delta t_2}{\Delta t_{2\omega=0}} = \frac{\Delta t_2}{\frac{\Delta(q/A)}{h}} = \sin\omega\tau$$

Special case for K=0 (or $\rho Cp = \infty$)

$$t_2 = 0 \qquad \frac{t_2}{t_{2\omega=0}} = \frac{t_2}{\frac{\Delta(q/A)}{h}} = 0$$

$$\theta_2 = \frac{\Delta(q/A)}{h}\sin\omega\tau \qquad \frac{\theta_2}{\theta_{2\omega=0}} = \frac{\theta_2}{\frac{\Delta(q/A)}{h}} = \sin\omega\tau$$

$$\Delta t_2 = \frac{\Delta(q/A)}{h}\sin\omega\tau \qquad \frac{\Delta t_2}{\Delta t_{2\omega=0}} = \frac{\Delta t_2}{\frac{\Delta(q/A)}{h}} = \sin\omega\tau$$

TABLE IV (CONT'D)

(b) $\tau u/x \geq 1$

Temperature	Dimensionless Temperature	Amplitude-Ratio	Phase-Shift
$t_2 = \frac{\Delta(q_A)}{h}\frac{(1-\cos\omega\tau)}{\frac{\omega}{K}} - \frac{\Delta(q_A)}{h}\frac{(1-\cos\omega\tau^*)}{\frac{\omega}{K}}$ $= \frac{\Delta(q_A)}{h}\frac{\cos\omega\tau^* - \cos\omega\tau}{\frac{\omega}{K}}$	$\frac{t_2}{t_{2\omega=0}} = \frac{t_2}{\frac{\Delta(q_A)}{h}\frac{Kx}{u}} = \frac{\cos\omega\tau - \cos\omega\tau^*}{\frac{\omega x}{u}}$ $= \frac{2(1-\cos\frac{\omega x}{u})}{\frac{\omega x}{u}}\sin\left[\omega\tau - \tan^{-1}\left(\frac{1-\cos\frac{\omega x}{u}}{\sin\frac{\omega x}{u}}\right)\right]$	$\lvert\bar{F}_t(i\omega)\rvert = \frac{(T_\infty)_{\omega=\omega}}{(T_\infty)_{\omega=0}} = \frac{\sqrt{2(1-\cos\frac{\omega x}{u})}}{\frac{\omega x}{u}}$	$\alpha_t = \tan^{-1}\left(\frac{1-\cos\frac{\omega x}{u}}{\sin\frac{\omega x}{u}}\right)$
$\theta_2 = \frac{\Delta(q_A)}{h}\frac{(1-\cos\omega\tau)}{\frac{\omega}{K}} + \frac{\Delta(q_A)}{h}\sin\omega\tau$ $- \frac{\Delta(q_A)}{h}\frac{(1-\cos\omega\tau^*)}{\frac{\omega}{K}}$ $= \frac{\Delta(q_A)}{h}\frac{(\cos\omega\tau^* - \cos\omega\tau + \frac{\omega}{K}\sin\omega\tau)}{\frac{\omega}{K}}$	$\frac{\theta_2}{\theta_{2\omega=0}} = \frac{\theta_2}{\frac{\Delta(q_A)}{h}(1+\frac{Kx}{u})} = \frac{\cos\omega\tau^* - \cos\omega\tau + \frac{\omega}{K}\sin\omega\tau}{\frac{\omega}{K}(1+\frac{Kx}{u})}$ $= \frac{\frac{K}{\omega}}{1+\frac{Kx}{u}}\sqrt{(\cos\frac{\omega x}{u}-1)^2 + (\frac{\omega}{K}+\sin\frac{\omega x}{u})^2}$ $\cdot \sin\left[\omega\tau - \tan^{-1}\left(\frac{1-\cos\frac{\omega x}{u}}{\frac{\omega}{K}+\sin\frac{\omega x}{u}}\right)\right]$	$\lvert\bar{F}_\theta(i\omega)\rvert = \frac{(\Theta)_{\omega=\omega}}{(\Theta_\infty)_{\omega=0}}$ $= \frac{\frac{K}{\omega}}{1+\frac{Kx}{u}}\sqrt{(\cos\frac{\omega x}{u}-1)^2 + (\frac{\omega}{K}+\sin\frac{\omega x}{u})^2}$	$\alpha_\theta = \tan^{-1}\left(\frac{1-\cos\frac{\omega x}{u}}{\frac{\omega}{K}+\sin\frac{\omega x}{u}}\right)$
$\Delta t_2 = \frac{\Delta(q_A)}{h}\sin\omega\tau$	$\frac{\Delta t_2}{\Delta t_{2\omega=0}} = \frac{\Delta t_2}{\frac{\Delta(q_A)}{h}} = \sin\omega\tau$	$\lvert\bar{F}_{\Delta t}(i\omega)\rvert = \frac{(\Delta T_\infty)_{\omega=\omega}}{(\Delta T_\infty)_{\omega=0}} = 1$	$\alpha_{\Delta t} = 0$

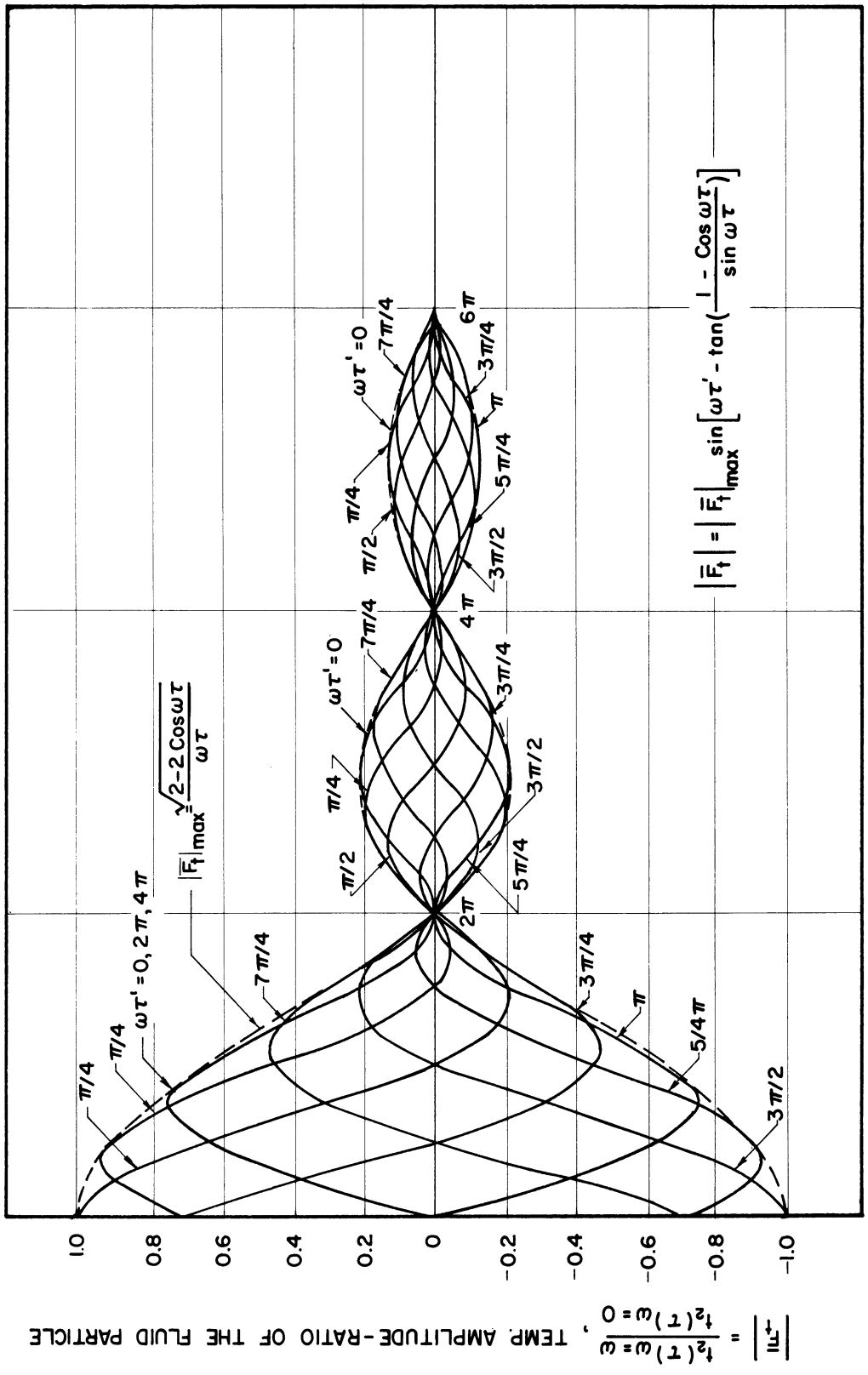

Figure 27. Change of the Temperature Amplitude-Ratio of the Fluid Particles After Entering the Heat Exchanger Having the Time-Dependent Sinusoidal Heat Sources for M=0.

Equation (121), which indicates that the temperature of the particle $t(\tau)$ is equal to the temperature of the steady-state component $t_1(\tau)$ when $\omega\tau = 2n\pi$ irrespective of its inlet lag $\omega\tau'$. This is a result of the total heat generation during each 2π period being equal to its steady-state heat generation and consequently there is no net change in enthalpy for all the fluid particles. Since x/u is the physical time required for a fluid particle flowing at a velocity u to traverse the distance x, the dimensionless time $\omega\tau$ can be expressed by $\omega x/u$. Consequently one may conclude that the transient components of the fluid temperature, or the amplitude-ratio is equal to zero at $\omega x/u = 2\pi, 4\pi, 6\pi, \ldots$.

If one substitutes $\omega\tau$ by $\omega\frac{x}{u}$ in Figure 27, the envelope of the temperature amplitude-ratio formed by the particles having different inlet lags is identical with the amplitude-ratio response of the fluid temperature shown in Figure 25 -a.

4. Frequency Response of the Heat Exchanger Having the Sinusoidal Inlet Fluid Temperature*

The frequency response characteristics when the internal heat generation is held constant and a sinusoidal disturbance is given to the inlet fluid temperature is obtained as follows from Equation (39) by substituting $\bar{\phi} = 0$,

$$\bar{t}_2 = \bar{t}_0^* e^{-\frac{S\left(\frac{M}{K^2}S+\frac{M+1}{K}\right)\frac{Kx}{u}}{1+\frac{M}{K}S}} \tag{144}$$

The transfer function is defined as

$$\bar{F}_t(S) = \frac{\bar{t}_2}{\bar{t}_0^*} = e^{\frac{-S\left(\frac{M}{K^2}S+\frac{M+1}{K}\right)\frac{Kx}{u}}{1+\frac{M}{K}S}} \tag{145}$$

* See Reference 7, 8 and 20.

Upon the substitution of $s = i\omega$ into Equation (145), one obtains

$$\bar{F}(i\omega) = e^{-\frac{Kx}{U}\left[\frac{(\frac{M\omega}{K})^2}{1+(\frac{M\omega}{K})^2}\right]} \; e^{-i\left[\frac{\omega x}{U} + \frac{M\frac{\omega x}{U}}{1+(\frac{M\omega}{K})^2}\right]} \tag{146}$$

According to Equations (20) and (21), the amplitude-ratio and phase-shift relationship between the temperature of the fluid at the outlet and inlet is the maximum value of Equation (146) which is expressed as

$$\frac{T_\infty(x)}{t^*_{o_{max}}(\tau)} = \frac{t_{max}(x,\tau) - t(x,0)}{t_{o_{max}}(\tau) - t_o} = e^{-\frac{Kx}{U}\left[\frac{(\frac{M\omega}{K})^2}{1+(\frac{M\omega}{K})^2}\right]} \tag{147}$$

and

$$\alpha_t = \frac{\omega x}{U} + \frac{M\frac{\omega x}{U}}{1+(\frac{M\omega}{K})^2} \tag{148}$$

The limiting value of the amplitude-ratio at $\omega = \infty$ can be obtained from Equation (147) as

$$\lim_{\omega \to \infty} \frac{T_\infty(x)}{t^*_{o_{max}}} = e^{-\frac{Kx}{U}} \tag{149}$$

The amplitude-ratio and phase-shift responses indicated by Equations (147) and (148) are also graphically presented in Figures 28-a, to -f.

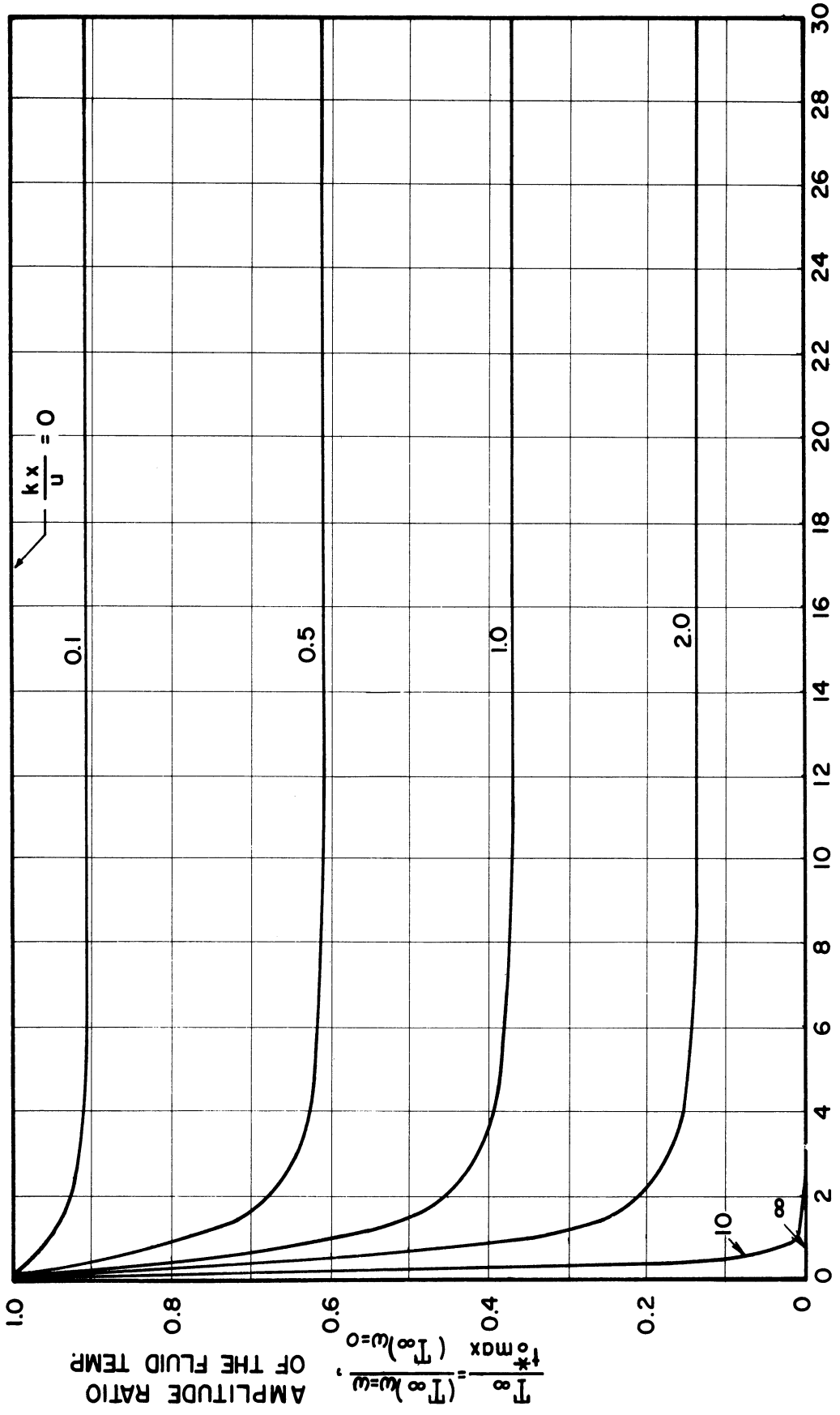

Figure 28-a. Amplitude-Ratio Response of the Fluid Temperature with the Inlet Fluid Temperature as the Sinusoidal Disturbance.

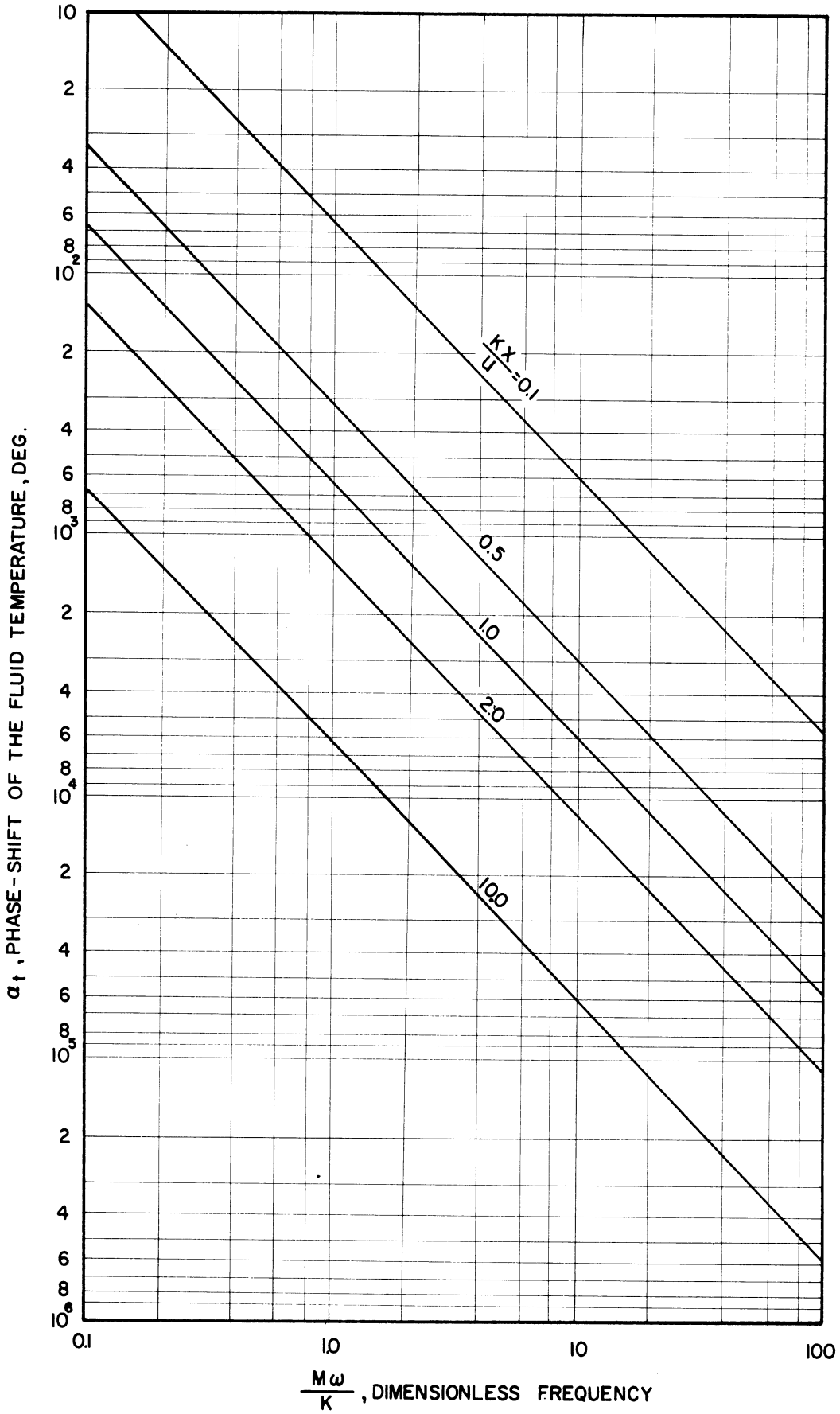

Figure 28-b. Phase-Shift Response of the Fluid Temperature with Inlet Fluid Temperature as the Sinusoidal Disturbance for M = 0.1.

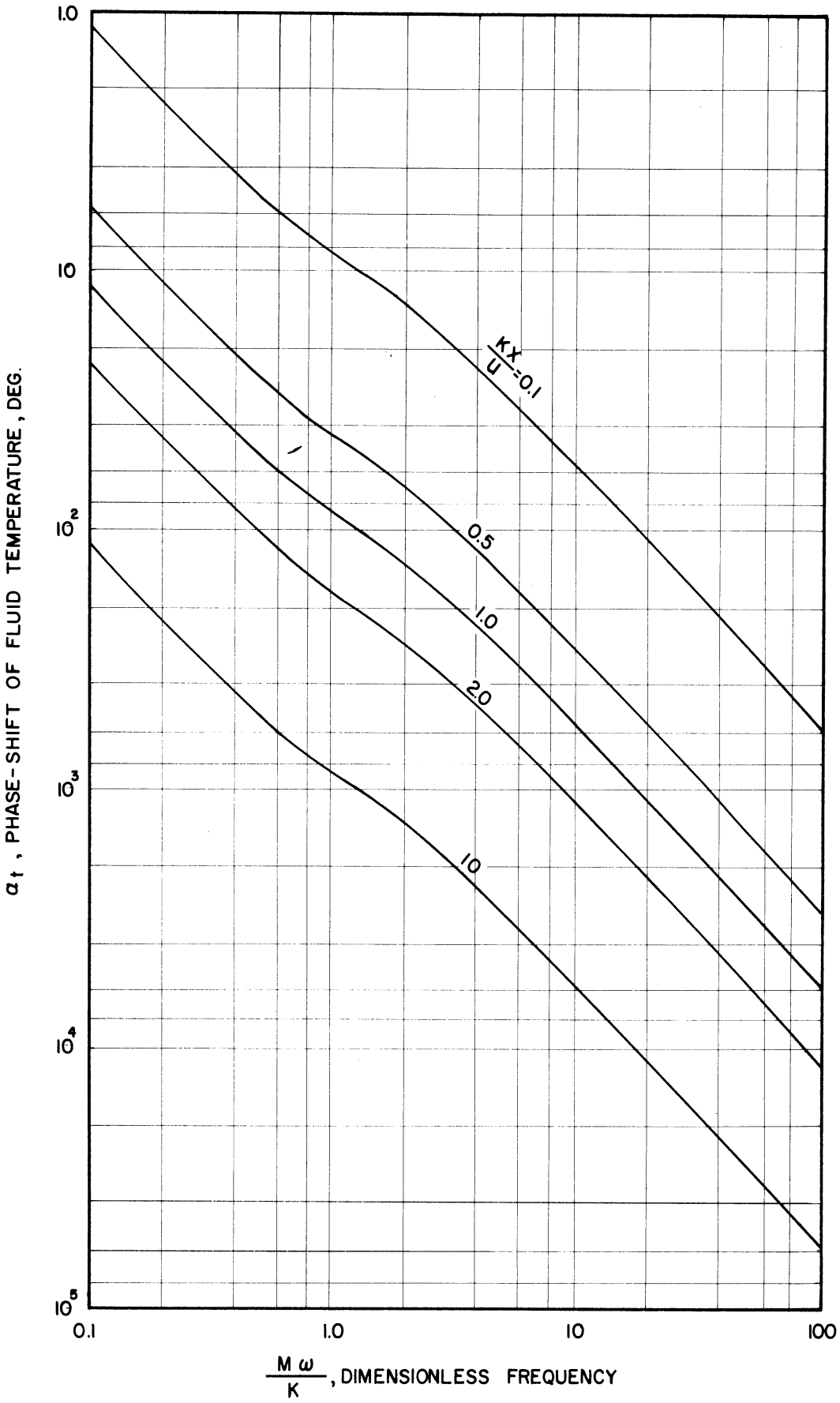

Figure 28-c. Phase-Shift Response of the Fluid Temperature with the Inlet Fluid Temperature as the Sinusoidal Disturbance for M=1.

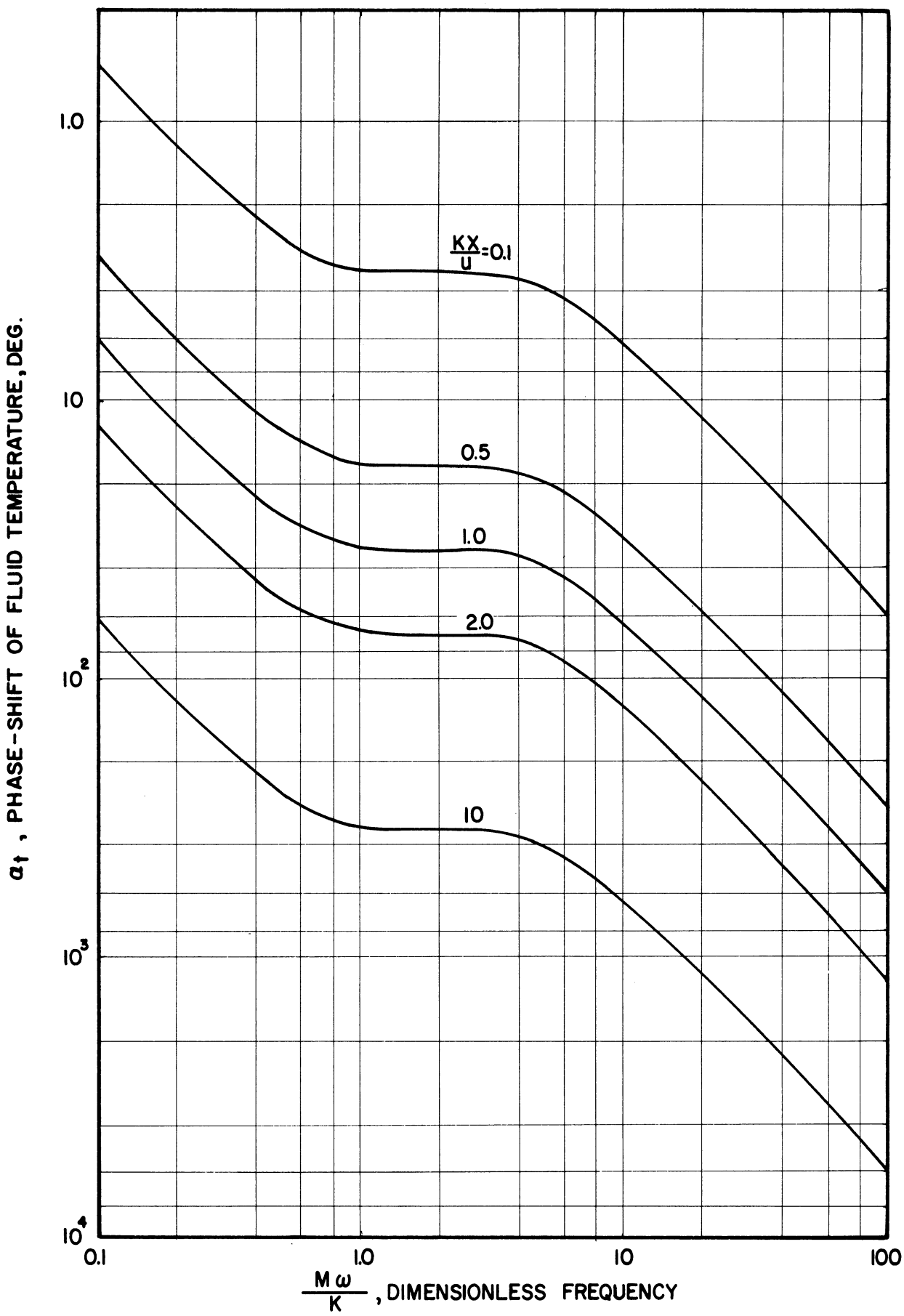

Figure 28-d. Phase-Shift Response of the Fluid Temperature with the Inlet Fluid Temperature as the Sinusoidal Disturbance, M = 10.

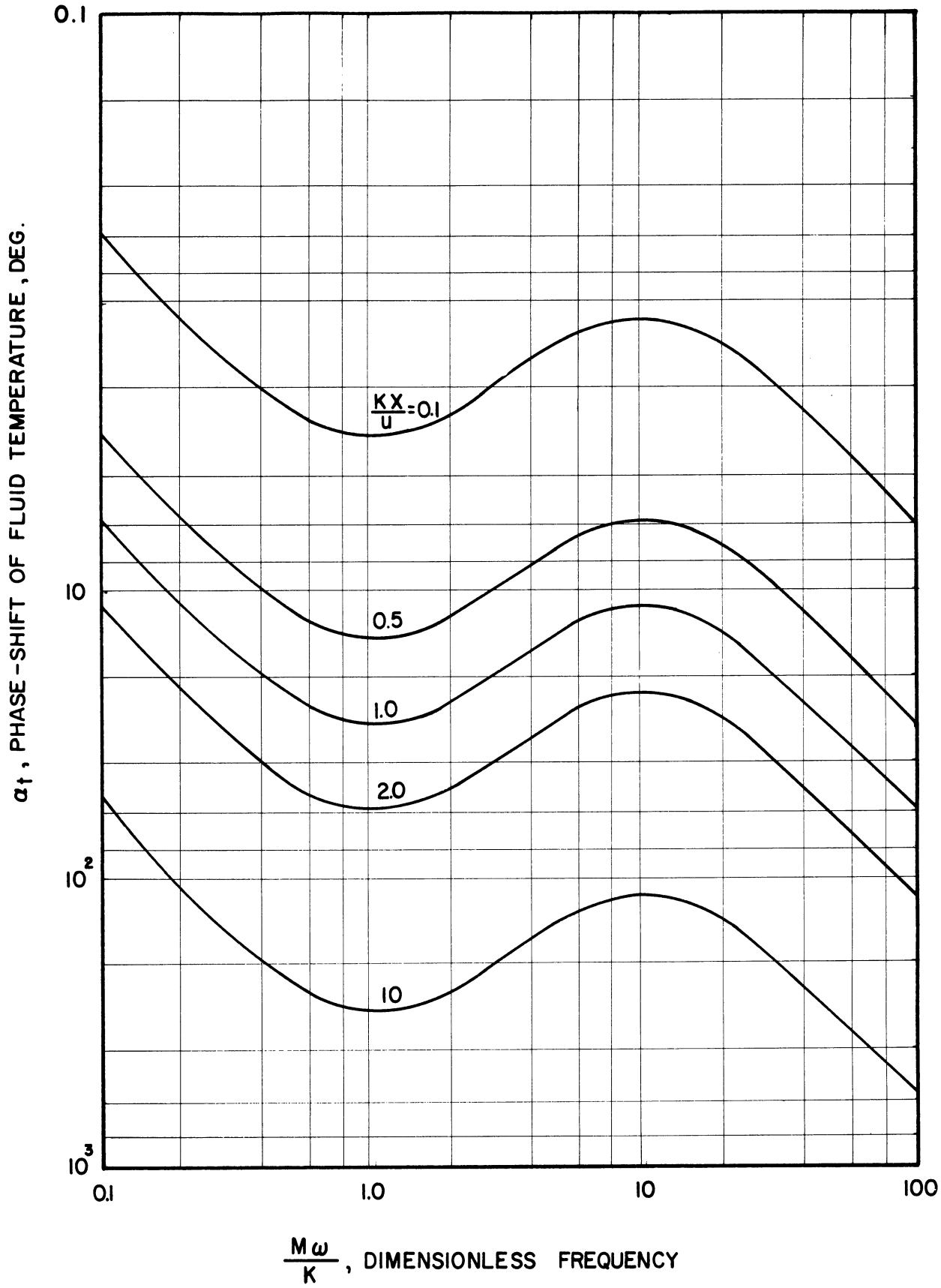

Figure 28-e. Phase-Shift Response of the Fluid Temperature with the Inlet Fluid Temperature as the Sinusoidal Disturbance for M=100.

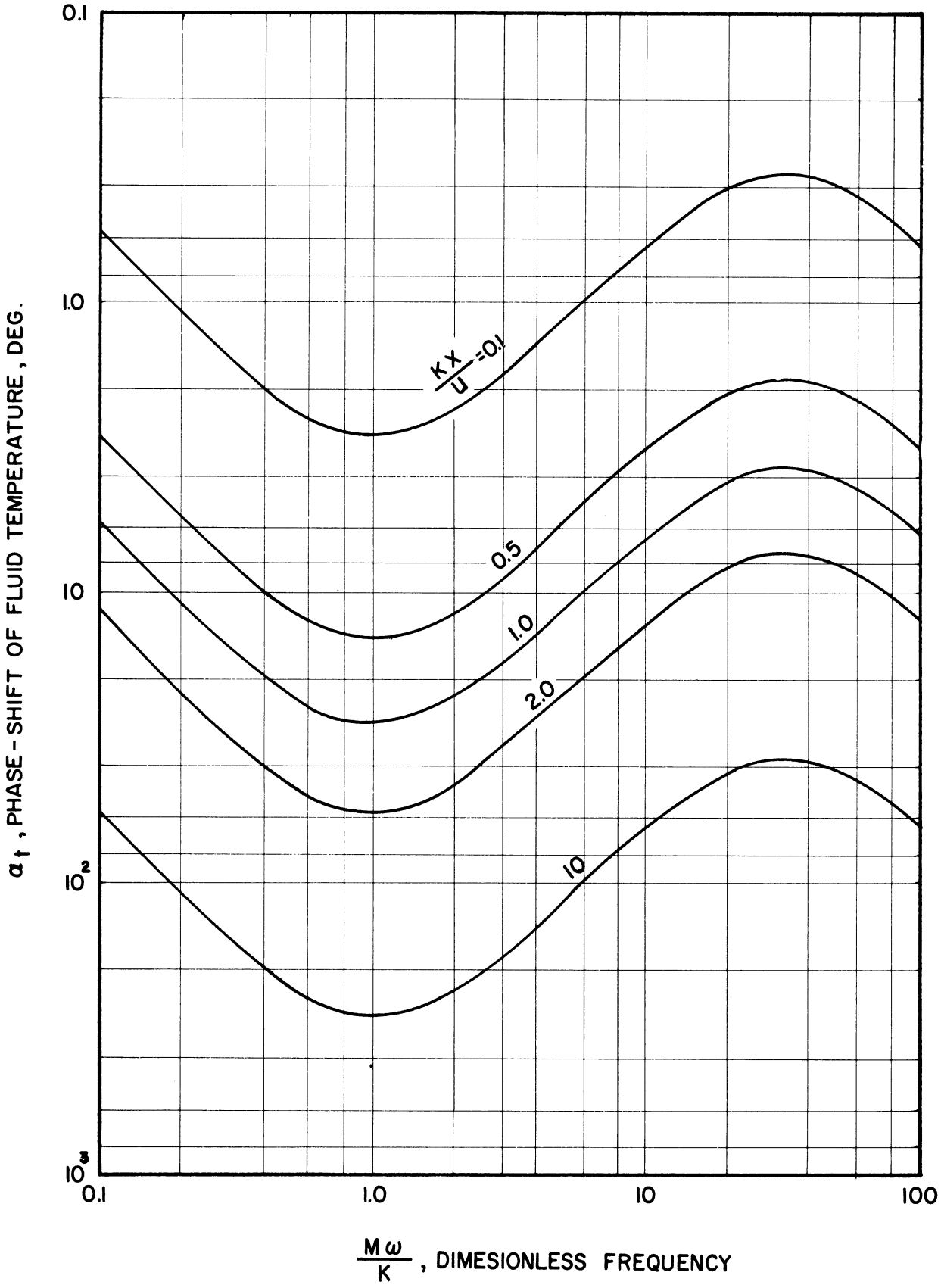

Figure 28-f. Phase-Shift Response of the Fluid Temperature with the Inlet Fluid Temperature as the Sinusoidal Disturbance for M=1000.

These figures demonstrate that the system is also of the distributed parameter type where the amplitude-ratio approaches a limiting value $e^{-Kx/u}$ for increase in frequency and the phase-shift increases indefinitely with increasing frequency. Figure 28-a shows the amplitude-ratio decreases with increase in Kx/u and Mω/K. Decrease in the amplitude-ratio with increase in Mω/K is very rapid at the small values of Mω/K then asymptotic to a constant $e^{-Kx/u}$. Figures 28-b to -f show that the phase-shift increases with increase in Kx/u, M and Mω/K. It is interesting to note that the phase-shift at the large values of M has one "resonance" which was also indicated in Reference 20. Profos[20] dealt with the dynamic characteristics of the steam superheater and pointed out that when the system consists of a light gas (low pressure steam) and a metal tube (i.e., large value of M) the phase-shift has a "resonance."* The dynamic characteristics of the wall temperature and the fluid-wall temperature difference are investigated as follows by substituting $\Phi = 0$ into Equation (40) and (41).

Wall Temperature

$$\bar{\theta}_2 = \bar{t}_0^* \frac{e^{-\frac{Kx}{u}\frac{S\left(\frac{M}{K}S+\frac{MH}{K}\right)}{(1+\frac{M}{K}S)}}}{1+\frac{MS}{K}} \tag{150}$$

Fluid wall temperature-difference

$$\Delta\bar{t}_2 = -\bar{t}_0^* \frac{\frac{MS}{K}}{1+\frac{MS}{K}} e^{-\frac{Kx}{u}\frac{S\left(\frac{MS}{K^2}+\frac{M+1}{K}\right)}{(1+\frac{MS}{K})}} \tag{151}$$

* Reference 4 has the same form of the phase-shift response in which they ignored the possibility of one "resonance" at the high values of the wall-fluid heat capacity ratio.

The transfer functions for the wall temperature and the fluid-wall temperature difference are defined as

Wall temperature

$$\bar{F}_\theta(s) = \frac{\bar{\theta}_2}{\bar{t}_0^*} = \frac{e^{-\frac{Kx}{u}\frac{s\left(\frac{Ms}{K^2}+\frac{M+1}{K}\right)}{\left(1+\frac{Ms}{K}\right)}}}{1+\frac{Ms}{K}} \tag{152}$$

Fluid-wall temperature difference

$$\bar{F}_{\Delta t}(s) = \frac{\Delta\bar{t}_2}{\bar{t}_0^*} = -\frac{\frac{Ms}{K}}{1+\frac{Ms}{K}} e^{-\frac{Kx}{u}\frac{s\left(\frac{Ms}{K^2}+\frac{M+1}{K}\right)}{1+\frac{Ms}{K}}} \tag{153}$$

Substituting s = iω into Equations (152) and (153), one obtains

$$\begin{aligned}\bar{F}_\theta(i\omega) &= \frac{1}{1+\frac{Mi\omega}{K}} e^{-\frac{Kx}{u}\frac{(i\omega)\left(\frac{Mi\omega}{K^2}+\frac{M+1}{K}\right)}{1+\frac{Mi\omega}{K}}} \\ &= \frac{e^{-\frac{Kx}{u}\left[\frac{\left(\frac{M\omega}{K}\right)^2}{1+\left(\frac{M\omega}{K}\right)^2}\right]}}{1+\left(\frac{Mi\omega}{K}\right)^2} e^{-i\left[\frac{\omega x}{u}+\frac{M\omega x}{u}\frac{1}{1+\left(\frac{M\omega}{K}\right)^2}+\tan^{-1}\left(\frac{M\omega}{K}\right)\right]}\end{aligned} \tag{154}$$

and

$$\begin{aligned}\bar{F}_{\Delta t}(i\omega) &= -\frac{\frac{Mi\omega}{K}}{1+\frac{Mi\omega}{K}} e^{-\frac{Kx}{u}\frac{(i\omega)\left(\frac{Mi\omega}{K^2}+\frac{M+1}{K}\right)}{1+\frac{Mi\omega}{K}}} \\ &= \frac{\frac{M\omega}{K}\, e^{-\frac{Kx}{u}\left[\frac{\left(\frac{M\omega}{K}\right)^2}{1+\left(\frac{M\omega}{K}\right)^2}\right]}}{1+\left(\frac{M\omega}{K}\right)^2} e^{-i\left[\frac{\omega x}{u}+\frac{Mi\omega x}{u}\frac{1}{1+\left(\frac{M\omega}{K}\right)^2}+\tan^{-1}\left(\frac{M\omega}{K}\right)+\frac{\pi}{2}\right]}\end{aligned} \tag{155}$$

Thus one finds the amplitude-ratio and phase-shift of the wall temperature and fluid-wall temperature and their relationship with those of the fluid

temperature as follows:

Wall temperature

$$\frac{\Theta_\infty}{t^*_{o\,max}} = \frac{e^{-\frac{Kx}{u}\left[\frac{\left(\frac{M\omega}{K}\right)^2}{1+\left(\frac{M\omega}{K}\right)^2}\right]}}{\sqrt{1+\left(\frac{M\omega}{K}\right)^2}} = \frac{1}{\sqrt{1+\left(\frac{M\omega}{K}\right)^2}} \frac{T_\infty}{t^*_{o\,max}} \tag{156}$$

$$\alpha_\theta = \frac{\omega x}{u} + \frac{M\frac{\omega x}{u}}{1+\left(\frac{M\omega}{K}\right)^2} + \tan^{-1}\left(\frac{M\omega}{K}\right) = \alpha_t + \tan^{-1}\left(\frac{M\omega}{K}\right) \tag{157}$$

Fluid-wall temperature difference

$$\frac{\Delta T_\infty}{t^*_{o\,max}} = \frac{\frac{M\omega}{K}}{\sqrt{1+\left(\frac{M\omega}{K}\right)^2}} e^{-\frac{Kx}{u}\left[\frac{\left(\frac{M\omega}{K}\right)^2}{1+\left(\frac{M\omega}{K}\right)^2}\right]} = \frac{M\omega}{K}\frac{\Theta_\infty}{t^*_{o\,max}} = \frac{\frac{M\omega}{K}}{\sqrt{1+\left(\frac{M\omega}{K}\right)^2}} \frac{T_\infty}{t^*_{o\,max}} \tag{158}$$

$$\alpha_{\Delta t} = \frac{\omega x}{u} + \frac{M\frac{\omega x}{u}}{1+\left(\frac{M\omega}{K}\right)^2} + \tan^{-1}\left(\frac{M\omega}{K}\right) + \frac{\pi}{2}$$

$$= \alpha_\theta + \frac{\pi}{2} = \alpha_t + \tan^{-1}\left(\frac{M\omega}{K}\right) + \frac{\pi}{2} \tag{159}$$

Equations (156) through (159) are graphically presented in Figures 28-g to -m. It must be noted that this work and Reference 20 are physically different. The heat exchangers in this work have constant heat generation while Reference 20 investigates those heated isothermally by steam, although the differential equations governing the dynamic characteristics and the external disturbance are identical.

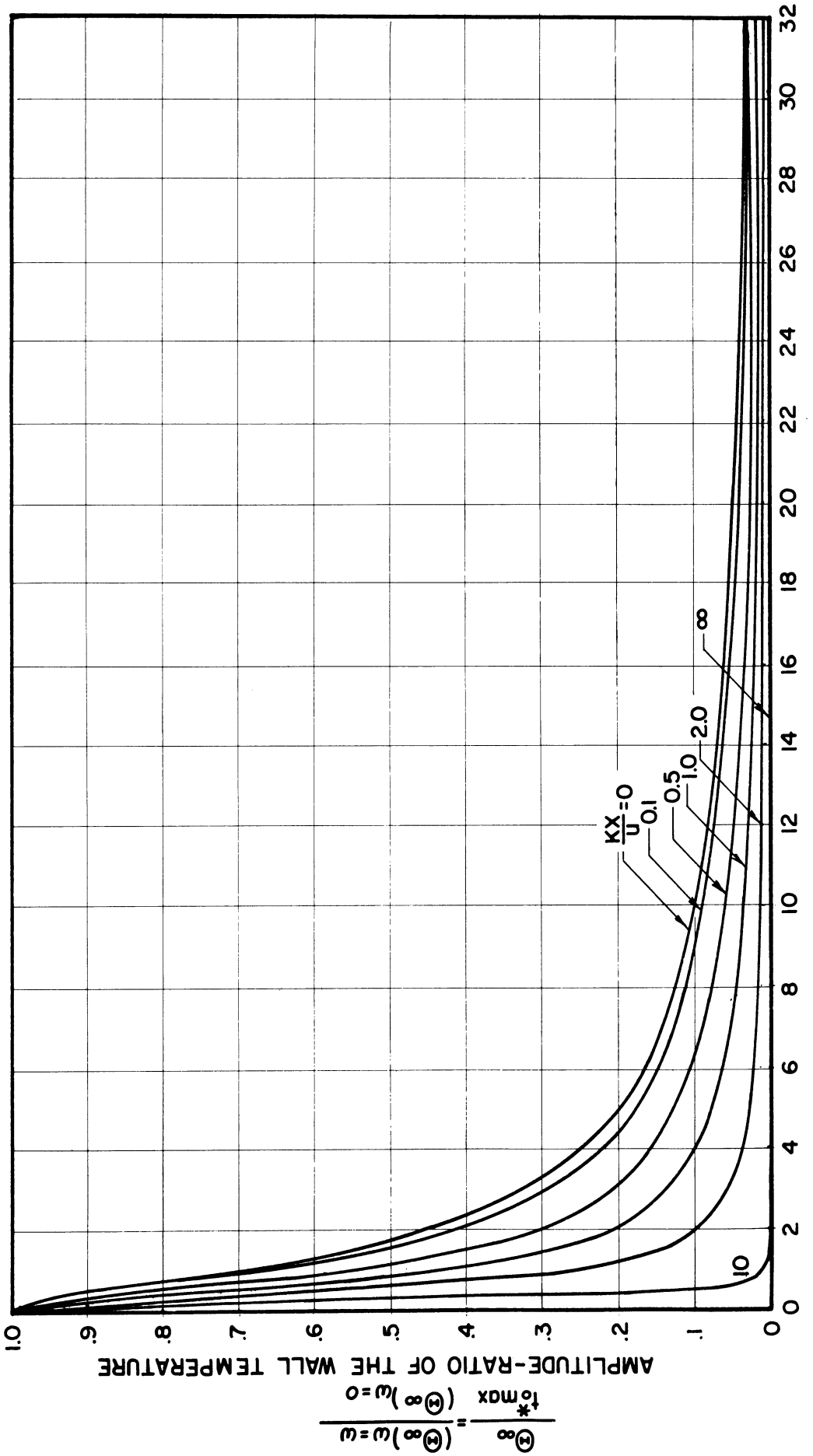

Figure 28-g. Amplitude-Ratio Response of the Wall Temperature with the Inlet Fluid Temperature as the Sinusoidal Disturbance.

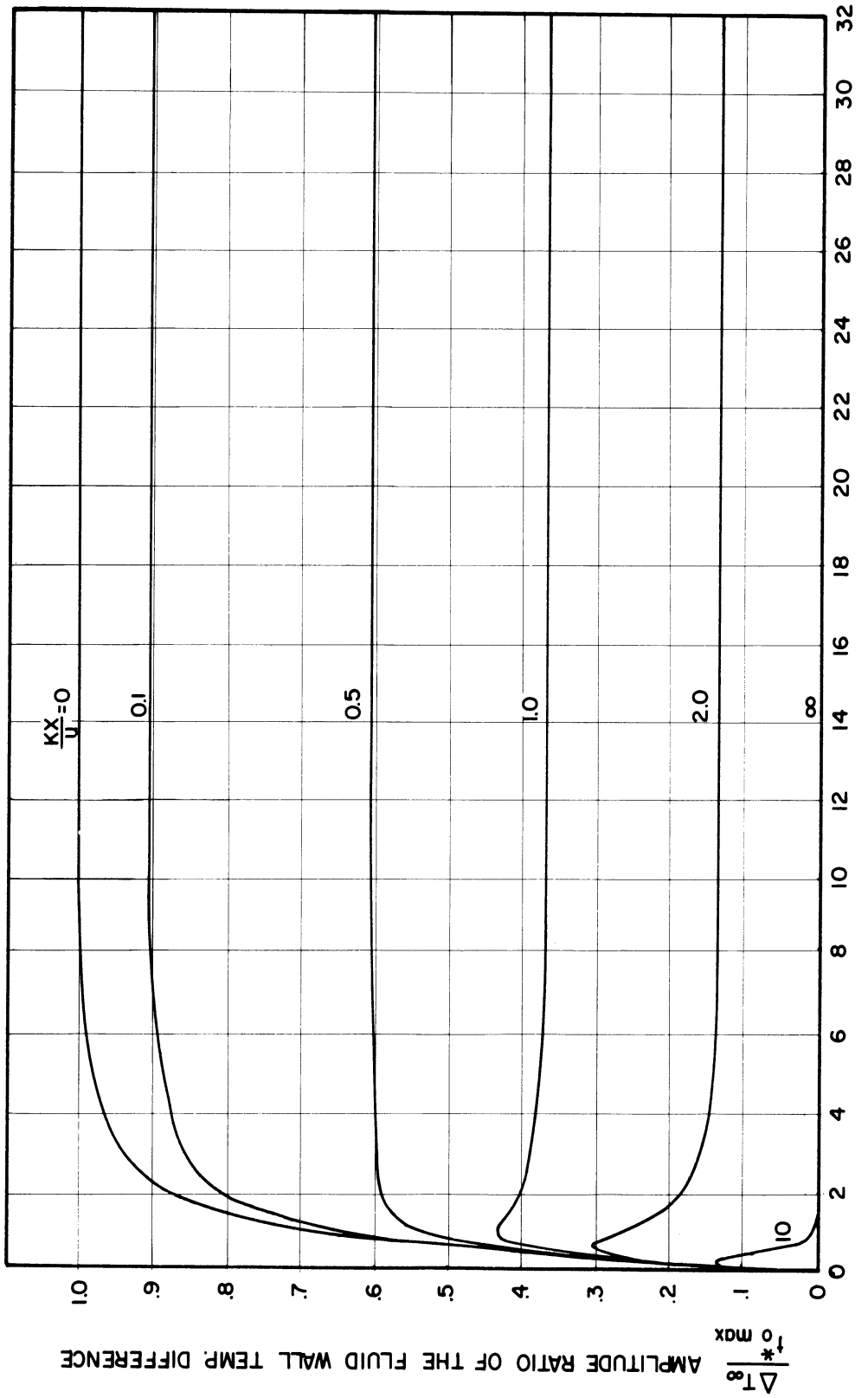

Figure 28-h. Amplitude-Ratio Response of the Fluid-Wall Temperature Difference with the Inlet Fluid Temperature as the Sinusoidal Disturbance.

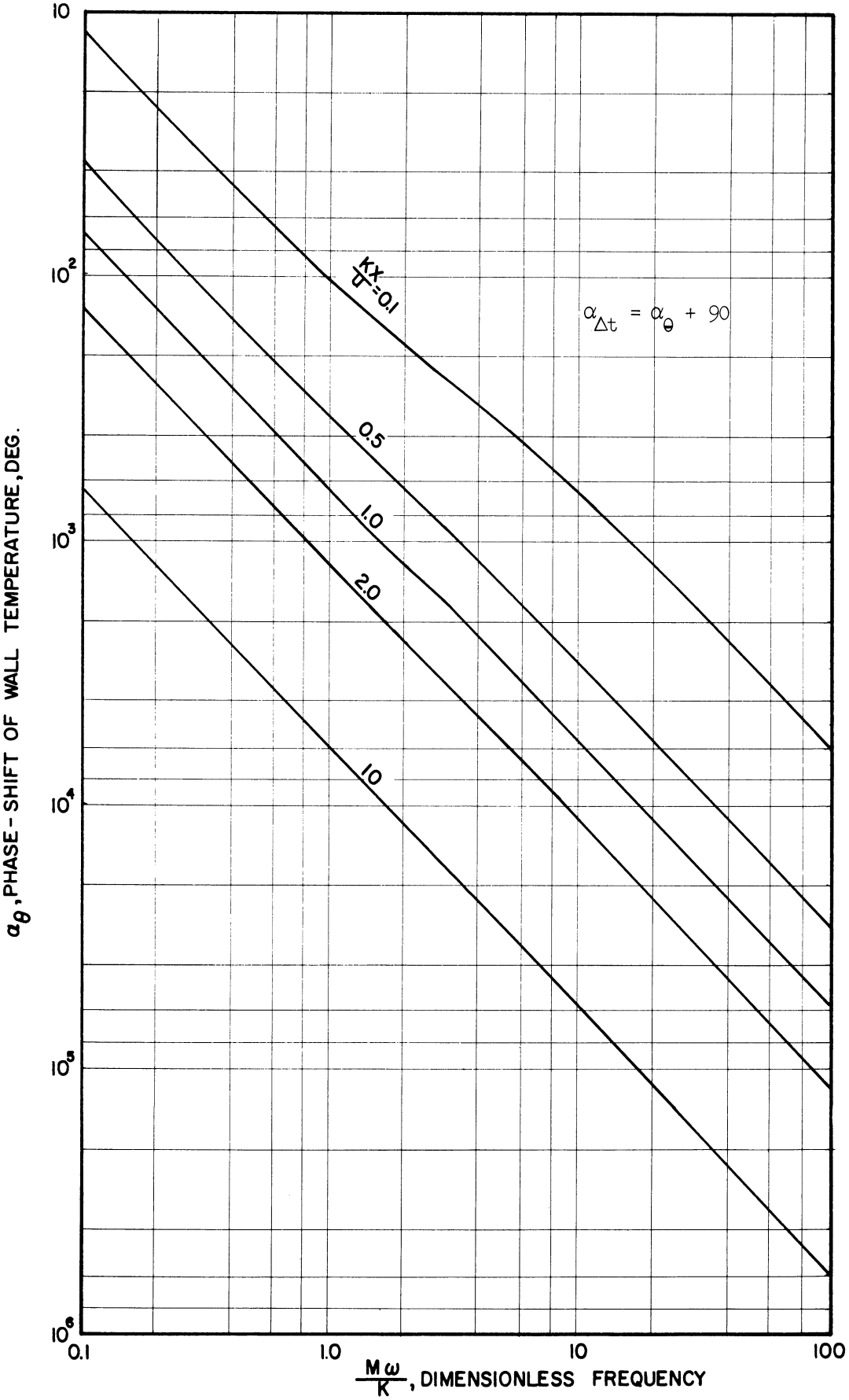

Figure 28-i. Phase-Shift Response of the Wall Temperature and Fluid-Wall Temperature Difference with the Inlet Fluid Temperature as the Sinusoidal Disturbance for M=0.1.

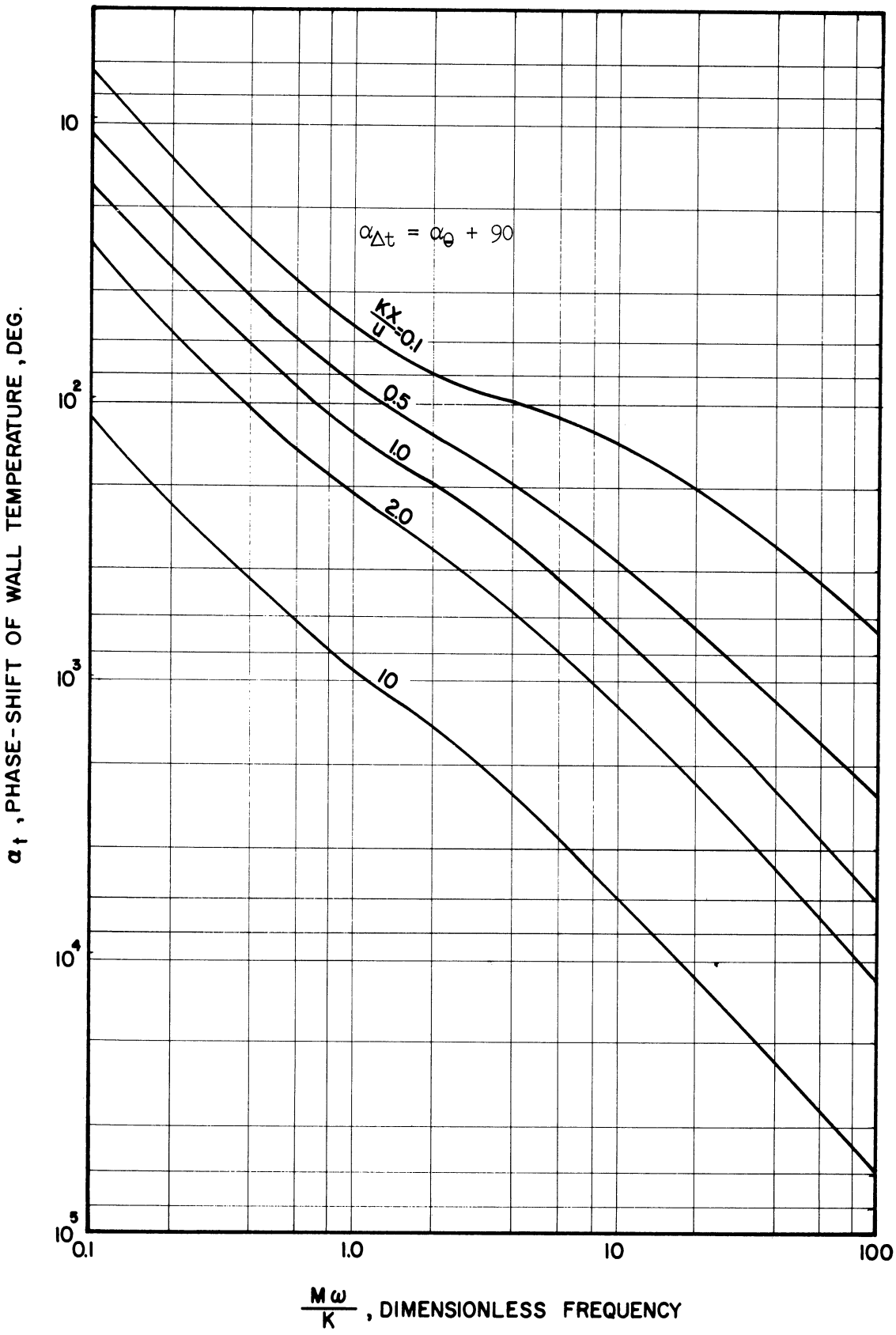

Figure 28-j. Phase-Shift Response of the Wall Temperature and Fluid-Wall Temperature Difference with the Inlet Fluid Temperature as the Sinusoidal Disturbance for M=1.

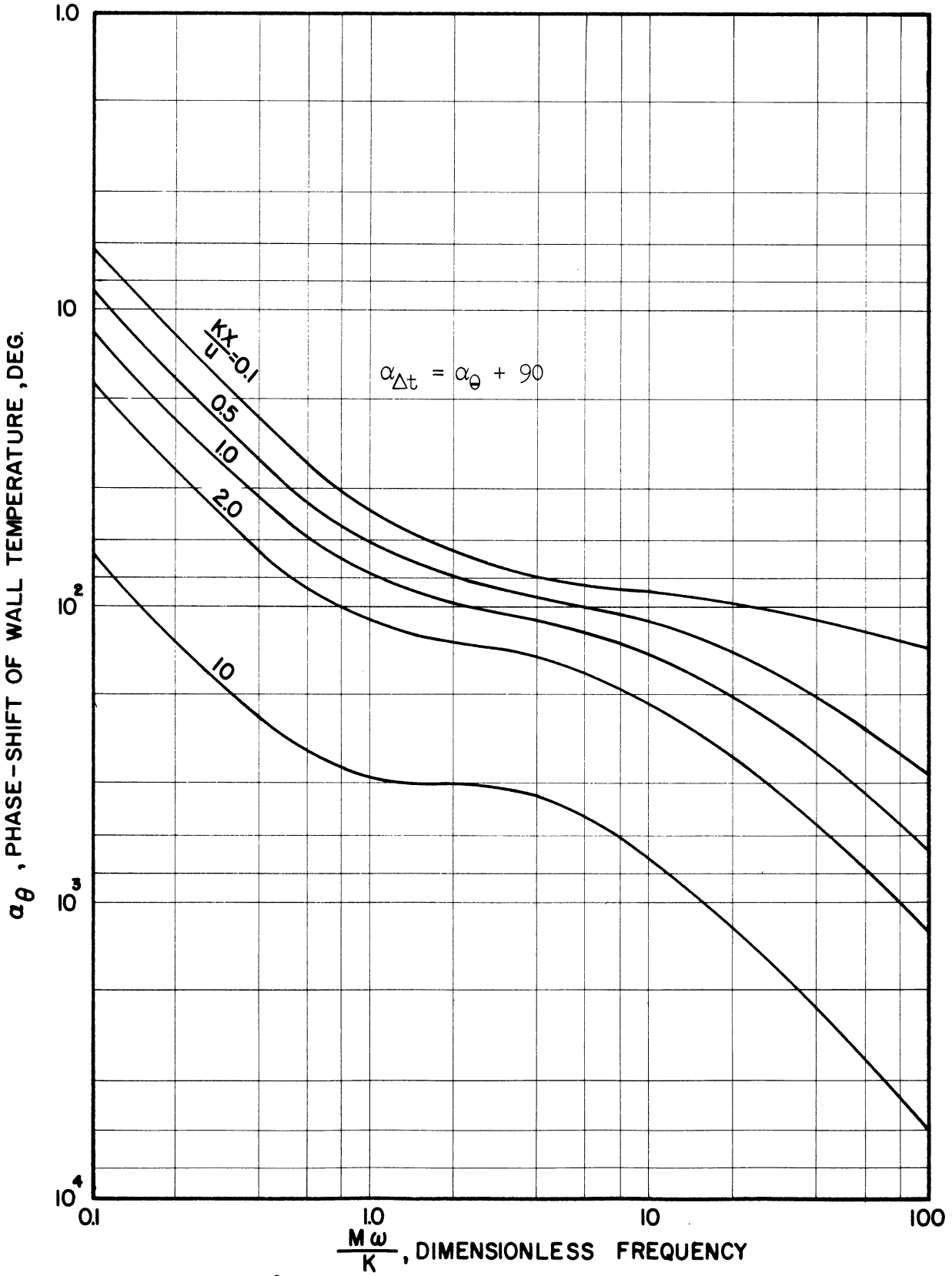

Figure 28-k. Phase-Shift Response of the Wall Temperature and Fluid-Wall Temperature Difference with the Inlet Fluid Temperature as the Sinusoidal Disturbance, M = 10.

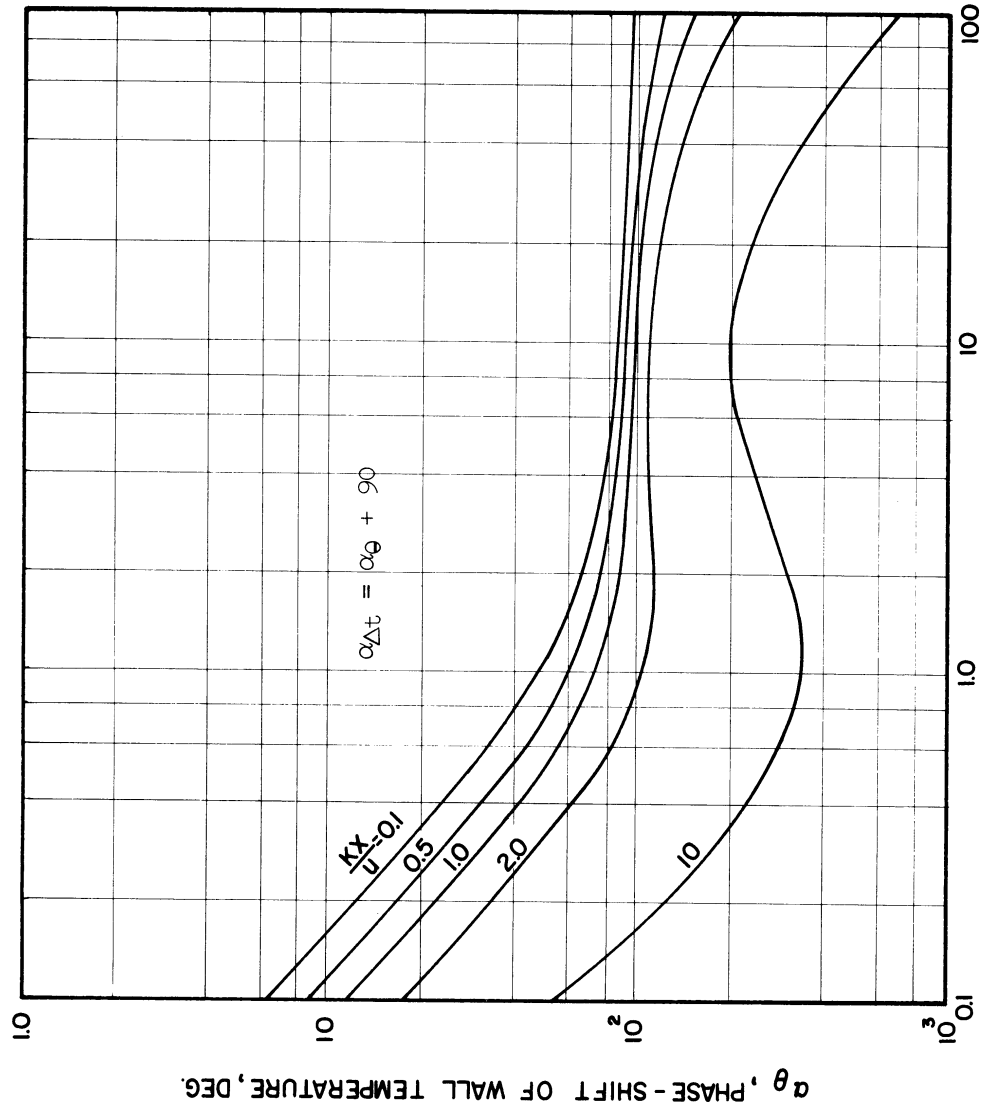

Figure 28-ℓ. Phase-Shift Response of the Wall Temperature and Fluid-Wall Temperature Difference with the Inlet Fluid Temperature as the Sinusoidal Disturbance for M=100.

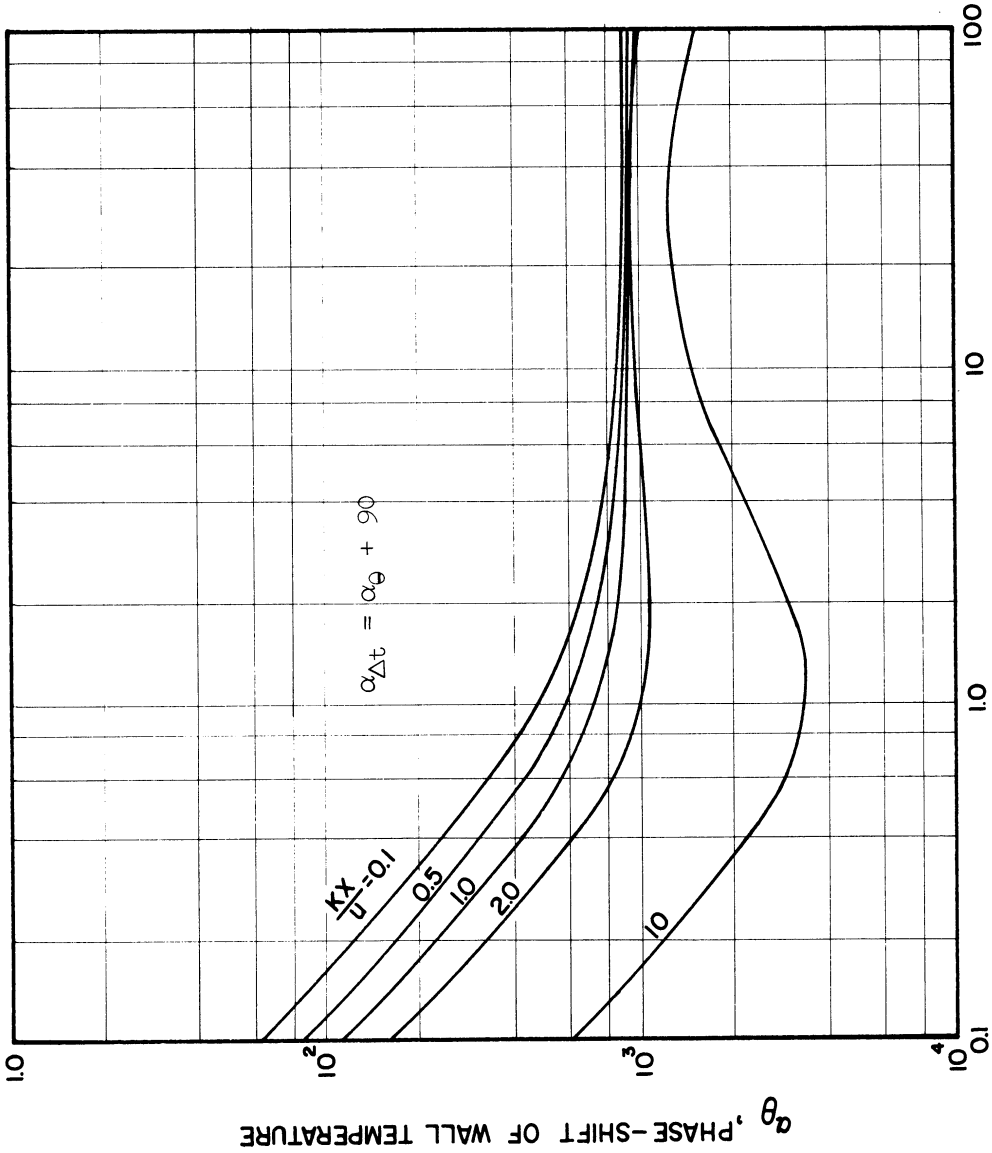

Figure 28-m. Phase-Shift Response of the Wall Temperature and Fluid-Wall Temperature Difference with the Inlet Fluid Temperature as the Sinusoidal Disturbance, M = 1000.

CHAPTER IV

EXPERIMENTS

The dynamic characteristics of a physical system may be determined experimentally, without even writing its equations. This can be done by simply applying all frequencies from very low to very high and recognizing the fact that the ratio of steady output with a sinusoidal input of frequency ω to the input is equal to the frequency response $F(i\omega)$.

The determination of frequency response has been applied to problems ranging from simple to complicated systems. The method is recommended to be used when there exists a lack of accurate information of its characteristics or the systems are too complicated to theoretically calculate the frequency response.

A. Experimental Apparatus

The apparatus as shown in Figure 29-a consisted of a horizontal water-cooled electrically heated 304 stainless steel tube BWG 16 (0.495 in. I.D., 5/8 in. O.D.), 3 ft. in length. Electrical current connections were copper connectors silver-soldered at each end of the tube to which power leads were attached. The hydrodynamic calming section which preceded the test section was 3 ft. and on it a 304 stainless steel tube 34 inch length 1 in. ID and 1-1/8 in. OD was mounted concentrically. A stream of cooling water taken from the same water supply as the coolant flowed through the concentric space in order to maintain the coolant temperature as uniform as possible up to the inlet of the test section. The tube between the test section and the hydrodynamic calming section was reduced

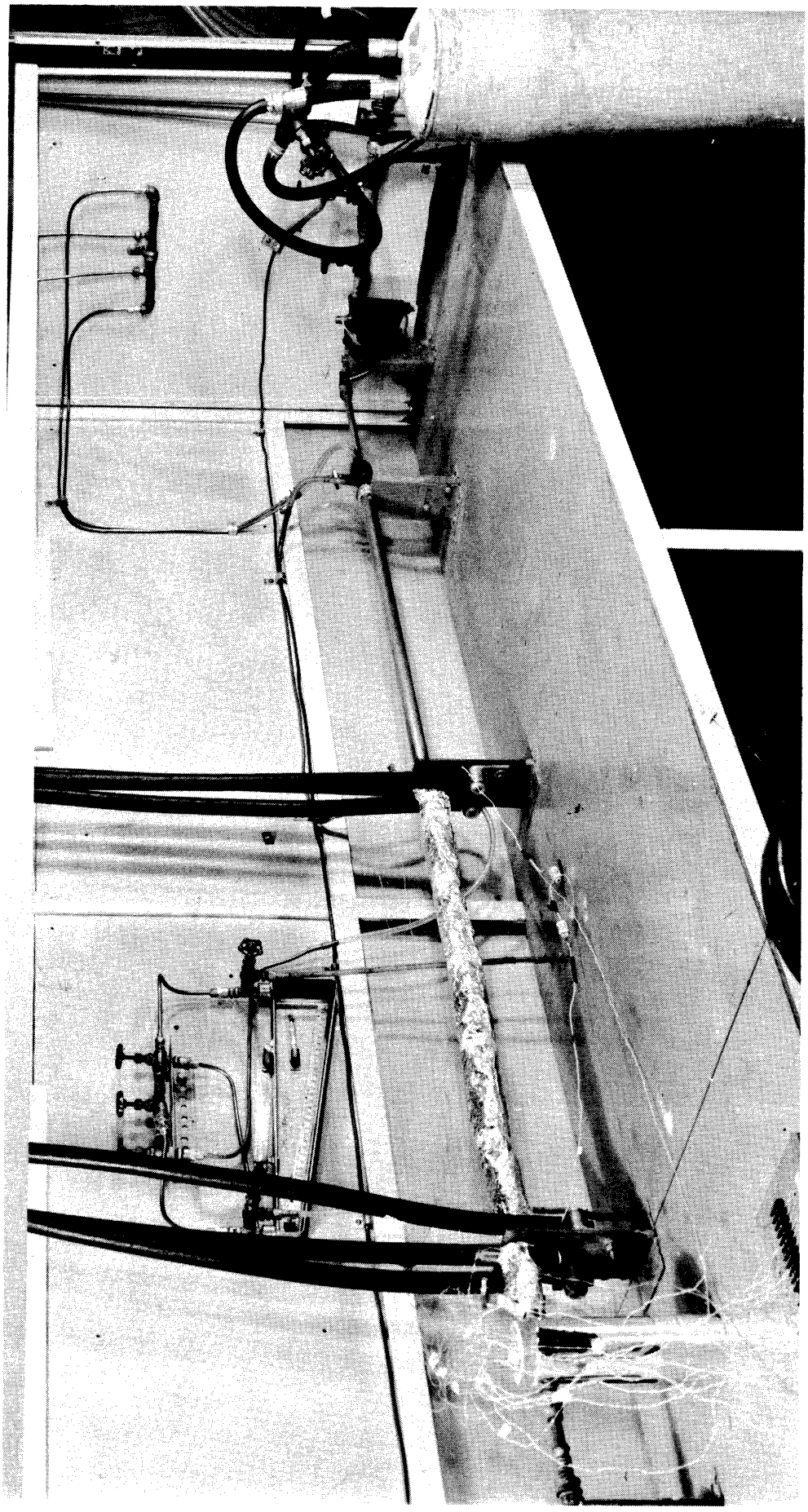

Figure 29-a. Test Section.

in cross sectional area in order to reduce axial heat conduction loss from the heat generating section. A schematic drawing of the system is shown in Figure 29-b.

A once-through water system was used to avoid the necessity of recirculation loops, heat exchangers, and pumps. Water was supplied directly from the city water lines through a water softener and its flow rate through the test section was regulated by a control valve and was measured by a calibrated sharp-edge orifice with a manometer using a 2.00 specific weight indicating liquid. Electric power was dissipated in the stainless-steel tube to provide the source for internal heat generation. In order to produce a sinusoidal heat generation, a four bar linkage as shown in Figure 29-c was designed to oscillate the auto transformer input of a 50 kw Germanium Rectifier. The four bar linkage was driven by three phase induction motor, through a 3/4 hp hydraulic speed control and a 10-1 Boston reduction gear. The locations of the wall and fluid thermocouples are shown in Figure 29-d. Fluid thermocouples were located at the beginnings of the unheated hydrodynamic calming section, and the test section, at the end of the test section and at the location immediately after a mixing baffle. The fluid thermocouple at the end of the test section was mounted as in Figure 29-e so that it can traverse the tube cross-section to measure the temperature profile.

Seven wall thermocouples whose positions are shown in Figures 29-f and 29-g, were spot-welded directly on the tube-wall by a condenser discharge process. The DC voltage picked up by those wall thermocouples during a sudden increase in test section voltage were carefully calibrated using a Minneapolis-Honeywell Visicorder at several recording

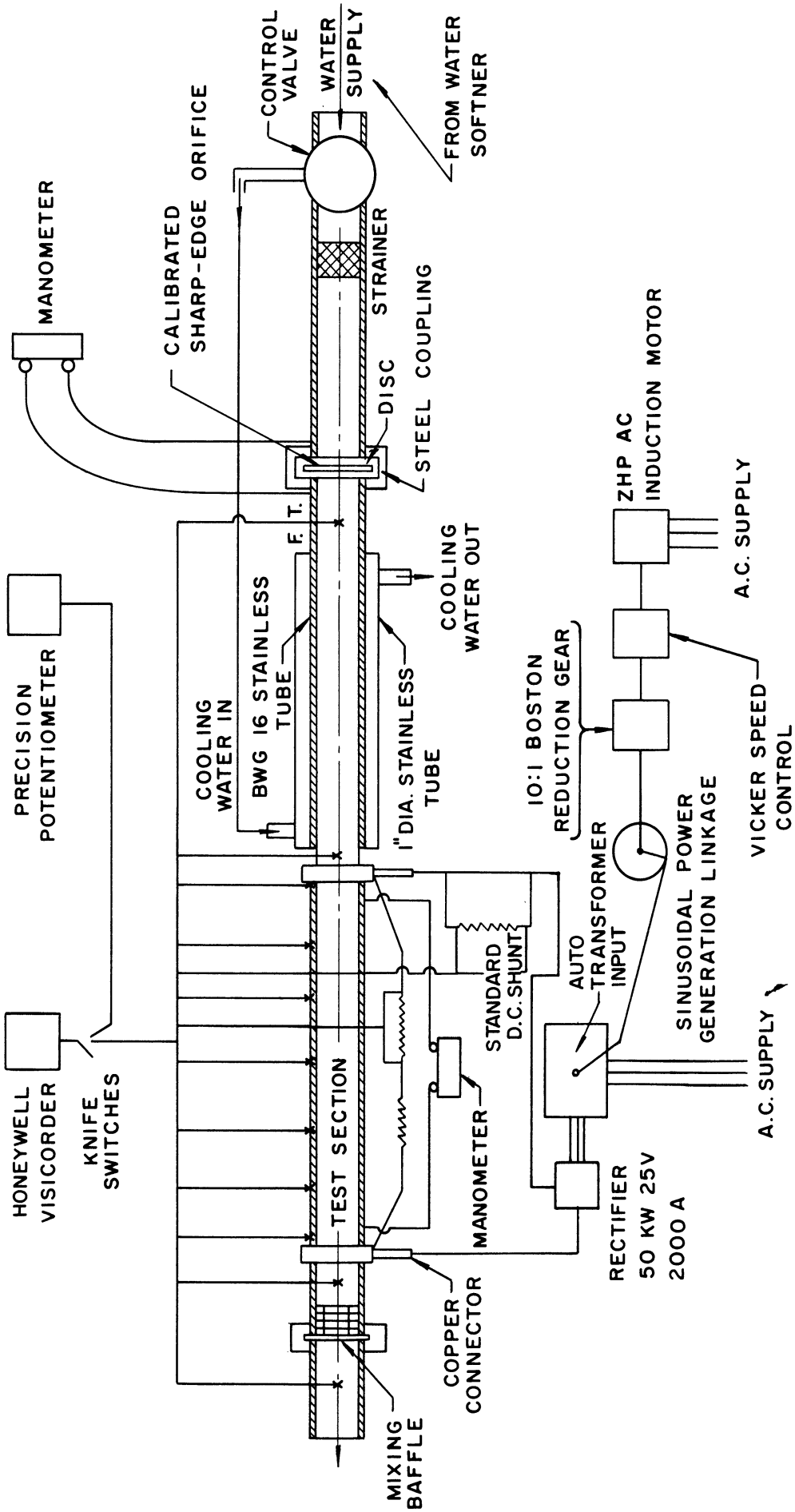

Figure 29-b. Schematic Diagram of Experimental Apparatus.

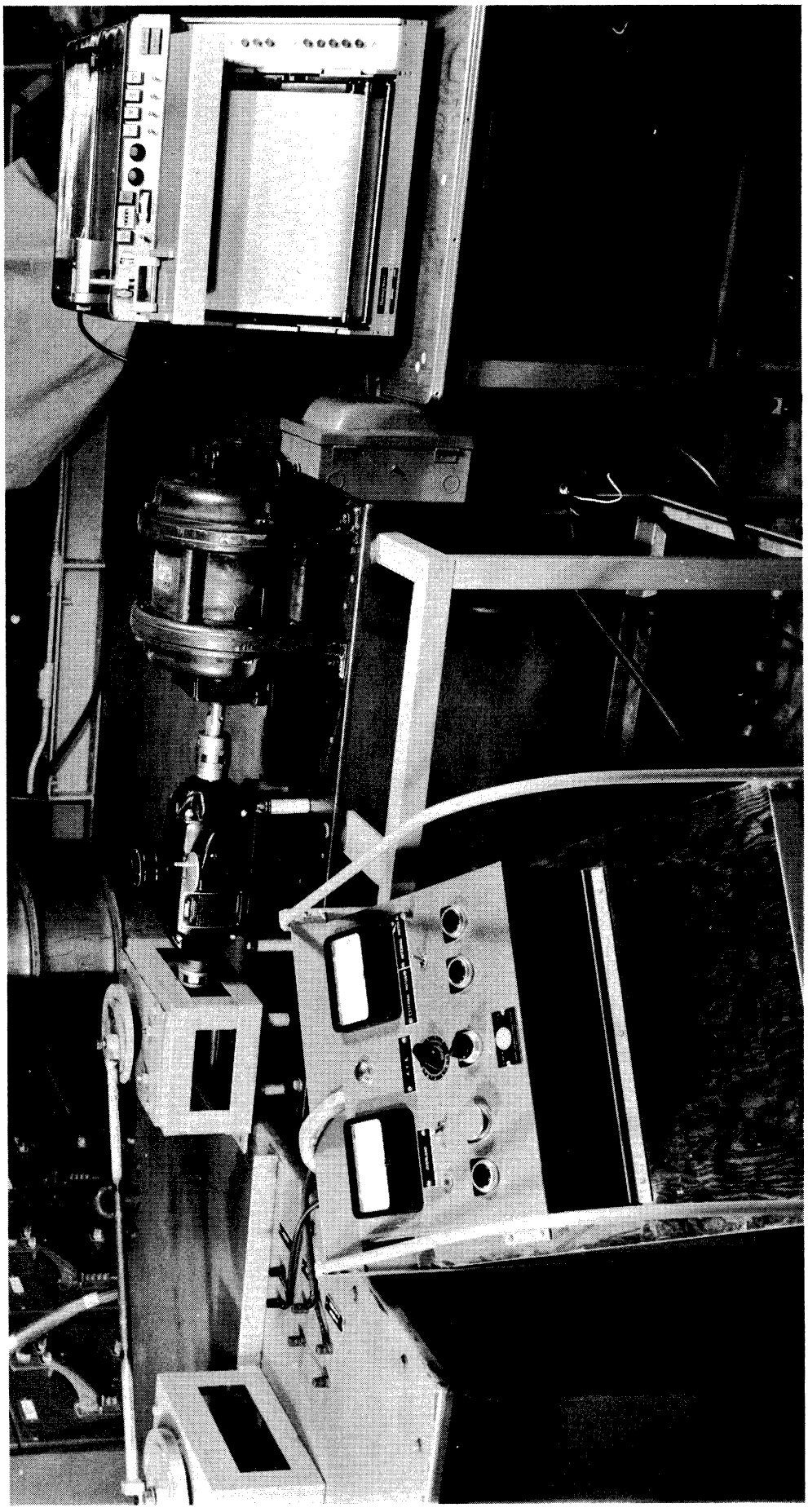

Figure 29-c. Driving Mechanism and Visicorder.

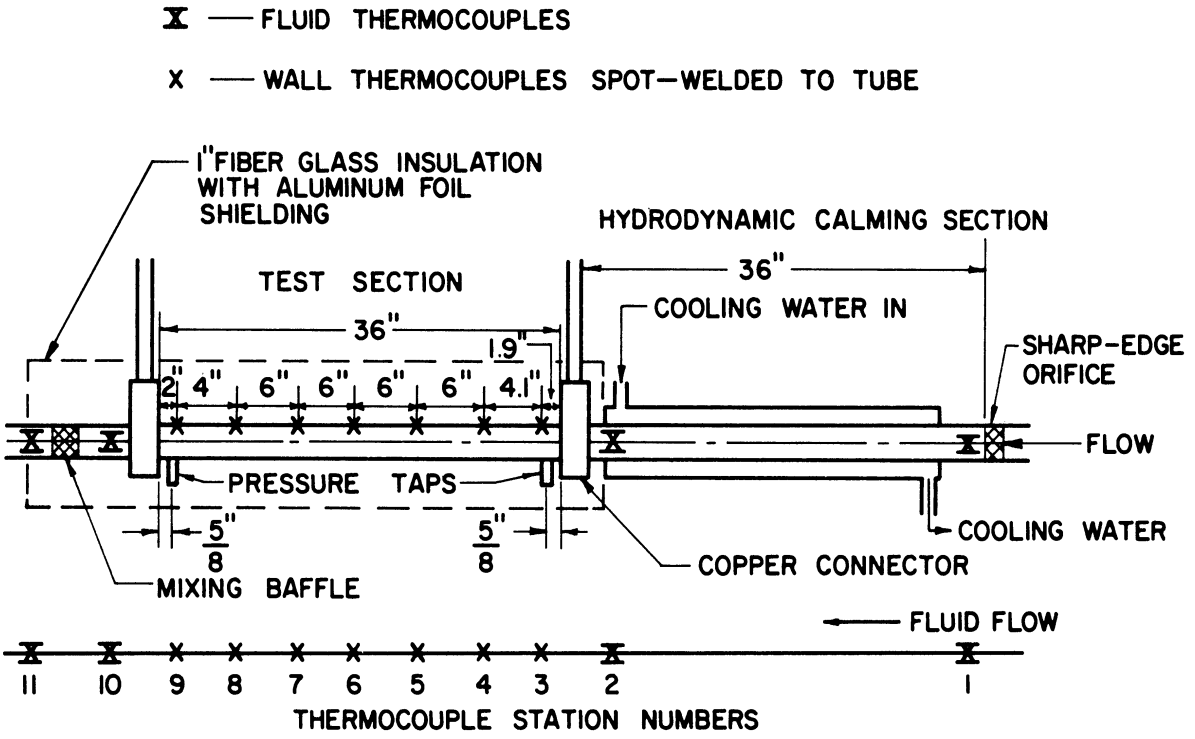

Figure 29-d. Detail of Test Section and Hydrodynamic Entrance Section.

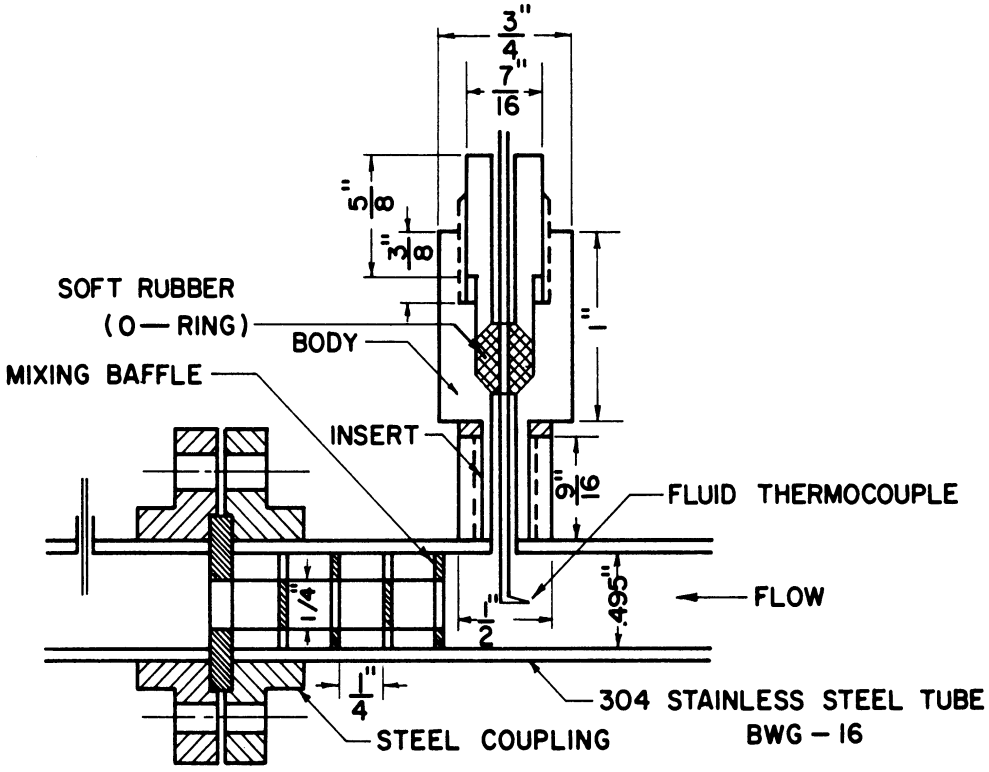

Figure 29-e. Fluid Thermocouple Mount and Mixing Baffle.

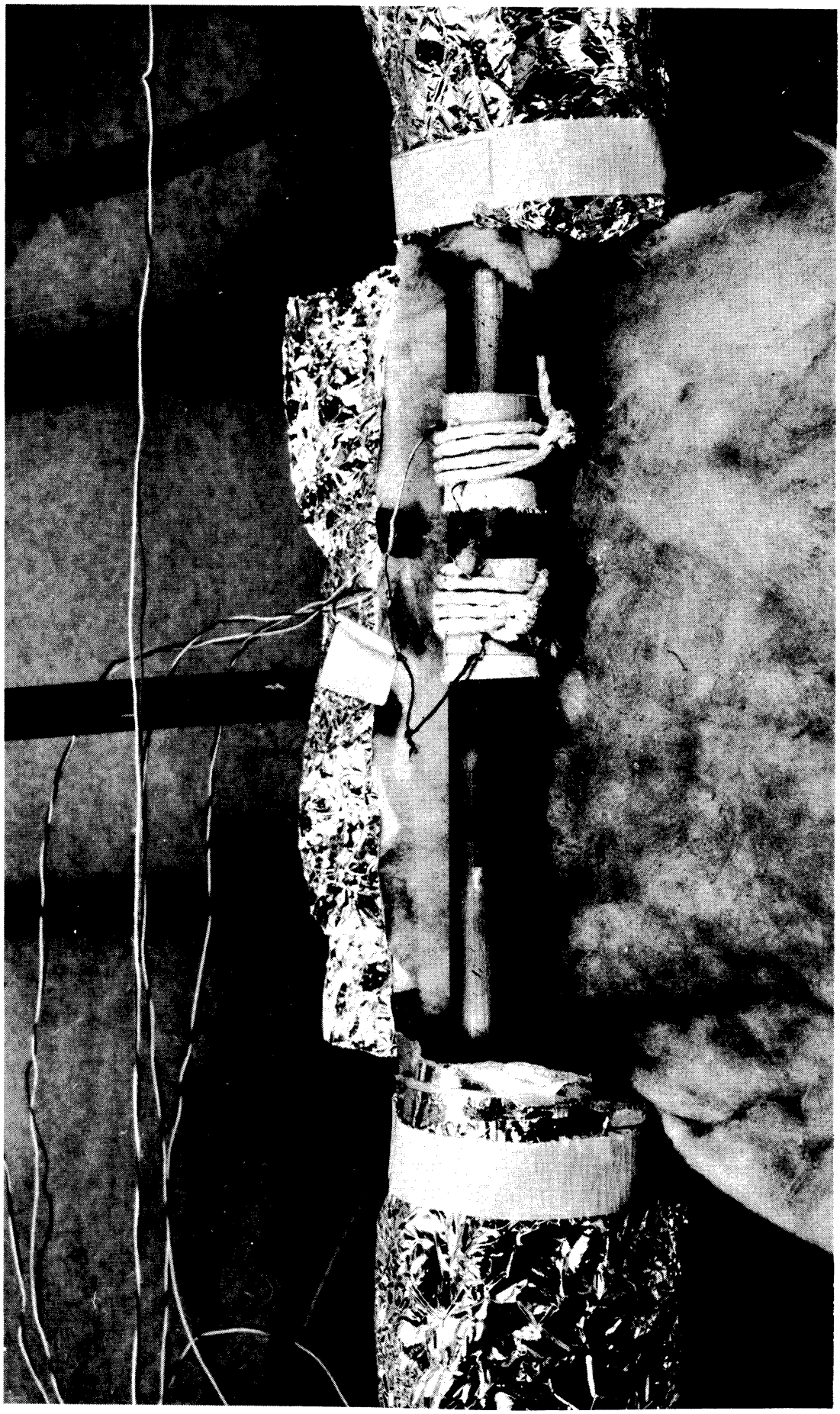

Figure 29-f. Test Section and Welded Wall Thermocouple.

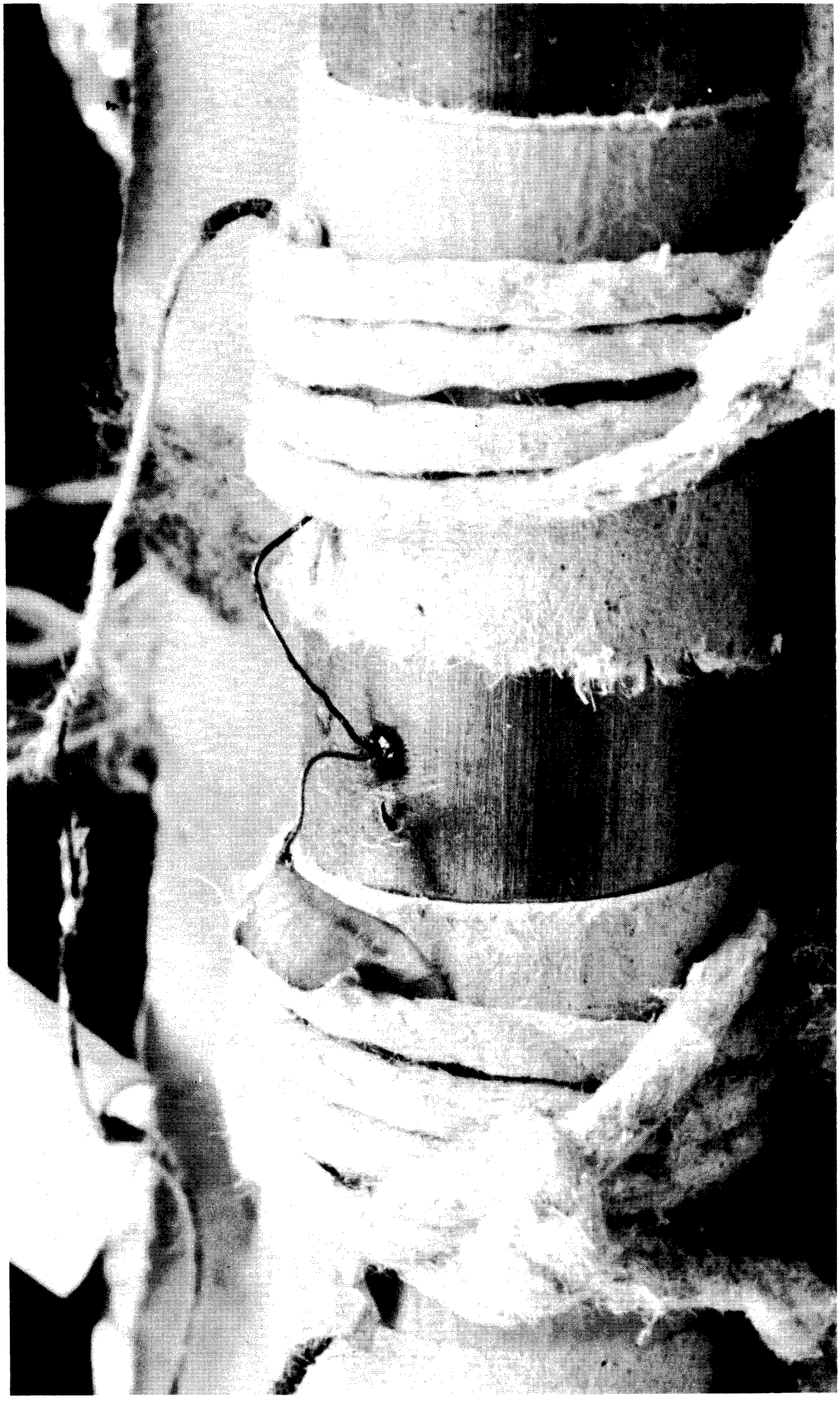

Figure 29-g. Welded Wall Thermocouple.

speeds. All fluid and wall thermocouples were made from 30 gage iron and constantan thermocouple wires and were chosen because of their higher thermal emf per degree of temperature difference. The response of the water thermocouples were corrected analytically for their inherent lag, which was not significant. Two 24 gage copper wires were connected to the ends of the test section the other two wires connected to a DC shunt for purposes of measuring the potential drops across the test section and the shunt. All thermocouple lead wire, and test section and shunt voltage leads were connected to double-throw copper knife switches with one side connected to a precision laboratory potentiometer (L&N 8662) for the steady-state readings and with the other side to a Minneapolis-Honeywell Visicorder (Model 1012) for the transient as well as steady-state recordings. A mixing baffle of negligible heat capacity was installed just upstream from the outlet fluid thermocouple as in Figure 29-e. It was found in the previous experiments[1,2,3] that measuring the coolant bulk temperature by means of a single, stationary thermocouple in the center of the stream provided a source of uncertainty which required a correction to obtain the bulk temperature.

The pressure drop across the test section were measured by a calibrated draft gage with a 2.00 specific weight indicating liquid.

B. Test Procedure

Three major experimental programs were scheduled: steady-state transient-periodic state and steady-periodic state.

The steady-state heat transfer experiments consisted of several runs with Reynolds number ranging from 10,000 to 35,000, in which both

heat transfer and pressure drop data were obtained. Temperatures were measured by the potentiometer and at the same time recorded by the Visicorder with the object of checking the calibrations of its galvanometers.

The experimental program of the steady periodic-state response included the frequencies ranging from 0.85 to 50 cycles per minute. Approximately 5 to 10 minutes were allowed for the attainment of steady state as determined by the Visicorder recordings.

For the transient periodic-state response, the starting positions of the four-bar linkage was set at the mean power output, followed by a sudden starting of the driving motor. The range of frequencies was limited to 20-25 cpm to prevent damage to the transformer shaft and the hydraulic speed control.

C. Analysis of Data

In the experimental investigation of the processes of heat exchange the local heat transfer coefficient along the test section is required. The local heat transfer coefficient is defined as

$$h_x = \frac{(q/A)_x}{\theta_{ix} - t_x} \tag{160}$$

where $(q/A)_x$ is the local heat flux evaluated from the equation

$$\left(\frac{q}{A}\right)_x = \frac{3412 (I^2 \rho_x)}{(\pi d_i)^2 \delta} \tag{161}$$

The current I is obtained from the measured voltage drop across the DC shunt, ρ_x is the local electrical resistivity and δ is the wall thickness. Figure 30 shows a typical curve of the local heat flux distribution indicating that the heat flux is practically constant except at the

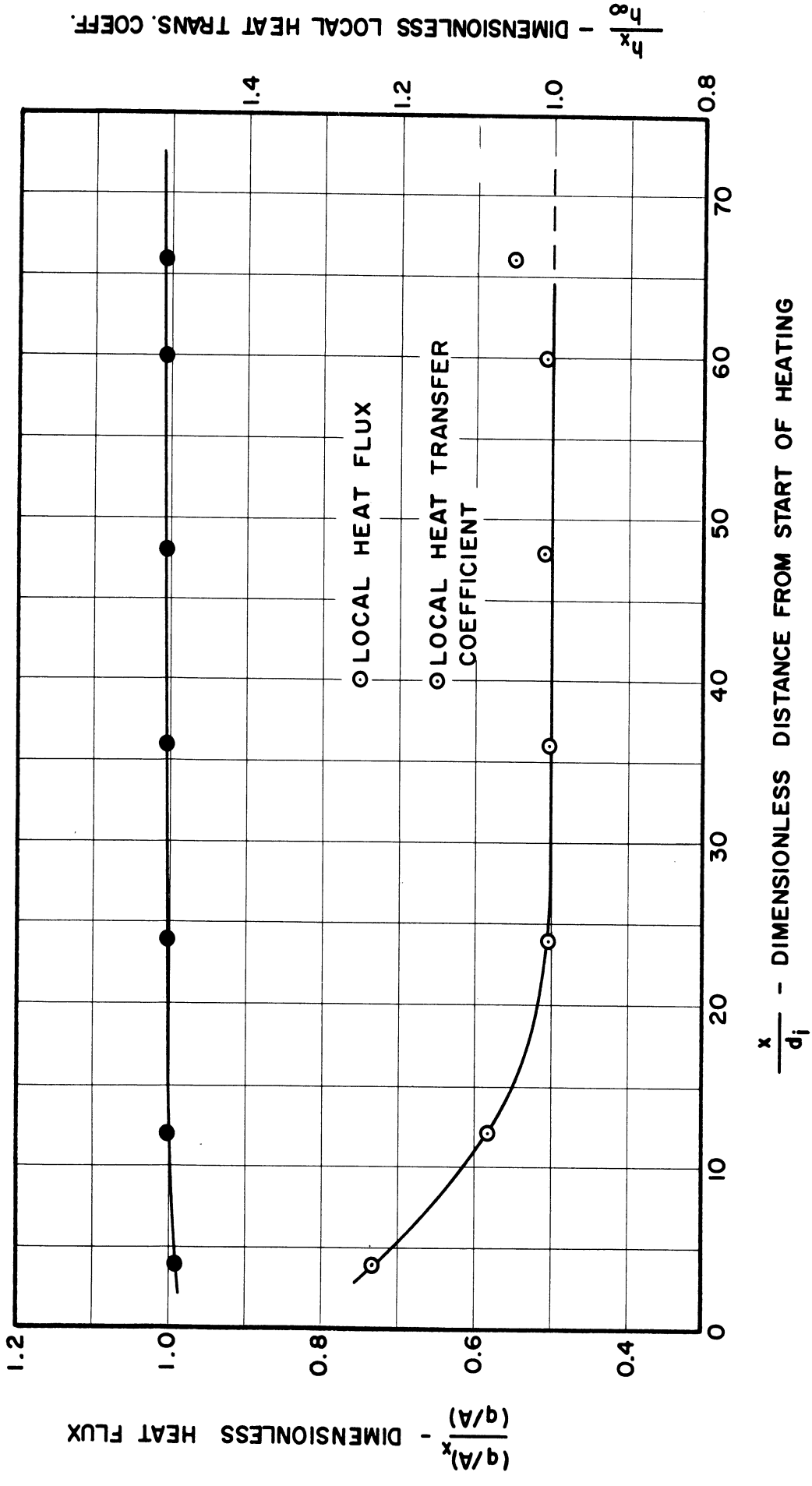

Figure 30. Typical Local Heat Flux and Heat Transfer Coefficient Distribution at Steady State, Re = 21,000.

thermal entrance region where the values are lower. The local inner-wall temperature θ_{ix} shown in Figure 31 is obtained from the measured temperature of the outer-wall which is insulated,

$$\theta_i = \theta_o - \frac{p''_x}{2k_x}\left[r_o^2 \ln\frac{r_o}{r_i} - \frac{1}{2}(r_o^2 - r_i^2)\right] \tag{162}$$

This is the equation for a hollow tube being heated by passing electric current through it, under the assumption that k_x is independent of r.

The variation of the temperature of the water along the length of the pipe could be determined by computation using the equation

$$t_x = t_o + \int_0^x \frac{(q/A)_x \pi d_i \, dx}{WC_p} \tag{163}$$

From the computations, curves are constructed showing the variation of the water temperature along the length of the test section for each run. The most typical one is shown in Figure 31.

After the curves for the temperature variation of the water and of the wall along the test section are obtained, the local heat transfer coefficients are computed from Equation (160). The dimensionless local heat transfer coefficients are shown in Figure 30.

The integrated mean heat transfer coefficient is defined as

$$h_m = \frac{1}{x}\int_0^x h \, dx \tag{164}$$

These computations allow constructing curves showing the variation of the integrated mean heat transfer coefficients along the length of the test section. Figure 32 shows the variation in dimensionless form.

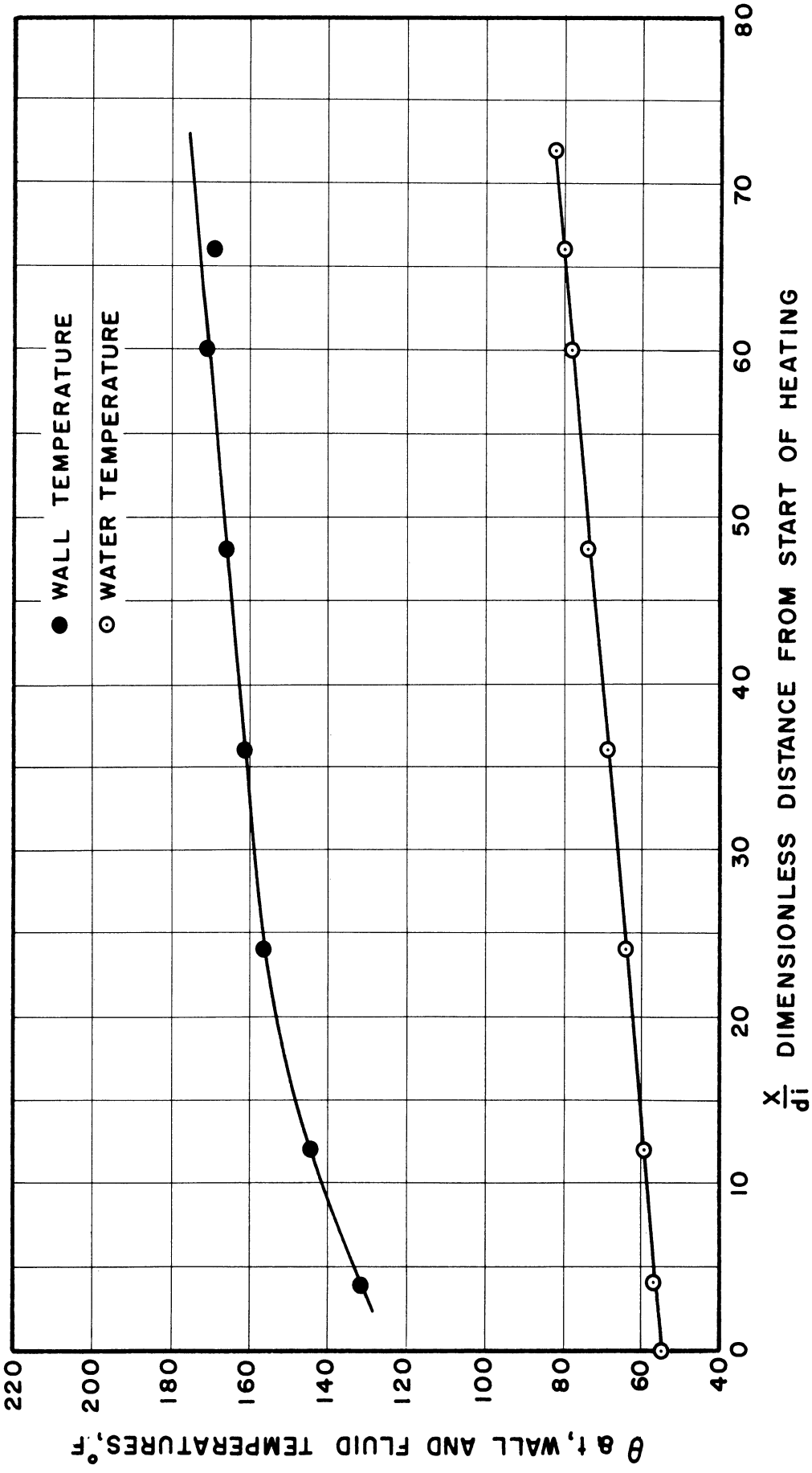

Figure 31. Typical Wall and Water Temperature Distribution at Steady-State Re = 21,000.

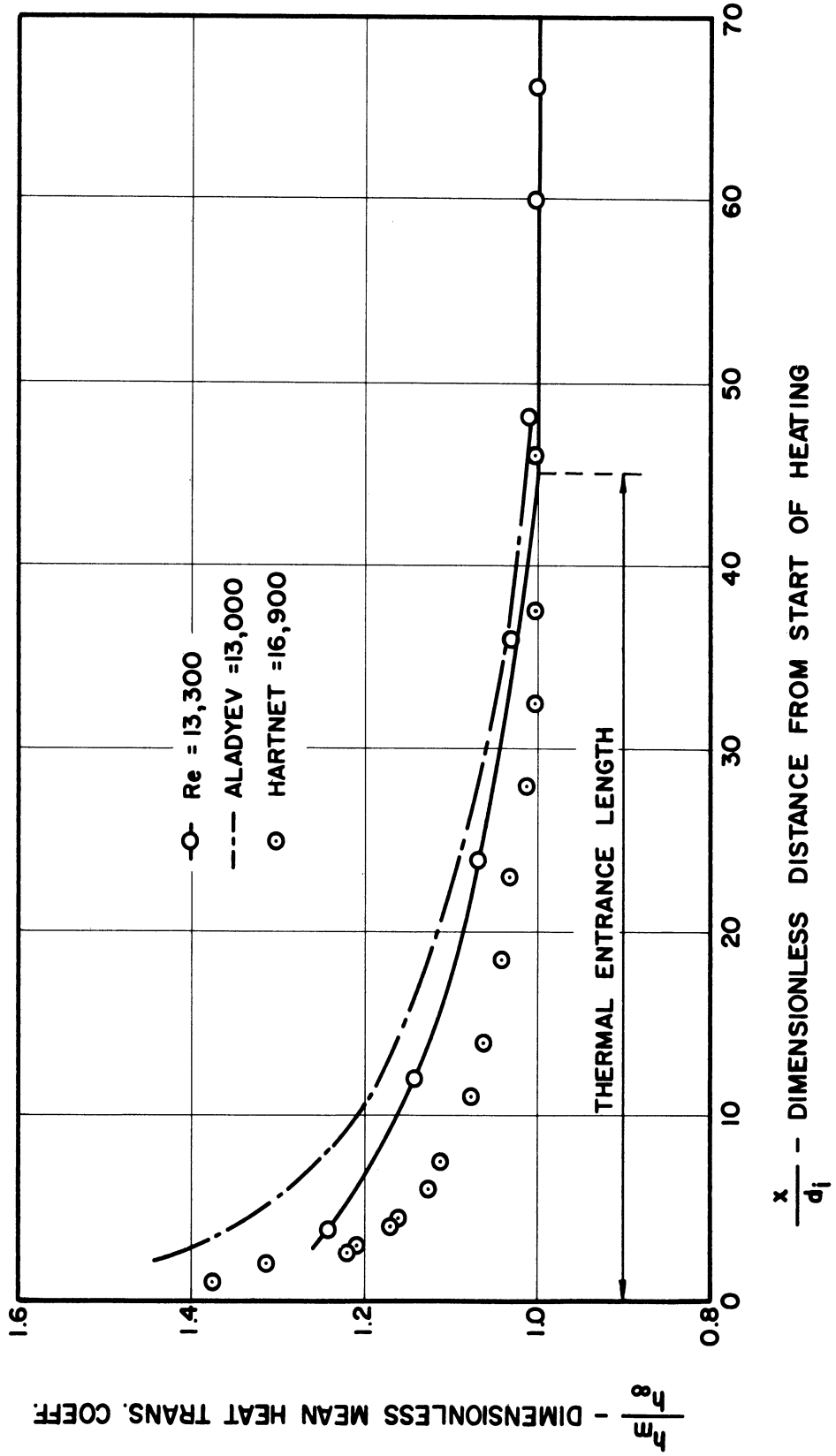

Figure 32. Comparison of Steady-State Results with Previous Investigations (Based on Re at Bulk Temperature).

In the experimental investigation of the transient behavior of the test section, temperatures as well as voltages are recorded by the Visicorder. Fourteen galvanometers used were of Heiland type No. M 40-120 with an undamped voltage sensitivity of 7.00 in/mv (or 0.143 mv/in) and nominal coil resistance of 21.4 ohms. A 120 ohm damping resistor was used in series with the galvanometer circuit. Each of the galvanometer circuits was calibrated in terms of deflection versus emf at its open terminals by using two precision potentiometers one to supply emf to the galvanometer the other to measure the emf supplied. Total resistance of each complete external thermocouple circuit was measured by a Wheatstone Bridge. The relationship between the DC voltage applied to the galvanometers and the corresponding (open circuit) thermal emf generated by the thermocouples was calculated for each circuit.

Each thermocouple was calibrated at the liquid nitrogen, steam and tin points. Due to the fact that the voltage applied to the test section is DC and the wall thermocouples were spot welded to the wall surface, the Visicorder would record the thermal emf as well as DC pick-up. A step input in DC voltage was applied to the test section and the sudden deflection of the galvanometer at that moment was measured.

Figure 33 shows the calibrations of DC voltage pickup by the wall thermocouples, which indicates the direct proportionality of the galvanometer deflection with DC voltage supplied to the test section. The wall thermocouples located at stations 6 and 9 showing no such DC pick up. The temperatures then are obtained after these several corrections to the recordings are made.

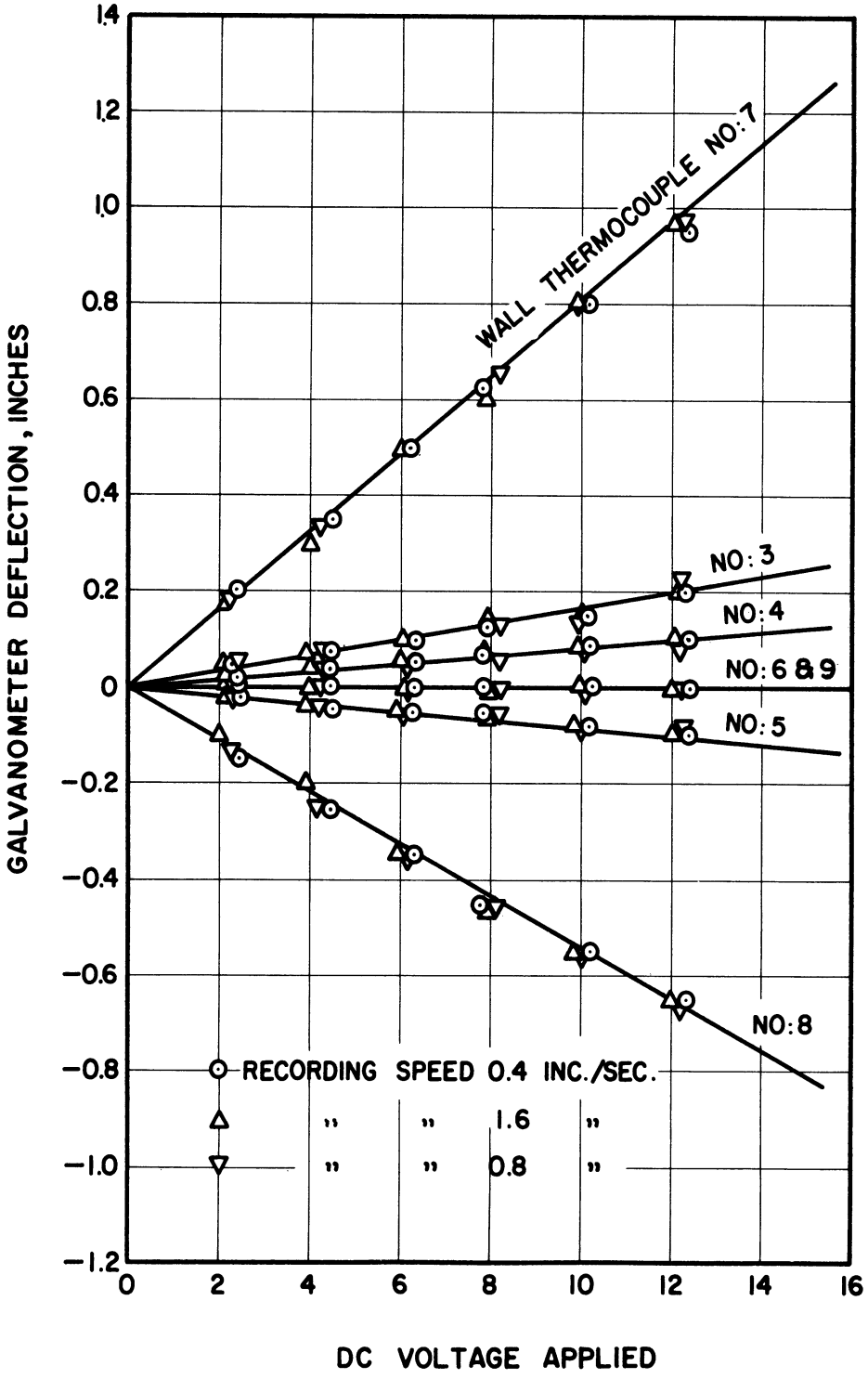

Figure 33. Calibration of DC Voltage Pickup by the Wall Thermocouples.

D. Results and Discussion

The hydrodynamic condition of the experiment is that the velocity distribution is fully established but the temperature profile is uniform at the entrance of the heated section.

1. Steady-State

The wall temperature distribution is shown in Figure 31. The gradient shown at the entrance is due to the formation and thickening of a thermal boundary layer. The drop in the wall temperature at the tube exit is due to conduction heat losses to the bus bar and the pressure tap.

Figure 30 indicates that the local heat transfer coefficient continuously decreases along the length of the test section up to a length to diameter ratio of 24 from the entrance for Reynolds numbers ranging from 10,000 to 35,000. The temperature profile downstream from this point is practically developed. The local heat transfer coefficients are independent of x when x/d_i is greater than 24.

Figures 32 and 34 show the comparison between the present results and that previously obtained by Aladev[32] for the constant wall temperature and Hartnett[33] for constant heat flux. Aladyev shows the thermal entrance length is approximately $40d_i$ while Hartnett indicates it should be $12d_i$ for the same ranges of the Reynolds Number. The present results show a fully developed condition exists at x/d_i of 24, which falls between the results of Aladyev and Hartnett.

The integrated mean heat transfer coefficients also decrease with increase in distance from the heated entrance, up to a length of

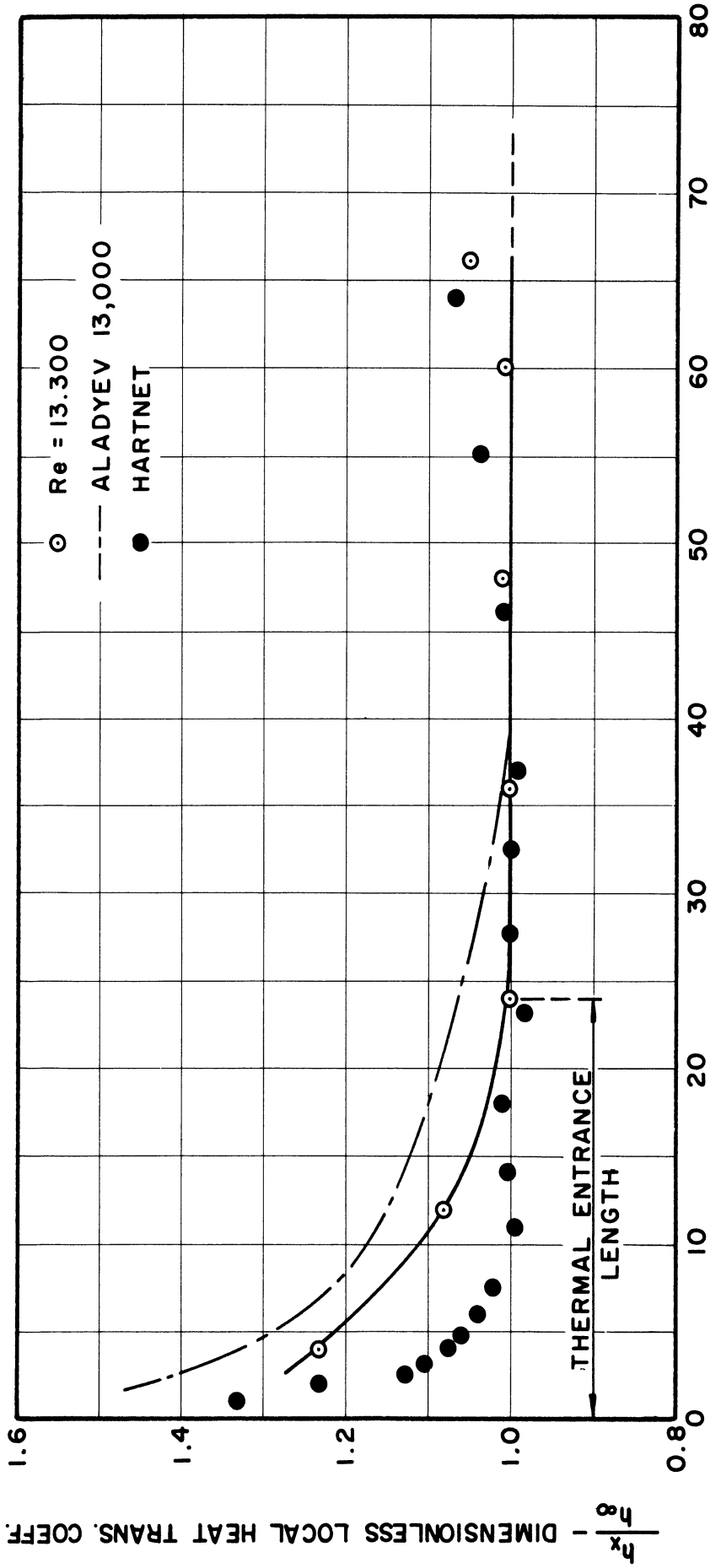

Figure 34. Comparison of Steady-State Results (Local Heat Transfer Coefficient) with Previous Investigations.

$x/d_i \approx 45$, where the thermal conditions are practically stablized. Aladyev gives a higher value of 50, while Hartnett, a lower one of approximately 30 for this condition. The experimental integrated mean heat transfer data correlated as shown in Figure 36 are 10 per cent lower than that predicted by McAdams' Equation (9-10b), Reference 37.

2. Steady-Periodic State

Figure 37-a demonstrates a typical result for comparisons between the actually recorded changes in the voltage and current applied to the test section, the water bulk temperature at x = 3 ft., and the wall temperature at x = 2.825 ft., and their theoretical sinusoidal changes. The applied voltage and current have flat tops, higher values at the first half period and lower values at the last half one, probably due to the four bar linkage itself and the generation of the induced voltage in the transformer while it is sinusoidally oscillating. It is estimated that this small discrepancy in the voltage and current would produce negligible error on the results as a whole. Appendix H shows the principle of the mechanism and its error estimation. It must be stressed here that the four bar linkage can produce an approximately sinusoidal angular displacement only on the transformer shaft.

Figure 37-b is a typical visicorder recording of the frequency response. The response recordings of the wall thermocouples at stations No. 6 and 9 (θ_6 and θ_9), which are free of the DC pick-up, are almost purely sinusoidal although the other wall thermocouples having a DC pick-up are less sinusoidal in their response. This is due to the fact that the magnitude of the DC pick-up by each wall thermocouple are different

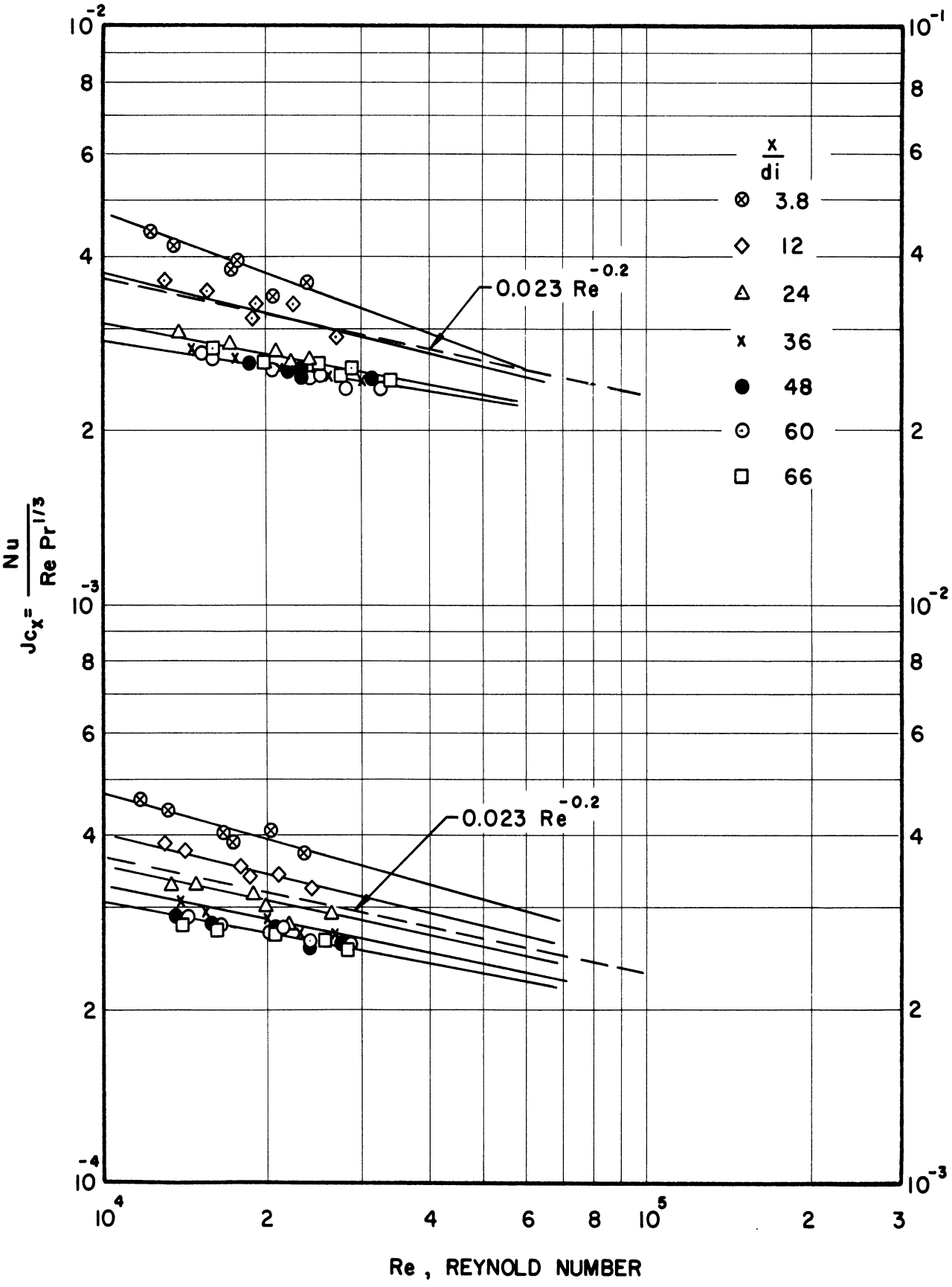

Figure 35. Correlation of Local and Local Mean Values of Heat Transfer Data.

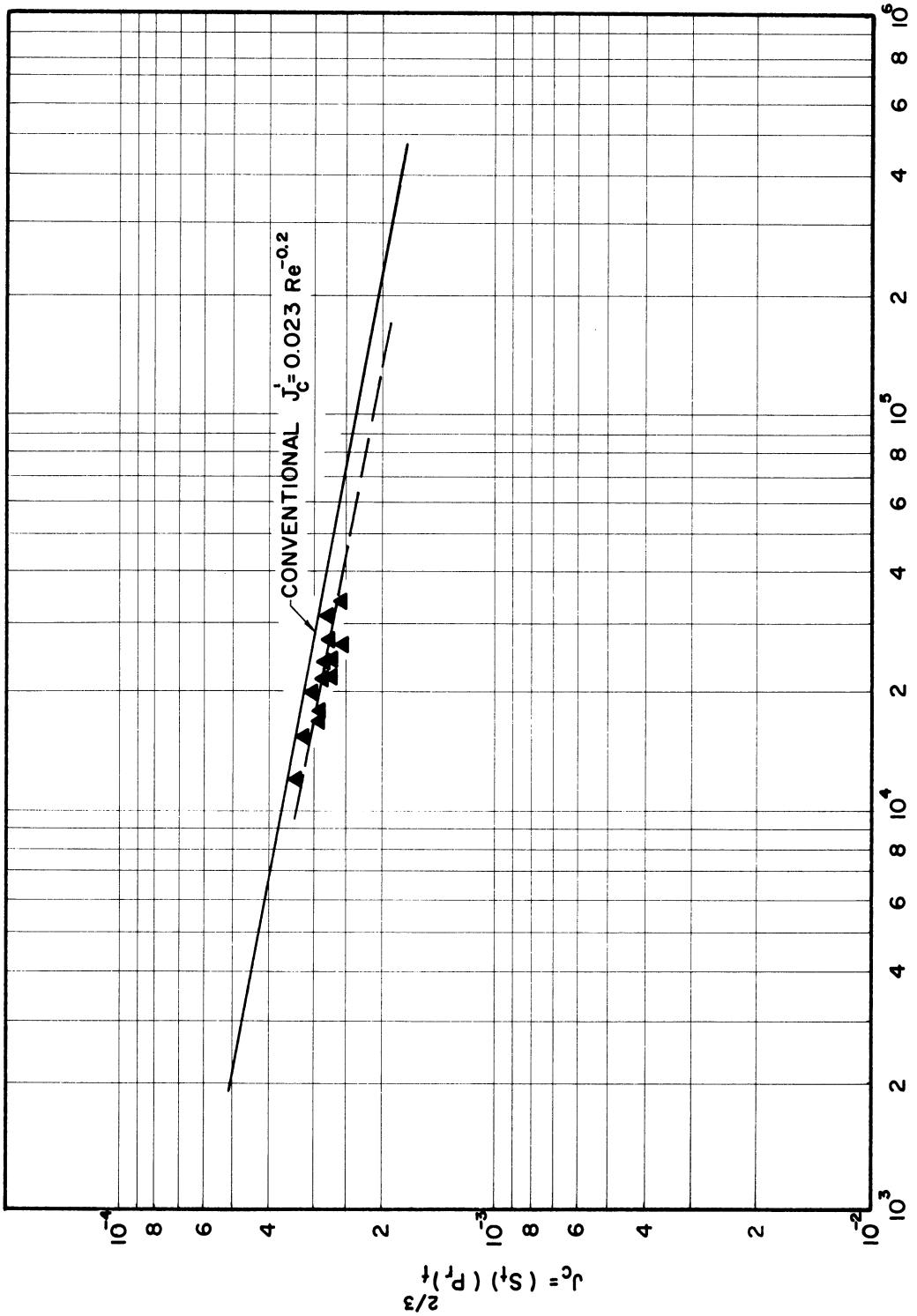

Figure 36. Correlation of Length-Mean Heat Transfer Data.

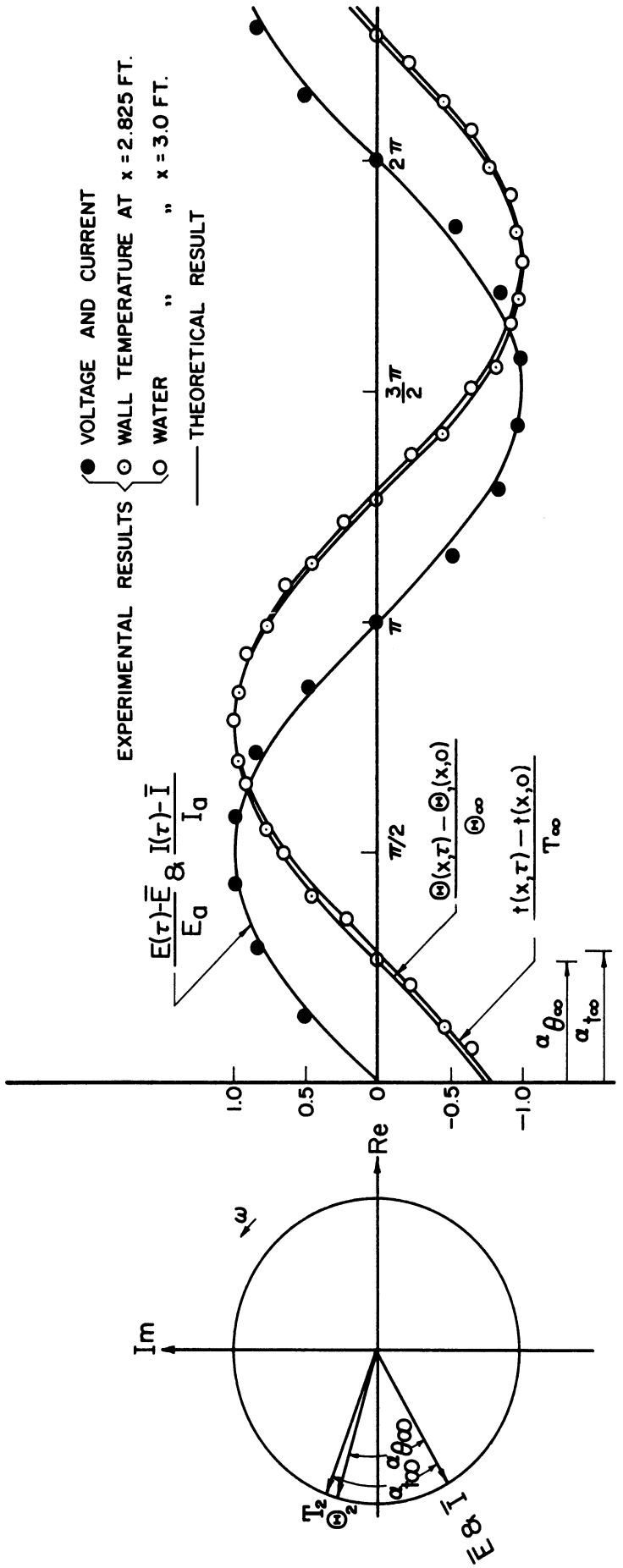

Figure 37-a. Steady Periodic Responses of the Wall and Water Temperatures, M = 0.561, K_w = 2470, P_a/P_{xo}" = 0.218, Mw/K = 0.653, Kx/u for Water = 0.321, for Wall = 0.161.

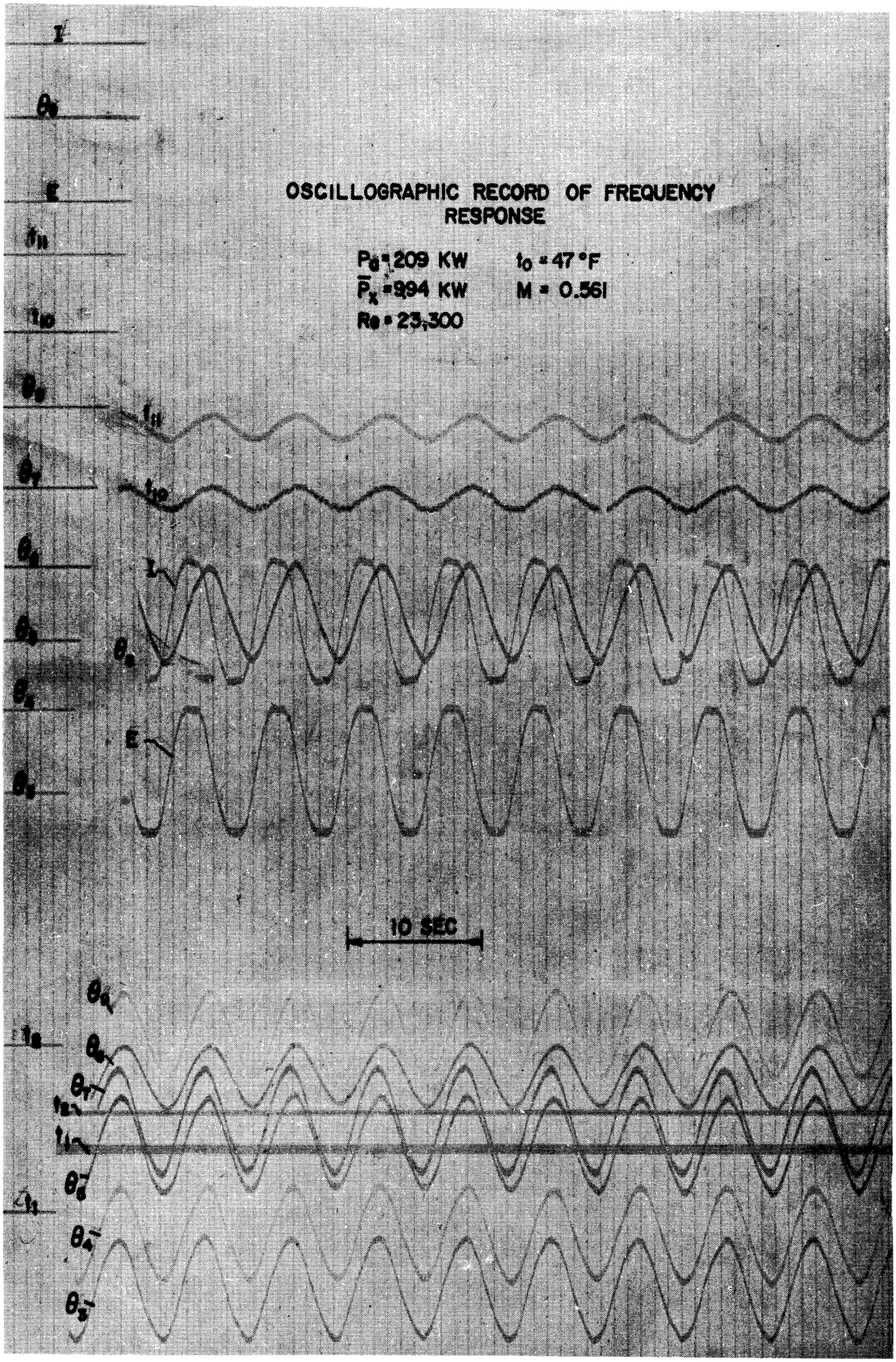

Figure 37-b. Oscillographic Record of Frequency Response.

with different voltage applied to the test section. For this reason, the frequency response of the wall temperatures shown in Figures 7 and 8 are investigated at stations No. 6 and 9 only. Figures 7 and 8 show the frequency response characteristics of the wall temperatures at Kx/u equal to 0.161 and 0.302. Figures 7 and 8 indicate that the experimental results of the wall temperature amplitude-ratio falls below the theoretical results, particularly at high frequency. The phase-shift response on the contrary is higher than but almost parallel to the theoretical one, and agree fairly well at the high frequency.

This discrepancy is probably due to the heat capacity lag of the wall thermocouples. The wall thermocouple at station No. 9 is close to the bus bar on one side and the pressure tap on the other. The uncertainty estimations for confidence limits on the mean of 95% are evaluated for the amplitude-ratio and phase-shift of the wall and fluid temperature by the method of Reference 36. The uncertainty intervals increase with increase in frequency, since at high frequency the galvanometer deflections corresponding to the temperature amplitude and mean temperature become very small.

For the wall temperatures at Kx/u = 0.161 and ω = 50 cycles per minute, the uncertainty intervals of the amplitude-ratio response is $\pm$ 35.3 per cent, and for the phase-shift response it is $\pm$ 34.3 per cent of their corresponding mean values for 95% confidence in the mean. At Kx/u = 0.302 those values decrease to $\pm$ 24.4 per cent and $\pm$ 34.3 per cent, respectively.

The frequency response of the water bulk temperature, shown in Figures 6-a and -b is measured at station 11, located after the mixing baffle and corresponds to that at test section exit. The experimental

results of both amplitude-ratio and phase-shift responses agree well with their theoretical curves. The uncertainty intervals are also shown for 95% of confidence in the mean. The heat transfer coefficient used in the theoretical computation is the integrated mean value where fluid properties are based on the film temperature.

Resonance phenomena both in the amplitude-ratio and phase-shift response of the water temperature occur at the frequencies of 95 cycles per minute for the former and 80 cycles per minute for the latter.

Owing to the increasing percentage in uncertainty interval at high frequency and the difficulties in making a physical measurement as the thermal emf of the temperature amplitude at the first point of resonance is the order of 1 to 3 microvolts for operating conditions shown in Figure 6-a, which is lower than the output noise level of the ordinary DC amplifier, these experimental data have not been extended to sufficiently high frequencies in this thesis to demonstrate the resonance indicated by the theoretical computations because of the physical restrictions of the experimental apparatus. However, it is believed to be possible to obtain the resonance phenomena experimentally by providing a longer test section (approximately 4 times longer than the present one with the same diameter) and using a different fluid-wall system having a smaller heat-capacity ratio M.

3. Transient Periodic-State

The typical transient-periodic state responses of water and wall temperatures are shown in Figures 38 and 39. Figure 38 shows the experimental data of the water bulk temperature response to agree very

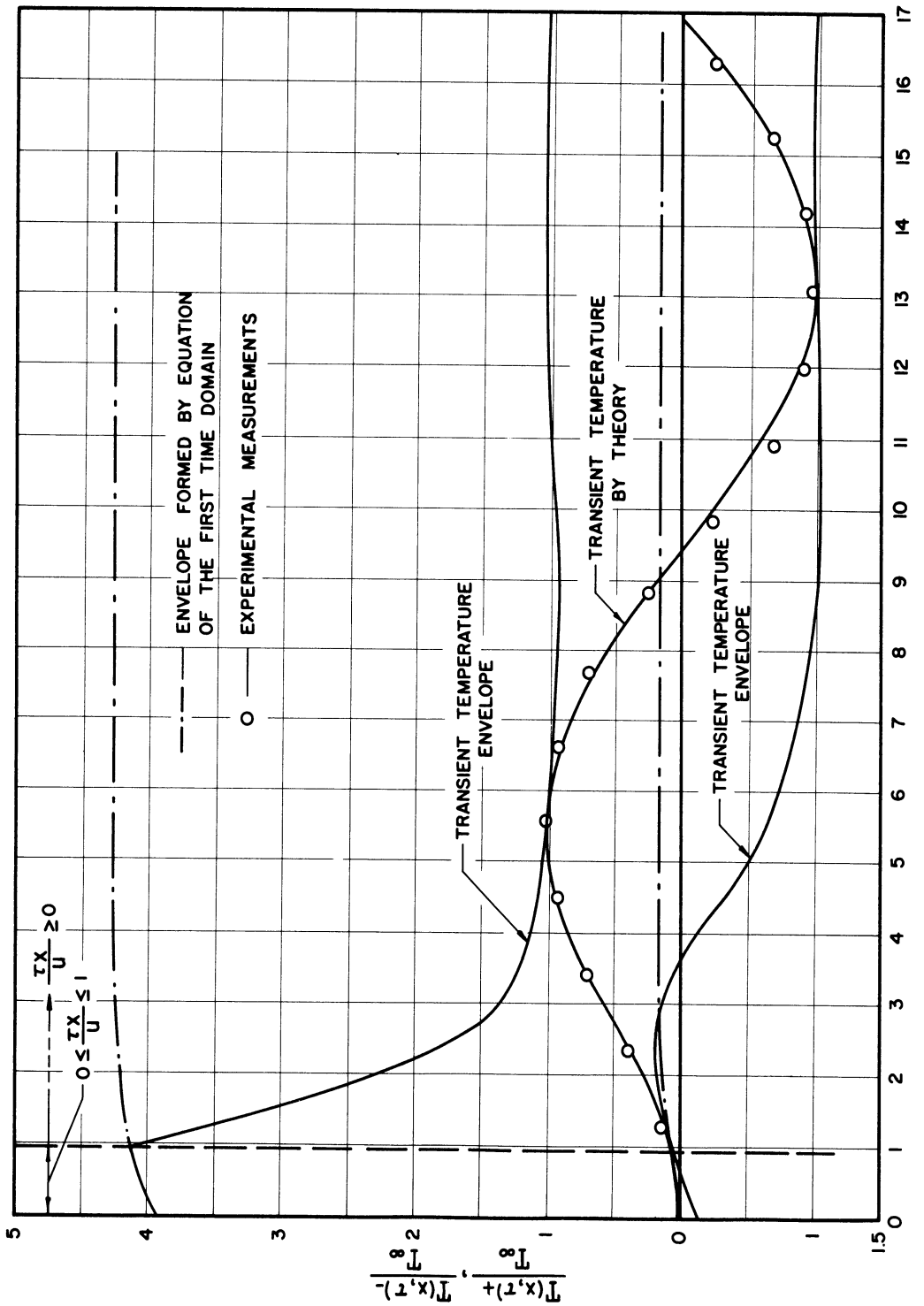

Figure 38. Transient Periodic-State Response of Water Temperature at $Kx/u = 0.321$, $M = 0.561$, $K_w = 2470$, $P_a/P_{ox}" = 0.218$, $M\omega/K = 0.653$.

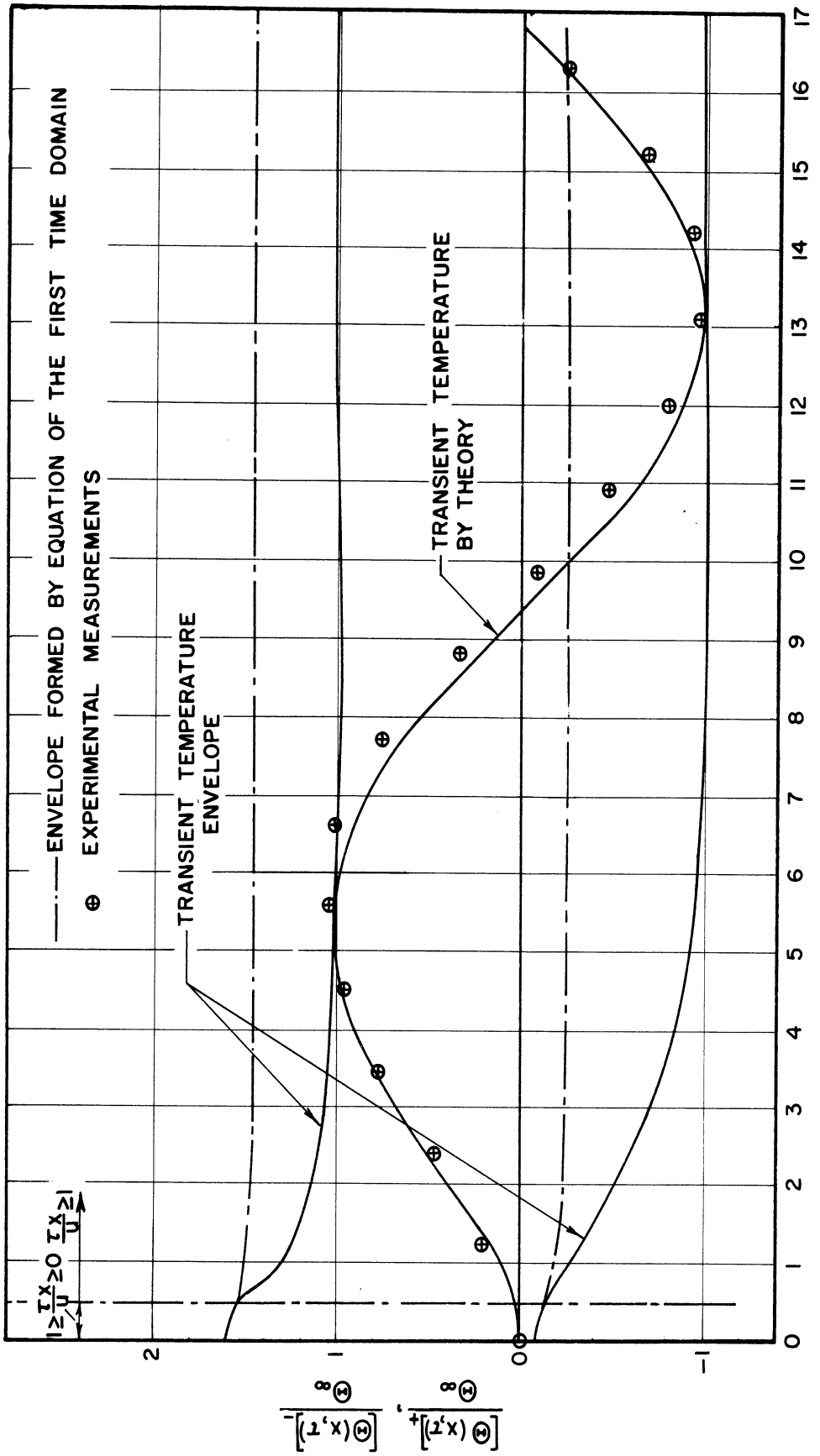

Figure 39. Transient Periodic-State Response of Wall Temperature at $Kx/u = 0.161$, $M = 0.561$, $K_w = 2470$, $P_a/P_{ox}'' = 0.218$, $M\omega/K = 0.218$.

well with the theoretical curve in this state. The experimental results of wall temperature response shown in Figure 39 fall fairly well on the theoretical curve, except that the phase-shift is larger. The physical time intervals in the first time domain for the both responses are very short but the recordings show they agree well with the theoretical calculations.

CHAPTER V

CONCLUSION

It is concluded from this study that:

1. In the steady turbulent flow of a fluid in a pipe with steady uniformly distributed heat sources, the local values of the heat transfer coefficients decrease along the length of the pipe practically up to a section of the distance $x = 24d_i$ from the start of heating where the velocity profile of the flow is fully developed. The thermal-entry length is a function of the Reynolds number Re (based on the film temperature) and decreases with increase in the latter, but starting from $x = 24d_i$ the local heat transfer coefficients become independent of x/d.

The integrated mean heat transfer coefficient decreases with increase in the relative length of the pipe. The length of the thermally stabilized section for the mean heat transfer coefficient is a function of Re and decreases with increase in the latter. The integrated mean heat transfer coefficient become practically independent of x/d starting from $x = 45d_i$.

2. The frequency-response characteristics of the wall and fluid temperatures and the fluid-wall temperature difference have been analyzed, and it has been shown that those response characteristics are functions of four parameters M, Kx/u, $M\omega/u$ and $\omega x/u$, among which one is the dependent parameter. The frequency-response characteristics of the fluid and wall temperatures, and fluid-wall temperature difference exhibit the phenomena

of resonance in amplitude-ratio and phase-shift. For a system of zero wall-fluid heat capacity ratio (M=0) the dynamic characteristics depend upon parameters $\omega x/u$ and Kx/u, and the phenomena of resonance in amplitude-ratio and phase-shift occur periodically in intervals of 2π in $\omega x/u$. Resonance occurs at $\pi x/u = 3\pi/2$, $5\pi/2$, $7\pi/2$, etc. for the amplitude-ratio and $\omega x/u = 2\pi$, 4π, 6π, etc. for the phase-shift, for the fluid temperature only. For the wall temperature the points of resonance depends on Kx/u. The amplitude-ratio decreases and the phase-shift increases with increase in heat capacity ratio. These results are found in Figures 9, 10, 11, 12, 25 and 26.

3. The transient-periodic state of the response of the wall and fluid temperatures and the fluid-wall temperature difference are functions of four parameters, M, $K\tau/M$, $M\Theta/K$, and $\omega\tau$, of which $\omega\tau$ is dependent in the first time domain. In the second time domain these temperatures are functions of six parameters, M, $K\tau/M$, $M\Theta/K$, $\omega\tau$, Kx/u and $\omega x/u$ of which two parameters $\omega x/u$ and $\omega\tau$ are dependent. The transient-periodic state, in general, decays exponentially. The dynamic behavior of the wall and fluid temperatures and the fluid-wall temperature difference are confined within defineable envelopes.

4. From this study it is concluded that resonance phenomena in the amplitude-ratio and phase-shift are the characteristics of distributed-parameter systems under distributed disturbances. These results are contrary to those of Paynter[21] who classified these systems in the category of those having monotonic characteristics. The method of approximating the process characteristics by means of stochastic processes* as suggested by him in Reference 1 is undesirable in this instance.

---

* See Reference 1 for Paynter's comments on the generalized percolation problem.

APPENDICES

APPENDIX A

DERIVATION OF THE BASIC DIFFERENTIAL EQUATIONS*

The system analyzed is shown in Figure 4 and consists of a constant-diameter circular tube through which a fluid (coolant) is pumped steadily and in the walls of which energy is dissipated.

With the assumptions and conditions as indicated in Chapter III, two differential equations, one for the wall and one for the fluid, may be derived from the First Law of Thermodynamics and the law of conservation of mass for an incompressible fluid.(1)

Fluid

$$\frac{\partial(\rho e)}{\partial \tau} + \frac{\partial(\rho h u)}{\partial x} = \frac{hC}{a}(\theta - t) \qquad \text{(A-1)}$$

Wall

$$\frac{\partial(\rho e)_w}{\partial \tau} = -\frac{hC}{a'}(\theta - t) + p''_{xo} + \phi(\tau) \qquad \text{(A-2)}$$

Where

- a flow wetted cross-sectional area (πr_i^2 for circular tube)
- c wetted perimeter ($2\pi r_i$ for circular tube)
- a' gross-sectional area of duct wall ($\pi r_o^2 - \pi r_i^2$ for circular tube)
- p_{xo}'' initial volumetric heat generation rate
- $\phi(\tau)$ arbitrary transient in volumetric heat generation rate
- e internal energy per lbm in absence of the effects of motion, capillarity, and so forth

* See Reference 3.

Equations (A-1) and (A-2) may be reduced to the following

$$\theta - t = \frac{\rho C_p a}{h}\left(\frac{\partial t}{\partial \tau}\right) + \frac{\rho C_p a u}{hC}\left(\frac{\partial t}{\partial x}\right) \tag{A-3}$$

$$= \frac{\rho C_p r_i}{2h}\left(\frac{\partial t}{\partial \tau}\right) + \frac{\rho C_p r_i u}{2h}\left(\frac{\partial t}{\partial x}\right) \tag{A-4}$$

$$= \frac{1}{K}\left(\frac{\partial t}{\partial \tau}\right) + \frac{u}{K}\left(\frac{\partial t}{\partial x}\right) \tag{A-5}$$

Equation (A-4) is for circular tube geometry and (A-5) is for generalized geometry. Both are equivalent to Equation (35).

For the wall, Equation (A-2) may be rearranged to

$$-(\theta - t) + \frac{a'}{hC}\left[P''_{x0} + \phi(\tau)\right] = \frac{a'(\rho C_p)_w}{hC}\left(\frac{\partial \theta}{\partial \tau}\right) \tag{A-6}$$

$$-(\theta - t) + \frac{r_o^2 - r_i^2}{2hr_i}\left[P''_{x0} + \phi(\tau)\right] = \frac{(\rho C_p)_w (r_o^2 - r_i^2)}{2r_i h}\left(\frac{\partial \theta}{\partial \tau}\right) \tag{A-7}$$

$$-(\theta - t) + \frac{1}{(\rho C_p)_w K_w}\left[P''_{x0} + \phi(\tau)\right] = \frac{1}{K_w}\left(\frac{\partial \theta}{\partial \tau}\right) \tag{A-8}$$

Equation (A-7) is for circular-tube geometry and (A-8) is for generalized geometry. Both are equivalent to Equation (34).

For this particular problem, it is convenient to partition both temperatures $\theta(x,\tau)$ and $t(x,\tau)$ into transient and steady-state components at this point. It is defined that

$$\theta(x,\tau) = \theta_1(x,0) + \theta_2(x,\tau) \tag{A-9}$$

$$t(x,\tau) = t_1(x,0) + t_2(x,\tau) \tag{A-10}$$

Where Θ_1 and t_1 are the steady-state and Θ_2 and t_2 the transient components. For the steady-state conditions, Θ_1 and t_1 satisfy the following differential equations which are Equations (A-5) and (A-8) with all time derivatives and $\phi(\tau)$ set equal to zero,

$$(\Theta_1 - t_1) = \frac{u}{K}\left(\frac{\partial t_1}{\partial x}\right) \tag{A-11}$$

$$-(\Theta_1 - t_1) + \frac{1}{(\rho C_p)_w K_w} P''_{x0} = 0 \tag{A-12}$$

With the introduction of assumption g, one obtains from Equations (A-11) and (A-12)

$$t_1(x,0) = t_0 + \frac{(q/A)_0}{WC_p} Cx \tag{A-13}$$

$$\Theta_1(x,0) = t_0 + \frac{(q/A)_0}{WC_p} Cx + \frac{(q/A)_0}{h} \tag{A-14}$$

where $(a/A)_0$ is the initial steady-state heat flux at $\tau=0$, t_0 is the temperature of the fluid entering the duct at the initial steady-state $\tau=0$. Substitution of Equations (A-9) and (A-10) into Equations (A-5) and (A-8), and subtracting Equations (A-11) and (A-12) from the results give

$$\Theta_2 - t_2 = \frac{1}{K}\left(\frac{\partial t_2}{\partial \tau}\right) + \frac{u}{K}\left(\frac{\partial t_2}{\partial x}\right) \tag{A-15}$$

$$-(\Theta_2 - t_2) + \frac{1}{(\rho C_p)_w K_w} \phi(\tau) = \frac{1}{K_w}\left(\frac{\partial \Theta_2}{\partial \tau}\right) \tag{A-16}$$

These equations are the same as Equations (37) and (38) and are subjected to the following initial and boundary conditions. Since the initial and boundary conditions are

$$\theta(x,0)=\theta_1(x,0) \tag{A-17}$$

$$t(x,0)=t_1(x,0) \tag{A-18}$$

$$t(0,\tau)=t_0+t_0^*(\tau) \tag{A-19}$$

and

$$t_1(0,0)=t_0 \tag{A-20}$$

the boundary conditions for the transient components become

$$\theta_2(x,0)=0 \tag{A-21}$$

$$t_2(x,0)=0 \tag{A-22}$$

$$t_2(0,\tau)=t_0^*(\tau)\ ,\ t_2(0,\tau)=0 \text{ if } t(0,\tau)=t_0 \tag{A-23}$$

Equations (A-13) and (A-14) show both θ_1 and t_1 are independent of τ, the dynamic characteristics of the system is free of the initial effect due to θ_1 and t_1 and the transient components constitute the complete dynamic behavior.

The response equations for the fluid and wall temperatures may be found from Equations (A-15) and (A-16) as

$$a_2a_3\frac{\partial^2 t_2}{\partial\tau^2}+a_2a_4\frac{\partial^2 t_2}{\partial\tau\partial x}+(a_2+a_3)\frac{\partial t_2}{\partial\tau}+a_4\frac{\partial t_2}{\partial x}=a_1\phi \tag{A-24}$$

$$a_2a_3\frac{\partial^2\theta_2}{\partial\tau^2}+a_2a_4\frac{\partial^2\theta_2}{\partial\tau\partial x}+(a_2+a_3)\frac{\partial\theta_2}{\partial\tau}+a_4\frac{\partial\theta_2}{\partial x}=a_1\phi+a_1a_3\frac{\partial\phi}{\partial\tau} \tag{A-25}$$

APPENDIX B

DERIVATION OF TRANSFER FUNCTIONS

Apply the method of Laplace transform to Equation (A-24) and its initial condition $t_2(x,0)=0$, one obtains a subsidiary equation for the fluid temperature as

$$a_4(a_2S+1)\frac{d\bar{t}_2}{dx}+S(b_2S+b_1)\bar{t}_2=a_1\bar{\Phi} \tag{B-1}$$

The general solution of Equation (B-1) is

$$\bar{t}_2=C_1e^{-\frac{S(b_2S+b_1)x}{a_4(1+a_2S)}}+\frac{a_1\bar{\Phi}}{S(b_2S+b_1)} \tag{B-2}$$

where the integration constant c_1 is determined by the boundary conditions. There are three different sets of the boundary conditions, (i), (ii) and (iii) below, which are:

(i) The inlet fluid temperature is kept constant, i.e. $\bar{t}_0^* = 0$, and energy (heat) generation within the walls is constant with length but is time dependent. Equation (B-2) then becomes

$$\bar{t}_2=\bar{\Phi}\frac{a_1}{S(b_2S+b_1)}\left[1-e^{\frac{-S(b_2S+b_1)x}{a_4(1+a_2S)}}\right] \tag{B-3}$$

Substituting Equation (B-3) into the Laplace transform of Equation (A-16), gives an equation for the transformed wall temperature as

$$\bar{\theta}_2=\bar{\Phi}\frac{a_1}{S(b_2S+b_1)}\left[1+a_3S-\frac{1}{1+a_2S}e^{-\frac{S(b_2S+b_1)x}{a_4(1+a_2S)}}\right] \tag{B-4}$$

(ii) The temperature of the fluid entering the duct is time-dependent and the energy generation within the wall is constant with length and time, that is $\bar{\phi} = 0$. For this case Equation (B-2) becomes

$$\bar{t}_2 = \bar{t}_0^* \, e^{-\frac{s(b_2 s + b_1)x}{a_4(1+a_2 s)}} \tag{B-5}$$

Substituting into the Laplace transform of Equation (A-16) with $\Phi = 0$, gives for the wall,

$$\bar{\theta}_2 = \frac{\bar{t}_0^*}{1+a_2 s} e^{-\frac{s(b_2 s + b_1)x}{a_4(1+a_2 s)}} \tag{B-6}$$

(iii) For the general case, both the inlet fluid temperature and the energy generation in the wall are time-dependent, that is $\bar{\phi}$ and $\bar{t}_2^*$ are the disturbances. Equations for $\bar{t}_2$ and $\bar{\theta}_2$ may be found by principle of superposition. By superposing Equations (B-3) with (B-5) and (B-4) with (B-6), one obtains

$$\bar{t}_2 = \bar{t}_0^* e^{-\frac{s(b_2 s + b_1)x}{a_4(1+a_2 s)}} + \bar{\phi} \frac{a_1}{s(b_2 s + b_1)} \left[1 - e^{-\frac{s(b_2 s + b_1)x}{a_4(1+a_2 s)}} \right] \tag{B-7}$$

and

$$\bar{\theta}_2 = \frac{\bar{t}_0^*}{1+a_2 s} e^{-\frac{s(b_2 s + b_1)x}{a_4(1+a_2 s)}} + \bar{\phi} \frac{a_1}{s(b_2 s + b_1)} \left[1 + a_3 s - \frac{1}{1+a_2 s} e^{-\frac{s(b_2 s + b_1)x}{a_4(1+a_2 s)}} \right] \tag{B-8}$$

Subtracting Equations (B-8) by (B-7), yields

$$\Delta\bar{t}_2=\bar{\theta}_2-\bar{t}_2=-\frac{a_2 s\bar{t}_o^*}{1+a_2 s}\,e^{-\frac{s(b_2 s+b_1)x}{a_4(1+a_2 s)}}+\frac{\bar{\phi}a_1}{b_2 s+b_1}\left[a_3+\frac{a_2}{1+a_2 s}\,e^{-\frac{s(b_2 s+b_1)x}{a_4(1+a_2 s)}}\right] \qquad \text{(B-9)}$$

The dynamic response due to the disturbance on the fluid inlet temperature $\bar{t}_o^*$ was investigated by Profos[20], Takahashi[7] and Rizika.[11] The response to a step increase in heat generation $\bar{\phi}$ with constant fluid inlet temperature ($\bar{t}_o^* = 0$), was studied, by Clark and Arpaci.[1,2,3] Since the two processes are linear in nature, their individual dynamic responses are superposable in the output, that is the wall and fluid temperatures and fluid-wall temperature difference.

If the temperature of the fluid entering the coolant channel is constant and equal to t_o, then Equations (B-7), (B-8) and (B-9) become

$$\bar{t}_2=\frac{a_1}{s(b_2 s+b_1)}\left[1-e^{-\frac{s(b_2 s+b_1)x}{a_4(1+a_2 s)}}\right]\bar{\phi} \qquad \text{(B-10)}$$

$$\bar{\theta}_2=\frac{a_1}{s(b_2 s+b_1)}\left[1+a_3 s-\frac{1}{1+a_2 s}e^{-\frac{s(b_2 s+b_1)x}{a_4(1+a_2 s)}}\right]\bar{\phi} \qquad \text{(B-11)}$$

$$\Delta\bar{t}_2=\frac{a_1}{b_2 s+b_1}\left[a_3+\frac{a_2}{1+a_2 s}e^{-\frac{s(b_2 s+b_1)x}{a_4(1+a_2 s)}}\right]\bar{\phi} \qquad \text{(B-12)}$$

By rearranging Equations (B-10), (B-11) and (B-12), one obtains

$$\frac{\bar{t}_2}{\bar{\Phi}\frac{a_1 x}{a_4}} = \frac{a_4}{b_2 x\, s\left(s+\frac{b_1}{b_2}\right)}\left[1 - e^{-\frac{s(b_2 s+b_1)x}{a_4(1+a_2 s)}}\right] \tag{B-13}$$

$$\frac{\bar{\Theta}_2}{\bar{\Phi} a_1\left(1+\frac{x}{a_4}\right)} = \frac{1}{b_2\left(1+\frac{x}{a_4}\right)s\left(s+\frac{b_1}{b_2}\right)}\left[1+a_3 s - \frac{1}{1+a_2 s}\, e^{-\frac{s(b_2 s+b_1)x}{a_4(1+a_2 s)}}\right] \tag{B-14}$$

$$\frac{\Delta\bar{t}_2}{\bar{\Phi} a_1} = \frac{1}{b_2\left(s+\frac{b_1}{b_2}\right)}\left[a_3 + \frac{a_2}{1+a_2 s}\, e^{-\frac{s(b_2 s+b_1)x}{a_4(1+a_2 s)}}\right] \tag{B-15}$$

At zero frequency a heat balance of the system gives the following relationship:

$$\frac{\Phi a_1 x}{a_4} = \frac{\Delta\left(\frac{q}{A}\right)}{h}\frac{x}{a_4} = t_1^*(x) - t_1(x,0) = \left[T_\infty(x)\right]_{\omega=0} \tag{B-16}$$

$$\Phi a_1\left(1+\frac{x}{a_4}\right) = \frac{\Delta\left(\frac{q}{A}\right)}{h}\left(1+\frac{x}{a_4}\right) = \Theta_1^*(x) - \Theta_1(x,0) = \left[\Theta_\infty(x)\right]_{\omega=0} \tag{B-17}$$

$$\Phi a_1 = \frac{\Delta\left(\frac{q}{A}\right)}{h} = t_1^*(x) - t_1(x,0) = \left[\Delta T_\infty(x)\right]_{\omega=0} \tag{B-18}$$

where $t_1^*(x)$, $\Theta^*(x)$ and $\Delta t_1^*(x)$ are the steady-state fluid and wall temperatures and fluid-wall temperature difference at x for $p_x'' = p_{xo}'' + \Phi$. But $\phi(\tau) = \Phi \sin\omega\tau$, for sinuscinal input disturbances (heat generation), hence

$$\phi(\tau)\frac{a_1 x}{a_4} = \left[T_\infty(x)\right]_{\omega=0} \sin\omega\tau \tag{B-19}$$

$$\phi(\tau)a_1\left(1+\frac{x}{a_4}\right) = \left[\Theta_\infty(x)\right]_{\omega=0} \sin\omega\tau \tag{B-20}$$

$$\phi(\tau)a_1 = \left[\Delta T_\infty(x)\right]_{\omega=0} \sin\omega\tau \tag{B-21}$$

If Equations (B-19), (B-20) and (B-21) are taken as the disturbances instead of $\phi(\tau)$, then $\overline{\phi}\ \frac{a_1 x}{a_4}$, $\overline{\phi}\ a_1(1 + \frac{x}{a_4})$ and $\overline{\phi}\ a_1$ are the Laplace transform of the disturbances. Since $\overline{t}_2$, $\overline{\Theta}_2$ and $\overline{\Delta t}_2$ are the Laplace transform of the outputs, Equations (B-13), (B-14) and (B-15) may be defined as the transfer functions of the fluid and wall temperatures and the fluid-wall temperature difference, which are designated by $\overline{F}_t(s)$, $\overline{F}_\Theta(s)$ and $\overline{F}_{\Delta t}(s)$.

APPENDIX C

FREQUENCY RESPONSE*

According to the general theory in Chapter II the transfer functions of frequency response of the fluid and wall temperatures and the fluid-wall temperature difference can be obtained as follows by replacing s by iω in the transfer functions expressed by Equations (B-13), (B-14) and (B-15.

Fluid temperature

$$\bar{F}_t(i\omega) = \frac{a_4}{b_2 x (i\omega)(i\omega + \frac{b_1}{b_2})}\left[1 - e^{-\frac{(i\omega)(b_2 i\omega + b_1)}{a_4(1 + a_2 i\omega)}}\right] = \left|\bar{F}_t(i\omega)\right| e^{i\alpha_t} \qquad (C\text{-}1)$$

where

$$\left|\bar{F}_t(i\omega)\right| = \frac{\left\{\left[-\frac{e^{\delta}}{\sqrt{1+(\frac{b_1}{b_2\omega})^2}} + \sin\left(\gamma + \tan^{-1}\frac{b_2\omega}{b_1}\right)\right]^2 + \left[-\frac{e^{\delta}}{\sqrt{1+(\frac{b_2\omega}{b_1})^2}} + \cos\left(\gamma + \tan^{-1}\frac{b_2\omega}{b_1}\right)\right]^2\right\}^{1/2}}{\frac{e^{\delta}}{\sqrt{1+(\frac{b_1}{b_2\omega})^2}}\left[1 + (\frac{b_2\omega}{b_1})^2\right]\frac{x}{a_4}\frac{b_1^2}{b_2}} \qquad (C\text{-}2)$$

$$\alpha_t = \tan^{-1}\left\{\frac{\frac{e^{\delta}}{\sqrt{1+(\frac{b_2\omega}{b_1})^2}} - \cos\left(\gamma + \tan^{-1}\frac{b_2\omega}{b_1}\right)}{-\frac{e^{\delta}}{\sqrt{1+(\frac{b_1}{b_2\omega})^2}} + \sin\left(\gamma + \tan^{-1}\frac{b_2\omega}{b_1}\right)}\right\} \qquad (C\text{-}3)$$

$$\delta = \frac{(a_2\omega)^2}{1+(a_2\omega)^2}\frac{x}{a_4} \qquad (C\text{-}4)$$

*See Chapter III, Section A.

and

$$\gamma = \frac{(b_1 + a_2 b_2 \omega^2)\omega}{1 + (a_2\omega)^2} \frac{x}{a_4} \tag{C-5}$$

wall temperature

$$\bar{F}_\theta(i\omega) = \frac{1}{b_2\left(1+\frac{x}{a_4}\right)(i\omega)\left(i\omega+\frac{b_1}{b_2}\right)}\left[1 + a_3 i\omega - \frac{e^{\frac{-(i\omega)(b_2 i\omega + b_1)x}{a_4(1+a_2 i\omega)}}}{1+a_2 i\omega}\right] = \left|\bar{F}_\theta(i\omega)\right| e^{i\phi_\theta} \tag{C-6}$$

where

$$\left|\bar{F}_\theta(i\omega)\right| = \frac{\sqrt{\left(\frac{b_1}{b_2\omega} - a_2\omega\right)^2 + \left(1+\frac{a_2 b_1}{b_2}\right)^2}}{\left[1+\left(\frac{b_1}{b_2\omega}\right)^2\right] b_2\omega^2\left(1+\frac{x}{a_4}\right)\left(1+a_2^2\omega^2\right)e^{\delta}} \left\{\left[\frac{\frac{a_3}{a_2}e^{\delta}\left(1+a_2^2\omega^2\right)}{\sqrt{\left(\frac{b_1}{b_2\omega} - a_2\omega\right)^2 + \left(1+\frac{a_2 b_1}{b_2}\right)^2}} + \sin\left(\gamma + \tan^{-1}\frac{1+\frac{a_2 b_1}{b_2}}{\frac{b_1}{b_2\omega} - a_2\omega}\right)\right]^2 + \left[\frac{\left(-\frac{b_1}{b_2\omega} - a_3\omega\right)e^{\delta}\left(1+a_2^2\omega^2\right)}{\sqrt{\left(\frac{b_1}{b_2\omega} - a_2\omega\right)^2 + \left(1+\frac{a_2 b_1}{b_2}\right)^2}} + \cos\left(\gamma + \tan^{-1}\frac{1+\frac{a_2 b_1}{b_2}}{\frac{b_1}{b_2\omega} - a_2\omega}\right)\right]^2\right\}^{1/2} \tag{C-7}$$

$$\alpha_\theta = \tan^{-1}\left\{\frac{\frac{\left(\frac{b_1}{b_2\omega} + a_3\omega\right)e^{\delta}\left(1+a_2^2\omega^2\right)}{\sqrt{\left(\frac{b_1}{b_2\omega} - a_2\omega\right)^2 + \left(1+\frac{a_2 b_1}{b_2}\right)^2}} - \cos\left(\gamma + \tan^{-1}\frac{1+\frac{a_2 b_1}{b_2}}{\frac{b_1}{b_2\omega} - a_2\omega}\right)}{\frac{\frac{a_3}{a_2}e^{\delta}\left(1+a_2^2\omega^2\right)}{\sqrt{\left(\frac{b_1}{b_2\omega} - a_2\omega\right)^2 + \left(1+\frac{a_2 b_1}{b_2}\right)^2}} + \sin\left(\gamma + \tan^{-1}\frac{1+\frac{a_2 b_1}{b_2}}{\frac{b_1}{b_2\omega} - a_2\omega}\right)}\right\} \tag{C-8}$$

Fluid-wall temperature difference

$$\bar{F}_{\Delta t}(i\omega)=\frac{1}{b_2(i\omega+\frac{b_1}{b_2})}\left[a_3+\frac{a_2}{1+a_2 i\omega}e^{-\frac{(i\omega)(b_2 i\omega+b_1)x}{a_4(1+a_2 i\omega)}}\right]=\left|\bar{F}_{\Delta t}(i\omega)\right|e^{i\alpha_{\Delta t}} \qquad \text{(C-9)}$$

where

$$\left|\bar{F}_{\Delta t}(i\omega)\right|=\frac{\sqrt{\left(-\frac{b_1}{b_2\omega}+a_2\omega\right)^2+\left(\frac{b_1a_2}{b_2}+1\right)^2}}{a_3\omega\left[1+\left(\frac{b_1}{b_2\omega}\right)^2\right](1+a_2^2\omega^2)e^{\delta}}\left\{\left[\frac{\frac{b_1}{a_2^2\omega}(1+a_2^2\omega^2)e^{\delta}}{\sqrt{\left(-\frac{b_1}{b_2\omega}+a_2\omega\right)^2+\left(\frac{b_1a_2}{b_2}+1\right)^2}}-\sin\left(\gamma+\tan^{-1}\frac{-\frac{b_1}{b_2\omega}+a_2\omega}{\frac{b_1a_2}{b_2}+1}\right)\right]^2+\left[\frac{\frac{a_3}{a_2}(1+a_2^2\omega^2)e^{\delta}}{\sqrt{\left(-\frac{b_1}{b_2\omega}+a_2\omega\right)^2+\left(\frac{b_1a_2}{b_2}+1\right)^2}}+\cos\left(\gamma+\tan^{-1}\frac{-\frac{b_1}{b_2\omega}+a_2\omega}{\frac{b_1a_2}{b_2}+1}\right)\right]^2\right\}^{1/2} \qquad \text{(C-10)}$$

and

$$\alpha_{\Delta t}=\tan^{-1}\frac{\frac{a_3}{a_2}(1+a_2^2\omega^2)e^{\delta}}{\sqrt{\left(-\frac{b_1}{b_2\omega}+a_2\omega\right)^2+\left(\frac{b_1a_2}{b_2}+1\right)^2}}+\cos\left(\gamma+\tan^{-1}\frac{-\frac{b_1}{b_2\omega}+a_2\omega}{\frac{b_1a_2}{b_2}+1}\right)}{\frac{\frac{b_1}{a_2^2\omega}(1+a_2^2\omega^2)e^{\delta}}{\sqrt{\left(-\frac{b_1}{b_2\omega}+a_2\omega\right)^2+\left(\frac{b_1a_2}{b_2}+1\right)^2}}-\sin\left(\gamma+\tan^{-1}\frac{-\frac{b_1}{b_2\omega}+a_2\omega}{\frac{b_1a_2}{b_2}+1}\right)} \qquad \text{(C-11)}$$

At the steady-periodic state, the oscillations of the fluid and wall temperatures and fluid-wall temperature difference may be expressed as

$$t_2(x,\tau) = \left[T_\infty(x)\right]_{\omega=\omega} \sin(\omega\tau - \alpha_t) \tag{C-12}$$

$$\theta_2(x,\tau) = \left[\Theta_\infty(x)\right]_{\omega=\omega} \sin(\omega\tau - \alpha_\theta) \tag{C-13}$$

and

$$\Delta t_2(x,\tau) = \left[\Delta T_\infty(x)\right]_{\omega=\omega} \sin(\omega\tau - \alpha_{\Delta t}) \tag{C-14}$$

Equations (B-19), (B-20), and (B-21) are in the forms of Equation (16) and Equations (C-12), (C-13) and (C-14) are in the forms of Equation (17). Therefore according to Equation (21), Equations (C-2), (C-7) and (C-10) are the amplitude-ratios of the fluid and wall temperatures and fluid-wall temperature difference, which express the ratio of the amplitude at $\omega = \omega$ to $\omega = 0$. Equations (C-3), (C-8), and (C-11) express the phase-shift, of the fluid and wall temperature and fluid-wall temperature difference respectively. Substituting the following physical parameters, into Equations (C-2), (C-3), (C-7), (C-8), (C-10) and (C-11) one obtains equations for circular-tube geometory, which are identical with Equations (55), (56), (57), (58), (59) and (60).

$$\zeta = \frac{\frac{Kx}{u}\left(\frac{M\omega}{K}\right)^2}{1+\left(\frac{M\omega}{K}\right)^2} \tag{C-15}$$

$$\gamma = \frac{kx}{u}\left[\frac{\frac{M\omega}{K}}{1+\left(\frac{M\omega}{K}\right)^2} + \frac{1}{M}\left(\frac{M\omega}{K}\right)\right] \qquad \text{(C-16)}$$

$$\frac{a_3}{a_2} = \frac{K_w}{K} = \frac{1}{M} \qquad \frac{x}{a_4} = \frac{kx}{u} \qquad \frac{b_1}{b_2\omega} = \frac{M+1}{\frac{M\omega}{K}}$$

$$a_2\omega = \frac{M\omega}{K} \qquad a_3\omega = \frac{1}{M}\frac{M\omega}{K}$$

APPENDIX D

INVERSE LAPLACE TRANSFORMATION OF EQUATIONS (B-11) AND (B-12)

In order to obtain the whole transient solutions of the wall temperature and fluid-wall temperature difference, the inverse Laplace transformations must be performed on Equations (B-11) and (B-12), which can be rewritten as:

$$\bar{\theta}_2 = \frac{a_1}{b_1} F_{13}(s)\bar{\phi}(s) - \frac{a_1}{a_2 b_1} e^{-\frac{x}{a_4}} e^{-\frac{x}{u}} F_{14}(s)\bar{\phi}(s) \qquad \text{(D-1)}$$

$$\Delta\bar{t}_2 = \frac{a_1 a_3}{b_2} F_{15}(s)\bar{\phi}(s) + \frac{a_1}{b_2} e^{-\frac{x}{a_4}} e^{-\frac{x}{u}s} F_{15}(s)F_{16}(s)\bar{\phi}(s) \qquad \text{(D-2)}$$

where the Laplace-transformed functions F_{13}, F_{14}, F_{15}, and F_{16} and its inverse transformed functions G are listed in the following table:

	$F(s)$		$G(\tau)$	Restriction
F_{13}	$a_3\left(\frac{b_1}{b_2}\right)\frac{s+\frac{1}{a_3}}{s\left(s+\frac{b_1}{b_2}\right)}$	G_{13}	$1+\frac{a_3}{a_2}e^{-\frac{b_1}{b_2}\tau}$	$\tau>0$
F_{14}	$\frac{b_1}{b_2}\frac{1}{s\left(s+\frac{b_1}{b_2}\right)}$	G_{14}	$1-e^{-\frac{b_1}{b_2}\tau}$	$\tau>0$
F_{15}	$\frac{1}{s+\frac{b_1}{b_2}}$	G_{15}	$e^{-\frac{b_1}{b_2}\tau}$	$\tau>0$
F_{16}	$\frac{e^{\frac{x}{a_2 a_4\left(s+\frac{1}{a_2}\right)}}}{s+\frac{1}{a_2}}$	G_{16}	$e^{-\frac{\tau}{a_2}} I_0\left[2\left(\frac{x\tau}{a_2 a_4}\right)^{\frac{1}{2}}\right]$	$\tau>0$

Hence the transformed equations in physical domain of x and τ which are the solutions to the differential Equations (34) and (35), and for the boundary and initial conditions of Equations (A-21) and (A-22) are found to be*:

Case 1 $0 \leq \frac{\tau u}{x} \leq 1$

wall temperature

$$\theta_2(\tau) = \frac{a_1}{b_1}\int_0^{\tau} \phi(\xi)\left[1 + \frac{a_3}{a_2} e^{-\frac{b_1}{b_2}\tau} e^{\frac{b_1}{b_2}\xi}\right] d\xi \qquad \text{(D-3)}$$

Fluid-wall temperature difference

$$\Delta t_2(\tau) = \frac{a_1 a_3}{b_2} e^{-\frac{b_1}{b_2}\tau} \int_0^{\tau} \phi(\xi) e^{\frac{b_1}{b_2}\xi} d\xi \qquad \text{(D-4)}$$

Case 2 $\frac{\tau u}{x} \geq 1$

wall temperature

$$\theta_2(x,\tau) = \theta_2(\tau) - \frac{a_1}{a_2 b_1} e^{-\frac{x}{a_4}} \int_0^{\tau^*} \pi(\tau - \xi) e^{-\frac{\xi}{a_2}} I_o\left[2\left(\frac{x\xi}{a_2 a_4}\right)^{1/2}\right] d\xi \qquad \text{(D-5)}$$

Fluid-wall temperature difference

$$\Delta t_2(x,\tau) = \Delta t_2(\tau) + \frac{a_1}{b_2} e^{-\frac{x}{a_4}} \int_0^{\tau^*} \Lambda(\tau - \xi) e^{-\frac{\xi}{a_2}} I_o\, 2\left(\frac{x\xi}{a_2 a_4}\right)^{1/2} d\xi \qquad \text{(D-6)}$$

*See Reference 3.

where

$$\Lambda(\tau) = e^{-\frac{b_1}{b_2}\tau}\int_0^\tau \phi(z)\, e^{\frac{b_1}{b_2}z}\, dz \qquad \text{(D-7)}$$

$$\Pi(\tau) = \int_0^\tau \phi(z)\, dz - \Lambda(\tau) \qquad \text{(D-8)}$$

$$\tau^* = \tau - \frac{x}{u} \qquad \text{(D-9)}$$

$\phi(\tau)$ = arbitrary time-variant volumetric heat generation rate

Special Case of Transient in $\phi(\tau)$ Being Sinusoidal in Time

In the case $\phi(\tau)$ be represented by a sinusoidal function of time such as

$$\phi(\tau) = \Phi \sin \omega\tau \qquad \text{(D-10)}$$

Equations (D-3), (D-4), (D-5), (D-6), (D-7) and (D-8) become

Case 1 $\quad 1 \geq \frac{\tau u}{x} \geq 0$

wall temperature

$$\theta_2(\tau) = \frac{a_1}{b_1}\int_0^\tau \Phi \sin\omega\xi \cdot \left[1 + \frac{a_2}{a_2} e^{-\frac{b_1}{b_2}(\tau-\xi)}\right] d\xi$$

$$\frac{\theta_2(\tau)}{a_1\left(1+\frac{x}{a_4}\right)\Phi} = \frac{1}{b_2\omega\left(1+\frac{x}{a_4}\right)}\left\{1 - \cos\omega\tau + \frac{a_3}{a_2}\frac{1}{1+\left(\frac{b_1}{b_2\omega}\right)^2}\left[\frac{b_1}{b_2\omega}\sin\omega\tau + e^{-\frac{b_1}{b_2}\tau} - \cos\omega\tau\right]\right\} \qquad \text{(D-11)}$$

Fluid-wall temperature difference

$$\frac{\Delta t_2(\tau)}{a_1 \Phi} = \frac{1}{b_2\omega}\frac{1+\frac{a_2}{a_3}}{1+\left(\frac{b_1}{b_2\omega}\right)^2}\left[\left(\frac{b_1}{b_2\omega}\right)\sin\omega\tau - \cos\omega\tau + e^{-\frac{b_1}{b_2}\tau}\right] \tag{D-12}$$

Fluid-temperature

$$\frac{t_2(x,\tau)}{\frac{a_1 x}{a_4}\Phi} = \frac{a_4}{b_1\omega x}\left\{1-\cos\omega\tau - \frac{1}{1+\left(\frac{b_1}{b_2\omega}\right)^2}\left[\frac{b_1}{b_2\omega}\sin\omega\tau - \cos\omega\tau + e^{-\frac{b_1}{b_2}\tau}\right]\right\} \tag{D-13}$$

Case 2 $\frac{\tau u}{x} \geq 1$

$$\Lambda(\tau) = e^{-\frac{b_1}{b_2}\tau}\int_0^\tau \Phi \sin\omega z\, e^{\frac{b_1}{b_2}z}\, dz$$

$$= \frac{\omega\Phi}{\left(\frac{b_1}{b_2}\right)^2+\omega^2}\left[\frac{b_1}{b_2\omega}\sin\omega\tau - \cos\omega\tau + e^{-\frac{b_1}{b_2}\tau}\right] \tag{D-14}$$

$$\Pi(\tau) = \int_0^\tau \Phi \sin\omega z\, dz - \Lambda(\tau)$$

$$= \Phi\frac{(1-\cos\omega\tau)}{\omega} - \frac{\omega\Phi}{\left(\frac{b_1}{b_2}\right)^2+\omega^2}\left[\frac{b_1}{b_2\omega}\sin\omega\tau - \cos\omega\tau + e^{-\frac{b_1}{b_2}\tau}\right] \tag{D-15}$$

wall temperature

$$\frac{\theta_2(x,\tau)}{a_1\Phi(1+\frac{x}{a_4})} = \frac{\theta_2(x)}{a_1\Phi(1+\frac{x}{a_4})} - \frac{e^{-\frac{x}{a_4}}}{b_1\omega(1+\frac{x}{a_4})}\left\{\psi_2^{**}(s,q^*) - \frac{a_3}{a_2}\frac{e^{-\frac{b_1}{b_2}\tau^*}}{1+(\frac{b_1}{b_2\omega})^2}\psi_4(r,\gamma^*)\right.$$

$$-\frac{\frac{b_1}{b_2\omega}}{1+(\frac{b_1}{b_2\omega})^2}\left[(\frac{b_1}{b_2\omega}\cos\omega\tau^* + \sin\omega\tau^*)\psi_7(s,q^*,\Omega)\right.$$

$$\left.\left.+(\frac{b_1}{b_2\omega}\sin\omega\tau^* - \cos\omega\tau^*)\psi_8(s,q^*,\Omega)\right]\right\} \qquad \text{(D-16)}$$

Fluid-wall temperature difference

$$\frac{\Delta t_2(x,\tau)}{a_1\Phi} = \frac{\Delta t_2(\tau)}{a_1\Phi} + \frac{1}{b_1\omega}\frac{1+\frac{a_2}{a_3}e^{-\frac{x}{a_4}}}{1+(\frac{b_1}{b_2\omega})^2}\left\{\frac{a_3}{a_2}e^{-\frac{b_1}{b_2}\tau^*}\psi_4(r,\gamma^*)\right.$$

$$+(\frac{b_1}{b_2\omega}\sin\omega\tau^* - \cos\omega\tau^*)\psi_7(s,q^*,\Omega)$$

$$\left.-(\frac{b_1}{b_2\omega}\cos\omega\tau^* + \sin\omega\tau^*)\psi_8(s,q^*,\Omega)\right\} \qquad \text{(D-17)}$$

Fluid temperature

$$\frac{t_2(x,\tau)}{\frac{a_1x}{a_4}\Phi} = \frac{t_2(\tau)}{\frac{a_1x}{a_4}\Phi} + \frac{a_4e^{-\frac{x}{a_4}}}{b_1\omega x}\left\{-\psi_2^{**}(s,q^*) - \frac{e^{-\frac{b_1}{b_2}\tau^*}}{1+(\frac{b_1}{b_2\omega})^2}\psi_4(r,\gamma^*)\right.$$

$$+\frac{1}{1+(\frac{b_1}{b_2\omega})^2}\left\{\left[(\frac{b_1}{b_2\omega})^2+1+\frac{a_2}{a_3}\right]\cos\omega\tau - \frac{a_2}{a_3}\frac{b_1}{b_2\omega}\sin\omega\tau\right\}\psi_7(s,q^*,\Omega)$$

$$\left.+\left\{\left[(\frac{b_1}{b_2\omega})^2+1+\frac{a_2}{a_3}\right]\sin\omega\tau + \frac{a_2}{a_3}\frac{b_1}{b_2\omega}\cos\omega\tau\right\}\psi_8(s,q^*\Omega)\right\} \qquad \text{(D-18)}$$

The function in these equations are defined. The functions ψ_2**(s,q^*) and $\psi_4(r,\gamma^*)$ are identical with those have been presented in Reference 3. These functions are also presented here in Figures 40 and 41. $\psi_7(s,q,\Omega)$ and $\psi_8(s,q,\Omega)$ are new functions which have been computed and presented in Figures 42-57. The numerical solutions and their elementary properties are presented in Appendix G.

$$\psi_4(x,\tau^*) = \frac{1}{a_2}\int_0^{\tau^*} e^{\frac{\xi}{a_3}} I_0\left[2\left(\frac{x\xi}{a_2 a_4}\right)^{1/2}\right] d\xi$$

$$= \frac{1}{a_2}\sum_{k=0}^{\infty} \frac{\left(\frac{x}{a_2 a_4}\right)^k}{(k!)^2}\int_0^{\tau^*} e^{\frac{\xi}{a_3}} \xi^k d\xi$$

$$= \frac{a_3}{a_2}\sum_{k=0}^{\infty} \frac{\left(\frac{a_3 x}{a_2 a_4}\right)^k}{(k!)^2}\int_0^{\frac{\tau^*}{a_3}} e^z z^k dz$$

$$= \frac{a_3}{a_2}\sum_{k=0}^{\infty} \frac{r^k}{(k!)^2}\int_0^{\gamma^*} e^z z^k dz$$

$$= \frac{a_3}{a_2}\psi_4(r,\gamma^*)$$

$$= \frac{a_3}{a_2}\psi_4\left(\frac{a_3 x}{a_2 a_4}, \frac{\tau^*}{a_3}\right) \qquad \text{(D-19*)}$$

---

* See References 1, 2, and 3

$$\psi_2^{**}(x,\tau^*) = \frac{1}{a_2}\int_0^{\tau^*} e^{-\frac{\xi}{a_2}} I_0\left[2\left(\frac{x\xi}{a_2 a_4}\right)^{1/2}\right] d\xi$$

$$= \frac{1}{a_2}\sum_{k=0}^{\infty} \frac{\left(\frac{x}{a_2 a_4}\right)^k}{(k!)^2}\int_0^{\tau^*} e^{-\frac{\xi}{a_2}} \xi^k d\xi$$

$$= \sum_{k=0}^{\infty} \frac{\left(\frac{x}{a_4}\right)^k}{(k!)^2}\int_0^{\frac{\tau^*}{a_2}} e^{-z} z^k dz$$

$$= \sum_{k=0}^{\infty} \frac{s^k}{(k!)^2}\int_0^{q^*} e^{-z} z^k dz$$

$$= \psi_2^{**}(s, q^*) \qquad \text{(D-20**)}$$

$$\psi_7(x,\tau^*,\omega) = \frac{1}{a_2}\int_0^{\tau^*} e^{-\frac{\xi}{a_2}} I_0\left[2\left(\frac{x\xi}{a_2 a_4}\right)^{1/2}\right] \cos\omega\xi\, d\xi$$

$$= \frac{1}{a_2}\sum_{k=0}^{\infty} \frac{\left(\frac{x}{a_2 a_4}\right)^k}{(k!)^2}\int_0^{\tau^*} e^{-\frac{\xi}{a_2}} \xi^k \cos\omega\xi\, d\xi$$

$$= \sum_{k=0}^{\infty} \frac{\left(\frac{x}{a_4}\right)^k}{(k!)^2}\int_0^{\frac{\tau^*}{a_2}} e^{-z} z^k \cos\Omega z\, dz$$

$$= \sum_{k=0}^{\infty} \frac{(s)^k}{(k!)^2}\int_0^{q^*} e^{-z} z^k \cos\Omega z\, dz$$

$$= \psi_7(s, q^*, \Omega) \qquad \text{(D-21)}$$

** See References 1,2,3 and 9

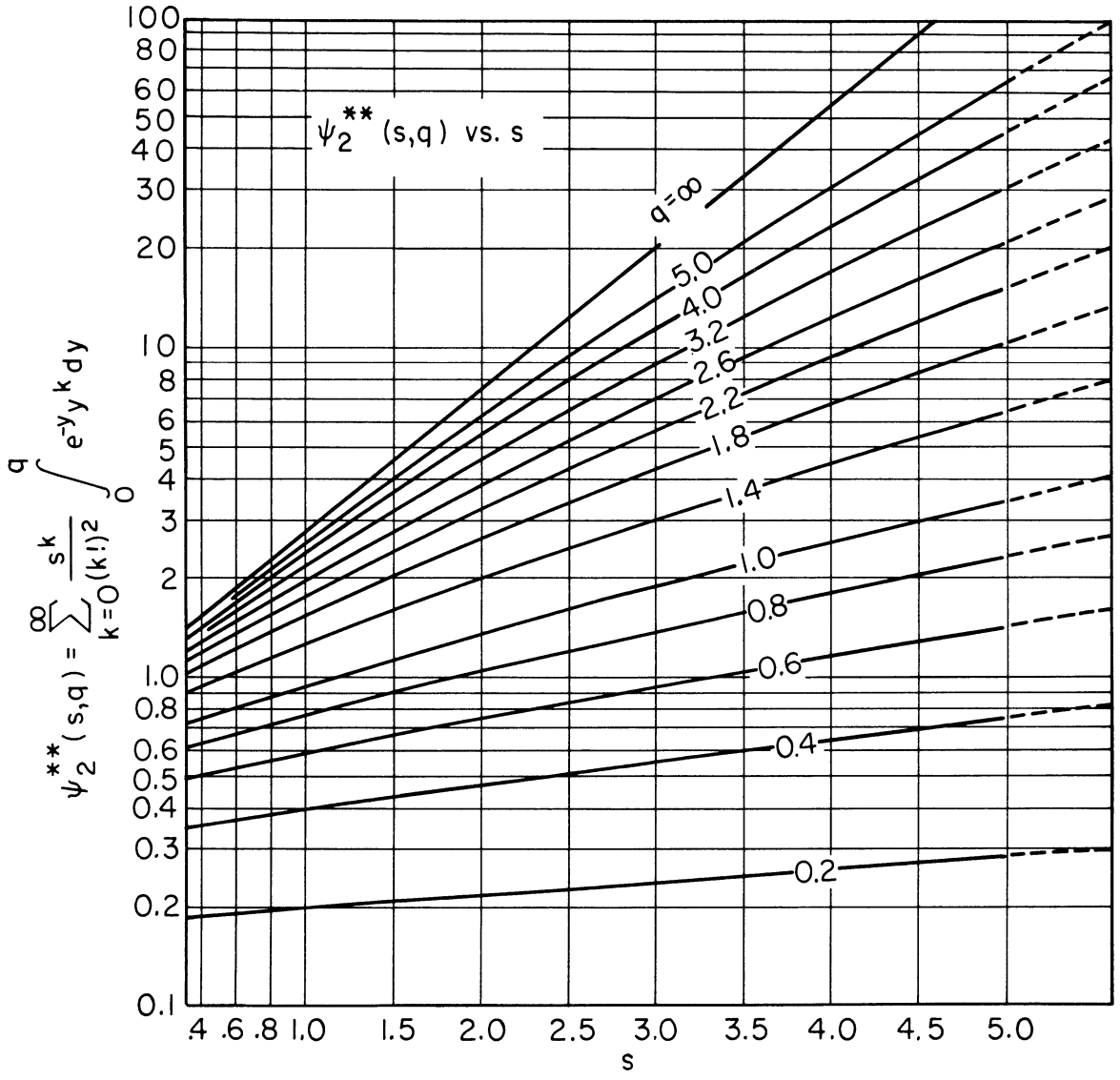

Figure 40. $\psi_2^{**}(s,q)$ versus s.

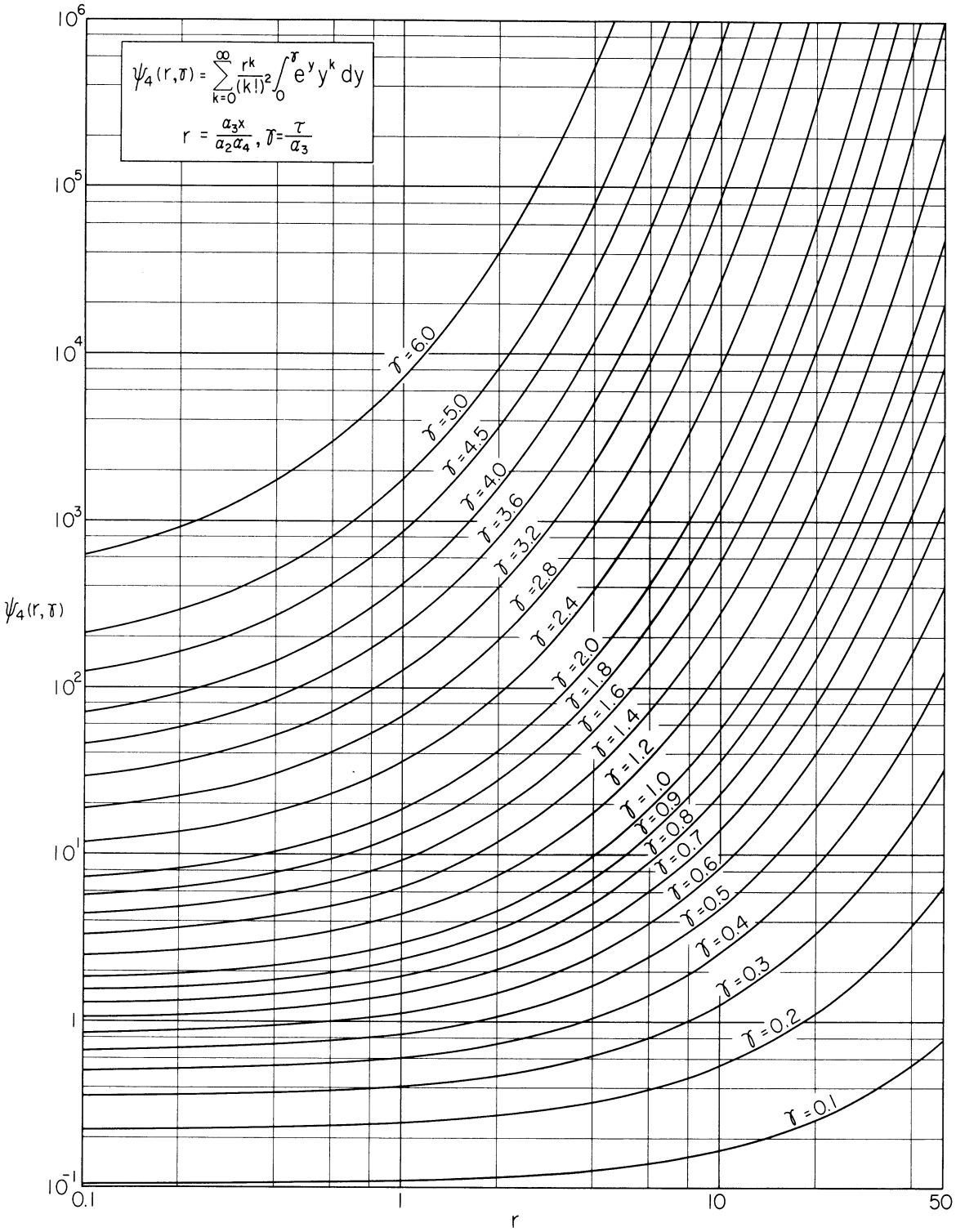

Figure 41. $\psi_4(r,\gamma)$ versus r.

$$\psi_8(x,\tau^*,\omega) = \frac{1}{a_2}\int_0^{\tau^*} e^{-\frac{\xi}{a_2}} I_0\left[2\left(\frac{x\xi}{a_2 a_4}\right)^{\frac{1}{2}}\right]\sin\omega\xi\, d\xi$$

$$= \frac{1}{a_2}\sum_{K=0}^{\infty}\frac{\left(\frac{x}{a_2 a_4}\right)^K}{(K!)^2}\int_0^{\tau^*} e^{-\frac{\xi}{a_2}}\xi^K \sin\omega\xi\, d\xi$$

$$= \sum_{K=0}^{\infty}\frac{\left(\frac{x}{a_4}\right)^K}{(K!)^2}\int_0^{\frac{\tau^*}{a_2}} e^{-z} z^K \sin\Omega z\, dz$$

$$= \sum_{K=0}^{\infty}\frac{(s)^K}{(K!)^2}\int_0^{q^*} e^{-z} z^K \sin\Omega z\, dz$$

$$= \psi_8(s, q^*, \Omega) \qquad \text{(D-22)}$$

The variables given in Equations (D-19) through (D-21) are defined

$$\gamma = \frac{a_3 x}{a_2 a_4} = \frac{1}{M}\frac{Kx}{u}$$

$$q = \frac{\tau}{a_2} = \frac{K\tau}{M} \qquad s = \frac{x}{a_4} = \frac{Kx}{u}$$

$$\gamma = \frac{\tau}{a_2} = K\tau \qquad \Omega = a_2\omega = \frac{M\omega}{K} \qquad \text{(D-23)}$$

APPENDIX E

DERIVATION OF EQUATIONS FOR THE
TRANSIENT-PERIODIC OSCILLATIONS OF TEMPERATURES

It will be shown in Equations (E-2), (E-3), (E-4), (E-11), (E-14), and (E-17) that Equations (D-11), (D-12), (D-13), (D-16), (D-17) and (D-18) may be expressed in a general form as follows:

$$y_2 = Y_1 + Y_2 e^{-\eta\tau} + Y_3 \sin(\omega\tau + \varphi) \qquad \text{(E-1)}$$

where η is a constant and Y_1, Y_2, Y_3 and φ are functions of x, ω and τ. The envelope formed by $y_2 = Y_1 + Y_2 e^{-\eta\tau} \pm Y_3$ is tangent to the curves expressed by Equation (E-1). However the points of tangency fall slightly to the left of the point of maximum amplitude of the function y_2. Generally this discrepancy is negligible, and the amplitude at the point of tangency may be taken equal to the maximum amplitude. This envelope encloses all the possible oscillations of the temperature change.

A. Equations for the Transient-Periodic Oscillation of Temperature

Case 1 $1 \geq \frac{\tau u}{x} \geq 0$

By rearranging Equations (D-11), (D-12), and (D-13), one obtains the equations for the transient-periodic oscillation of the fluid and wall temperatures and the fluid-wall temperature difference as follows:

$$\frac{\Theta(\tau)}{a_1\left(1+\frac{x}{a_4}\right)\Phi} = \frac{1}{b_1\omega\left(1+\frac{x}{a_4}\right)}\left\{1+\frac{\frac{a_3}{a_2}e^{-\frac{b_1}{b_2}\tau}}{1+\left(\frac{b_1}{b_2\omega}\right)}\right.$$

$$\left. + \frac{\sqrt{\left(\frac{a_3}{a_2}\frac{b_1}{b_2\omega}\right)^2+\left[1+\frac{a_3}{a_2}+\left(\frac{b_1}{b_2\omega}\right)^2\right]^2}}{1+\left(\frac{b_1}{b_2\omega}\right)^2}\sin\left[\omega\tau-\tan^{-1}\frac{1+\frac{a_3}{a_2}+\left(\frac{b_1}{b_2\omega}\right)^2}{\frac{a_3}{a_2}\frac{b_1}{b_2\omega}}\right]\right\} \qquad \text{(E-2)}$$

Fluid-wall temperature difference

$$\frac{\Delta t_2(\tau)}{a_1 \Phi} = \frac{1}{a_2 \omega \left[1+\left(\frac{b_1}{b_2\omega}\right)^2\right]} \left\{ e^{-\frac{b_1}{b_2}\tau} + \sqrt{1+\left(\frac{b_1}{b_2\omega}\right)^2} \sin\left(\omega\tau - \tan^{-1}\frac{b_2\omega}{b_1}\right) \right\} \qquad \text{(E-3)}$$

Fluid temperature

$$\frac{t_2(\tau)}{\frac{a_1 x}{a_4}\Phi} = \frac{a_4}{b_1 \omega x} \left\{ 1 - \frac{e^{-\frac{b_1}{b_2}\tau}}{1+\left(\frac{b_1}{b_2\omega}\right)^2} + \frac{\frac{b_1}{b_2\omega}\sqrt{1+\left(\frac{b_1}{b_2\omega}\right)^2}}{1+\left(\frac{b_1}{b_2\omega}\right)^2} \sin\left[\omega\tau - \tan^{-1}\left(-\frac{b_1}{b_2\omega}\right)\right] \right\} \qquad \text{(E-4)}$$

Equations for the temperature amplitude in the transient period $1 \geq \frac{\tau u}{x} \geq 0$ may be obtained from Equations (E-2), (E-3) and (E-4) by substituting sine by + 1 and - 1 as follows:

wall temperature

$$\frac{\left[\Theta(x,\tau)\right]_{+,-}}{a_1\left(1+\frac{x}{a_4}\right)\Phi} = \frac{1}{b_2\omega\left(1+\frac{x}{a_4}\right)} \left\{ 1 + \frac{\frac{a_3}{a_2} e^{-\frac{b_1}{b_2}\tau}}{1+\left(\frac{b_1}{b_2\omega}\right)^2} \pm \frac{\sqrt{\left(\frac{a_3}{a_2}\frac{b_1}{b_2\omega}\right)^2 + \left[1+\frac{a_3}{a_2}+\left(\frac{b_1}{b_2\omega}\right)^2\right]^2}}{1+\left(\frac{b_1}{b_2\omega}\right)^2} \right\} \qquad \text{(E-5)}$$

Fluid-wall temperature difference

$$\frac{\left[\Delta T(x,\tau)\right]_{+,-}}{a_1\Phi} = \frac{1}{a_2\omega\left[1+\left(\frac{b_1}{b_2\omega}\right)^2\right]} \left\{ e^{-\frac{b_1}{b_2}\tau} \pm \sqrt{1+\left(\frac{b_1}{b_2\omega}\right)^2} \right\} \qquad \text{(E-6)}$$

Fluid temperature

$$\frac{\left[T(x,\tau)\right]_{+,-}}{\frac{a_1 x}{a_4}\Phi} = \frac{a_4}{b_1\omega x} \left\{ 1 - \frac{e^{-\frac{b_1}{b_2}\tau}}{1+\left(\frac{b_1}{b_2\omega}\right)^2} \pm \frac{\frac{b_1}{b_2\omega}\sqrt{1+\left(\frac{b_1}{b_2\omega}\right)^2}}{1+\left(\frac{b_1}{b_2\omega}\right)^2} \right\} \qquad \text{(E-7)}$$

Case 2 $\frac{\tau u}{x} \geq 1$

Since

$$\tau = \tau^* + \frac{x}{u} \tag{E-8}$$

$$\cos\omega\tau = \cos\omega\tau^* \cos\frac{\omega x}{u} - \sin\omega\tau^* \cos\frac{\omega x}{u} \tag{E-9}$$

$$\sin\omega\tau = \sin\omega\tau^* \cos\frac{\omega x}{u} + \cos\omega\tau^* \sin\frac{\omega x}{u} \tag{E-10}$$

by substituting Equations (E-9) and (E-10) into Equations (D-16), (D-17) and (D-18), one obtains:

wall temperature

$$\frac{\theta_2(x,\tau)}{a_1\left(1+\frac{x}{a_4}\right)\Phi} = \frac{1}{b_1\omega\left(1+\frac{x}{a_4}\right)}\left\{\left[1+\frac{\frac{a_3}{a_2}e^{-\frac{b_1}{b_2}\tau}}{1+\left(\frac{b_1}{b_2\omega}\right)^2}\right.\right.$$

$$\left.\left. - e^{-\frac{x}{a_4}}\left[\psi_2^{**}(S,q^*) - \frac{\frac{a_3}{a_2}e^{-\frac{b_1}{b_2}\tau^*}}{1+\left(\frac{b_1}{b_2\omega}\right)^2}\psi_4(r,\gamma^*)\right]\right]\right.$$

$$\left. + \sqrt{A_\theta^2 + B_\theta^2}\,\sin^{-1}\left[\omega\tau^* - \tan^{-1}\left(-\frac{B_\theta}{A_\theta}\right)\right]\right\} \tag{E-11}$$

where

$$A_\theta = \sin\frac{\omega x}{u} + \frac{\frac{a_3}{a_2}}{1+\left(\frac{b_1}{b_2\omega}\right)^2}\left(\frac{b_1}{b_2\omega}\cos\frac{\omega x}{u} + \sin\frac{\omega x}{u}\right)$$

$$+ \frac{e^{-\frac{x}{a_4}\left(\frac{b_1}{b_2\omega}\right)}}{1+\left(\frac{b_1}{b_2\omega}\right)^2}\left[\frac{b_1}{b_2\omega}\psi_8(s,\eta^*,\Omega) + \psi_7(s,\eta^*,\Omega)\right] \qquad \text{(E-12)}$$

$$B_\theta = -\cos\frac{\omega x}{u} + \frac{\frac{a_3}{a_2}}{1+\left(\frac{b_1}{b_2\omega}\right)^2}\left(\frac{b_1}{b_2\omega}\sin\frac{\omega x}{u} - \cos\frac{\omega x}{u}\right)$$

$$+ \frac{e^{-\frac{x}{a_4}\left(\frac{b_1}{b_2\omega}\right)}}{1+\left(\frac{b_1}{b_2\omega}\right)^2}\left[\frac{b_1}{b_2\omega}\psi_7(s,\eta^*,\Omega) - \psi_8(s,\eta^*,\Omega)\right] \qquad \text{(E-13)}$$

Fluid-wall temperature difference

$$\frac{\Delta t_2(x,\tau)}{a_1\Phi} = \frac{1}{a_2\omega\left[1+\left(\frac{b_1}{b_2\omega}\right)^2\right]}\left\{e^{-\frac{b_1}{b_2}\tau} + \frac{a_3}{a_2}e^{-\frac{x}{a_4}}e^{-\frac{b_2}{b_2}\tau^*}\psi_4(r,\gamma^*)\right. \qquad \text{(E-14)}$$

$$\left. + \sqrt{A_{\Delta t}^2 + B_{\Delta t}^2}\,\sin\left[\omega\tau^* - \tan^{-1}\left(-\frac{B_{\Delta t}}{A_{\Delta t}}\right)\right]\right\}$$

where

$$A_{\Delta t} = -\frac{b_1}{b_2\omega}\cos\frac{\omega x}{u} + \sin\frac{\omega x}{u} + e^{-\frac{x}{a_4}}\left[\frac{b_1}{b_2\omega}\psi_7(s,\eta^*,\Omega) - \psi_8(s,\eta^*,\Omega)\right] \qquad \text{(E-15)}$$

$$B_{\Delta t} = \frac{b_1}{b_2\omega}\sin\frac{\omega x}{u} - \cos\frac{\omega x}{u} + e^{-\frac{x}{a_4}}\left[-\psi_7(s,\eta^*,\Omega) - \frac{b_1}{b_2\omega}\psi_8(s,\eta^*,\Omega)\right] \qquad \text{(E-16)}$$

Fluid temperature

$$\frac{t_2(x,\tau)}{\frac{a_1 x}{a_4}\Phi} = \frac{a_4}{b_1\omega x}\left\{1 - \frac{e^{-\frac{b_1}{b_2}\tau}}{1+\left(\frac{b_1}{b_2\omega}\right)^2} + e^{-\frac{x}{a_4}}\left[-\psi_2^{**}(s,\eta^*)\right.\right.$$

$$\left.\left. - \frac{e^{-\frac{b_1}{b_2}\tau^*}}{1+\left(\frac{b_1}{b_2\omega}\right)^2}\psi_4(r,\gamma^*)\right] + \sqrt{A_{\Delta t}^2 + B_{\Delta t}^2}\,\sin\left[\omega\tau^* - \tan^{-1}\left(-\frac{B_{\Delta t}}{A_{\Delta t}}\right)\right]\right\} \qquad \text{(E-17)}$$

where

$$A_t = \sin\frac{\omega x}{u} - \frac{1}{1+\left(\frac{b_1}{b_2\omega}\right)^2}\left(\frac{b_1}{b_2\omega}\cos\frac{\omega x}{u} + \sin\frac{\omega x}{u}\right) + \frac{e^{-\frac{x}{a_4}}}{1+\left(\frac{b_1}{b_2\omega}\right)^2}\left[\left(\frac{b_1}{b_2\omega}\right)^2 + 1 + \frac{a_2}{a_3}\right]$$

$$\cdot \left\{\psi_8(s,q^*,\Omega) - \frac{a_2}{a_3}\left(\frac{b_1}{b_2\omega}\right)\psi_7(s,q^*,\Omega)\right\} \qquad \text{(E-18)}$$

where

$$B_t = -\cos\frac{\omega x}{u} - \frac{1}{1+\left(\frac{b_1}{b_2\omega}\right)^2}\left(\frac{b_1}{b_2\omega}\sin\frac{\omega x}{u} - \cos\frac{\omega x}{u}\right) + \frac{e^{-\frac{x}{a_4}}}{1+\left(\frac{b_1}{b_2\omega}\right)^2}\left[\left(\frac{b_1}{b_2\omega}\right)^2 + 1 + \frac{a_2}{a_3}\right]$$

$$\cdot \left\{\psi_7(s,q^*,\Omega) + \frac{a_2}{a_3}\left(\frac{b_1}{b_2\omega}\right)\psi_8(s,q^*,\Omega)\right\} \qquad \text{(E-19)}$$

Equations for the temperature amplitude in the transient period $\frac{\tau u}{x} \geq 1$ may be obtained from Equations (E-11), (E-14) and (E-17) by substituting sine by + 1 and - 1 as follows:

wall temperature

$$\frac{\left[\Theta(x,\tau)\right]_{+,-}}{a_1\left(1+\frac{x}{a_4}\right)\Phi} = \frac{1}{b_1\omega\left(1+\frac{x}{a_4}\right)}\left\{1 + \frac{a_3}{a_2}\frac{e^{-\frac{b_1}{b_2}\tau}}{1+\left(\frac{b_1}{b_2\omega}\right)^2} - e^{-\frac{x}{a_4}}\left[\psi_{12}^{**}(s,q^*) - \frac{a_3}{a_2}\frac{e^{-\frac{b_1}{b_2}\tau^*}}{1+\left(\frac{b_1}{b_2\omega}\right)^2}\psi_4(r,\gamma^*)\right] \pm \sqrt{A_\theta^2 + B_\theta^2}\right\} \qquad \text{(E-20)}$$

Fluid-wall temperature difference

$$\frac{\left[\Delta T(x,\tau)\right]_{+,-}}{a_1\Phi} = \frac{1}{a_2\omega\left(1+\left(\frac{b_1}{b_2\omega}\right)^2\right)}\left\{e^{-\frac{b_1}{b_2}\tau} + \frac{a_3}{a_2}e^{-\frac{x}{a_4}}e^{-\frac{b_1}{b_2}\tau^*}\psi_4(r,\gamma^*) \pm \sqrt{A_{\Delta t}^2 + B_{\Delta t}^2}\right\} \qquad \text{(E-21)}$$

Fluid temperature

$$\frac{T(x,\tau)_{+,-}}{\frac{a_1 x}{a_4}\Phi} = \frac{a_4}{b_1\omega x}\left\{1 - \frac{e^{-\frac{b_1}{b_2}\tau}}{1+\left(\frac{b_1}{b_2\omega}\right)^2} + e^{-\frac{x}{a_4}}\left[-\psi_2^{**}(s,q^*)\right.\right.$$

$$\left.\left. - \frac{e^{-\frac{b_1}{b_2}\tau^*}}{1+\left(\frac{b_1}{b_2\omega}\right)^2}\psi_4(r,\gamma^*)\right] \pm \sqrt{A_t^2 + B_t^2}\right\} \qquad \text{(E-22)}$$

B. Equations for the Steady-Periodic Oscillation of Temperature

After the transient-periodic state, the oscillation of the temperatures become steady. These occur at large values of τ (infinite) at which $e^{-K\tau}$ and $e^{-K\tau^*}$ became essentically zero. Hence

$$1 - e^{-\frac{x}{a_4}}\psi^{**}(r,\infty) = 1 - e^{-\frac{x}{a_4}}e^{\frac{x}{a_4}} = 0 \qquad \text{(E-23)}$$

Substituting $\tau = \infty$, $\tau^* = \infty$ and Equation (E-23) into Equations (E-11), (E-14) and (E-17). The following equations for the oscillations of the temperatures in the steady-periodic state are obtained:

wall temperature

$$\frac{\theta_2(x,\tau)}{a_1\left(1+\frac{x}{a_4}\right)\Phi} = \frac{1}{b_1\omega\left(1+\frac{x}{a_4}\right)}\sqrt{A_{\theta\infty}^2 + B_{\theta\infty}^2}\,\sin\left[\omega\tau - \frac{\omega x}{u} - \tan^{-1}\left(-\frac{B_{\theta\infty}}{A_{\theta\infty}}\right)\right] \qquad \text{(E-24)}$$

where $$A_{\theta\infty} = \sin\frac{\omega x}{u} + \frac{\frac{a_3}{a_2}}{1+\left(\frac{b_1}{b_2\omega}\right)^2}\left(\frac{b_1}{b_2\omega}\cos\frac{\omega x}{u} + \sin\frac{\omega x}{u}\right)$$

$$+ \frac{e^{-\frac{x}{a_4}\left(\frac{b_1}{b_2\omega}\right)}}{1+\left(\frac{b_1}{b_2\omega}\right)^2}\left[\frac{b_1}{b_2\omega}\psi_8(S,\infty,\Omega) + \psi_7(S,\infty,\Omega)\right] \qquad \text{(E-25)}$$

$$B_{\theta\infty} = -\cos\frac{\omega x}{u} + \frac{\frac{a_3}{a_2}}{1+\left(\frac{b_1}{b_2\omega}\right)^2}\left(\frac{b_1}{b_2\omega}\sin\frac{\omega x}{u} - \cos\frac{\omega x}{u}\right)$$

$$+ \frac{e^{-\frac{x}{a_4}\left(\frac{b_1}{b_2\omega}\right)}}{1+\left(\frac{b_1}{b_2\omega}\right)^2}\left[\frac{b_1}{b_2\omega}\psi_7(S,\infty,\Omega) - \psi_8(S,\infty,\Omega)\right] \qquad \text{(E-26)}$$

Fluid-wall temperature difference

$$\frac{\Delta t_2(x,\tau)}{a_1\Phi} = \frac{1}{a_2\omega\left[1+\left(\frac{b_1}{b_2\omega}\right)^2\right]}\sqrt{A_{\Delta t_\infty}^2 + B_{\Delta t_\infty}^2}\,\sin\left[\omega\tau - \frac{\omega x}{u} - \tan^{-1}\left(-\frac{B_{\Delta t}}{A_{\Delta t}}\right)\right] \qquad \text{(E-27)}$$

where

$$A_{\Delta t\infty} = \frac{b_1}{b_2\omega}\cos\frac{\omega x}{u} + \sin\frac{\omega x}{u} + e^{-\frac{x}{a_4}}\left[\frac{b_1}{b_2\omega}\psi_7(S,\infty,\Omega) - \psi_8(S,\infty,\Omega)\right] \qquad \text{(E-28)}$$

$$B_{\Delta t_\infty} = \frac{b_1}{b_2\omega}\sin\frac{\omega x}{u} - \cos\frac{\omega x}{u} + e^{-\frac{x}{a_4}}\left[\psi_7(S,\infty,\Omega) - \frac{b_1}{b_2\omega}\psi_8(S,\infty,\Omega)\right] \qquad \text{(E-29)}$$

Fluid temperature

$$\frac{t_2(x,\tau)}{\frac{a_1 x}{a_4}\Phi} = \frac{a_4}{b_1\omega x}\sqrt{A_{t_\infty}^2 + B_{t_\infty}^2}\,\sin\left[\omega\tau - \frac{\omega x}{u} - \tan^{-1}\left(-\frac{B_{t\infty}}{A_{t_\infty}}\right)\right] \qquad \text{(E-30)}$$

where

$$A_{t\infty} = \sin\frac{\omega x}{u} - \frac{1}{1+\left(\frac{b_1}{b_2\omega}\right)^2}\left(\frac{b_1}{b_2\omega}\cos\frac{\omega x}{u} + \sin\frac{\omega x}{u}\right)$$

$$+ \frac{e^{-\frac{x}{a_4}}}{1+\left(\frac{b_1}{b_2\omega}\right)^2}\left\{\left[\left(\frac{b_1}{b_2\omega}\right)^2 + 1 + \frac{a_2}{a_3}\right]\psi_8(s,\infty,\Omega)\right.$$

$$\left. - \frac{a_2}{a_3}\left(\frac{b_1}{b_2\omega}\right)\psi_7(s,\infty,\Omega)\right\} \qquad \text{(E-31)}$$

$$B_{t\infty} = -\cos\frac{\omega x}{u} - \frac{1}{1+\left(\frac{b_1}{b_2\omega}\right)^2}\left(\frac{b_1}{b_2\omega}\sin\frac{\omega x}{u} - \cos\frac{\omega x}{u}\right)$$

$$+ \frac{e^{-\frac{x}{a_4}}}{1+\left(\frac{b_1}{b_2\omega}\right)^2}\left\{\left[\left(\frac{b_1}{b_2\omega}\right)^2 + 1 + \frac{a_2}{a_3}\right]\psi_7(s,\infty,\Omega)\right.$$

$$\left. + \frac{a_2}{a_3}\left(\frac{b_1}{b_2\omega}\right)\psi_8(s,\infty,\Omega)\right\} \qquad \text{(E-32)}$$

The amplitude-ratio and phase-shift responses can be found from Equations (E-24), (E-27) and (E-30) as follows:

wall temperature

$$\left|\bar{F}_\theta(i\omega)\right| = \frac{\sqrt{A_{\theta\infty}^2 + B_{t\infty}^2}}{b\omega\left(1+\frac{x}{a_4}\right)} \qquad \text{(E-33)}$$

$$\alpha_{\theta\infty} = \frac{\omega x}{u} + \tan^{-1}\left(-\frac{B_{\theta\infty}}{A_{\theta\infty}}\right) \tag{E-34}$$

Fluid-wall temperature difference

$$\left|\bar{F}_{\Delta t}(i\omega)\right| = \frac{\sqrt{A^2_{\Delta t\infty} + B^2_{\Delta t\infty}}}{a_2\omega\left[1+\left(\frac{b_1}{b_2\omega}\right)^2\right]} \tag{E-35}$$

$$\alpha_{\Delta t\infty} = \frac{\omega x}{u} + \tan^{-1}\left(-\frac{B_{\Delta t\infty}}{A_{\Delta t\infty}}\right) \tag{E-36}$$

Fluid temperature

$$\left|\bar{F}_t(i\omega)\right| = \frac{\sqrt{A^2_{t\infty} + B^2_{t\infty}}}{\frac{b_1\omega x}{a_4}} \tag{E-37}$$

$$\alpha_{t\infty} = \frac{\omega x}{u} + \tan^{-1}\left(-\frac{B_{t\infty}}{A_{t\infty}}\right) \tag{E-38}$$

Equations (E-33) through (E-38) are identical with Equations (55), (56), (57), (58), (59) and (60) by u sing s = iω.

APPENDIX F

DERIVATION OF EQUATIONS FOR THE DYNAMIC RESPONSE OF A HEAT EXCHANGER WITH ZERO WALL-FLUID HEAT-CAPACITY RATIO

The first law of thermodynamics in a heat exchanger with zero wall-fluid heat-capacity ratio can be expressed as follows:

$$(\rho a\,dx)C_p\frac{\partial t}{\partial \tau}+\rho u a C_p\frac{\partial t}{\partial x}dx=a^1 dx\,p_x''(\tau) \qquad \text{(F-1)}$$

or

$$\frac{\partial t}{\partial \tau}+\frac{\partial t}{\partial(\frac{x}{u})}=\frac{V_w}{\rho C_p V}p_x''(\tau) \qquad \text{(F-2)}$$

where $p_x''(\tau) = p_{xo}'' + \Phi(\tau) = p_{xo}'' + \Phi\cos(\omega\tau-\eta)$ and η is a constant.

The steady-state component of the fluid temperature can be obtained from Equation (F-2) as

$$t_1(x,0)=\frac{V_w}{\rho C_p V}p_{xo}''\frac{x}{u} \qquad \text{(F-3)}$$

From Equations (F-2) and (F-3), one obtains an equation for the transient component of the fluid temperature as

$$\frac{\partial t_2}{\partial \tau}+\frac{\partial t_2}{\partial(\frac{x}{u})}=\frac{V_w}{\rho C_p V}\Phi(\tau) \qquad \text{(F-4)}$$

performing the Laplace transformation on Equation (F-4) it yields,

$$s\bar{t}_2 + \frac{d\bar{t}_2}{d(\frac{x}{u})} = \frac{V_w}{\rho C_p V}\bar{\Phi} \tag{F-5}$$

With the same boundary conditions as Equations (A-21), (A-22) and (A-23), one obtains

$$\bar{t}_2 = \frac{V_w}{\rho C_p V}(1 - e^{-s\frac{x}{u}}) + \bar{t}_o^* e^{-s\frac{x}{u}} \tag{F-6}$$

For the constant inlet fluid temperature, Equation (F-6) reduces to

$$\bar{t}_2 = \frac{V_w}{\rho C_p V}(1 - e^{-s\frac{x}{u}}) \tag{F-7}$$

Substituting

$$\bar{\Phi} = \Phi\frac{s}{s^2+\omega^2}\cos\eta + \Phi\frac{\omega}{s^2+\omega^2}\sin\eta \tag{F-8}$$

into Equation (F-7), gives

$$\bar{t}_2 = \frac{\Phi V_w}{\rho C_p V s}\left[\frac{s}{s^2+\omega^2}\cos\eta - \frac{\omega}{s^2+\omega^2}\right]\sin\eta \tag{F-9}$$

performing the inverse Laplace transformation on Equation (F-9), yields two solutions as follows

i $1 \geq \frac{\tau u}{x} \geq 0$

$$t(\tau) - t_1(0) = \frac{\Phi V_w}{\rho C_p V}\left[\frac{\cos\eta}{\omega}\sin\omega\tau + \frac{\sin\eta}{\omega}(1-\cos\omega\tau)\right] \tag{F-10}$$

ii $\frac{\tau u}{x} \geq 1$

$$t(x,\tau)-t_1(x,0)=\frac{\Phi V_w}{\rho C_p V}\left[\frac{\cos\eta}{\omega}\sin\omega\tau+\frac{\sin\eta}{\omega}(1-\cos\omega\tau)\right.$$

$$\left.-\frac{\cos\eta}{\omega}\sin\omega\tau^*+\frac{\sin\eta}{\omega}(1-\cos\omega\tau^*)\right]$$

$$=\frac{\Phi V_w}{\rho C_p V}\left\{\frac{\cos\eta}{\omega}\sqrt{2(1-\cos\frac{\omega x}{u})}\cos\left[\omega\tau-\tan^{-1}\left(\frac{1-\cos\frac{\omega x}{u}}{\sin\frac{\omega x}{u}}\right)\right]\right.$$

$$\left.+\frac{\sin\eta}{\omega}\sqrt{2(1-\cos\frac{\omega x}{u})}\sin\left[\omega\tau-\tan^{-1}\left(\frac{1-\cos\frac{\omega x}{u}}{\sin\frac{\omega x}{u}}\right)\right]\right\}$$

$$=\frac{\Phi V_w}{\rho C_p V}\frac{\sqrt{2(1-\cos\frac{\omega x}{u})}}{\omega}\cos\left[\omega\tau-\eta-\tan\left(\frac{1-\cos\frac{\omega x}{u}}{\sin\frac{\omega x}{u}}\right)\right] \qquad \text{(F-11)}$$

For zero frequency, Equation (F-4) reduces to

$$\frac{\partial t_2}{\partial\tau}+\frac{\partial t_2}{\partial(\frac{x}{u})}=\frac{\Phi V_w}{\rho C_p V} \qquad \text{(F-12)}$$

Solving Equation (F-12), one obtains two solutions as

i $1 \geq \frac{\tau u}{x} \geq 0$

$$t_{w=0}(\tau) - t_i(0) = \frac{\Phi V_w \tau}{\rho C_p V} \tag{F-13}$$

ii $\frac{\tau u}{x} \geq 1$

$$t_{w=0}(x,\tau) - t_i(x,0) = \frac{\Phi V_w \tau}{\rho C_p V} - \frac{\Phi V_w \tau^*}{\rho C_p V} = \frac{\Phi V_w \frac{x}{u}}{\rho C_p V} \tag{F-14}$$

Dividing Equations (F-10) and (F-11) by (F-13) and (F-14), yields

i $1 \geq \frac{\tau u}{x} \geq 0$

$$\frac{t(\tau) - t_i(0)}{t_{w=0}(\tau) - t_i(0)} = \frac{\cos\eta \sin\omega\tau}{\omega\tau} + \frac{\sin\eta(1-\cos\omega\tau)}{\omega\tau} \tag{F-15}$$

ii $\frac{\tau u}{x} \geq 1$

$$\frac{t(x,\tau) - t_i(x,0)}{t_{w=0}(x,\tau) - t_i(x,0)} = \frac{\sqrt{2(1-\cos\frac{\omega x}{u})}}{\sin\frac{\omega x}{u}} \cos\left[\omega\tau - \eta - \tan^{-1}\left(\frac{1-\cos\frac{\omega x}{u}}{\sin\frac{\omega x}{u}}\right)\right] \tag{F-16}$$

Equations (F-15) and (F-16) express the oscillation of the fluid temperature in the two time domains, beside that Equation (F-16) also demonstrates the responses of the amplitude-ratio and phase-shift as

$$\frac{[T_\infty(x)]_{\omega=\omega}}{[T_\infty(x)]_{\omega=0}} = \frac{\sqrt{2(1-\cos\frac{\omega x}{u})}}{\frac{\omega x}{u}} \tag{F-17}$$

$$\alpha_t = \tan^{-1}\left(\frac{1-\cos\frac{\omega x}{u}}{\sin\frac{\omega x}{u}}\right) \qquad \text{(F-18)}$$

In case the observer is on the fluid particle and again $p''_x = p''_{xo}$ + $\Phi \cos(\omega\tau-\eta-\lambda)$ where λ is the inlet lag of the particle, the analysis as shown below follows.

Heat balance of the particle, gives

$$\rho C_p V\frac{dt}{d\tau} = P''_{xo}V_w + \Phi V_w \cos(\omega\tau-\eta-\lambda) \qquad \text{(F-19)}$$

Rearranging Equation (F-19) as

$$dt = \frac{P''_{xo}V_w}{\rho C_p V}d\tau + \frac{\Phi V_w}{\rho C_p V}\cos(\omega\tau-\eta-\lambda)d\tau \qquad \text{(F-20)}$$

and integrating it from $\tau = 0$ to $\tau = \tau$, one obtains

$$t(\tau)-t_o = \frac{P''_{xo}V_w\tau}{\rho C_p V} + \frac{\Phi V_w}{\rho C_p V}\frac{\cos(\eta+\lambda)}{\omega}\sin\omega\tau + \frac{\Phi V_w}{\rho C_p V}\frac{\sin(\eta+\lambda)}{\omega}(1-\cos\omega\tau) \qquad \text{(F-21)}$$

At a steady-state, heat balance gives

$$\rho C_p V\frac{dt}{d\tau} = P''_{xo}V_w \qquad \text{(F-22)}$$

Integrating Equation (F-22), yields

$$t_1(\tau) - t_0 = \frac{P''_{x0} V_w \tau}{\rho C_p V} \tag{F-23}$$

For zero frequency, heat balance is

$$\rho C_p V \frac{dt}{d\tau} = (P''_{x0} + \Phi) V_w \tag{F-24}$$

and

$$t_{w=0}(\tau) - t_0 = \frac{(P''_{x0} + \Phi) V_w \tau}{\rho C_p V} \tag{F-25}$$

From Equations (F-21), (F-23) and (F-25), one finds

$$t(\tau) - t_1(\tau) = \frac{\Phi V_w}{\rho C_p V} \left[\frac{\cos(\eta+\lambda)}{\omega} \sin\omega\tau + \frac{\sin(\eta+\lambda)}{\omega} \cos\omega\tau \right] \tag{F-26}$$

and

$$t_{w=0}(\tau) - t_1(\tau) = \frac{\Phi V_w \tau}{\rho C_p V} \tag{F-27}$$

Dividing (F-26) by (F-27), one obtains

$$\frac{t(\tau) - t_1(\tau)}{t_{w=0}(\tau) - t_1(\tau)} = \frac{\cos(\eta+\lambda)\sin\omega\tau}{\omega\tau} + \frac{\sin(\eta+\lambda)(1-\cos\omega\tau)}{\omega\tau}$$

$$= \frac{\sqrt{2(1-\cos\omega\tau)}}{\omega\tau} \cos\left[\eta + \lambda - \tan^{-1}\left(\frac{1-\cos\omega\tau}{\sin\omega\tau}\right)\right] \tag{F-28}$$

Equation (F-28) shows that

$$\frac{t(\tau)-t_1(\tau)}{t_{w=0}(\tau)-t_1(\tau)} = \pm \frac{\sqrt{2(1-\cos\omega\tau)}}{\omega\tau} \qquad \text{(F-29)}$$

when

$$\eta+\lambda = 2n\pi + \tan^{-1}\left(\frac{1-\cos\omega\tau}{\sin\omega\tau}\right) \quad \text{for + sign} \qquad \text{(F-30)}$$

and

$$\eta+\lambda = (2n+1)\pi + \tan^{-1}\left(\frac{1-\cos\omega\tau}{\sin\omega\tau}\right) \quad \text{for - sign} \qquad \text{(F-31)}$$

where

$$n = 0, 1, 2, \ldots .$$

Equation (F-26) shows that $t(\tau)$ equals to $t_1(\tau)$ when

$$\omega\tau = 2n\pi \quad \text{and} \quad \omega\tau - 2(\eta+\lambda) = (2n+1)\pi \qquad \text{(F-32)}$$

Equations (124) and (125) for the wall temperature may be derived independently directly from the energy equations as follows:

Taking the wall as a system, heat balance may be expressed as

$$-hA(\theta-t) + V_w P_x''(\tau) = 0 \qquad \text{(F-33)}$$

Since

$$hA(\theta_1-t_1) = V_w P_{x0}'' \qquad \text{(F-34)}$$

one obtains the equation governing the transient component from Equation (F-33) and (F-34) as

$$\theta_2 - t_2 = \frac{V_w}{hA}\phi(\tau) \tag{F-35}$$

performing the Laplace transformation on Equation (F-35), yields

$$\bar{\theta}_2 - \bar{t}_2 = \frac{V_w}{hA}\bar{\phi} \tag{F-36}$$

Substituting (F-6) into (F-36), one finds

$$\bar{\theta}_2 = \frac{V_w\bar{\phi}}{\rho C_p V s}\left(1 - e^{-s\frac{x}{u}}\right) + \frac{V_w}{hA}\bar{\phi} + \bar{t}_o^{*}e^{-s\frac{x}{u}} \tag{F-37}$$

For the constant fluid inlet temperature, (F-37) reduces to

$$\bar{\theta}_2 = \frac{V_w\bar{\phi}}{hA}\left(\frac{hA}{\rho C_p V}\,\frac{1-e^{-s\frac{x}{u}}}{s} + 1\right) \tag{F-38}$$

Since $K = hA/\rho C_p V$, and by rearranging Equation (F-38), one obtains

$$\frac{\bar{\theta}_2}{\frac{V_w\bar{\phi}}{hA}\left(1+\frac{Kx}{u}\right)} = \frac{1}{1+\frac{Kx}{u}}\left[\frac{K\left(1-e^{-s\frac{x}{u}}\right)}{s} + 1\right] \tag{F-39}$$

Since

$$\frac{V_w\Phi}{hA}\left(1+\frac{Kx}{u}\right) = \frac{\Delta\left(q/A\right)}{h}\left(1+\frac{Kx}{u}\right) = \left(\Theta_\infty\right)_{\omega=0} \tag{F-40}$$

and $\phi(\tau) = \Phi \sin\omega\tau$ Equation (F-39) expresses the transfer function of the wall temperature. By substituting $s = i\omega$ into Equation (F-39), the amplitude-ratio and phase-shift of the wall temperature may be obtained

as

$$\left|\bar{F}_\theta(i\omega)\right| = \frac{K}{\omega}\sqrt{\left(\cos\frac{\omega x}{u}-1\right)^2+\left(\frac{\omega}{K}+\sin\frac{\omega x}{u}\right)^2} \qquad \text{(F-41)}$$

$$\alpha_\theta = \tan^{-1}\left(\frac{1-\cos\frac{\omega x}{u}}{\frac{\omega}{K}+\sin\frac{\omega x}{u}}\right) \qquad \text{(F-42)}$$

Equations (135) and (136) for the fluid-wall temperature difference may also be obtained from Equation (F-35) as

$$\Delta t_2 = \frac{V_w}{hA}\Phi(\tau) \qquad \text{(F-43)}$$

or

$$\frac{\Delta t_2}{\frac{V_w \Phi}{hA}} = \sin\omega\tau \qquad \text{(F-44)}$$

$$\frac{V_w \Phi}{hA} = \frac{\Delta\left(\frac{q}{A}\right)}{h} = (\Delta T_\infty)_{\omega=0} \qquad \text{(F-45)}$$

From Equations (F-44) and (F-45), it is evident that

$$\left|\bar{F}_{\Delta t}(i\omega)\right| = 1 \qquad \text{(F-46)}$$

and

$$\alpha_{\Delta t} = 0 \qquad \text{(F-47)}$$

APPENDIX G

NUMERICAL SOLUTIONS OF FUNCTIONS $\psi_7(s,q,\Omega)$ AND $\psi_8(s,q,\Omega)$

Two functions $\psi_7(s,q,\Omega)$ and $\psi_8(s,q,\Omega)$ are defined as

$$\psi_7(s,q,\Omega)=\sum_{k=0}^{\infty}\frac{s^k}{(k!)^2}\int_0^q z^k e^{-z}\cos\Omega z\,dz \tag{G-1}$$

$$\psi_8(s,q,\Omega)=\sum_{k=0}^{\infty}\frac{s^k}{(k!)^2}\int_0^q z^k e^{-z}\sin\Omega z\,dz \tag{G-2}$$

By integrating the two functions $\psi_7(s,q,\Omega)$ and $\psi_8(s,q,\Omega)$ term by term, one obtains two infinite series

$$\psi_7(s,q,\Omega)=\sum_{k=0}^{\infty}A_k\frac{s^k}{(k!)^2} \tag{G-3}$$

$$\psi_8(s,q,\Omega)=\sum_{k=0}^{\infty}B_k\frac{s^k}{(k!)^2} \tag{G-4}$$

with their coefficients expressed as follow:

$$A_0=\frac{1}{1+\Omega^2}(1+M)$$

$$B_0=\frac{1}{1+\Omega^2}(\Omega-N)$$

$$A_1=\frac{1}{1+\Omega^2}\left[(A_0-\Omega B_0)+qM\right]$$

$$B_1=\frac{1}{1+\Omega^2}\left[(B_0+\Omega A_0)-qN\right]$$

$$A_2 = \frac{1}{1+\Omega^2}\left[2(A_1 - \Omega B_1) + q^2 M\right]$$

$$B_2 = \frac{1}{1+\Omega^2}\left[2(B_1 + \Omega A_1) - q^2 N\right]$$

$$A_3 = \frac{1}{1+\Omega^2}\left[3(A_2 - \Omega B_2) + q^3 M\right]$$

$$B_3 = \frac{1}{1+\Omega^2}\left[3(B_2 + \Omega A_2) - q^3 N\right]$$

or expressed in recurrence formula,

$$A_K = \frac{1}{1+\Omega^2}\left[K(A_{K-1} - \Omega B_{K-1}) + q^K M\right] \tag{G-5}$$

$$B_K = \frac{1}{1+\Omega^2}\left[K(B_{K-1} + \Omega A_{K-1}) - q^K N\right] \tag{G-6}$$

where

$$M = (\Omega \sin\Omega q - \cos\Omega q)\, e^{-q} \tag{G-7}$$

$$N = (\Omega \cos\Omega q + \sin\Omega q)\, e^{-q} \tag{G-8}$$

Substituting Equations (G-5) and (G-6) into Equations (G-3) and (G-4), it yields

$$\psi_7(S, q, \Omega) = \sum_{K=0}^{\infty} \frac{S^K}{(K!)^2(1+\Omega^2)}\left[K(A_{K-1} - \Omega B_{K-1}) + q^K(\Omega \sin\Omega q - \cos\Omega q)e^{-q}\right] \tag{F-9}$$

$$\psi_8(S, q, \Omega) = \sum_{K=0}^{\infty} \frac{S^K}{(K!)^2(1+\Omega^2)}\left[K(B_{K-1} + \Omega A_{K-1}) - q^K(\Omega \cos\Omega q + \sin\Omega q)e^{-q}\right] \tag{F-10}$$

Certain known elementary properties of the two functions may be recorded here for reference:

$$\psi_7(s,\infty,\Omega) = \frac{e^{\frac{s}{1+\Omega^2}}}{1+\Omega^2}\left(\cos\frac{s\Omega}{1+\Omega^2} - \Omega\sin\frac{s\Omega}{1+\Omega^2}\right) \tag{G-11}$$

$$\psi_8(s,\infty,\Omega) = \frac{e^{\frac{s}{1+\Omega^2}}}{1+\Omega^2}\left(\Omega\cos\frac{s\Omega}{1+\Omega^2} + \sin\frac{s\Omega}{1+\Omega^2}\right) \tag{G-12}$$

Equations (G-11) and (G-12) are obtained by integrating Equations (G-1) and (G-2) term by term from zero to infinite.

$$\psi_7(s,q,0) = \sum_{k=0}^{\infty}\frac{s^k}{(k!)^2}\int_0^q z^k e^{-z}dz = \psi_2^{**}(s,q) \tag{G-13}$$

$$\psi_8(s,q,0) = 0 \tag{G-14}$$

$$\psi_7(s,\infty,0) = \psi_2^{**}(s,\infty) = e^s \tag{G-15}$$

$$\psi_8(s,\infty,0) = 0 \tag{G-16}$$

$$\psi_7(0,q,\Omega) = 0 \tag{G-17}$$

$$\psi_8(0,q,\Omega) = 0 \tag{G-18}$$

$$\psi_7(0,q,0) = \psi_2(0,q) = 0 \tag{G-19}$$

$$\frac{\partial}{\partial q}\psi_7(s,q,0) = e^{-q}I_0(2\sqrt{sq}) \tag{G-20}$$

$$e^{-s}\psi_7(s,q,0) + e^{-q}\psi_7(s,q,0) + e^{-(s+q)}I_0(2\sqrt{sq}) = 1 \tag{G-21}$$

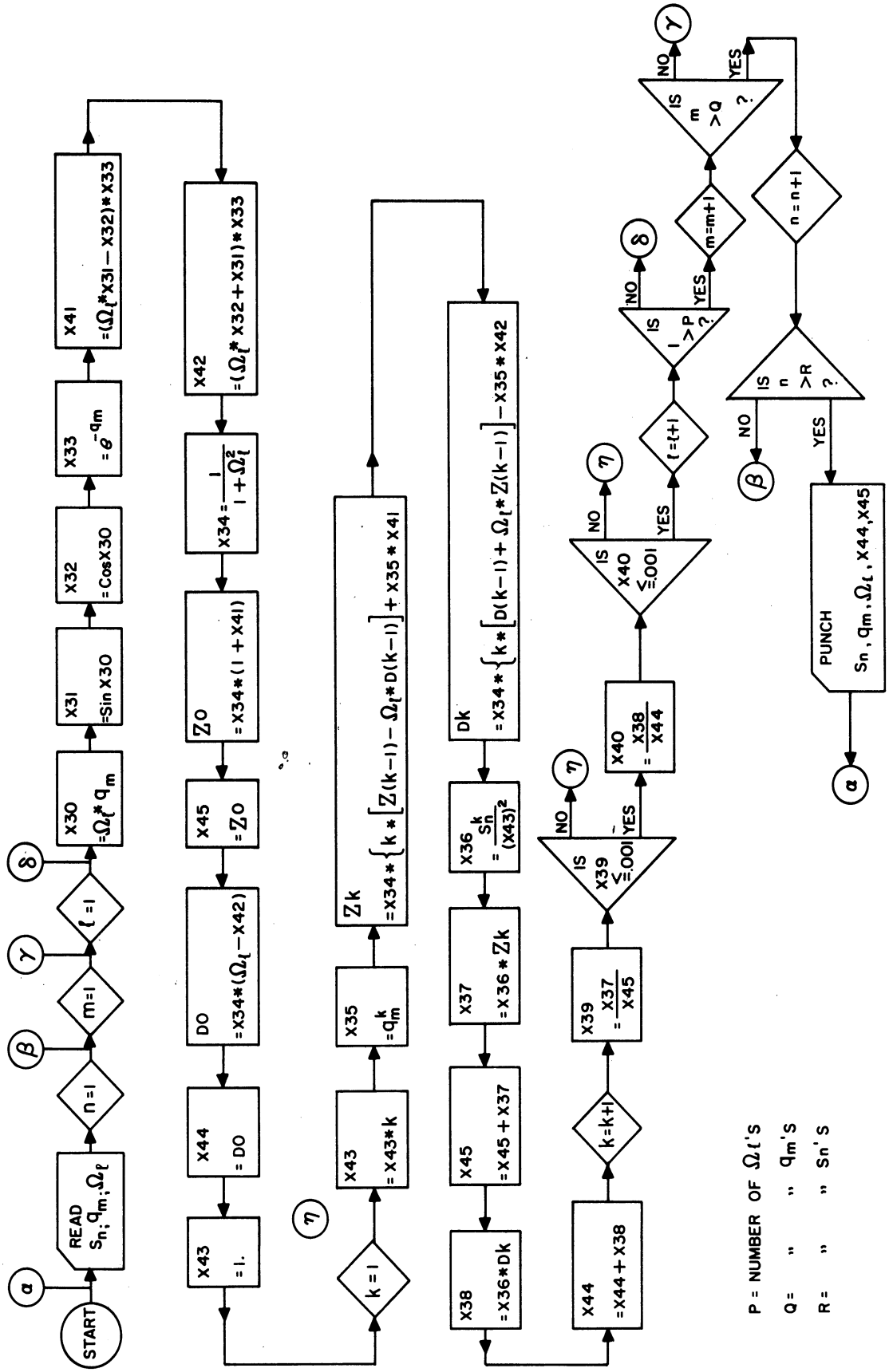

Flow Diagram

For the numerical evaluations of the two functions, the flow diagram and the program for IBM 704 computer have been worked out as follow:

Program for IBM 704 computer

```
    * Compile Fortran, print SAP execute
    Dimension C(50), D(2000), X(50), Y(50), Z(2000)
    Write output tape 6, 36
36. Format (8 H1Results)

 1. Read input tape 7, 34, NC, NX, NY, (C(I), I=1, NC), (X(I), I=1, NX),
    (Y(I), I=1, NY)
34. Format (3I3/(4F(5.2))
 2. DO 32 J0 = 1, NC
 3. DO 32 JI = 1, NX
 4. DO 32 J2 = 1, NY
 5. X(30) = Y(J2) * X(J1)
 6. X(31) = Sin F (X(30))
 7. X(32) = Cos F (X(30))
 8. X(33) = 1./2.7182818 ** X(J1)
 9. X(41) = (Y(J2) * X(31) - X(32) * X(33)
10. X(42) = (Y(J2) * X(32) + X(31) * X(33)
11. X(34) = 1./(1. + Y(J2) * Y(J2)
12. Z(1)  = X(34) * (1. + X(41))
13. X(45) = Z(1)
14. D(1)  = X(34) * (Y(J2) - X(42))
15. X(44) = D(1)
16. X(43) = 1
```

```
17.  K = 1
     Fk = K
18.  X(43) = X(43) * Fk
19.  X(53) * X'(J1) ** K
20.  Z(K+1) = X(34) * (FK*(X(K) - Y(J2)*D(K)) + X(35)*X(41))
21.  D(K+1) = X(34)*(FK*(D(K) + Y(J2)*Z(K)) - X(35)*X(42))
22.  X(36)  = C(J0)**K/(X(43)*X(43))
23.  X(37)  = X(36) *Z(k+1)
24.  X(45)  = X(45) + X(37)
25.  X(38)  = X(36)*D(K+1)
26.  X(44)  = X(44) + X(38)
27.  K = K+1
     FK = FK+1
28.  X(39) = X(37)/X(45)
29.  IF (ABSF(X(39))-0.001) 30,30,18
30.  X(40) = X(38)/X(44)
31.  IF(ABSF(X(40))-0.001) 32,32,18
32.  Write Output tape 6,35, J0, C(J0), J1, X(J1), J2, Y(J2), X(44), X(45)
35 Format (3H C(I3, 2H) = E12.5, 4H X(I3,2H) = 12.5, 4H Y(I3,2H) =
   E12.5, 8H X(44) = E12.5, 8H X(45) = E12.5)
33.  GO to 1
     End (1,1, 0, 1, 0)
```

Parts of the results are presented graphically in Figures 42-57, for ε = 0.1, 0.5, 1.0, 1.5, and 2.0. Both the results of IBM 650 and 704 for the program are available at the Heat Transfer and Thermodynamics

Laboratory, North Campus, upon the request. The combinations of the variables s, q and Ω are:

s = 0.1; 0.5; 1.0; 1.5; 2.0; 2.5; 3.0; 3.5; 4.0; 4.5; 5.0; 5.5; 6.0; 6.5; 7.0; 7.5; 8.0; 8.5; 9.0; 10.0,

q = 0.1; 0.2; 0.3; 0.4; 0.5; 0.6; 0.7; 0.8; 0.9; 1.0; 1.2; 1.4; 1.6; 1.8; 2.0; 2.4; 2.8; 3.2; 3.6; 4.0; 5.0; 10.0,

Ω = 0.1; 0.2; 0.4; 0.6; 0.8; 1.0; 1.2; 1.4; 1.6; 1.8; 2.0; 2.4; 2.8; 3.2; 3.6; 4.0; 5.0; 6.0; 8.0; 10.0.

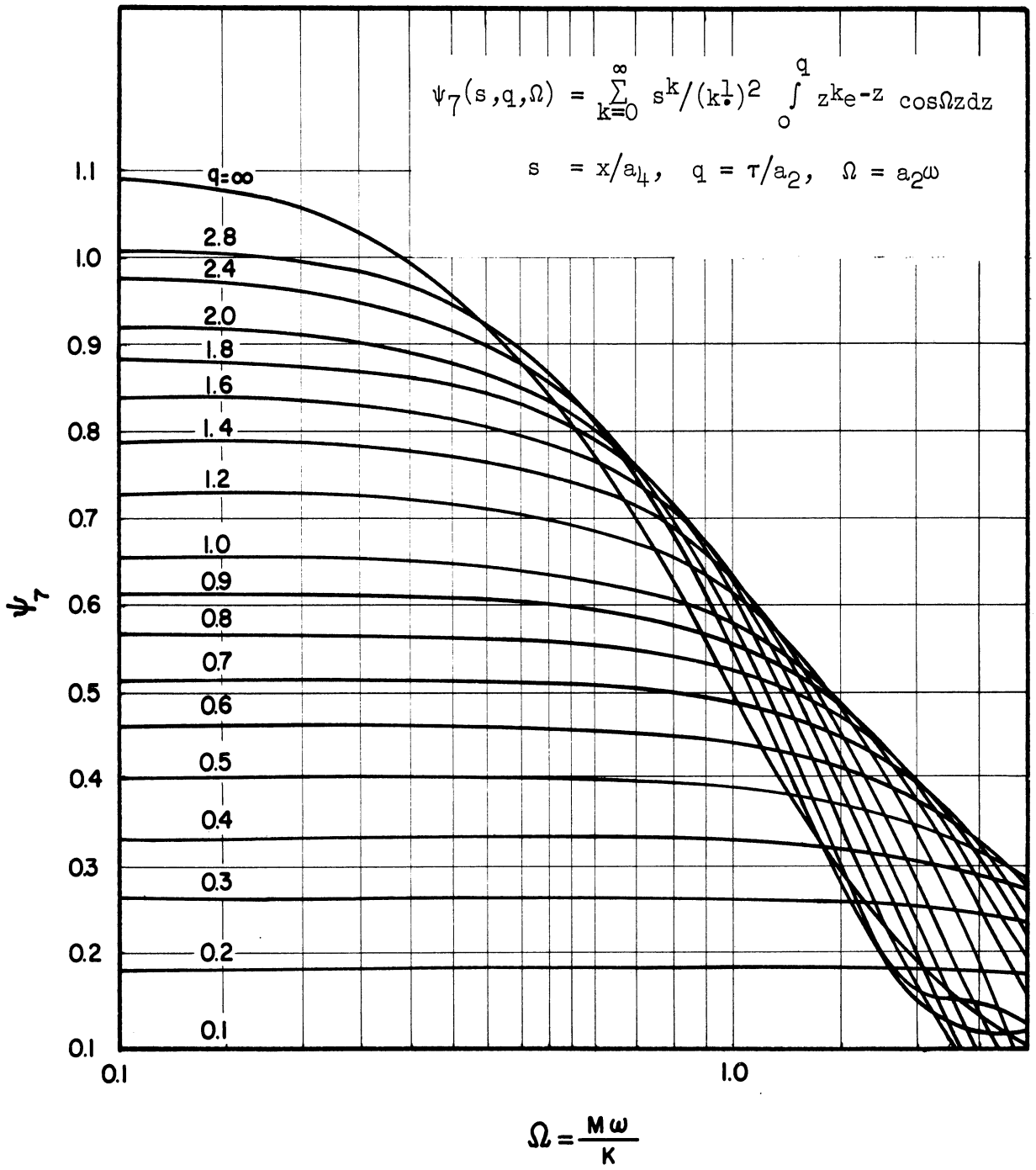

Figure 42. ψ_7 versus Ω, s = 0.1.

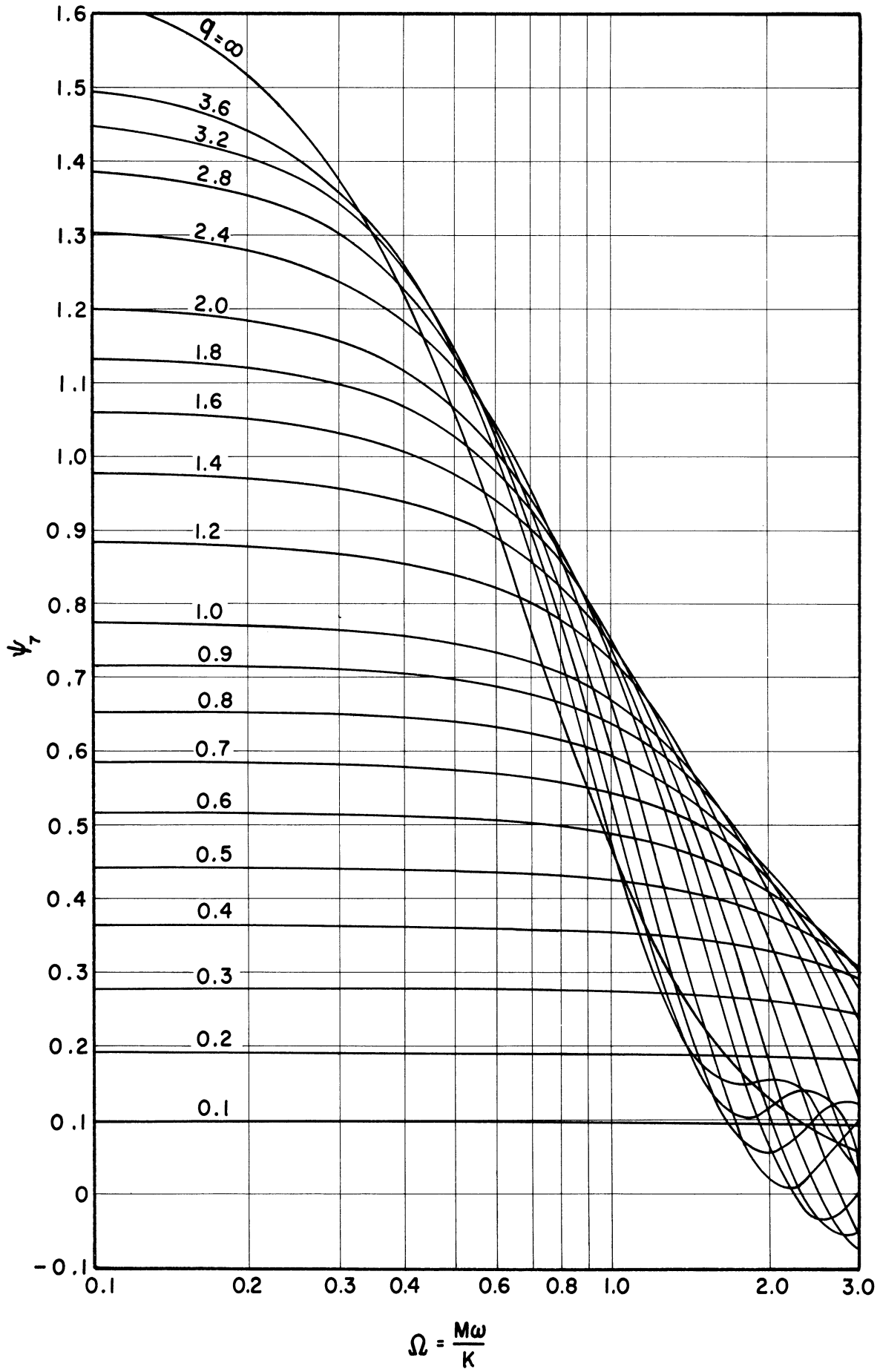

Figure 43. ψ_7 versus Ω, s = 0.5.

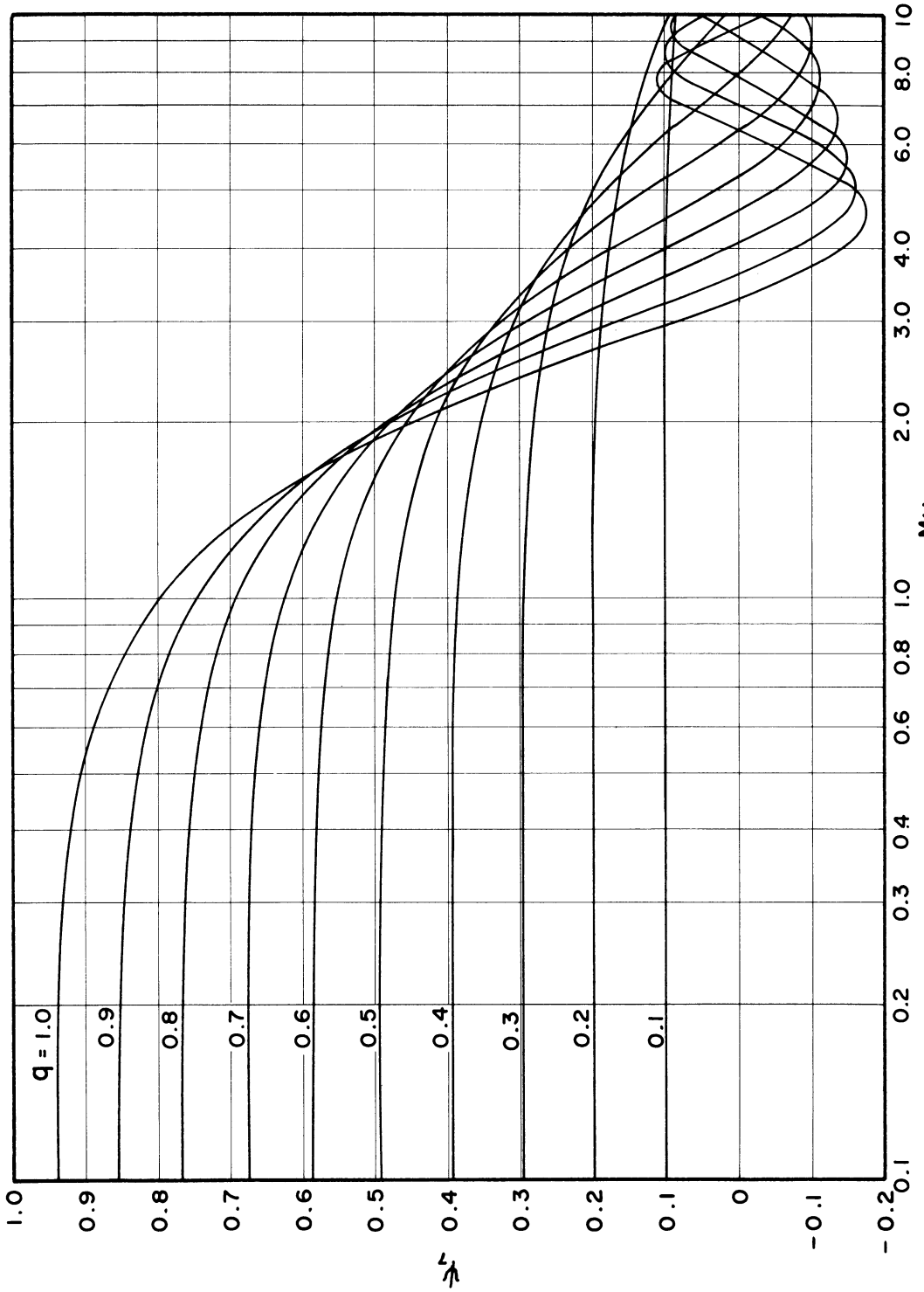

Figure 44. ψ_7 versus Ω, s = 1.0 (q = 0.1~1.0).

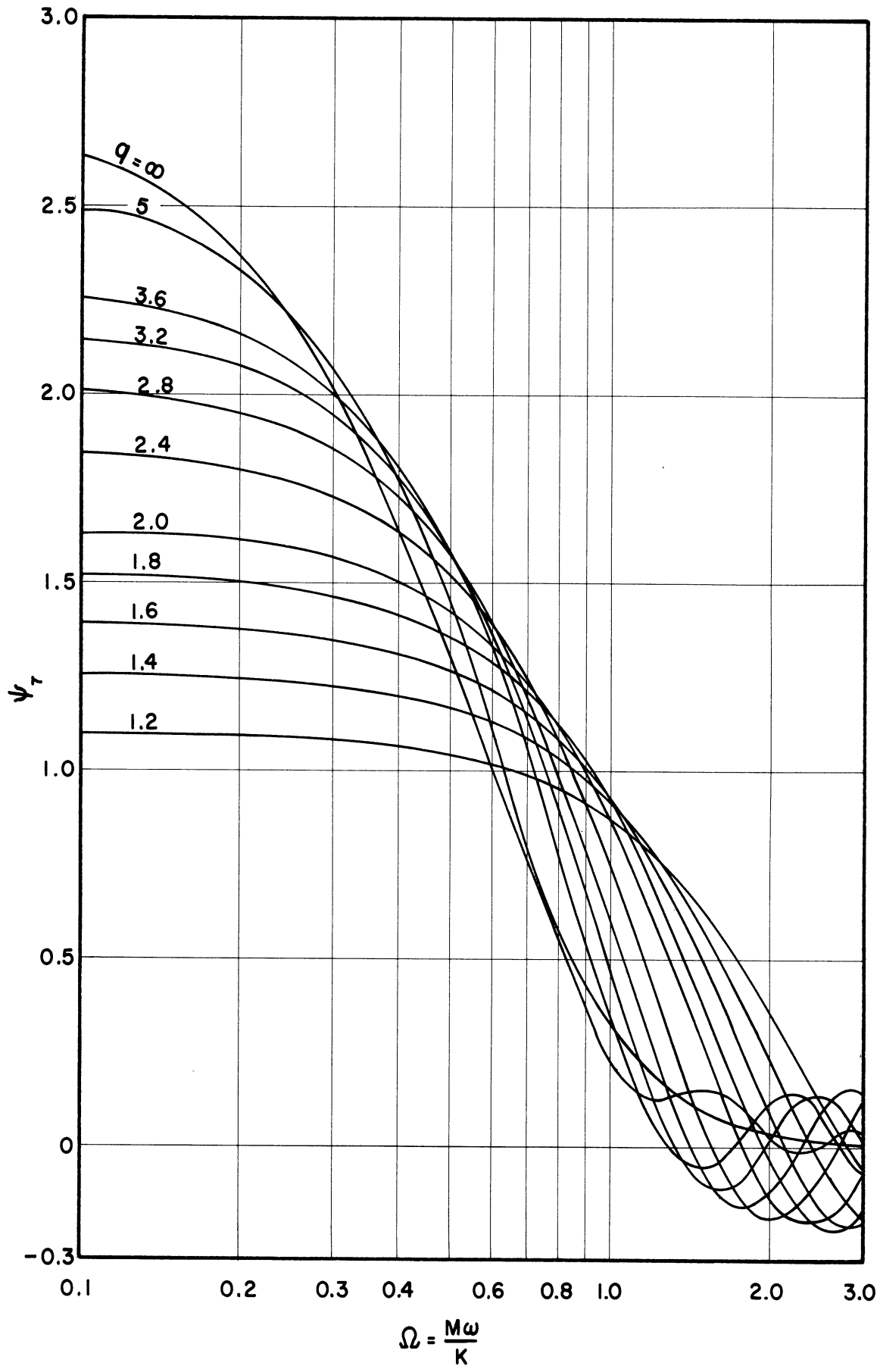

Figure 45. ψ_7 versus Ω, s = 1.0 (q = 1.2 $\sim \infty$).

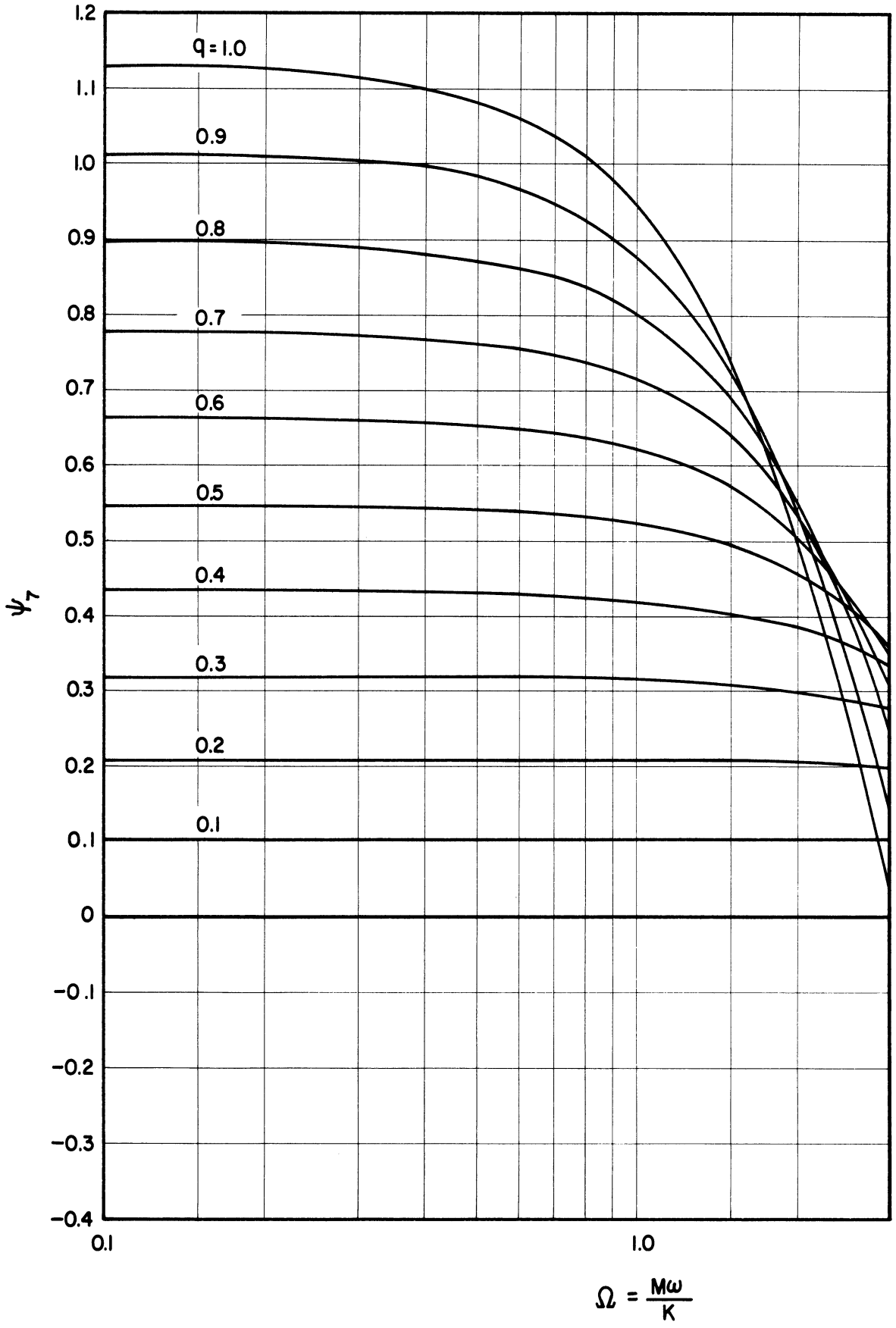

Figure 46. ψ_7 versus Ω, s = 1.5 (q = 0.1~1.0).

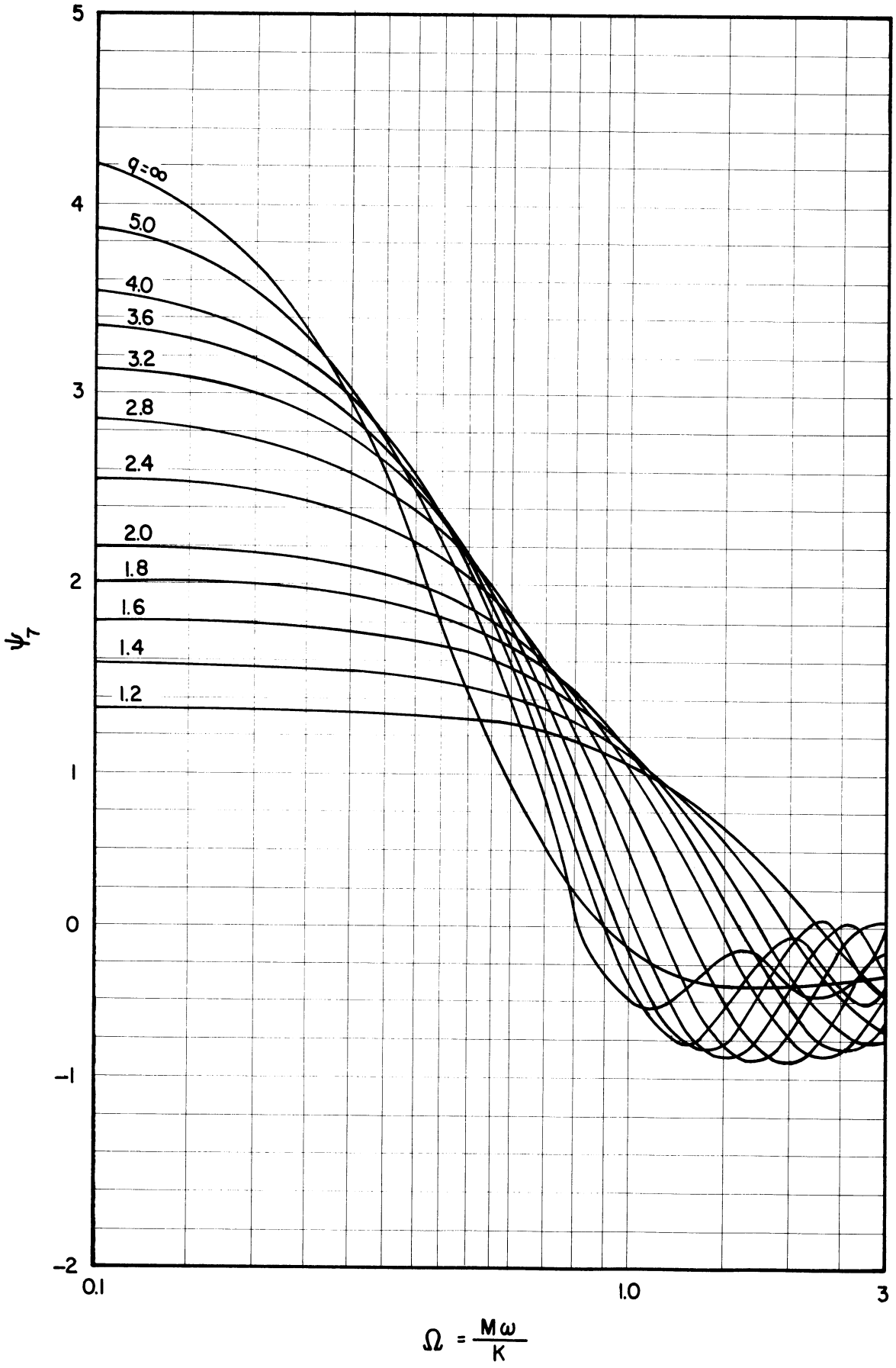

Figure 47. ψ_7 versus Ω, s = 1.5 (q = 1.2 $\sim \infty$).

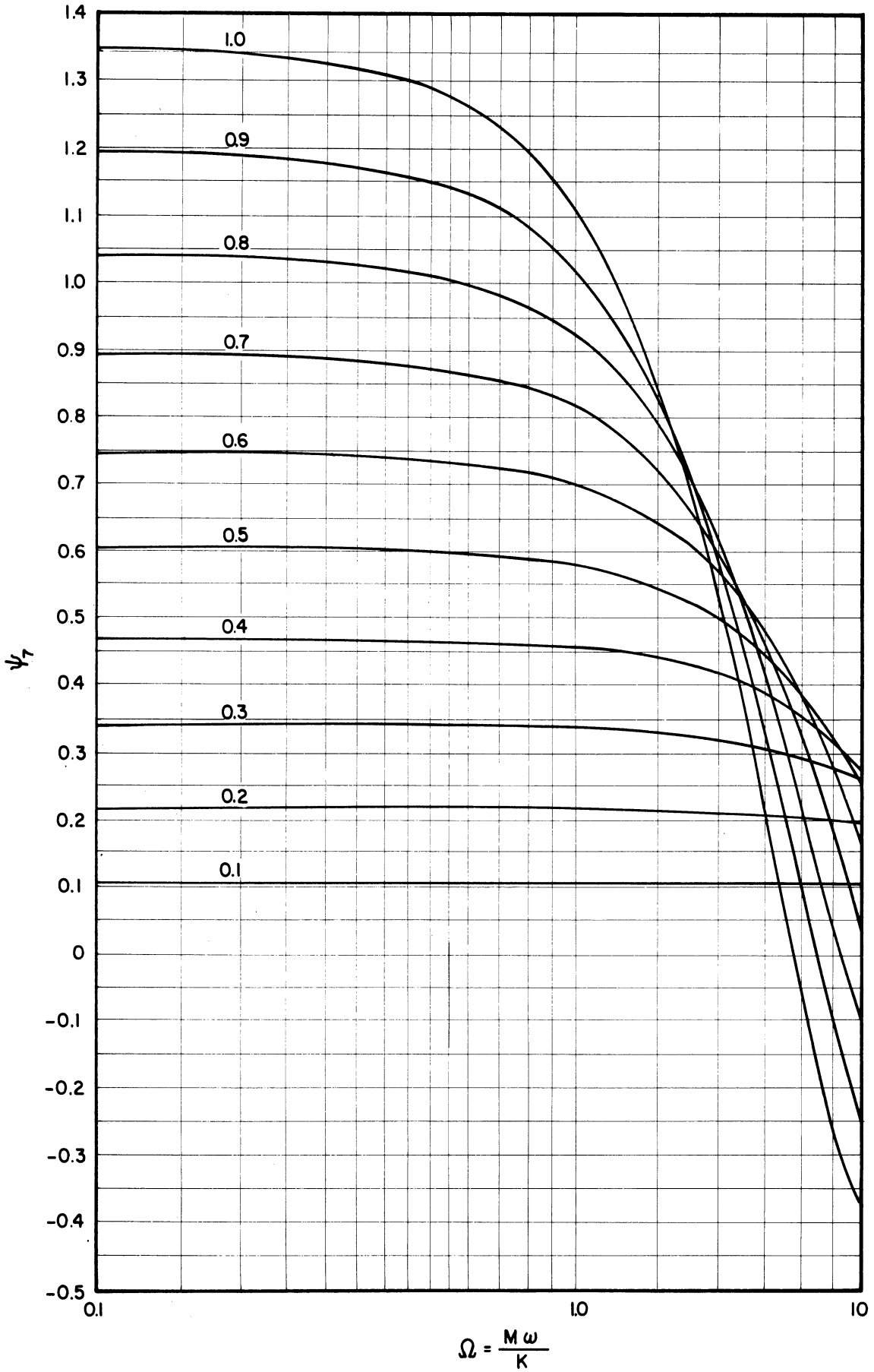

Figure 48. ψ_7 versus Ω, s = 2.0 (q = 0.1~1.0).

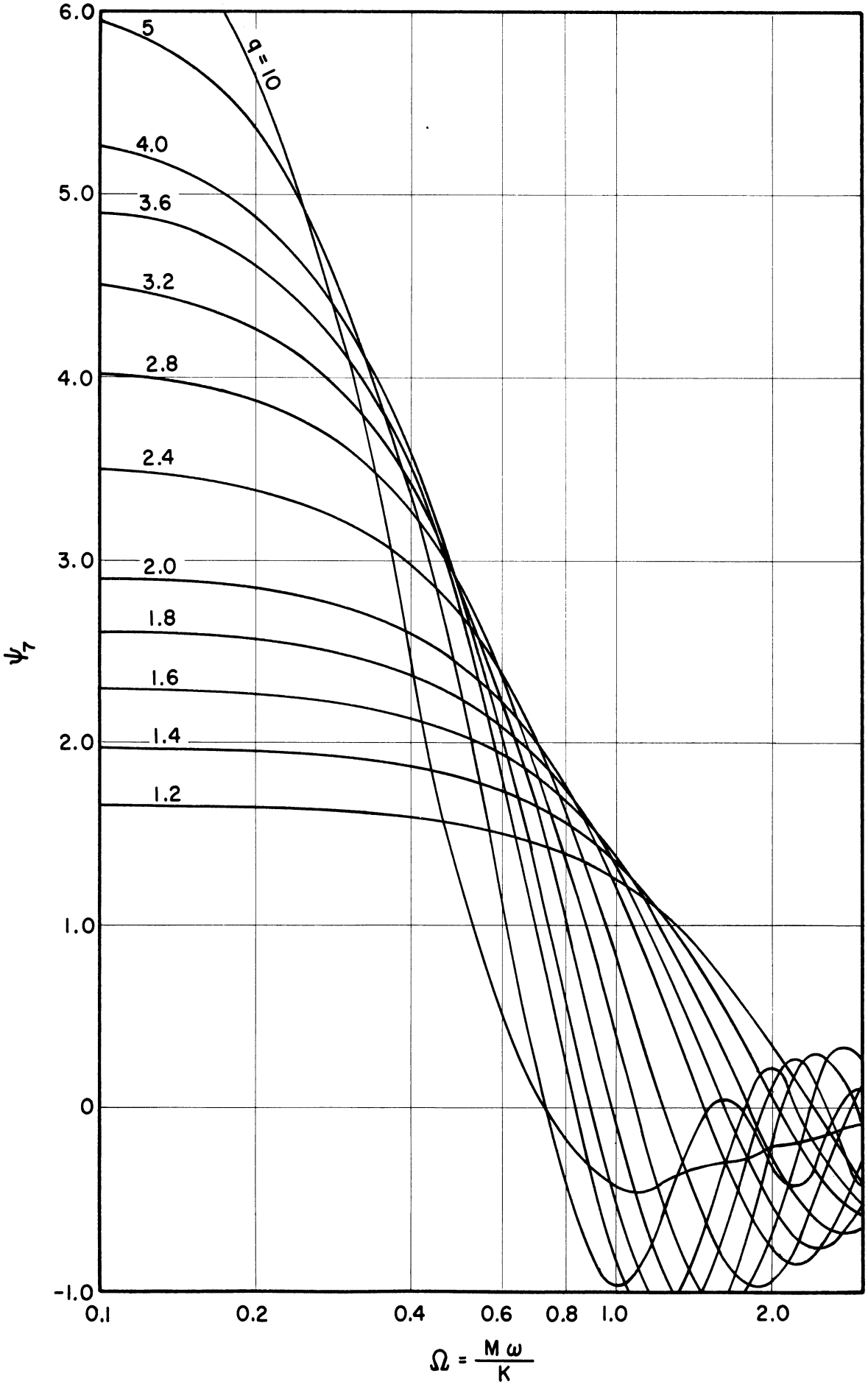

Figure 49. ψ_7 versus Ω, s = 2.0 (q = 1.2 ~ 10).

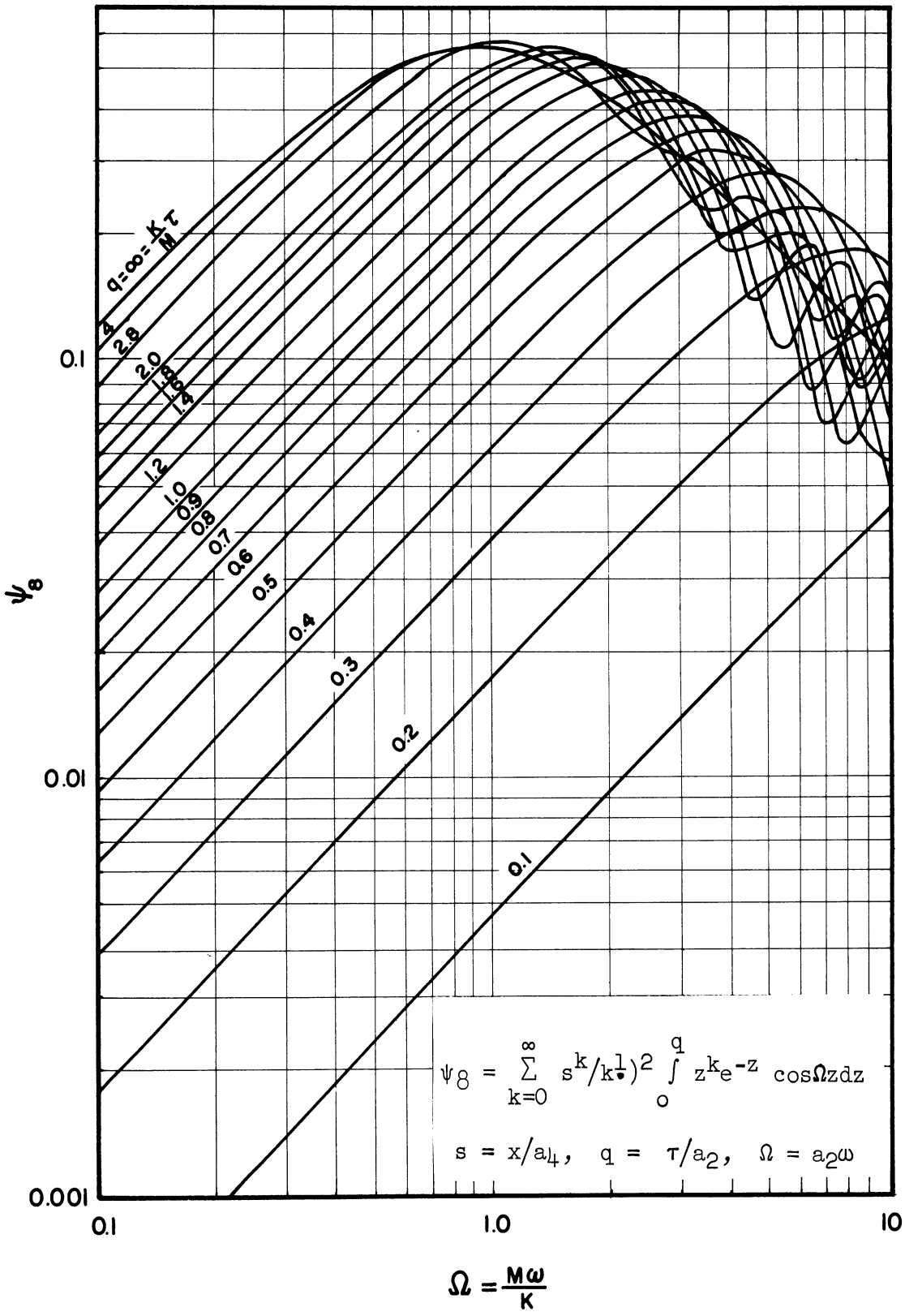

Figure 50. ψ_8 versus Ω, s = 0.1

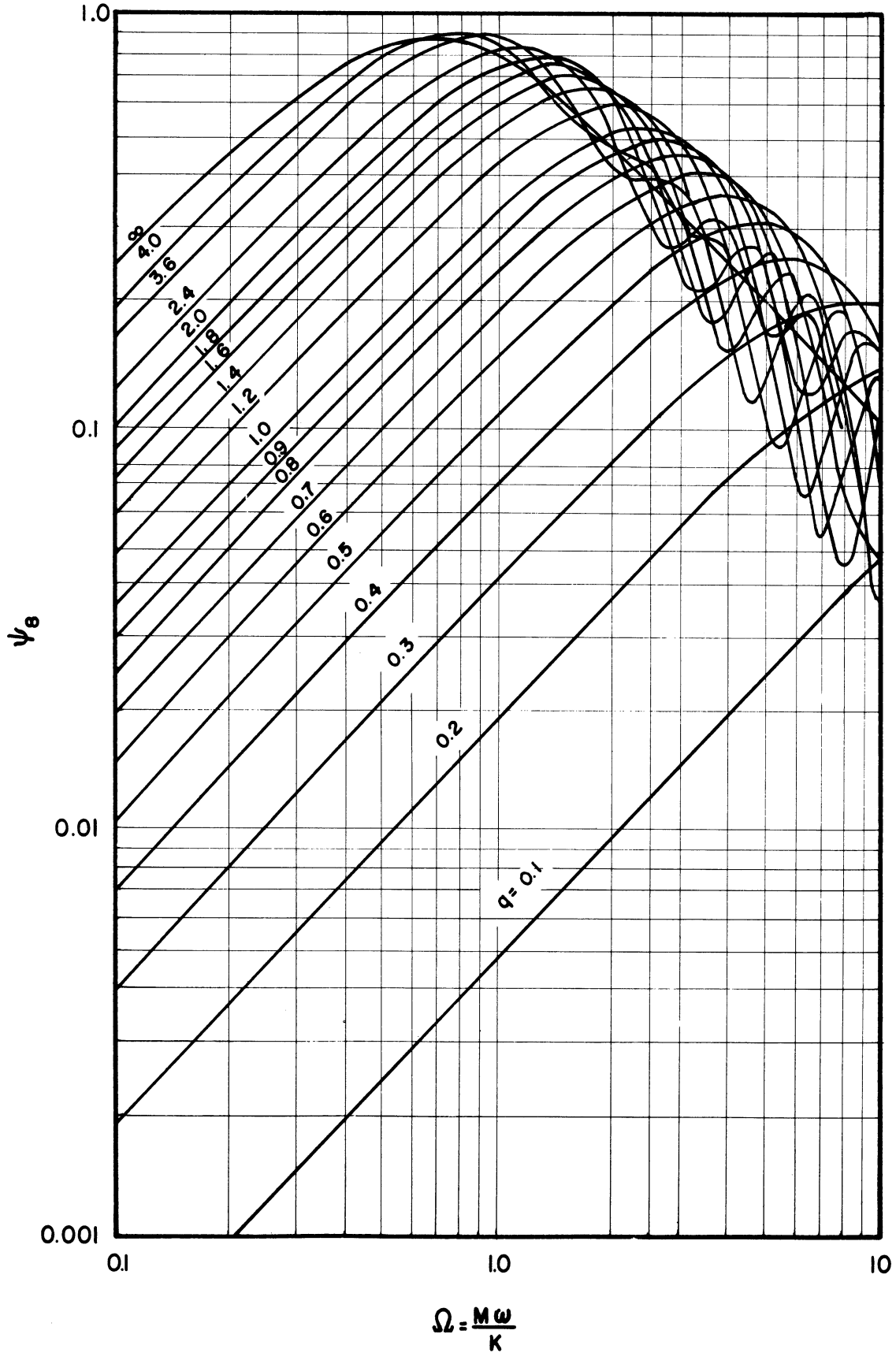

Figure 51. ψ_8 versus Ω, s = 0.5.

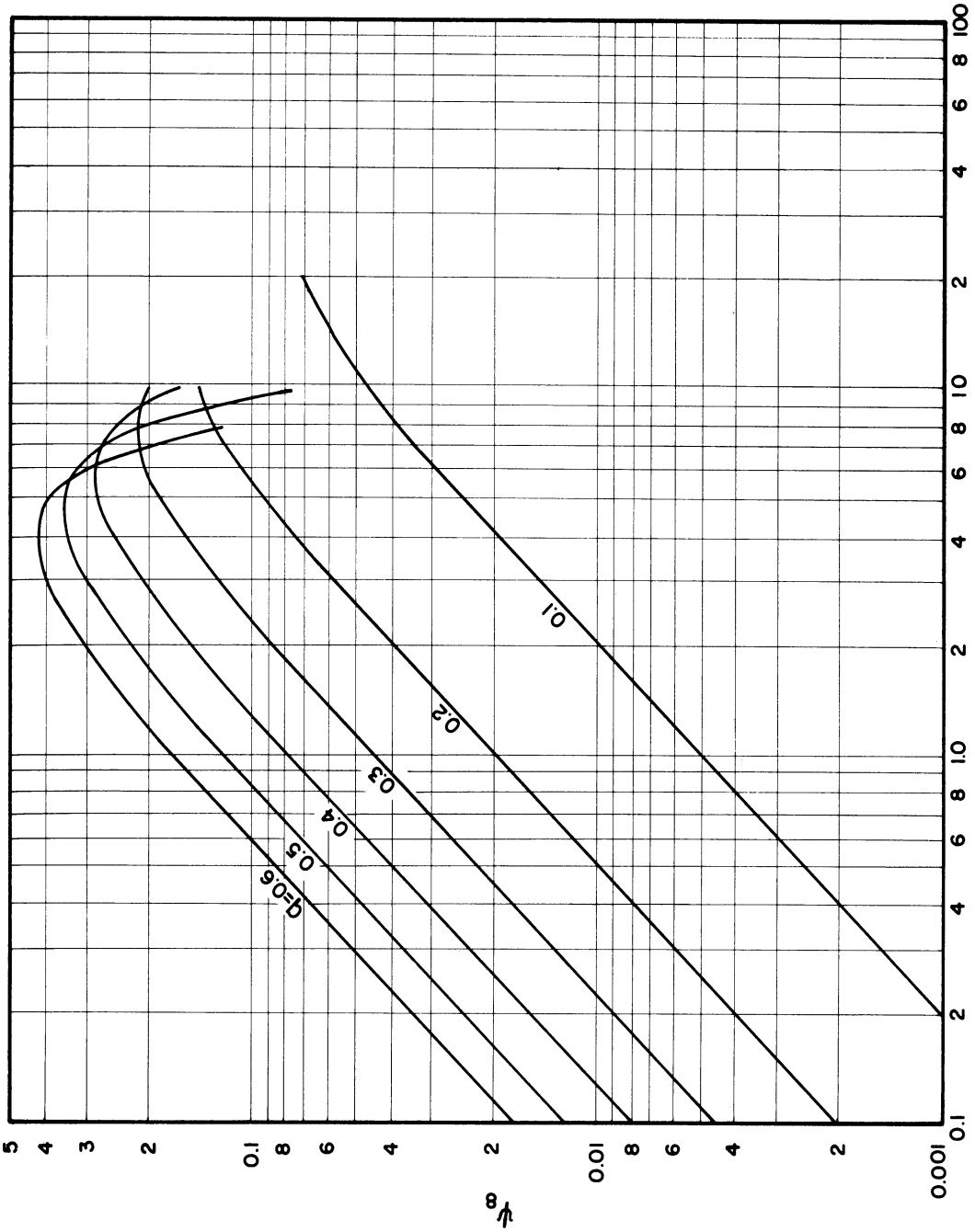

Figure 52. Ψ_8 versus Ω, s = 1.0 (q = 0.1~0.6).

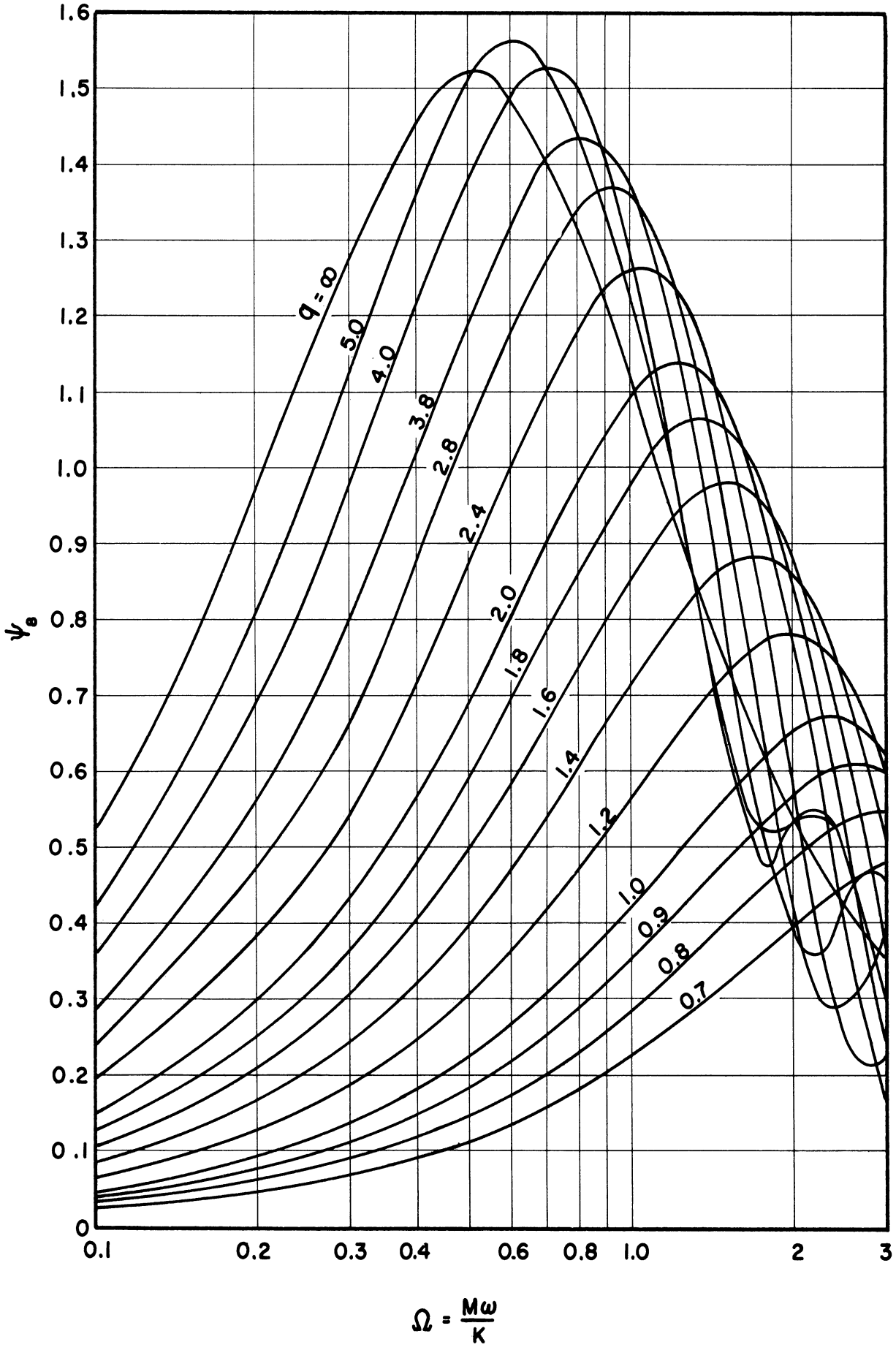

Figure 53. ψ_8 versus Ω, s = 1.0 (q = 0.7 ~ ∞).

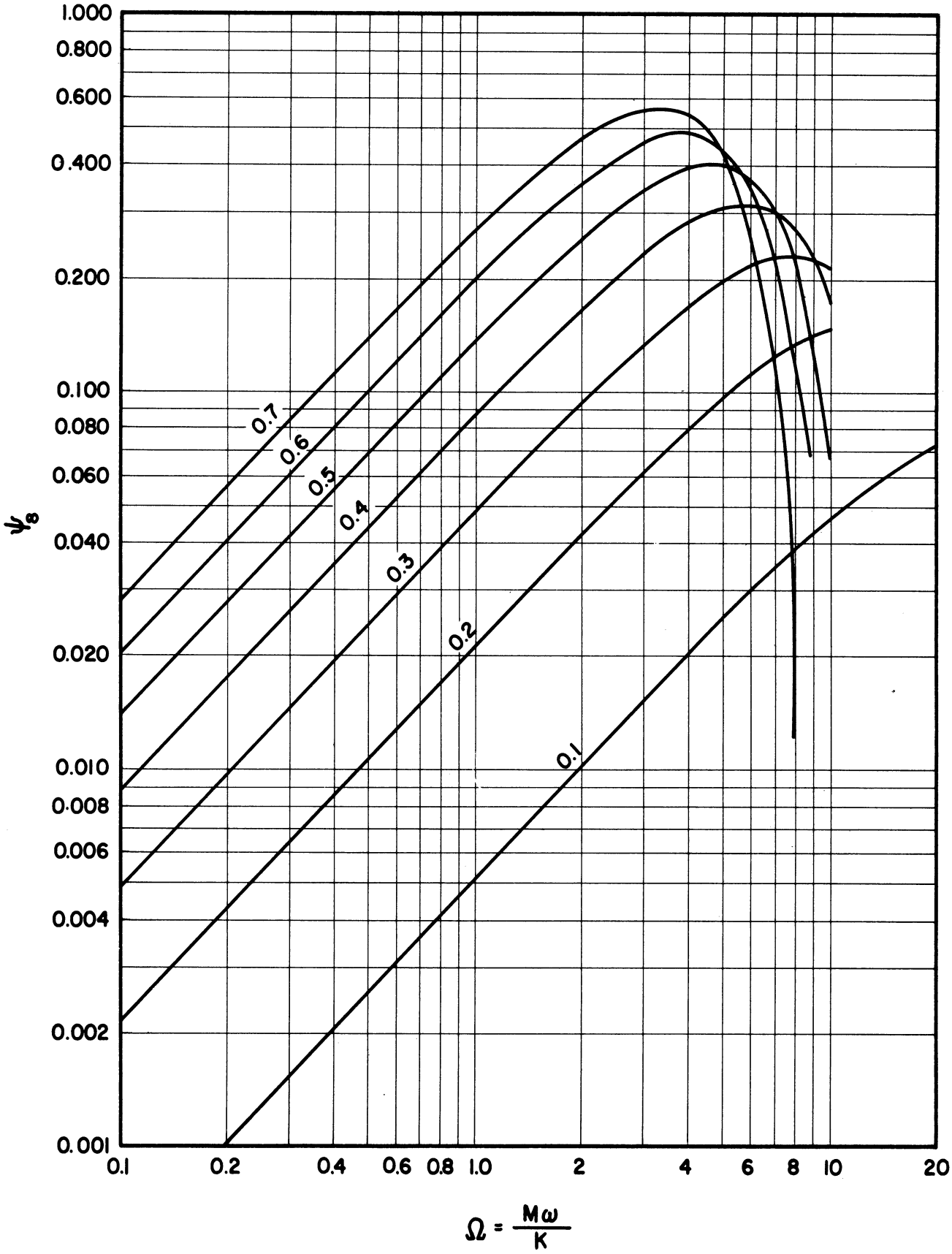

Figure 54. ψ_8 versus Ω, s = 1.5 (q = 0.1~0.7).

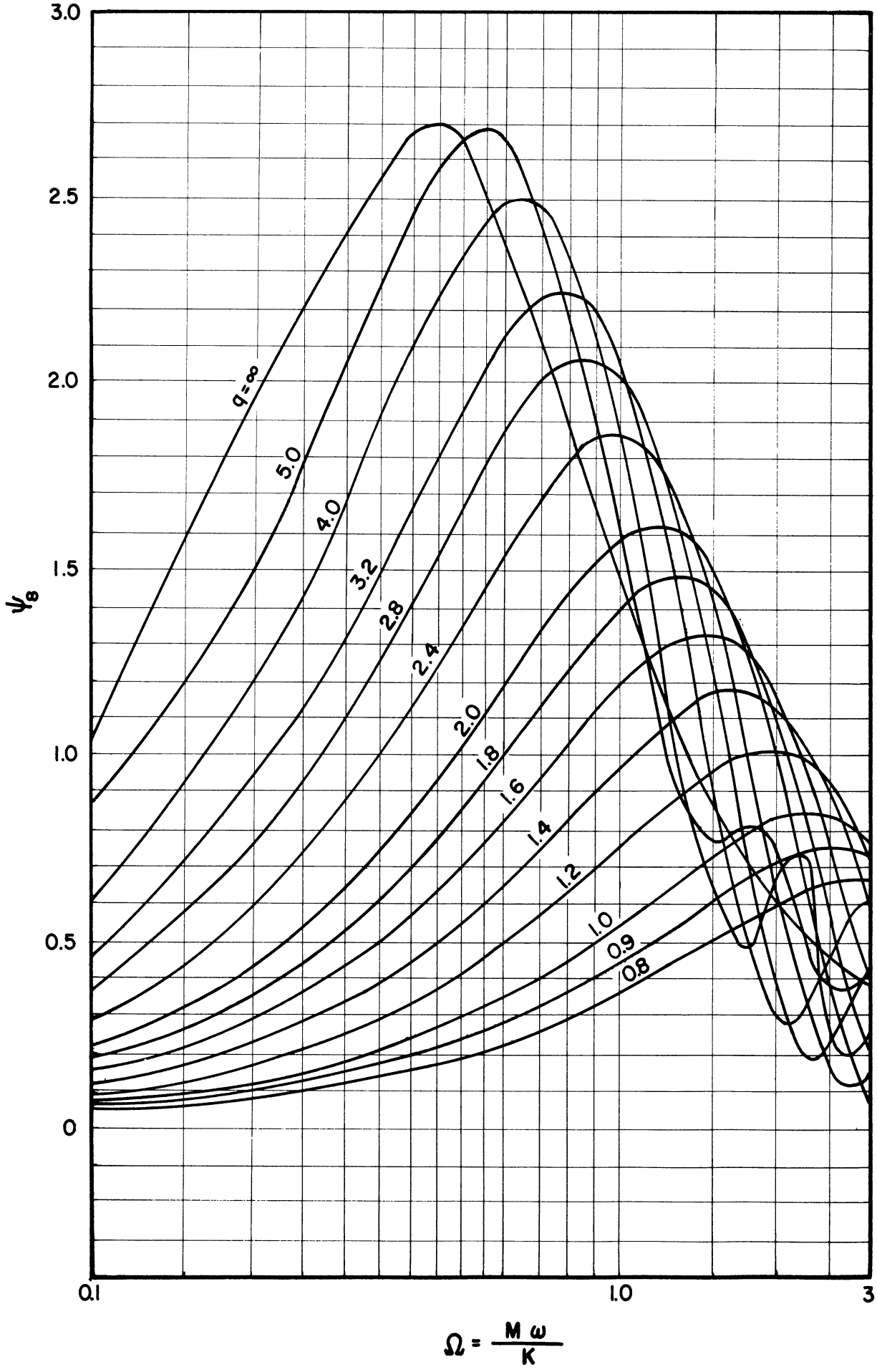

Figure 55. ψ_8 versus Ω, s = 1.5 (q = 0.8 ~ ∞).

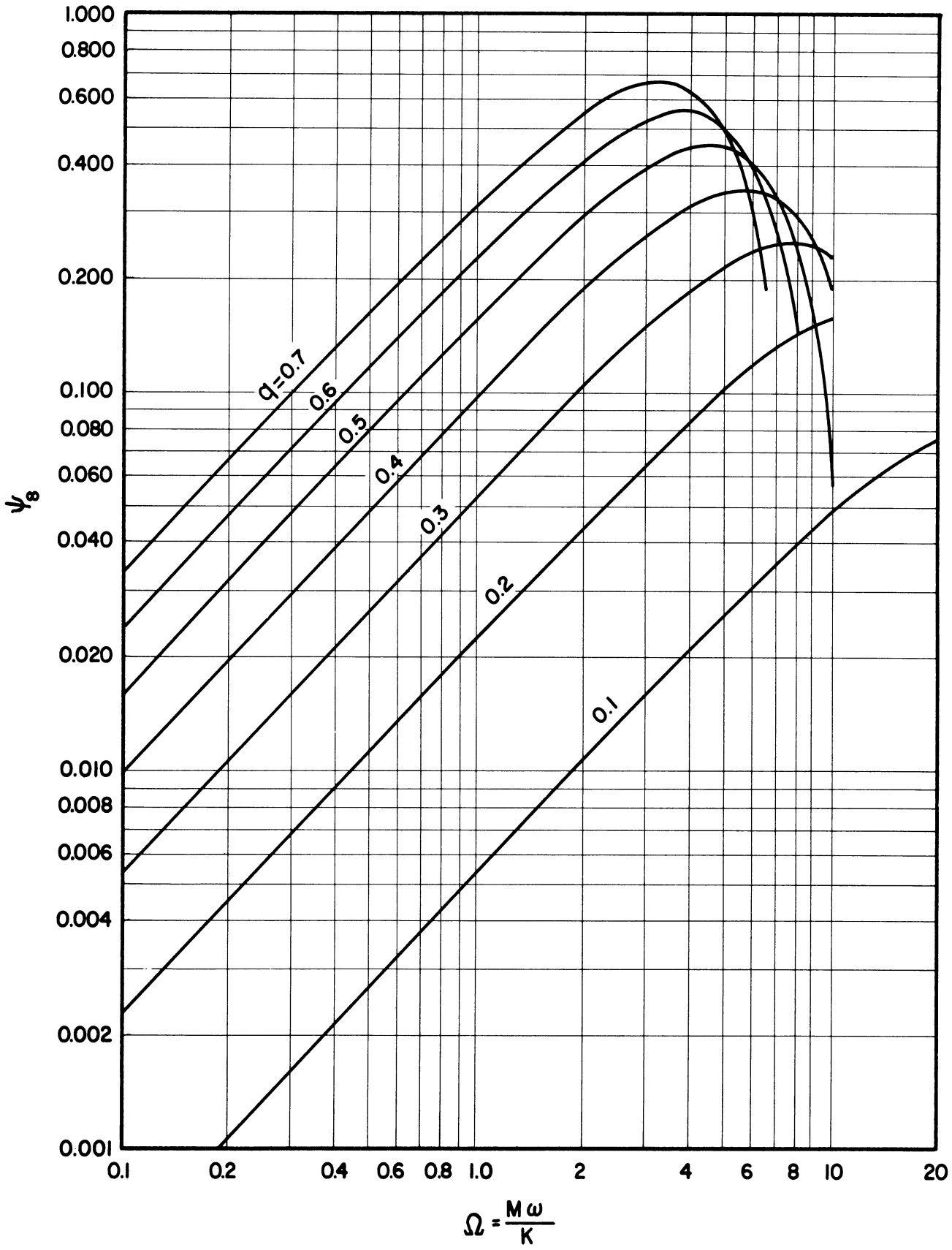

Figure 56. ψ_8 versus Ω, s = 2.0 (q = 0.1~0.7).

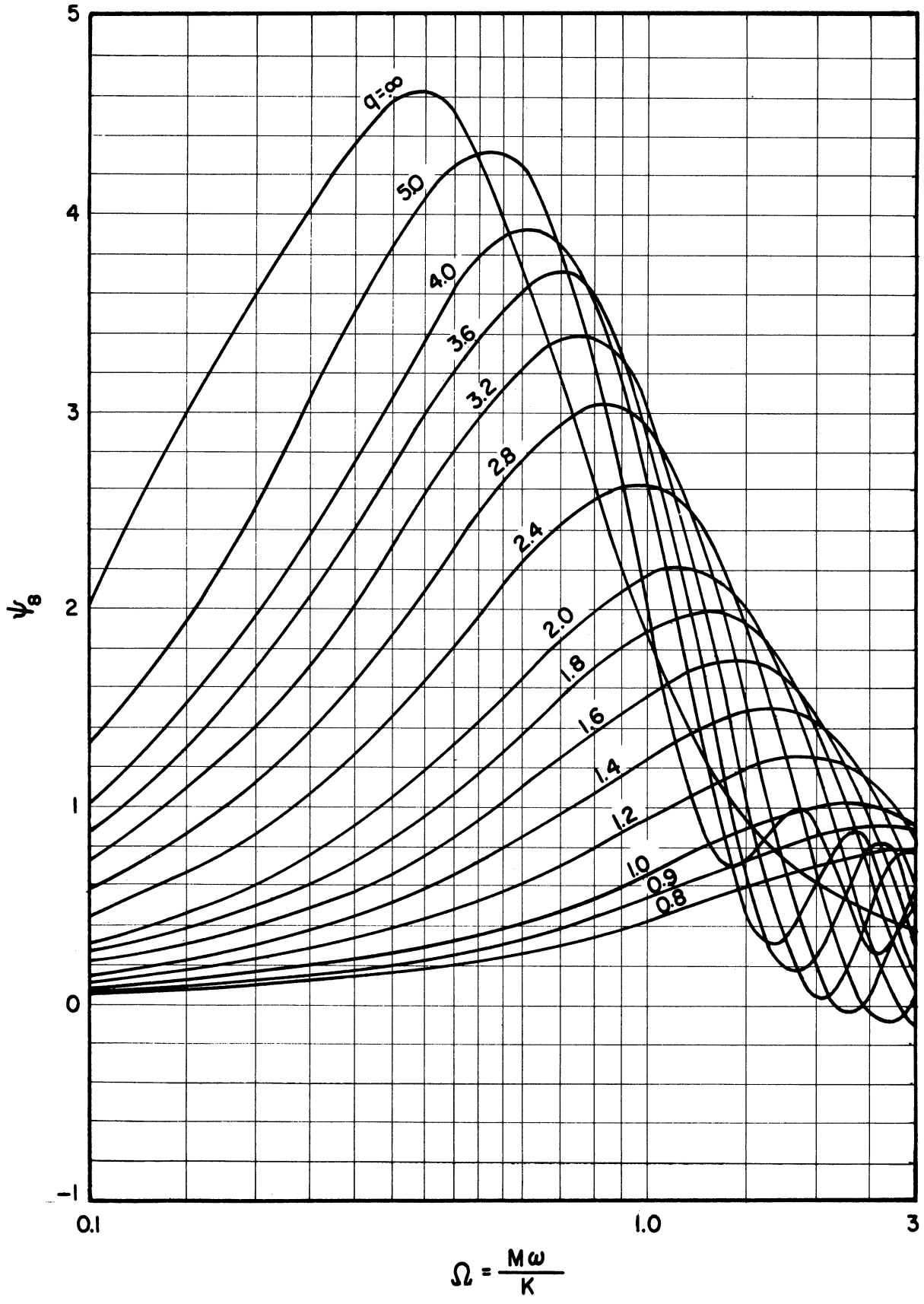

Figure 57. ψ_8 versus Ω, s = 2.0 (q = 0.8 ~ ∞).

APPENDIX H

DESIGN OF A FOUR-BAR LINKAGE TO PRODUCE THE SINUSOIDAL ANGULAR DISPLACEMENT OF THE TRANSFORMER SHAFT

The calibration of the 50 kw Rectifier shows that the voltage output is a linear function of the angular displacement of the transformer shaft. The four-bar linkage is designed to give the transformed shaft a sinusoidal angular displacement in order to obtain a sinusoidal voltage output from the rectifier. The relationship between the power output P_x'' of the rectifier and the angular displacement β of the transformer shaft is as follow:

$$\frac{P_x''(\tau)}{\bar{P}_x''} = \frac{E^2(\tau)}{\bar{E}^2} = \frac{\beta^2(\tau)}{\bar{\beta}} \qquad \text{(H-1)}$$

Assumpting the electrical resistance of the test section is constant, Equation (H-1) becomes

$$\frac{\beta(\tau)}{\bar{\beta}} = \sqrt{1 + \frac{P_{x0}''}{\bar{P}_x''} \sin\omega\tau}$$

$$= 1 + \frac{1}{2}\frac{P_{x0}''}{\bar{P}_x''}\sin\omega\tau - \frac{1}{8}\left(\frac{P_{x0}''}{\bar{P}_x''}\right)^2 \sin^2\omega\tau + \frac{1}{16}\left(\frac{P_{x0}''}{\bar{P}_x''}\right)^3 \sin^3\omega\tau + \cdots \qquad \text{(H-2)}$$

or

$$\frac{\beta(\tau)}{\bar{\beta}} \approx 1 + \frac{1}{2}\frac{P_{x0}''}{\bar{P}_x''}\sin\omega\tau \qquad \text{(H-3)}$$

Where $\bar{p}_x$", $\bar{E}$ and $\bar{\beta}$ are the mean (or initial) values of power input p_x" E voltage output and the angular displacement β. Equation (H-3) is a good approximation for $p_{xo}"/\bar{p}_x" \leq 0.23$.

In Figure 58, $O_2A_1B_1O_4$ is the position of the four-bar linkage at rest, corresponding to the position when β is at $\bar{\beta}$. As the linkage changes its position to $O_2A_2B_2O_4$ the following relationship holds if A_1B_1 is sufficiently long compared with O_4B_1.

$$A_2K_2 = B_2H_2 \tag{H-4}$$

i.e.

$$O_2A_2 \sin\omega\tau = O_4B_2 \sin\beta \tag{H-5}$$

Then

$$\beta(\tau) = \sin^{-1}\frac{O_2A_1}{O_4B_1}\sin\omega\tau$$

$$= \frac{O_2A_1}{O_4B_1}\sin\omega\tau + \frac{1}{6}\left(\frac{O_2A_1}{O_4B_1}\right)^3\sin^3\omega\tau + \frac{1\cdot3}{2\cdot4\cdot5}\left(\frac{O_2A_1}{O_4B_1}\right)^5\sin^5\omega\tau + \cdots\cdots \tag{H-6}$$

This relation holds for $(O_2A_1/O_4B_1)^2 < 1$. If O_2A_1/O_4B_1 is small, Equation (H-6) may be simplified as

$$\beta(\tau) \simeq \frac{O_2A_1}{O_4B_1}\sin\omega\tau \tag{H-7}$$

Therefore, if the ratio of power amplitude to the initial power is equal to or less than 0.23 and the ratio of O_2A_1 to O_4B_1 is small, an approximately sinusoidal heat generation may be obtained in the test section.

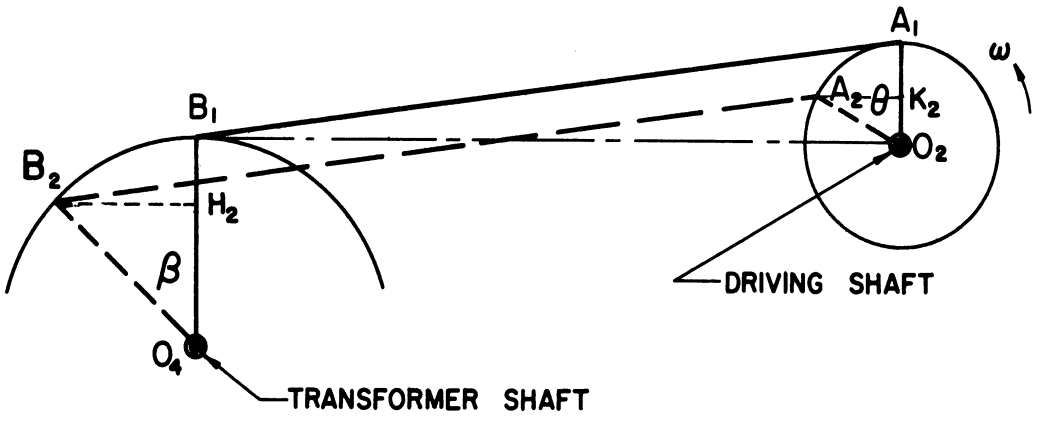

Figure 58. Four-Bar Linkage Designed to Produce the Sinusoidal Angular Displacement of the Transformer Shaft.

BIBLIOGRAPHY

1. Clark, J. A., Arpaci, V. S. and Treadwell, K. M. "Dynamic Response of Heat Exchangers Having Internal Heat Sources - Part I." Trans. ASME, 80, (1958), 612-624.

2. Arpaci, V. S. and Clark, J. A. "Dynamic Response of Heat Exchangers Having Internal Heat Sources - Part II." Trans. ASME, 80, (1958), 625-634.

3. Arpaci, V. S. and Clark, J. A. "Dynamic Response of Heat Exchangers Having Internal Heat Sources - Part III." ASME Paper No. 58-SA-39.

4. Cohen, W. C. and Johnson, E. F. "Dynamic Characteristics of Double-pipe Heat Exchangers." Industrial and Engineering Chemistry, 48, (June, 1956), 1031.

5. Mosley, J. M. "Predicting Dynamics of Concentric Pipe Heat Exchangers." Industrial and Engineering Chemistry, 48, (June, 1956), 1035.

6. Paynter, H. M. and Takahashi, Y. "New Method of Evaluating Dynamic Response of Counter Flow and Parallel-Flow Heat Exchangers." Trans. ASME, 78, (1956), 749-758.

7. Takahashi, Y. "You Need No Computers to Graphically Determine the Dynamics of Heat Percolation." Control Engineering, 2, (May, 1955), 46-50.

8. Takahashi, Y. "Transfer Function Analysis of Heat Exchangers." Automatic and Manual Control, ed. by A. Tustin, Buttersworth Science Publishing Co., London, England, (1952), 235.

9. Rizika, J. W. "Thermal Lags in Flowing Incompressible Fluid Systems Containing Heat Capacitors." Trans. ASME, 78, (1956), 1407.

10. Carslaw, H. S. and Jaeger, J. C. Conduction of Heat in Solids. London, England: Oxford University Press, (1948), 325-330.

11. Rizika, J. W. "Thermal Lags in Flowing Systems Containing Heat Capacitors." Trans. ASME, 76, (1954), 411.

12. Dusinberre, G. M. "Calculation of Transient Temperatures in Pipes and Heat Exchangers by Numerical Methods." Trans. ASME, 76, (1954),

13. Fritz, R. J. "Analysis of Temperature Transients in a Nuclear Power System." Preprint No. 234, Nuclear Engineering and Science Conference Cleveland, Ohio, December, 1955.

14. Silvers, J. P. and Dietrich, J. R. "The Reactor Handbook." 2, Engineering U.S. AEC, (May, 1955), 156-157.

15. Dabora, E. K. "Regenerative Heat Exchanger with Heat Loss Consideration Engineering Research Institute." Aircraft Propulsion Laboratory, Project 2284, University of Michigan, Ann Arbor, Aug., 1957.

16. Lambertson, T. J. "Performance Factors at a Periodic-Flow Heat Exchanger." Trans. ASME, 80, (1958), 586-592.

17. Cima, R. M. and London, A. L. "The Transient Response of Two-Fluid Counterflow Heat Exchanger - Gas Turbine Regeneration." ASME Paper No. 57-A-135.

18. Rea, S. E. and Ablow, C. M. "Transient Air Temperatures in a Duct." Trans. ASME, 79, (1957), 1536.

19. Siegel, R. "Transient Free Convection from a Vertical Flat Plate." Trans. ASME, 80, (1958), 347-359.

20. Profos, P. "Die Behandlung von Regelproblemen Vermittels des Frequenzganges des Regelkreises Und irhe Anwendung auf die Temperaturregelung Durchströmter Roheysteme." Zürich; Leemann and Co., 1943.

21. Paynter, H. M. "On an Analogy Between Stochastic Processes and Monotone Dynamic Systems." VDI/VDE Fachtagung Regelugstechnik, Heidelberg, Germany, September, 1956.

22. Leonbard, A. "Determination of Transient Response from Frequency Response." Frequency Response Symposium, Trans. ASME, 76, (Nov., 1954), 1215-1236.

23. Evans, W. R. "The Uses of Zeros and Poles for Frequency-Response or Transient Response." Frequency Response Symposium, Trans. ASME, 76, (November, 1954), 1335-1344.

24. Zoss, L. M., Gollin, N. W. and Edelman, R. I. "Dynamic Response Analysis of Air Heater Temperature Control System." Industrial and Engineering Chemistry, 48, (June, 1956), 1069-1073.

25. St. Clair, D. W., Coombs, W. F. Jr., and Owens, W. D. "Frequency-Response Analysis for Industrial Automatic-Control System." Trans. ASME, (Oct., 1952), 1138-1150.

26. Yang, W. J. "Dynamic Response of Plate-Finned Heat Exchangers" Report Engineering Research Office, Ford Motor Co., Dearborn, Dec., 1957.

27. Churchill, R. V. Modern Operational Mathematics in Engineering. Chapters 1, 2, 3, New York: McGraw-Hill Book Co., 1944.

28. Chestnut, H. and Mayer, R. W. Servomechanism and Regulating System Design. 1, Chapters 4, 5, 6, and 9, New York: John Wiley and Son Inc., Sep., 1953.

29. Tsien, H. S. Engineering Cybernetics. Chapters 1, 2, 3, and 4, New York: McGraw-Hill Book Co., Inc., 1954.

30. Oldenberg, R. C. and Sartorius, H. "The Dynamics of Automatic Controls." Translated and Edited by H. L. Mason, ASME, Chapters 1, 2, and 3, Feb., 1948.

31. Draper, C. S., McKay, W. and Lees, S. Instrument Engineering. 1, New York: McGraw-Hill Book Co., Inc., 1952.

32. Aladyev, I. T. "Experimental Determination of Localand Mean Coefficients of Heat Transfer for Turbulent Flow in Pipes." NaCA TM 1356, Feb., 1954.

33. Hartnett, J. P. "Experimental Determination of The Thermal-Entrance Length for the Flow of Water and of Oil in Circular Pipes." Trans. ASME, Nov., 1955.

34. Deissler, R. G. "Analysis of Turbulent Heat Transfer and Flow in the Entrance Regions of Smooth Passages." NACA TN 3016, Oct., 1953.

35. Kline, S. J. and McClintock, F. A. "Describing Uncertainties in Single-Sample Experiments." Mechanical Engineering, (Jan., 1953), 3-8.

36. McAdam, W. H. Heat Transmission. 3rd Edition, New York: McGraw-Hill Book Co., Inc., 1954.

37. Masubuchi, M. "Dynamic Response and Control of Multipass Heat Exchangers." ASME Trans., Series D, March, 1960.